SUPRAMOLECULAR POLYMER BLENDS FOR COMPOSITE MATRICES

A thesis submitted in part fulfilment of the degree of
Doctor of Philosophy

Kate J C Lim

Department of Chemistry

2016

Declaration of original authorship

I confirm that this is my own work and the use of all material from other sources has been properly and fully acknowledged.

_____   Kate J C Lim

Acknowledgments

Abstract

This research project reports a new approach to thermoplastic composite matrix design, in which a low-MW polymer additive acts as a plasticiser and flow-promoter at high temperatures, but as a non-covalent cross-linking agent at lower temperatures. Thus, poly(aryl ether ketone)s (PAEKs) are functionalised with π-electron rich terminal groups and blended with π-electron deficient polyimides. A non-covalent charge-transfer stacking interaction between the two polymers forms a self-assembled supramolecular network. Carbon fibre composites with matrices composed of these supramolecular polymer blends were produced, and the thermomechanical performance of these materials are reported.

In designing functionalised PAEKs, novel benzoyl-pyrene and -perylene derived compounds were synthesised. The synthesis of these compounds and their subsequent use as functional end-groups in polycondensations are also discussed.

During the course of polymer synthesis, the effect of varying polymerisation conditions involving different alkali metal carbonates was systematically investigated. It was found that monomer sequence distribution in PAEKs can be controlled by changing the alkali metal cation used in the nucleophilic synthesis. The mechanism of modifying monomer sequence distribution is presented herein.

Investigating the interaction of polycyclic aromatic molecules pyrene and perylene with binary co-polyimides containing both strongly-binding and weakly-binding diimide sequences results in the emergence of fractal-like patterns in the ^{1}H NMR spectra of the polyimide. The polyimide spectrum at high intercalator loadings shows self-similarity over a range of different length scales.

Table of Contents

List of abbreviations

Ar	Aromatic or aryl
Đ	Dispersity (polydispersity index)
DCM	Dichloromethane
DMA	Dynamic mechanical analysis
DMAc	*N,N*-Dimethylacetamide
DMF	*N,N*-Dimethylformamide
DMSO	Dimethyl sulfoxide
DSC	Differential scanning calorimetry
ESI	Electrospray ionisation
EtOH	Ethanol
h	Hour(s)
HFiPA	1,1,1,3,3,3-hexafluoro-2-propanol
η_{inh}	Inherent viscosity
IR	Infrared spectroscopy
min	Minute(s)
M_n	Number-average molecular weight
M_w	Weight-average molecular weight
N_i	Number of monomer molecules
NDA	1,4,5,8-naphthalenetetracarboxylic dianhydride
NDI	1,4,5,8-naphthalenetetracarboxylic diimide
NMP	1-methyl-2-pyrrolidinone
NMR	Nuclear magnetic resonance spectroscopy
PDA	Pyromellitic dianhydride
PDI	Pyromellitic diimide
PAEK	Poly(aryl ether ketone)
PEEK	Poly(ether ether ketone)
PEKK	Poly(ether ketone ketone)
PES	Poly(ethersulfone)
R_f	Chromatography retardation factor

s	Second(s)
T_c	Crystallisation temperature
T_{cc}	Cold crystallisation temperature
TFA	Trifluoroacetic acid
T_g	Glass transition temperature
THF	Tetrahydrofuran
T_m	Crystalline melting temperature
UV-Vis	Ultraviolet-visible spectroscopy
v/v	Volume ratio
wt	Weight
w/v	Weight to volume ratio
w/w	Weight ratio
XRD	X-ray diffraction
X_n	Number average degree of polymerisation
ΔH_f	Enthalpy of fusion for a crystal at the T_m

Chapter 1

Introduction

1.1 Research Motivation

Carbon fibre composites for high performance applications have traditionally been based on cross-linked resins such as the epoxies and bismaleimides.[1,2] However, the potential advantages of thermoplastic matrices, notably much increased toughness, have begun to be realised in more recent years.[3] The most notable development has been the introduction of long-fibre composites based on semi-crystalline engineering thermoplastics such as poly(1,4-phenylene sulfide) (PPS)[4] and the aromatic poly(ether ether ketone) (PEEK)[5] and poly(ether ketone ketone) (PEKK) (Figure 1.1)[6].
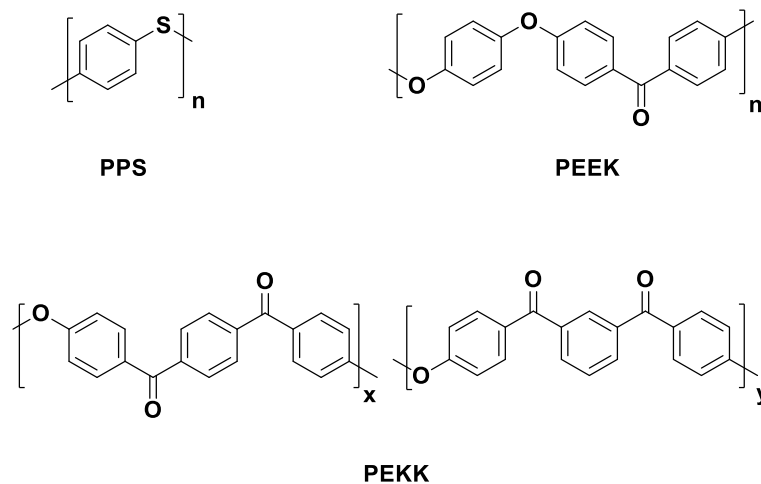
Figure 1.1. Some thermoplastic aromatic matrix polymers used in carbon fibre composites.

Poly(aryl ether ketone)s (PAEKs) such as PEEK and PEKK offer outstanding physiochemical and thermomechanical properties, which are primarily attributed to their crystalline character. They also exhibit high thermo-oxidative stability as a result of their aromatic nature and non-oxidisable linking groups. These features have allowed their use in a wide-variety of demanding applications that include the automotive, aerospace and biomedical industries.[7] In a typical application, three or more properties of the PAEKs may come into consideration. For instance, if a material is required to have a combination of chemical

resistance, structural strength as well as high operating temperatures, then PEEK (and its related PAEKs) is one of the few suitable materials.[8]

These properties of PAEKs, although highly desirable, can also be a hindrance in their synthesis and processing. Moreover, their resistance to dissolution in organic solvents remain an obstacle to detailed characterisation. In addition, their high melt-viscosities and the high processing temperatures required (*ca.* 400 °C) make their application as composite matrices, specifically the fibre impregnation step (pre-pregging) challenging and costly.[9]

The initial aim of this research project was therefore to improve the ease of processing of PAEKs to allow more facile carbon fibre composite production. A more comprehensive overview of the project objectives will be outlined at the end of the present Chapter. This is preceded by a literature review which presents the current synthesis routes to PAEKs and discusses their structure-related properties. Finally, the use of different polymeric blends of PAEKs, as an approach to improving the thermomechanical properties and processing of PAEKs, will be discussed.

1.2 Chemistry of PAEKs

Syntheses of PAEKs proceed by either electrophilic or nucleophilic polycondensation of aromatic monomers. A polycondensation reaction is a form of step-growth polymerisation wherein a repeated reaction between two reactive functional groups form a single functional group, so affording a polycondensate (a polymer), and is often accompanied by the displacement of a small molecule or ion at each step. In this regard, one route to PAEKs could be described simplistically as the formation of an ether bond from the reaction between an activated aromatic dihalide and an aromatic diphenolate salt, with the displacement of a halide anion.

The extent of a polycondensation reaction may be defined by the Carothers equation[10] (Equation 1.1), where X_n is the number-average degree of polymerisation, equal to the average number of monomer units in a polymer. The number of reacted functional groups is represented by p, which is defined by N_0, the initial number of monomer molecules and N, the number of monomer molecules after a given time. The equation therefore allows the degree of polymerisation to be calculated by the conversion of monomer units.

Equation 1.1. Carothers equation

$$X_n = \frac{1}{(1 - p)}$$
$$\text{where} \quad p = \frac{N_0 - N}{N_0}$$

This equation shows that a very high monomer conversion is required to achieve a high degree of polymerisation, or as p tends to unity, which is at the end of the reaction. This becomes increasingly difficult to achieve as the reaction progresses, with the decreasing frequency of reactive chain ends encountering depleting amounts of reactants. The highly crystalline nature of PAEKs could also have the disadvantage of crystallisation and consequent precipitation during polycondensation. Two main synthetic routes are available for production of high molecular weight PAEKs, and these are discussed below.

1.2.1 Nucleophilic polycondensation

The nucleophilic route to PAEKs is a base-promoted process where an ether bond is formed via nucleophilic displacement of an activated halide or nitro group by a phenolate anion.

This type of polycondensation ("polyetherification") was first used to produce poly(ether sulfone)s (PES).[11] In most cases, the base is an alkali metal carbonate such as Na_2CO_3 and/or K_2CO_3. The nucleophilic phenolate ion is formed *in situ* by the de-protonation of a bisphenol monomer by the base (this approach was the one mainly used in the present research project). The presence of a conjugated, electron-withdrawing substituent, such as a ketone or sulfone linkage *ortho-* or *para-* to the halide leaving group is essential to promote nucleophilic displacement and ether bond formation.[12]

A general reaction scheme for the nucleophilic aromatic substitution is presented in Scheme 1.1. The electron-withdrawing group and leaving group are represented by EWG and X respectively. The reaction proceeds via the S_NAr mechanism, with a resonance-stabilised intermediate known as the Meisenheimer complex. The *formation* of this intermediate (not its breakdown) is known to be the rate-determining step of the reaction.[13]
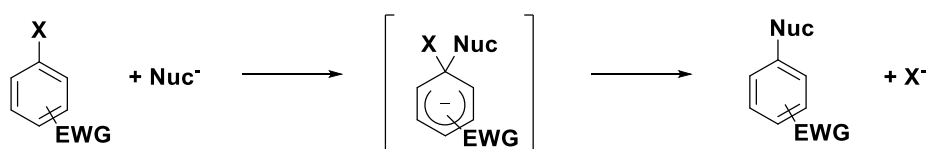
Scheme 1.1. A general reaction scheme for nucleophilic aromatic substitution, where EWG is an electron-withdrawing group conjugated with the aromatic ring, and X is a leaving group.

The orientation of the electron-withdrawing group relative to the leaving group is important for the kinetics of the reaction. In a study comparing the kinetics of different arenesulfonyl fluoride isomers, it was found that the rate of reaction decreased in the order: *para- > ortho- > meta-,* relative to the leaving group.[14] The reduced reactivity of the *o*-isomer compared with the *p*-isomer could be attributed to steric hindrance at the substitution position. The reduced reactivity of the *m*-isomer clearly arises from the lack of mesomeric stabilisation of the intermediate, as this isomer cannot delocalise the negative charge in the intermediate in the same way as the other two isomers.[15]

The halogen leaving group reactivity is in the order F^- >> Cl^- > Br^- > I^-.[16] The reactivity can be attributed to the high electronegativity of fluorine and thus it forms the most polar carbon-halide bond. This would make the corresponding carbon (in C-F) more susceptible to

nucleophilic attack. Additionally, F⁻ has the smallest ionic radius of the halides, and offers the least hindered carbon-halide bond for nucleophilic substitution reactions.

A high boiling solvent is required in order to achieve a high molecular weight PAEK. The first reported preparations of PEEK using such solvents as dimethyl sulfoxide or tetrahydrothiophene-1,1-dioxide (sulfolane) achieved temperatures of *ca*. 200 °C.[11] However, only brittle, low molecular weight materials were obtained, owing to early crystallisation of the product. Later, a method for performing the polymerisation at higher temperatures (up to 320 °C) in diphenyl sulfone was developed by Rose[17] and Attwood.[18] This allowed the polymer to remain in solution until high molecular weights were attained. Materials suitable for high performance applications were produced using this process. *N*-Methylpyrrolidone has also been reported as a solvent for this reaction, although its high volatility limits reaction temperatures to around 200 °C, or to pressurised systems.[19] Most recently, it was reported that PEEK was successfully synthesised in an ionic liquid by polycondensation reactions of hydroquinone with 4,4'-dihalobenzophenones at elevated temperatures (up to 320 °C). The materials produced were said to be similar to polymers prepared in commercial processes, i.e. in diphenyl sulfone, but with much lower molecular weights.[20] In the present research project, PAEKs obtained by the nucleophilic pathway employed diphenyl sulfone (for crystalline polymers) and DMAc (for amorphous ones) as solvents.

A side reaction that is known to occur during nucleophilic polycondensation of PAEKs is transetherification, through a reversible ether cleavage process.[21] The aryl ether bonds are activated towards nucleophilic cleavage by fluoride or phenolate anions present in the reaction mixture. The extent of the transetherification reaction depends on the type of base used in the reaction. Chapter 4 of this thesis will examine in detail the role of the alkali metal carbonate in transetherification during one specific polymer synthesis.

1.2.2 Electrophilic polycondensation

The first electrophilic route to PAEKs was reported by Bonner[22] and involved a Friedel-Crafts polyacylation between an aromatic diacyl halide and an aryl ether to produce PEKK (Scheme 1.2). Again, polymer crystallisation was a problem in these early studies, but later work showed that the electrophilic route to PAEKs can proceed successfully under two synthetic

conditions: either the use of strongly acidic solvents at ambient temperature or using a large an excess of Lewis acid; both conditions are briefly described herein.
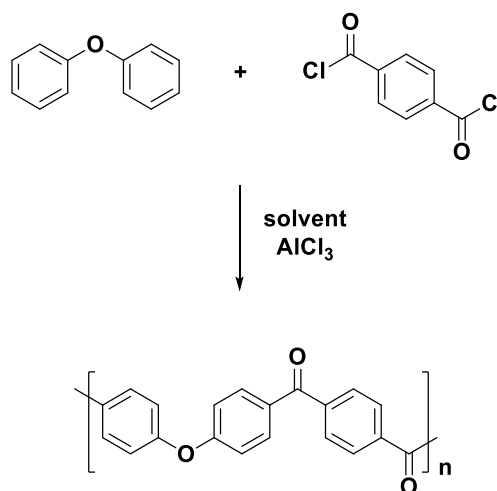
Scheme 1.2. A general synthesis of PEKK via the electrophilic route.

The first successful polycondensation via the electrophilic route in strong acidic media was carried out in HF using BF_3 as "catalyst", by Marks at Dupont.[23] Under well-controlled reaction conditions, high molecular weight PEK was obtained from 4-phenoxybenzoyl chloride at ambient temperature, using a large excess of HF/BF_3 to afford high molecular weight polymers.

PAEKs can also be produced with either neat polyphosphoric acid or anhydrous trifluoromethanesulfonic acid acting as both solvent and Friedel-Crafts catalyst. Iwakura and co-workers[24] reported the synthesis of PEK by the self-condensation of *p*-phenoxybenzoic acid using polyphosphoric acid as the solvent and catalyst. Colquhoun and Lewis[25] first reported the synthesis of various high molecular weight PAEKs via self-condensation of aryloxybenzoic acids in the neat trifluoromethanesulfonic acid system. Their work also demonstrated a selective 'through-bridge' deactivating effect in some acylated diphenyl ethers, which inhibits self-condensation, *ipso facto* producing only low molecular weight products in certain cases. Both the polyphosphoric acid and trifluoromethanesulfonic acid polycondensations are carried out at ambient temperature, with the PAEK remaining in solution as a result of the protonation of the carbonyl groups by the strong acid solvent. The reaction can thus yield high molecular weight products.

Electrophilic polycondensation in non-basic solvents (such as dichloromethane or 1,2-dichloroethane) can proceed with the addition of excess Lewis acid, $AlCl_3$. The Lewis acid catalyses the reaction and also acts to solubilise the polymer by forming a complex with the carbonyl groups of the polymer backbone.[26] $AlCl_3$ must then be hydrolysed and extracted from the polymer. The waste stream from this process thus contains organic compounds, aluminium salts and hydrochloric acid. Under these conditions, the polycondensation of diphenyl ether with mixtures of terephthaloyl chloride and isophthaloyl chloride is a low cost route to PEKK.[27] Polymerisations in the presence of a large excess of $AlCl_3$ when complexed with a Lewis base such as DMF or LiCl were reported to produce a higher molecular weight product.[28] The Lewis base can complex with $AlCl_3$ to prevent *ortho*-acylation of the monomers. The polar complex also increases the solubility of polymer complexes that lead to high molecular weight polymers. Finally, a two-step reaction has been reported[29] to yield polymer with maximum *para*-selectivity. In this approach (Scheme 1.3) 4,4'-diphenoxyterephthalophenone is first isolated from the reaction of excess diphenyl ether with terephthaloyl chloride, and is purified by recrystallisation. This compound then undergoes polycondensation with a mixture of isopthaloyl and terephthaloyl chlorides, the molar ratio of the two acid chlorides influencing the melting point and rate of crystallisation of the final polymer (a higher proportion of terephthaloyl chloride gives higher melting and faster-crystallising polymer).
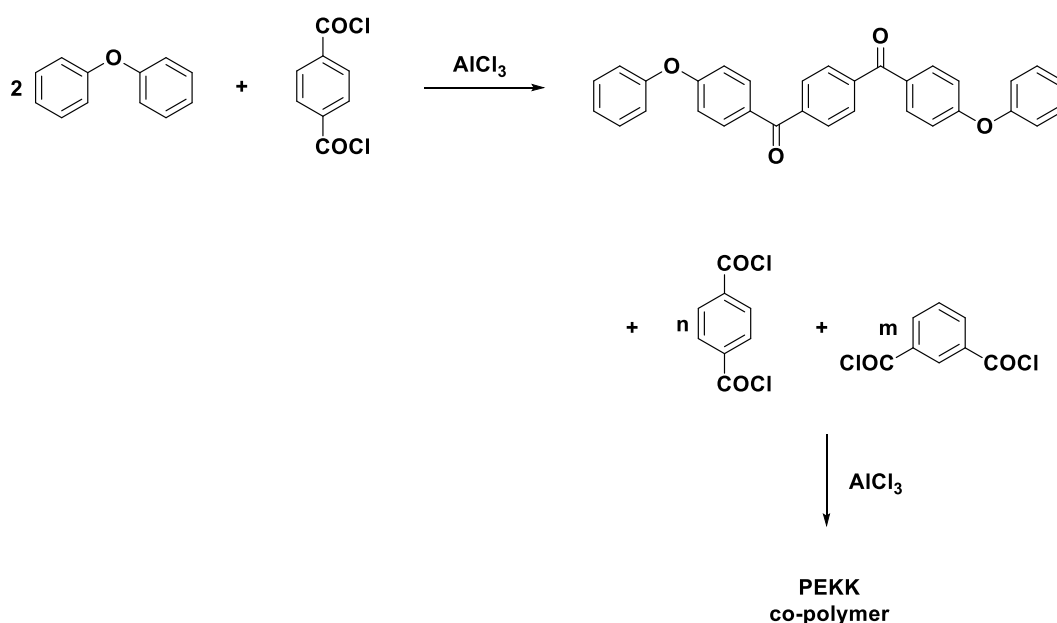
Scheme 1.3. Synthesis of commercial PEKK via the electrophilic route.

The electrophilic route has the advantage of using relatively cheap monomers and low reaction temperatures in comparison to the nucleophilic route. Nevertheless, the difficulties of disposing waste hydrolysis by-products of AlCl$_3$ and the safety hazards of using extremely strong acidic media limits the applicability of the electrophilic route in industrial processes.[20]

1.2.3 Industrial production of PEEK and related PAEKs

Since the early 1960s, the development of high performance polymers has been driven by corresponding requirements of technologically advanced industries, notably the aerospace and nuclear industries. The first reported attempts to synthesise PEKK[22] and PEK[30] (via the electrophilic route) as potentially useful industrial products were reported in patents granted to Dupont and Imperial Chemical Industries (ICI) in 1962 and 1964, respectively. This was quickly followed by production of the first commercially available poly(ether ketone) (PEK), which was introduced by Raychem Corporation (under licence from DuPont) in the mid-1970s under the trade name *Stilan*.[31] The product was a semi-crystalline polymer, made by the electrophilic synthesis (HF/BF$_3$ system), mainly for use in electrical wiring insulation. The rigorous conditions needed to make PEK, involving Friedel-Crafts chemistry and the use of an expensive catalyst (BF$_3$) combined with a highly hazardous solvent (liquid HF) meant it was very expensive to manufacture.

ICI was one of the major contributors to the development of high performance materials with its introduction of a nucleophilic approach to PEK in the late 1970s.[32] This was followed by the first patent to the nucleophilic route to PEEK[33] in 1982, and its eventual commercial production under the *Victrex* trade name. PEEK is a semi-crystalline PAEK prepared via nucleophilic aromatic substitution of hydroquinone with 4,4'-difluorobenzophenone, using a mixture of sodium and potassium carbonates as the base. Early work on PEEK had resulted in low molecular weight polymer, owing to the difficulty of keeping the crystallisable polymer in solution.[34] It was not until Rose and Staniland at ICI investigated the use of the solvent diphenyl sulfone (which has a boiling point at temperatures close to the melting point of the polymer) that high molecular weight PEEK was obtained. The discovery of *in situ* formation of the phenolate salt using alkali metal carbonates and its mixtures[35] eliminated the need for the separate synthesis of unstable phenolate salts as the reactive monomer (Scheme 1.4).
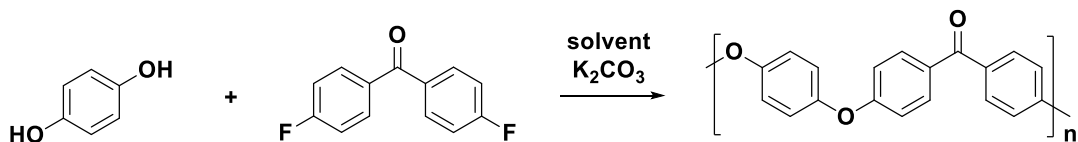
Scheme 1.4. General nucleophilic synthetic scheme for PEEK.

The core elements of the chemistry and industrial synthesis have remained largely unchanged ever since. The nucleophilic approach is still the most widely used route for the large scale production of PEEK and other related PAEKs. PAEKs are a true niche product, more expensive than other high-end polymers such as PPS or polyphthalamide, and they are sold in volumes much smaller than "commodity" polymers such as polyethylene or nylon. However, the superior properties of PAEKs have led to its success in many demanding applications. Recent years have seen a continued growth of the demand for and interest in PAEKs, with several newcomers in the polymer industry introducing new applications for PAEKs.[36]

1.3 Properties of PAEKs

The morphology of a PAEK may be described in terms of three general phases: amorphous, semi-crystalline and interphase. Amorphous regions do not possess long-range order of the polymer chains. The semi-crystalline morphology can be described as crystalline regions embedded within the amorphous regions, that is, short-range ordered regions within the random (amorphous) arrangement of polymer chains. There is now also a general recognition that, because the dimensions of polymer crystals are so small (often only a few hundred Å in diameter) there can be a substantial amount of material in the "interphase" region where polymer chains pass from the amorphous phase into the crystallite.

1.3.1 Glass transition temperature

The glass transition temperature (T_g) is often simply defined as the temperature at which an amorphous material changes from a relatively hard and rigid state into a softer, rubber-like state, as the temperature is increased. The T_g is the temperature at which the interactions that hold distinct components of an amorphous solid together yield to allow thermally

induced motions.[37] A T_g can therefore be only observed in an amorphous or semi-crystalline material, where there can be freedom of motion within the polymer chain segments.

The large-scale molecular motions above the T_g are dependent on the geometric arrangement of, and interactions within and between the chain segments. The mobility of the polymer chain segments within the amorphous phase greatly influences T_g. Resistance to cooperative motion and therefore the value of the T_g increase if the polymer chains possess strong intermolecular forces and high intramolecular rigidity (chain stiffness). The presence of attractive intermolecular forces or cross-linking groups restricts chain motion and consequently increases the T_g of the polymer. In terms of the present research project, π-electron-rich aromatic residues are introduced into different PAEKs which are then blended with a second polymer having a higher T_g and containing π-electron-poor subunits. An increase in the T_g of the PAEK would provide evidence for compatibilisation via complementary π-stacking between the PAEK and the second polymeric component.

The Flory-Fox equation (Equation 1.2) is an empirical formula that describes the T_g as a function of the number-average molecular weight of the polymer (M_n). $T_{g\infty}$ is the maximum glass transition temperature that can be achieved at a theoretical infinite molecular weight and K is an empirical parameter that is related to the free volume present in the polymer sample.

Equation 1.2. Flory-Fox equation

$$T_g = T_{g\infty} - \left[\frac{K}{M_n}\right]$$

Equation 1.2 indicates that the T_g increases with respect to M_n, as there is less free volume present within the polymer for molecular motion to occur. It is the chain-end unit of the polymer that exhibits greater free volume than units within the chain backbone. This is because the covalent bonds that make up the polymer are shorter than the intermolecular distances between polymers found at the end of the chain. A polymer sample with long chain lengths (high molecular weight) will have fewer chain ends per total units and less free volume than a polymer sample consisting of short chains. At low M_n, the molecular motion of polymer chains is dominated by that of chain-end groups and T_g is therefore relatively low.

The free volume model was proposed by Turnbull and Cohen[38] in order to explain the behaviour of polymers at the T_g. They defined the free volume of a polymer as the difference between the specific volume and the occupied volume. Fujita[39] later gave new evidence to corroborate the prevailing notion that the mobility of polymer chains at a given temperature is primarily controlled by the free volume. As shown in Figure 1.2, the occupied volume of a polymer remains relatively constant through the T_g, but the free volume (through which the polymer chains are able to move) increases. The sharp increase in both specific and free volume is derived from conformational motions within polymer chains, which then allows molecular motions above the T_g.
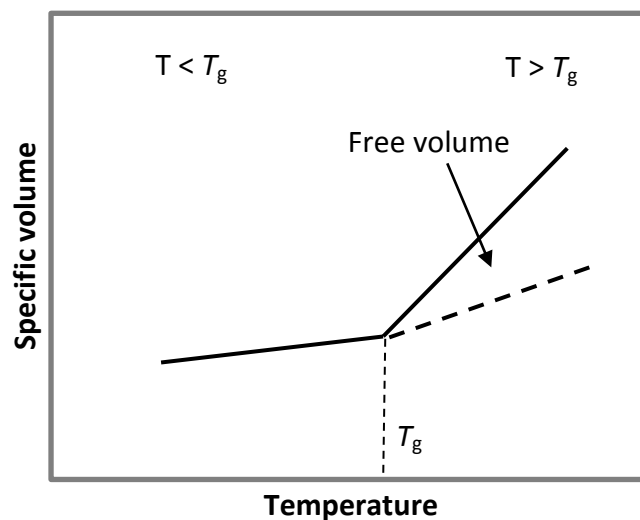
Figure 1.2. Temperature dependence of the specific volume within an amorphous or semi-crystalline polymer.[37]

Although the changes in T_g may be at least partially explained by the free volume model, the T_g of a material is more commonly identified with a change in specific heat capacity. The change in specific heat capacity at the T_g is not abrupt or discontinuous but is instead characterised by an progressive step change over a range of temperatures.[40] As illustrated in Figure 1.3, above the T_g, more energy is required to raise the temperature of the polymer than at the T_g. Despite the considerable changes in the physical properties of a material through its T_g, it is not itself a true phase transition of any kind. The T_g is rather an experimental phenomenon extending over a temperature range. Strictly speaking, the glass transition is a *region* and not a single temperature.[41] It is subject to the influence of different analytical techniques and heating/cooling rates[42].

$T < T_g$ $T > T_g$

Specific heat capacity

T_g
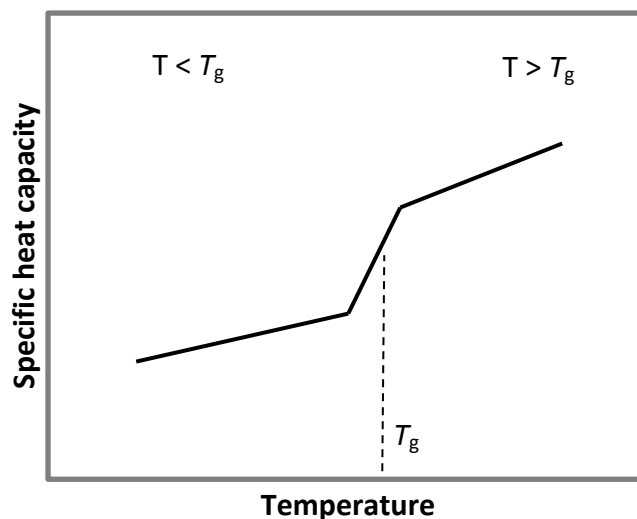
Temperature

Figure 1.3. Temperature dependence of the specific heat capacity of an amorphous or semi-crystalline polymer.[37]

1.3.2 Crystallinity

Polymers chains form irregular, entangled coils in the melt, and amorphous polymers retain such a disordered structure upon cooling below the T_g and thus yield amorphous solids. In semi-crystalline polymers, the chains rearrange upon cooling and form partly ordered regions. Although it would be energetically favourable for the polymer chains to align parallel, such alignment is hindered by the entanglement. Therefore, within the ordered regions, the polymer chains are both aligned and folded. The interphase region, comprising chain-folds and partly-ordered chains is therefore neither fully crystalline nor fully amorphous. The polymer chains fold together and form ordered, crystalline regions called lamellae, which in turn make up larger spherical structures called spherulites.[43] As illustrated in Figure 1.4, the lamellar crystallites consist of parallel chains that are connected by concertina-like folds. These lamellae then aggregate, via amorphous regions, to form the spherulite structures.[44]
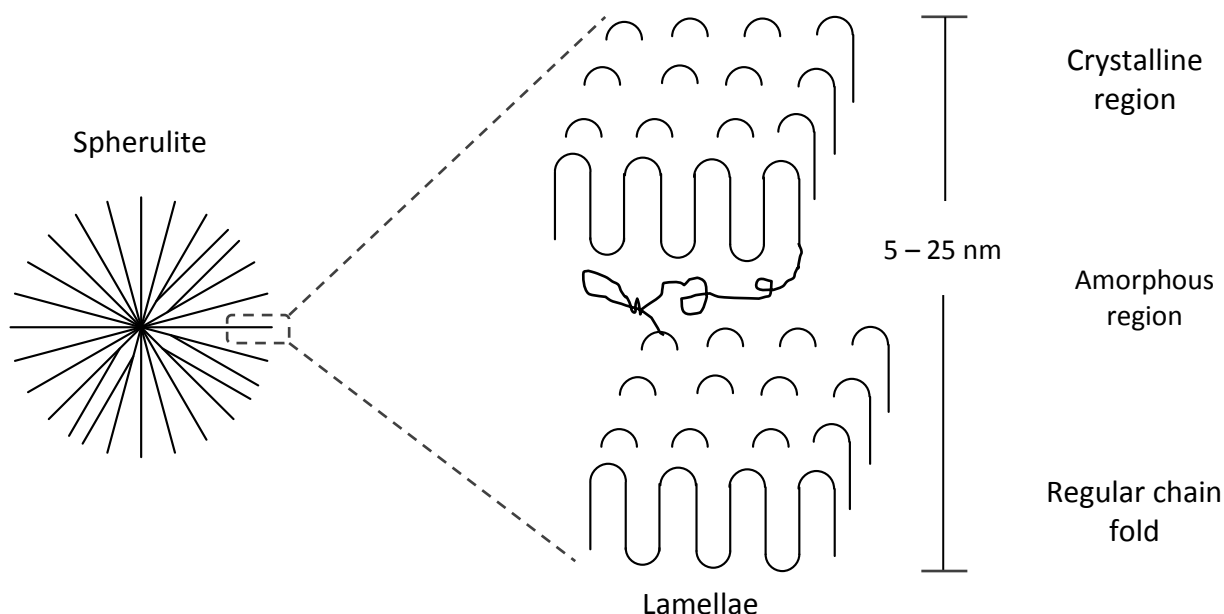
Figure 1.4. Schematic diagram of spherulite formation in a semi-crystalline polymer showing it is composed of ordered regions of chain-folded polymer (lamellae).[45,46]

Crystallisation in a polymer is associated with the partial alignment of its molecular chains. A degree of crystallinity (χ_c) is defined as the weight-percent ratio of crystalline to amorphous regions. A χ_c of 10-80% may be attained for semi-crystalline polymers, with a value closer to 40-70% for semi-crystalline PAEKs.[47] A polymer's mechanical properties such as yield stress and elastic modulus are strongly correlated with its χ_c. Most methods of evaluating the χ_c assume a mixture of perfectly crystalline and completely disordered areas. The value of χ_c in a polymer is most commonly and accurately determined by DSC.[47] Other methods include density gradients, powder XRD and IR spectroscopy.[48] Equation 1.3 allows the calculation of χ_c, where ΔH_f is the enthalpy of fusion, ΔH_{cc} is the enthalpy of cold crystallisation and $\Delta H_{f°}$ is the enthalpy of fusion of a fully crystalline material.

Equation 1.3.

$$\chi_c = \frac{\left(\Delta H_f - \Delta H_{cc}\right)}{\Delta H_{f°}}$$

The crystalline nature of PAEKs originates, in part, from the geometric equivalence of the diphenyl ether and diphenyl ketone groups in the unit cell, both having bond angles of approximately 120° and torsion angles of *ca.* 30° between the plane of each aromatic ring

and the plane of its associated linking unit [C-O-C or C-C(=O)-C].[49] This suggests that the two monomer residues should be crystallographically interchangeable.[50] Consequently, most PAEKs have a high packing density in the crystalline phase. This has a direct influence on the physical characteristics of the polymers.[51] The crystallinity of PAEKs is important in the context of the current project as, to overcome the difficulties of achieving good carbon fibre wetting, the current approach is to reduce the viscosity of PEEK by dissolving it in diphenyl sulfone at or near the polymer melting point (340 °C). This is successful at the pre-preg stage, but difficulties remain in consolidating a composite with a high melt-viscosity matrix. As a consequence, the molecular weight of the matrix polymer currently used is only just high enough to achieve a reasonable level of toughness. If it were any higher, the melt viscosity would make successful processing of the composite almost impossible.

1.4 Polymer blends of PAEKs with poly(ether imide)s

High performance polymers such as PAEKs are often blended with other polymers which have different properties in order to obtain new materials with intermediate properties that are useful for certain applications.[52] It is the balance of the properties of the individual polymers that lead to the final properties of the blended material.

One of the most widely studied blends containing PEEK is that with poly(ether imide) (PEI), most probably because these two polymers form a miscible blend across the whole composition range. PEI is an amorphous thermoplastic which can be described as a hybrid between poly(aryl ether)s and polyimides. The imide imparts high temperature performance and the inclusion of ether groups allows melt processing. PEI was developed and launched by General Electric under the trade name *Ultem* (Figure 1.5). It is used extensively in medical and chemical instrumentation because of its heat, solvent and flame resistance. Like other polyimides, it is typically coloured because of intermolecular charge transfer absorptions and intramolecular chain conjugation.
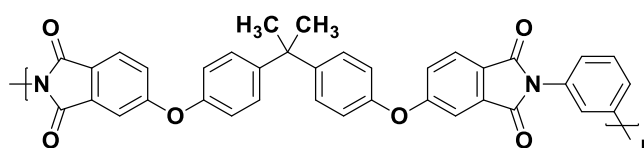
Figure 1.5. Structure of *Ultem* (PEI).

Blends of PAEKs and PEI (especially PEEK and PEKK) have been studied since the late 1980s,[53] presumably as the combination of the properties of the two polymers could address innumerable engineering requirements. The semi-crystalline nature of PAEKs would offer excellent mechanical properties as well as chemical resistance. In contrast, PEI is an amorphous polymer with a high T_g of 215 °C albeit with a lower chemical resistance compared with PEEK but would provide superior thermal resistance and facile melt processing.

1.4.1 T_g of polymeric blends

Although the two polymers differ substantially in chemical structure and crystallisability, they are completely miscible in the amorphous phase.[54] It was found by Crevecoeur and Groeninckx[55] that blends of PEEK with PEI exhibit a single T_g that obeys the Fox equation for miscible systems. The Fox equation estimates that for a well behaving miscible system, the T_g of the blend is the weighted average of its individual components.[56] A study of the thermal properties of miscible blends between commercial samples of PEKK and PEI by Derail and co-workers[54] concluded that positive T_g deviations occur when the crystallinity of the polymer blend was better controlled.

1.4.2 Crystallisation and morphology

It was reported by the same team (Crevecoeur and Groeninckx) that the rate of crystallisation of PEEK is substantially lowered by the addition of PEI to the blend. Moreover, it was shown that upon crystallisation of PEEK in the blends, phase separation occurs, and for blends containing up to 50 wt% PEEK, the segregation is nearly complete in that the amorphous phase consists of almost pure PEI. The team of Hsiao and Sauer[52] further investigated the crystallisation and morphology of PAEKs (specifically PEEK and PEKK) and PEI blends. They proposed three types of non-crystalline component segregation morphology in semi-crystalline/amorphous blend: interlamellar, interspherulitic and interfibrillar (Figure 1.7). Their observations were later confirmed by SAXS which showed that, in high-PEI-content blends, PEI is excluded from the interlamellar regions while in PEEK-rich blends, the opposite was found.[57]
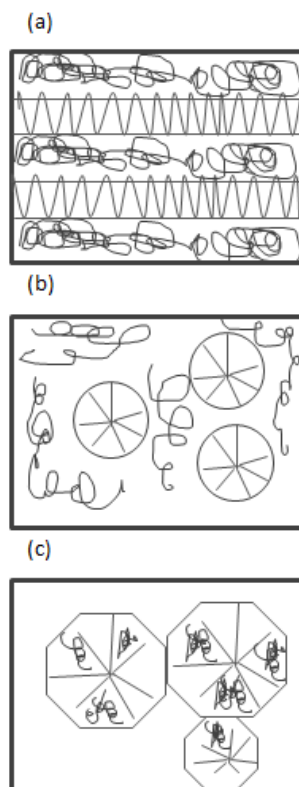
Figure 1.6. Three types of non-crystalline component segregation morphology in semi-crystalline/ amorphous blend (a) interlamellar, (b) intersperulitic, (c) interfibrillar.[52]

1.4.3 Blends with other polyimides

A number of publications in the patent literature[58,59] have referred to blends of PEEK with polyimides of varying chemical structure, all of which are different from *Ultem*. Additionally, a semi-crystalline thermoplastic polyimide launched as *Aurum* (Figure 1.8) was melt blended with various PAEKs. *Aurum* was found to be completely immiscible with PEEK. However, the polyimide showed varying degrees of miscibility with other PAEKs such as PEK, PEKEKK and PEKK. Cser and Goodwin[60] rationalised these observations in terms of chain flexibility and interactions between the chain components.
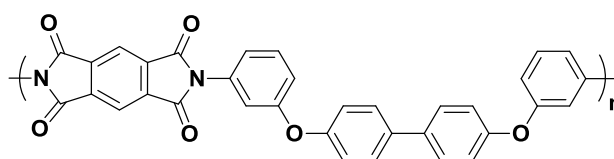
Figure 1.7. Structure of a semi-crystalline thermoplastic polyimide (*Aurum*) used in PAEK blends.

Karcha and Porter[61] found that the blend of PEEK with a poly(amide imide) is completely immiscible. Interestingly, the same poly(amide imide) when blended with sulfonated-PEEK, produced a miscible system with substantial increase of the T_g of sulfonated-PEEK. The blends were analysed by UV-Vis and FT-IR spectroscopy, and an explanation for the change in phase behaviour was proposed to involve the formation of electron donor-accepter complexes between the sulfonated-PEEK and the phenylene units of the poly(amide imide).[62] Weiss et al.[63] investigated a similar blend of sulfonated-PEKK with PEI for use in proton-exchange membranes, and also found that the sulfonated-PEKK produced a miscible blend with PEI compared with an unmodified PEKK. Weiss proposed that the miscibility of the polymers is influenced by the rigidity of the PEKK chain, and by intermolecular associations (hydrogen bonding interactions or electron donor-acceptor complexes), in accordance to the earlier findings of Karcha and Porter.

1.5 Requirements of a potential PAEK/polyimide blend

The literature discussed here has provided an overview of the work to date on PAEK/PEI blends. Novel materials with intermediate properties between PAEKs and polyimides are doubtless of industrial significance. There has also been interest in PAEK/polyimide block copolymers as an approach to materials that combine the complementary properties of both polymers.[64] A block copolymer comprises long sequences of one polymer, followed by long sequences of another polymer. The block copolymers pertinent to PAEKs/polyimide blends were synthesised by a condensation reaction of an amino-terminated PAEK oligomer with an acid-anhydride-terminated polyimide oligomer. This type of polymer remains beyond the scope of the present research project and will not be discussed further.

A blend of PAEKs with polyimides would ideally share the superior properties of each polymeric component. The primary requirement of a potential blend is for the two components to be miscible. It was shown that amorphous PEI had a tendency to separate from the semi-crystalline phase of PEEK.[55] It was later found that a donor-acceptor interaction promotes the miscibility between the two components.[62] The present research project introduced electron-donating moieties to PAEKs in order to produce a π-electron donating-accepting interaction between the two components. The polyimides described in this current work are capable of chain-folding to give a binding site for the electron-donating

residue of the PAEK. It was anticipated that electron donor-acceptor complexation may help avoid separation of the two components in the amorphous phase of a semi-crystalline blend.

A fully-miscible polymer blend must display a single weight-averaged T_g as per the Fox equation.[41] The T_g of the PAEK is expected to increase with the addition of a high-T_g polyimide in the blend and is expected to follow simple additive behaviour. It is therefore a requirement of this research project that a potential polymer blend must have increased T_g. With the incorporation of electron-donating residues to PAEKs, an increase in its T_g provides a qualitative test for interaction between the PAEKs and the polyimides.

The PAEK/polyimide blends described in the present chapter thus far are produced by melt blending of commercially-available polymers. The blend is then extruded before being moulded into the required objects. The majority of the research in this area has thus been confined to commercially available PAEKs and polyimides. In the present work however, novel π-electron donating end-groups are developed that can be incorporated into any PAEK, which may in turn allow blending with other polymers.

1.6 Supramolecular polymer blends

Self-assembled polymers are supramolecular motifs that result from the spontaneous association of molecules through non-covalent interactions such as hydrogen bonding, π-π stacking, or electrostatic forces. Non-covalent bonds are energetically weaker than covalent bonds but are crucial in determining the physical and thermodynamic properties of materials.[65] These interactions influence biological systems such as the assembly of DNA chains into double helices,[66] and are more generally important in template-directed synthesis,[67] materials science, and molecular recognition.

Although individual non-covalent interactions are often too weak to hold together monomeric units, supramolecular aggregates can be obtained when many such interactions cooperate to form a network. Given the previously discussed importance of electron donor-acceptor interactions[62,63] for a complementary polymer blend, non-covalent supramolecular self-assembly appeared to be a worthwhile approach to the design of high performance polymeric blends.

1.6.1 Aromatic π-π interactions

π-π Stacking interactions are attractive, non-covalent interactions between π-conjugated systems. The intermolecular interaction between benzene dimers has been extensively studied as an archetype for the π-π interaction.[68] It is widely accepted that the benzene dimer has three representative configurations as illustrated in Figure 1.8.
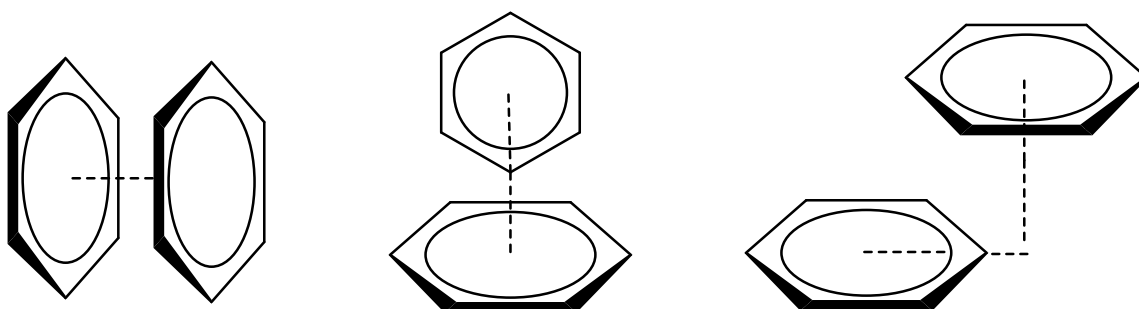
Figure 1.8. Sandwich, T-shape and parallel displaced (left to right) configurations of the benzene dimer.

Despite extensive theoretical[69,70] and experimental[71,72] investigations, there is no fully-accepted and unified description of the source of attraction in the benzene dimer or the origin of the directionality of the interaction.[73] However, Sanders and Hunter[74] formulated a model for the charge distribution in a π-system. Their study showed that π-π stacking interactions occur when the attractive interactions between π-electrons and the σ-ring outweigh unfavourable contributions such as π-electron repulsion. Their model predicts the geometry of the idealised aggregate as a function of the dimer orientation. An attractive interaction occurs from a perpendicular orientation (CH···π) with no offset (Figure 1.8, T-shape), as well as a parallel orientation (π-π) with an offset distance of 3 to 6 Å (Figure 1.8, parallel displaced). However, a weakness of this model is that it predicts a strong, attractive interaction between two parallel, electron-poor π-systems, for which there is little experimental evidence. The vast majority of strong π-π stacking interactions are instead found between complementary (i.e. π-electron poor / π-electron rich) aromatic molecules.

1.6.2 π-π Stacking interactions in supramolecular systems

Colquhoun and colleagues have studied π-π stacking interactions between electron-rich molecular tweezers that would bind strongly to complementary, electron-poor aromatic polyimides. The two components bind through intercalation of the pyrenyl tweezer-arms

into chain-folds of the polymer, and NH---O=C hydrogen bonding between tweezers and polymer (Figure 1.9).[75] Specific planar aromatic structures can be described as π-electron rich or π-electron poor, depending on the substituents. When these compounds are blended together, they interact with one another by means of charge transfer and the aromatic groups as a result stack alternately. Computational modelling suggested that intermolecular distance in a π-π stacked complex is *ca.* 3.5 Å,[76] a value confirmed by X-ray crystallography (Figure 1.9). This type of supramolecular interaction has been shown to aid self-assembly of a supramolecular polymer blend.
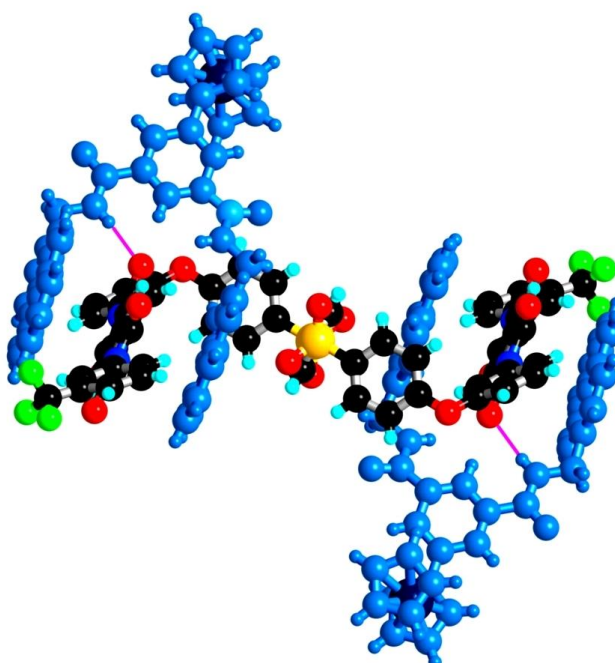
Figure 1.9. Single crystal X-ray structure of a π-π stacked complex between two pyrene-armed tweezer-molecules and a chain-folded bis-pyromellitimide oligomer. Hydrogen bonds (NH---O=C) are shown in magenta.[77]

Colquhoun et al. later reported[77] the synthesis of a homogenous (compatible) polymer blend between a pyrenyl-terminated polyamide (**2**) and a co-polyimide (**1**) containing a chain-folding motif (Figure 1.10). The significance of this type of supramolecular interaction was evaluated by comparison with a control material which contained benzyl rather than pyrenemethyl end-groups on the polyimide. The self-healing characteristics of the two blends were investigated by SEM, from which it was evident that only the designated supramolecular blend [**1+2**] exhibited healing behaviour when heated above 80 °C. UV-Vis

spectroscopy provided confirmation that this interaction occurs via charge-transfer, from the presence of a strong charge transfer band in the visible region at *ca.* 520 nm.
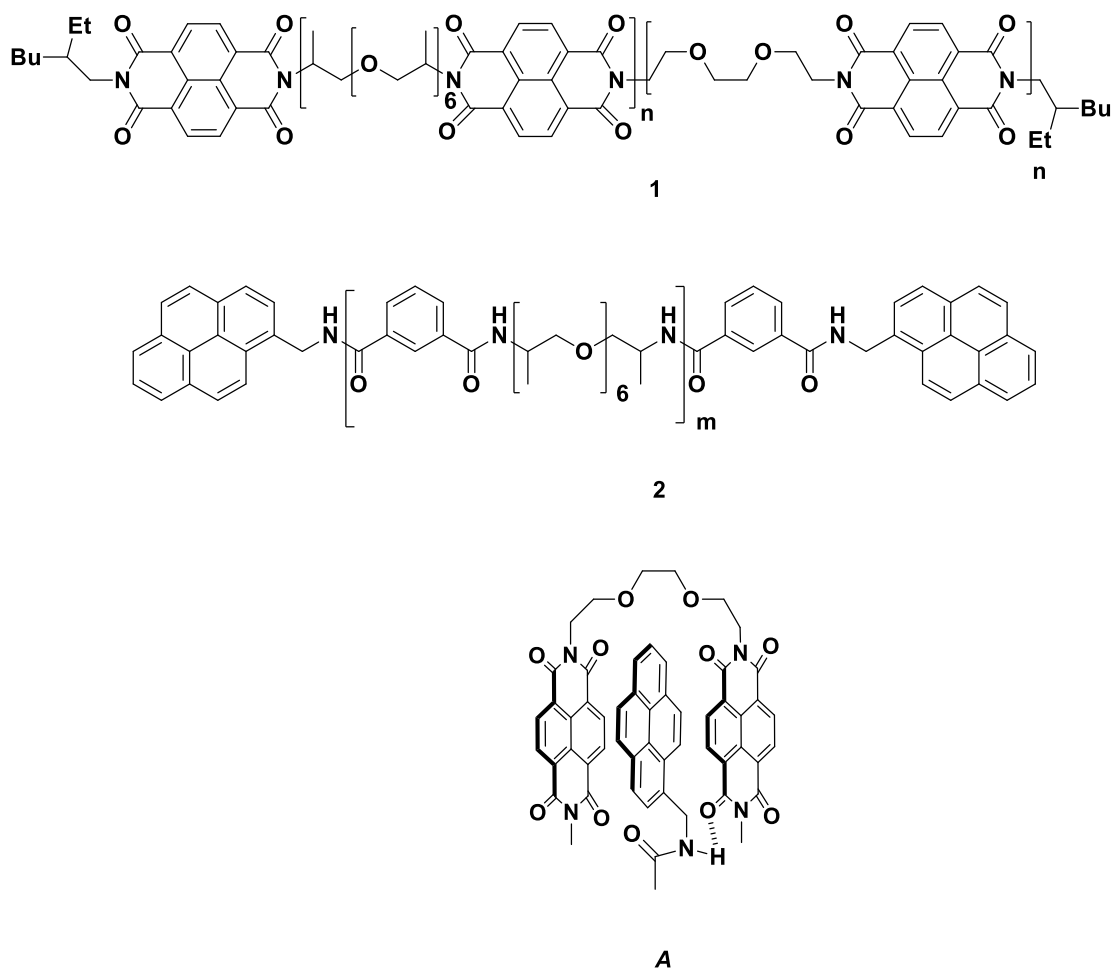
Figure 1.10. Polymer blend [**1+2**] in which the pyrenyl end-groups of the polyamide complex with the polyimide chain-folds as shown in structure ***A***.

Iverson et al.[78] reported the synthesis of a self-complexing polymer containing both electron-rich and electron-poor residues. Supramolecular networks involving electron-rich 1,5-dialkoxynaphthalene and electron-poor 1,4,5,8-naphthalenetetracarboxylic diimide linked by a flexible chain backbone are able to fold in such a way that consecutive aromatic units are stacked in a face-to-face conformation as illustrated in Figure 1.11. They also reported a charge-transfer interaction that was confirmed by UV-Vis and NMR spectroscopies. This work highlighted the most favoured, complementary π-π stacked conformation in such a supramolecular system.
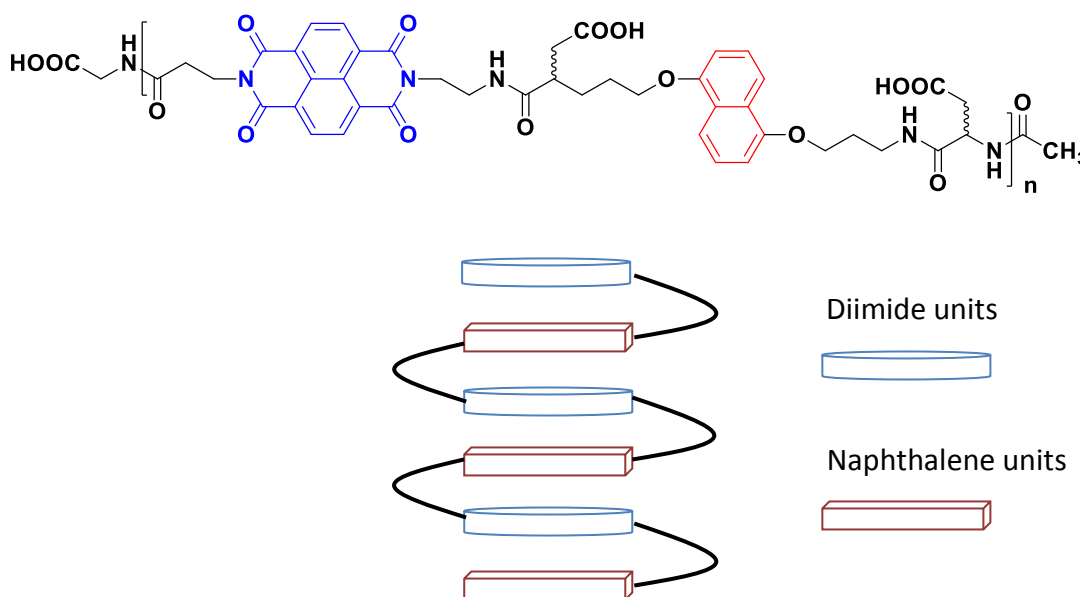
Figure 1.11. Structure of the Iverson self-complexing polymer and a schematic representation of its chain-folded π-π stacking interactions.

1.7 Aims and objectives of the project

The main aim of this research project is to extend the concept of supramolecular π-π stacking interactions to materials in which high levels of thermal and mechanical performance are to be expected, i.e. blends of PAEKs and polyimides. The broad objectives of the project may be summarised as follows:

- Develop the synthetic chemistry of novel π-electron rich terminal groups for end-functionalisation of PAEKs.
- Explore the potential for interactions between π-electron rich PAEKs and π-electron poor polyimides as a result of complementary π-π stacking interactions between the two components.
- Explore the use of different end-capping compounds and different polyimide systems as a way of enhancing compatibility of the polymer blend.
- Explore blends of low- to medium- molecular weight polymers in terms of thermomechanical properties for potential application as composite matrix materials.
- Explore the possibility of pre-pregging, fabricating and evaluating a new type of carbon fibre composite material based on a PAEK/polyimide blend as the matrix.

1.8 References

[1] R. J. Morgan, *Adv. Polym. Sci.*, 1985, **72**, 1-43.

[2] D. Landman, Advances in the chemistry and application of bismaleimides. In: G. Pritchard (ed.) *Developments in reinforced plastics, Vol. 5*. London: Elsevier, 1980, 39-81.

[3] F. N. Cogswell, *Thermoplastic aromatic polymer composites.* Oxford: Butterworth-Heinemann, 1992.

[4] A. M. Diez-Pascual and M. Naffakh, *Materials*, 2013, **6**, 3171-3193.

[5] A. Wood and D. Pandey, In: *SAMPE Conf. Proceedings*, Long Beach, USA, Vol 53, 2008, 325/1-325/11.

[6] R. L. Mazur, P. C. Oliveira and M. C. Rezende, *J. Reinf. Plast. Compos.*, 2014, **33**, 749-757.

[7] S. A. Baeurle, A. Hotta and A. A. Gusev, *Polymer*, 2006, **47**, 6243-6253.

[8] F. W. Mercer, M. M. Fone, V. N. Reddy and A. A. Goodwin, *Polymer*, 1997, **38**, 1989-1995.

[9] H. M. Colquhoun, P. Hodge, F. P. V. Paolini, P. T. McGrail and P. Cross, *Macromolecules*, 2009, **42**, 1955-1963.

[10] R. J. Young and P. A. Lovell, *Introduction to Polymers*, London: CRC Press, 3rd Edition, 2011.

[11] R. N. Johnson, A. G. Farnham, R. A. Clendinning, W. F. Hale and C. N. Merriam, *J. Polym. Sci., Part A-1*, 1967, **5**, 2375-2398.

[12] J. B. Rose, *Polymer*, 1974, **15**, 456-465.

[13] S. Maiti and B. K. Mandal, *Prog. Polym. Sci.*, 1986, **12**, 111-153.

[14] A. B. Newton and J. B. Rose, *Polymer*, 1972, **13**, 465-474.

[15] J. F. Burnett, *Q. Rev. Chem. Soc.*, 1958, **12**, 1-16.

[16] V. L. Rao, *J. Macromol. Sci-Rev. Macromol. Chem. Phys.*, 1995, **C35**, 661-712.

[17] J. B, Rose and P. A. Staniland, *Eur. Pat.*, 0001879 A1, 1979.

[18] T. E. Attwood, P. C. Dawson, J. L. Freeman, L. R. J. Hoy, J. B. Rose and P. A. Staniland, *Polymer*, 1981, **22**, 1096-1103.

[19] M. Toriida, T. Kuroki, T. Abe, A. Hasegawa, K. Takamatsu, Y. Taniguchi, I. Hara, S. Fujiyoshi, T. Nobori and S. Tamai, *Eur. Pat.*, EP 1464662 A1, 2002.

[20] H. Q. N. Gunaratne, C. R. Langerick, A. V. Puga, K. R. Seddon and K. Whiston, *Green Chem.,* 2013, **15**, 1166-1172.

[21] V. Carlier, J. Devaux, R. Legras, P. T. McGrail, *Macromolecules*, 1992, **25**, 6646-6650.

[22] W. H. Bonner (Du Pont), *US Pat.*, 3065205, 1962.

[23] B. M. Marks (Du Pont), *US Pat.*, 3441538, 1964.

[24] Y. Iwakura, K. Uno, T. Takiguchi, *J. Polym. Sci. Part A-1*, 1968, **6**, 3345-3355.

[25] H. M. Colquhoun and D. F. Lewis, *Polymer*, 1988, **29**, 1902-1908.

[26] M. I. Litter and C. S. Marvel, *J. Polym. Sci., Part A: Polym. Chem. Ed.*, 1985, **23**, 2205-2223.

[27] R. Clendinning, D. Kelsey, J. Botkin, P. Winslow, M. Yousefi, R. Cotter, R. Matzner, G. Kwiatowski, *Macromolecules*, 1993, **26**, 2361-2365.

[28] V. Jansons, H. C. Gors, S. Moore, R. H. Reamey, P. Becker, (Raychem Corp.), *US Pat.*, 4698393, 1987.

[29] D. R. Corbin and E. Kumpinsky (Du Pont), *US* Pat. 4,918,237, 1990.

[30] I. Goodman, J. E. McIntyre, W. Russell, (ICI), *UK Pat.*, GB971227, 1964.

[31] K. J. Dahl (Raychem Corp.), *US Pat.*, 3953400 1976.

[32] J. B. Rose, (ICI), *UK Pat.*, GB1414421 and GB1414422, 1975.

[33] J. B. Rose, P. A. Staniland, (ICI), *US Pat.*, 4320224, 1982.

[34] G. H. Melton, E. N. Peters and R. K. Arisman, Engineering thermoplastics. In: M. Kutz (ed.) *Applied plastics engineering handbook: processing and materials*, New York: Elsevier, 2011, p.17.

[35] M. B. Cinderey, J. B. Rose, (ICI), *US Pat.*, 4176222, 1979.

[36] A. H. Tullo, The high-end plastics boom, *Chemical & engineering news*, February 29, 2016; Vol. 94, Iss. 9, pp.23-24.

[37] J. Bicerano, *Encyclopedia of polymer science and technology*, New York: Wiley, 2013, pp.1-29.

[38] D. Turnbull and M. H. Cohen, *J. Chem. Phys.*, 1961, **34**, 120-124.

[39] H. Fujita, *Polym. J.*, 1991, **23,** 1499-1506.

[40] C. A. Angell, K. L. Ngai, G. B. McKenna, P. F. McMillan and S. W. Martin, *J. Appl. Phys.*, 2000, **88**, 3113-3157.

[41] W. Brostow, R. Chiu, I. M. Kalogeras and A. Vassilikou-Dova, *Mater. Lett.*, 2008, **62**, 3152-3155.

[42] P. G. Debenedetti, F. H. Stillinger, *Nature*, 2001, **410**, 259–267.

[43] M. Raimo, *Prog. Polym. Sci.*, 2007, **32**, 597-622.

[44] Y. Kong and J. N. Hay, *Eur. Polym. J.*, 2003, **39**, 1721-1727.

[45] N. B. McCrum, C. P. Buckley and C. B. Bucknall, *Principles of Polymer Engineering,* Oxford University Press, 1988.

[46] S. M. Jones, *PhD Thesis*, University of Reading, 2015.

[47] G. M. K. Ostberg and J. C. Seferis, *J. Appl. Polym. Sci.*, 1987, **33**, 29-39.

[48] G. W. Ehrenstein and R. P. Theriault, *Polymeric materials: structure, properties, applications*, 2001, Berlin: Hanser Verlag, pp. 67–78.

[49] H. M. Colquhoun, C. A. O'Mahoney and D. J. Williams, *Polymer*, 1993, **34**, 218-221.

[50] P. C. Dawson and D. J. Blundell, *Polymer*, 1980, **21**, 577-578.

[51] Z. Bashir, I. Al Aloush, I. Al Raqibah and M. Ibrahim, *Polym. Eng. Sci.*, 2000, **40**, 2442-2455.

[52] B. S. Hsiao and B. B. Sauer, *J. Polym. Sci: Part B: Polym. Phys.*, 1993, **31**, 901-915.

[53] J. E. Harris and L. M. Robeson, *J. Appl. Polym. Sci.*, 1988, **35**, 1877-1891.

[54] S. Dominguez, C. Derail, F. Léonardi, J. Pascal and B. Brulé, *Eur. Polym. J.*, 2015, **62**, 179-185.

[55] G. Crevecoeur and G. Groeninckx, *Macromolecules*, 1991, **24**, 1190-1195.

[56] T. G. Fox, *Bull. Am. Phys. Soc.*, 1956, **1**, 123.

[57] H. Saito and B. Stühn, *Polymer*, 1994, **35**, 475-479.

[58] T. Tsutsumi, S. Morikawa, T. Nakakura, K. Shimamura, T. Takahashi, N. Koga, M. Ohta, A. Morita and A. Yamaguchi *Eur. Pat.*, EP 0430640 A1, 1990.

[59] T. Tsutsumi, S. Morikawa, T. Nakakura, T. Takahashi, A. Morita and Y. Gotoh *US Pat.*, 5312866, 1994.

[60] F. Cser and A. Goodwin, *J. Therm. Anal. Cal.*, 2001, **65**, 69-86.

[61] R. J. Karcha and R. S. Porter, *J. Polym. Sci: Part B: Polym. Phys.*, 1989, **27**, 2153-2155.

[62] R. J. Karcha and R. S. Porter, *J. Polym. Sci: Part B: Polym. Phys.*, 1993, **31**, 821-830.

[63] S. Swier, M. T. Shaw, R. A. Weiss, *J. Mem. Sci.*, 2006, **270**, 22-31.

[64] C. Gao, S. Zhang, X. Li, S. Zhu, Z. Jiang, *Polymer*, 2014, **55**, 119-125.

[65] J. Clayden, N. Greeves, S. Warren and P. Wothers, *Organc chemistry,* Oxford University Press, 2001.

[66] S. K. Burley, G. A. Petsko, *Science*, 1995, **229**, 23.

[67] M. Asakawa, W. Dehaen, G. L'abbe, S. Menzer, J. Nouwen, F. M. Raymo, J. F. Stoddart and D. J. Williams, *J. Org. Chem.*, 1996, **61**, 9591-9595.

[68] H. J. Neusser, and H. Krause, *Chem. Rev.*, 1994, **94**, 1829-1843.

[69] K. S. Kim, P. Tarakeshwar and J. Y. Lee, *Chem. Rev.*, 2000, **100**, 4145-4186.

[70] P. Linse, *J. Am. Chem. Soc.*, 1992, **114**, 4366-4373.

[71] V. Spirko, O. Engkvist, P. Soldan, H. L. Selzle, E. W. Schlag and P. Hobza, *J. Chem. Phys.*, 1999, **111**, 572-582.

[72] H. Krause, B. Ernstberger and H. Neusser, *J. Chem. Phys. Lett.*, 1991, **184**, 411.

[73] S. Tsuzuki, K. Honda, T. Uchimaru, M. Mikami and K. Tanabe *J. Am. Chem. Soc.*, 2002, **12**, 104-112.

[74] J. K. M. Sanders and C. A. Hunter, *J. Am. Chem. Soc.*, 1990, **112**, 5525-5534.

[75] Z. Zhu, C. J. Cardin, Y. Gan and H. M. Colquhoun, *Nature Chem.*, 2010, **2**, 653-660.

[76] B. W. Greenland, S. Burattini, W. Hayes and H. M. Colquhoun, *Tetrahedron*, 2008, **64**, 8346-8354.

[77] S. Burattini, H. M. Colquhoun, J. D. Fox, D. Friedmann, B. W. Greenland, P. J. F. Harris, W. Hayes, M. E. Mackay and S. J. Rowan, *Chem. Commun.*, 2009, **44**, 6717-6719.

[78] A. J. Zych and B. L. Iverson, *J. Am. Chem. Soc.*, 2000, **122**, 8898-8909.

Chapter 2

Functional end-capping of poly(aryl ether ketone)s

2.1 Abstract

In this chapter, the syntheses of novel benzoylpyrene monomers for the end-functionalisation of PAEKs are detailed. Two different approaches to polycondensation, by nucleophilic and electrophilic routes, using different π-electron rich end-caps, are presented herein. Polymerisations were carried out under a range of different conditions, e.g. reaction temperatures, catalyst loading, and the resulting variations in the molecular weight of the polymers are discussed. This work was followed by preliminary studies of electronically complementary, intermolecular π-π stacking interactions as models for supramolecular polymer blends.

2.2 Introduction

A supramolecular polymer blend of PAEKs and polyimides would ideally display intermediate properties of both components. As discussed in the previous chapter, blends of amorphous poly(ether imide)s tend to form separate phases from the crystalline phase of PAEKs.[1] It was later reported by Karcha and Porter[2] that a donor-acceptor complex promotes the miscibility between a blend of two polymers. Computational modelling[3] has shown that polycyclic aromatic structures stack with intermolecular distance of approximately 3.5 Å. It was also demonstrated experimentally[4] that π-π stacked complexes arise from charge-transfer interactions between electron-rich and electron poor residues in polymers.

The present research project would incorporate electron-donating moieties to PAEKs in order to produce a π-electron donating-accepting interaction with a polyimide. It was envisioned that π-π stacking interactions would aid self-assembly of the PAEK and polyimide to afford a miscible supramolecular structure from relatively low molecular weight polymer chains. This chapter discusses the synthetic routes to produce novel π-electron rich terminal groups for end-functionalisation of PAEKs.

2.3 Results and discussion

2.3.1 Synthesis and characterisation of a functional PAEK

The first stage of this work was to synthesise a PAEK using high temperature polycondensation and simultaneously functionalise it with a commercially available π-electron rich end-cap. Scheme 2.1 shows the mechanism of the formation of the polymer chain from the nucleophilic polycondensation of 1,3-bisfluoro(4-fluorobenzoyl)benzene and 4,4'-dihydroxybenzophenone. The dihalide monomer is present in excess over its co-monomer to ensure production of a fluoro-terminated chain, so that the end-capping reaction gives the pyrenyl-terminated PAEK **2.4**. As can be seen in Scheme 2.1, the mechanism proceeds by deprotonation of the phenol by carbonate ions giving hydrogen carbonate ions $[HCO_3]^-$. The phenoxide ions then attack the bisfluoro- co-monomer to displace fluoride ions and form the ether linkage.
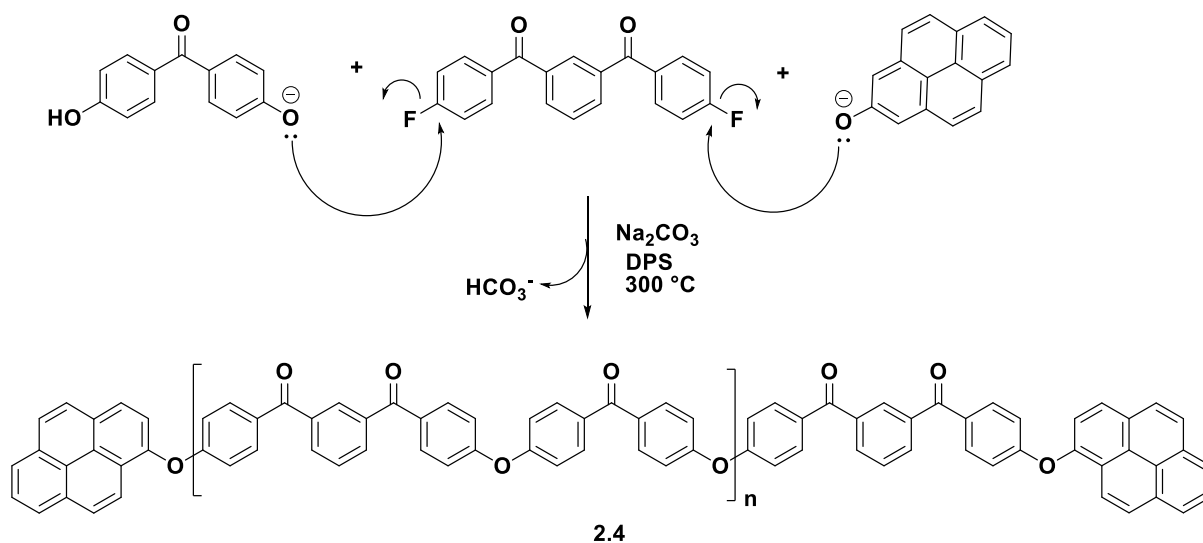
Scheme 2.1. Partial mechanism to show the nucleophilic polycondensation and end-capping to give **2.4**.

The 1-hydroxypyrene end cap was added with the co-monomers at the start of the reaction in order to achieve a one-pot high temperature polycondensation with *in situ* functionalisation. The end-cap was added at 20% molar ratio of the limiting co-monomer. The co-monomers 1,3-bis(4-fluorobenzoyl)benzene and 4,4'-dihydroxybenzophenone were

used in the molar ratio of 11:10, in order to afford a number-average degree of polymerisation (X_n) of approximately 10.

Addition of the end-cap at 20% per mole of the 4,4'-dihydroxybenzophenone allowed the functionalisation of the polymer chain to be confirmed by simple analytical methods such as ^{1}H NMR spectroscopy. Figure 2.1 shows the ^{1}H NMR of **2.4** with the resonances arising from the oxy-pyrene terminal groups highlighted. The ^{1}H NMR spectra of polymers tend to have broader resonances than the spectra of small molecules. Additionally, the similar (aromatic) proton environments of PAEKs and the terminal groups described here meant that there was significant overlap between resonances.[5] Nevertheless, ^{1}H NMR spectroscopy (Figure 2.1) confirms the successful functionalisation of the PAEK. The proton intensities of provide an estimate of the X_n of **2.4**. The triplet at 7.77 ppm which integrates to 9H can be assigned to the proton at the centre of the 3-ring, bis-fluoro co-monomer residue (labelled **b**). The doublet in the highest field which integrates to approximately 4H is end group related, and can be assigned to the protons of the two 3-ring residues at the termini of the polymer chain. Nine 1H in the polymer repeat unit and two 2H at each end sum to eleven 3-ring monomer residue, and therefore an approximate X_n of 10.
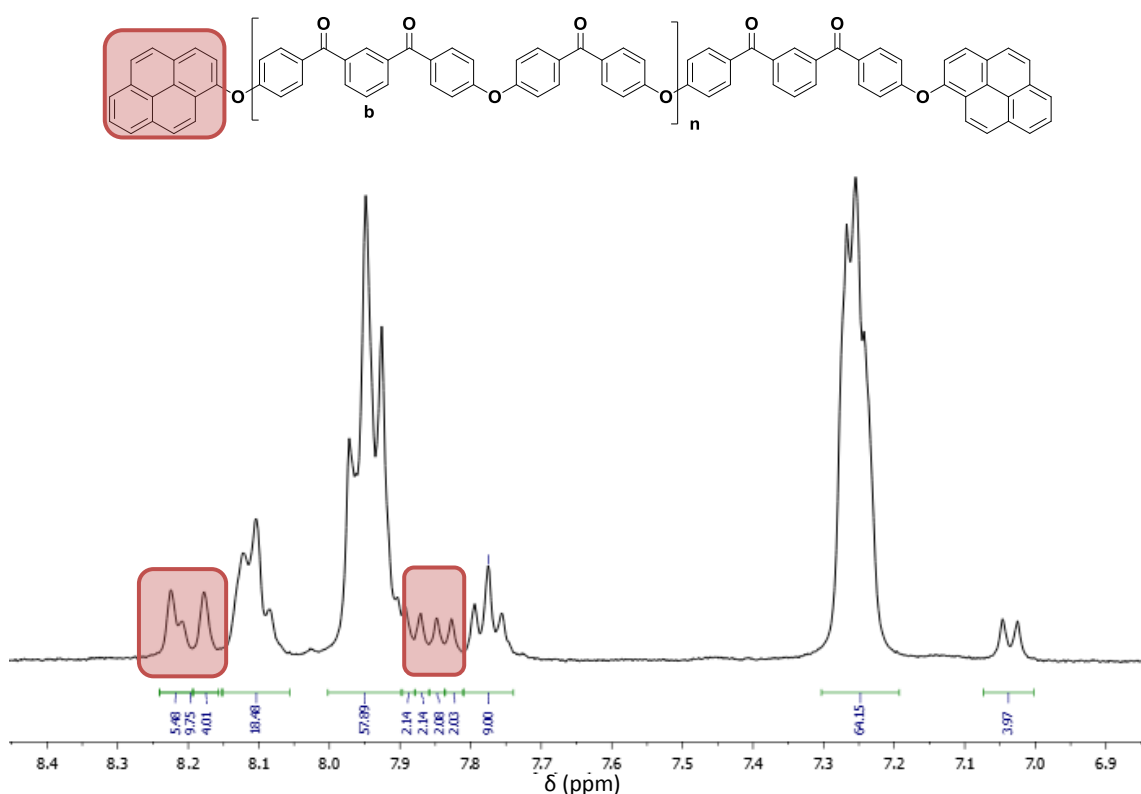

Figure 2.1. ^{1}H NMR spectrum (CDCl$_3$/(CF$_3$)COOH 3:1 v/v) of polymer **2.4**.

The molecular weight of **2.4** can also be analysed qualitatively by determining the solution inherent viscosity (η_{inh}) of the polymer. Polymer **2.4** had an η_{inh} of 0.19 dL g^{-1} in 96% H_2SO_4. This value is much lower than those associated with high molecular weight PAEKs which are typically reported to be around 0.5-1.0 dL g^{-1}.[6] The low value for the η_{inh} of **2.4** is consistent with successful functionalisation in the polycondensation as without the designed monomer imbalance and end-capping, the molecular weight and therefore η_{inh} would be anticipated to be much higher. This is because the degree of polymerisation would be larger in the absence of a growth-limiting terminal group.

Fluorescence spectroscopy is another useful, if qualitative technique to confirm actual end-capping of the polymer. Pyrenyl substituents are often used in fluorescence studies of labelled polymers.[7] The present analysis was conducted using a standard reference solvent of $CHCl_3$/TFA (3:1 v/v). A solution of the unfunctionalised analogue PEKEK*m*K was also prepared as a comparison (Figure 2.2). Irradiation using a spectrophotometer (λ = 310 nm) of a solution of 1-oxypyrene-terminated polymer **2.4** produced a strong fluorescence response originating from the pyrenyl terminal groups on **2.4** (Figure 2.3). In comparison, the control polymer did not fluoresce at all under the same conditions. This strongly supports the successful end-capping of polymer **2.4**. Similarly, polymer **2.4** in its powder form produced a visual fluorescence under a standard laboratory UV source, while the unfunctionalised PAEK did not.

PEKEK*m*K

2.4
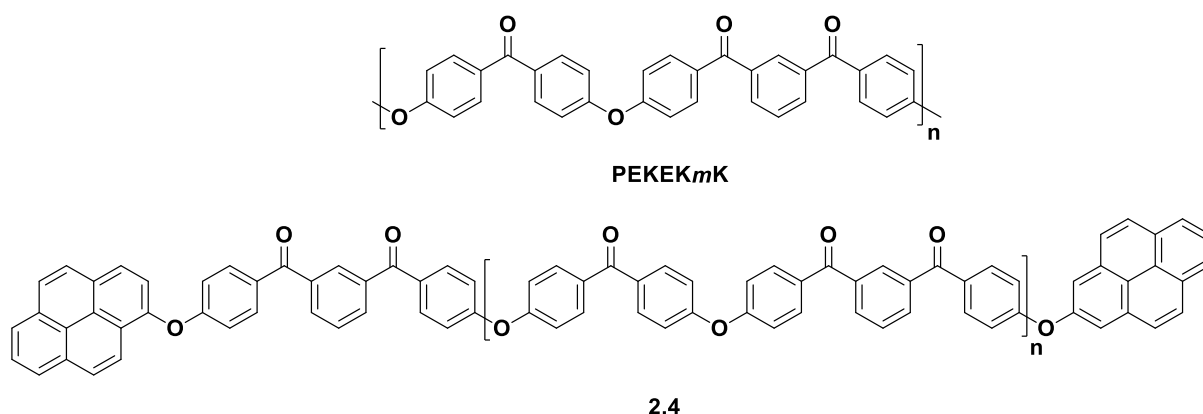
Figure 2.2. Structure of control polymer PEKEK*m*K and **2.4**.

Fluorescence spectra of **2.4** and PEKEK*m*K
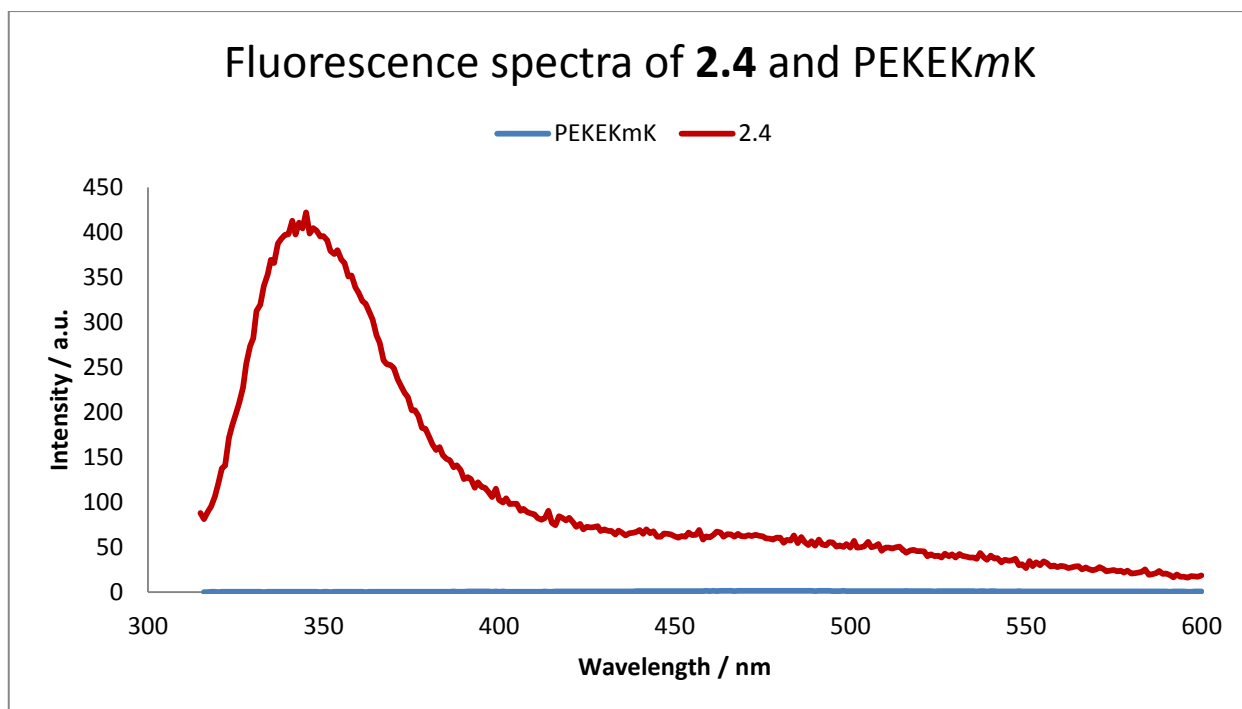
Figure 2.3. Fluorescence spectra of **2.4** and PEKEK*m*K (CHCl$_3$/TFA, 3:1 v/v, 10^{-7} M, λ = 310 nm).

2.3.2 Synthesis of benzoylpyrene end groups

Following the favourable results from the end-capping of a PAEK with commercially available (if extremely expensive) monofunctional pyrene, the next step was to synthesise novel π-electron rich end groups. These were novel hydroxy- and fluoro-benzoyl pyrene derivatives that are complementary to the types of co-monomers commonly used in polycondensation reactions (Figure 2.4).

X = F or OH
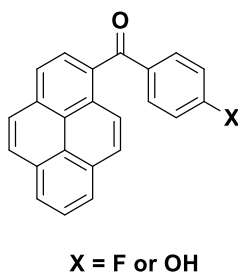
Figure 2.4. Structure of benzoylpyrene end-group

2.3.2.1 Syntheses in trifluoromethanesulfonic acid

Initially, the syntheses of the benzoylpyrene end-caps were carried out using neat trifluoromethanesulfonic acid (triflic acid) as both solvent and catalyst for a Friedel-Crafts acylation reaction with the free carboxylic acid. This approach to aromatic ketone synthesis was first reported by Colquhoun and Lewis, working at Imperial Chemical Industries in 1988.[8] The proposed mechanism of ketone formation in this type of reaction is shown in Scheme 2.2.
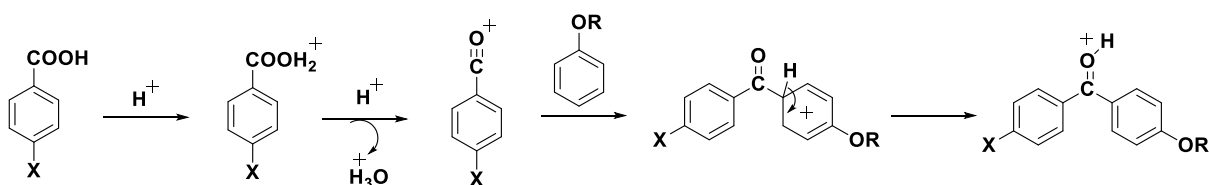
Scheme 2.2. Mechanism proposed by Colquhoun and Lewis for the formation of ketones by Friedel-Crafts acylation in triflic acid.

By adapting the method, the target fluoro- and hydroxy- benzoyl pyrenes were successfully synthesised. The reaction, as outlined in Scheme 2.3, simply required prolonged stirring of the reaction mixture at room temperature under an inert atmosphere. The work-up involved was relatively straightforward with precipitation and washing with water affording the desired pyrenylketone.
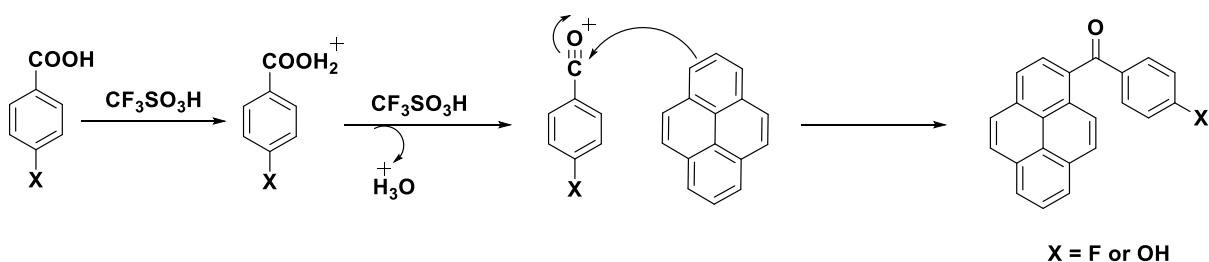
Scheme 2.3. Proposed mechanism of Friedel-Crafts acylation of pyrene by a benzoic acid.

2.3.2.1.1 1-(4-Fluorobenzoyl)-pyrene (**2.1**)

The first attempt to synthesise 1-(4-fluorobenzoyl)-pyrene (**2.1**) involved stirring a solution of pyrene and 4-fluorobenzoic acid in triflic acid for 16 h. Purification of the crude product by recrystallisation did afford **2.1**, but in extremely poor yield (2%). Nonetheless, the

amount obtained after recrystallisation was sufficient for a full characterisation of this novel compound. The ^{1}H NMR spectrum of **2.1** is shown in Figure 2.5. The two resonances corresponding to the 4-fluorobenzoyl ring (highlighted in blue and green) are a doublet of doublets at 7.88 ppm and a triplet at 7.39 ppm. This splitting pattern is a result of coupling to the fluorine atom (nuclear spin s = ½) that is four- or three- bonds distant respectively. The symmetry of pyrene has been broken by substitution at the 1-position, thus giving rise to a more complex multiplet at 8.45-8.13 ppm rather than the simple doublet, singlet and triplet splitting pattern for unsubstituted pyrene (Figure 2.6 shows the ^{1}H NMR spectrum of pyrene).
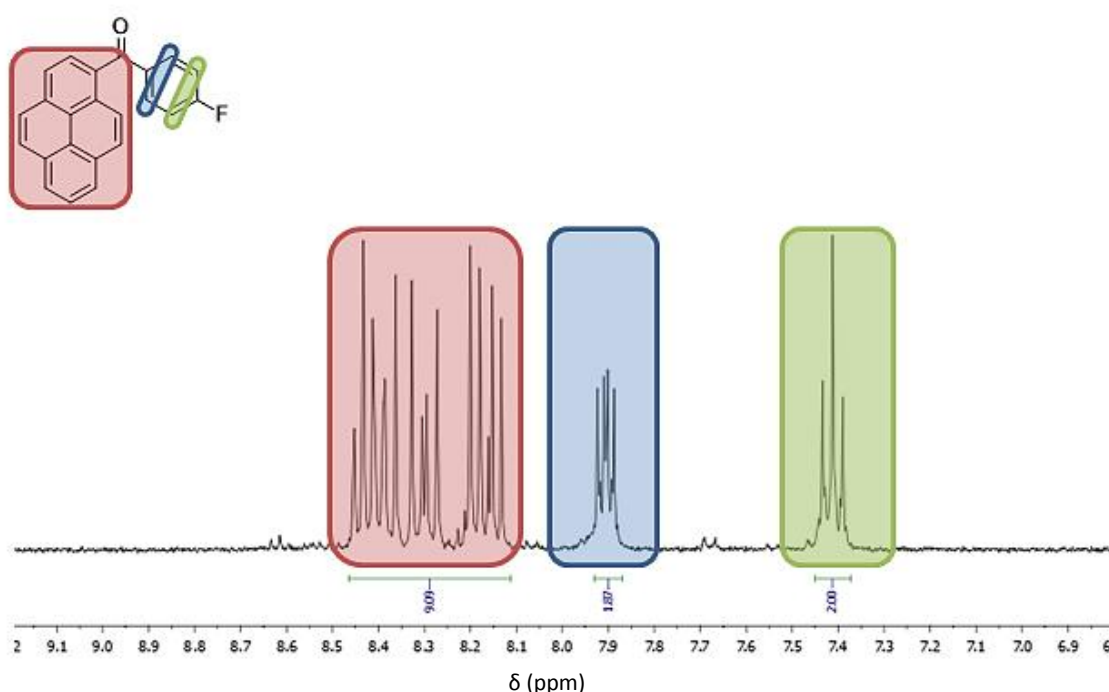
Figure 2.5. ^{1}H NMR spectrum of 4-fluorobenzoyl pyrene (**2.1**).

2.3.2.1.2 1-(4-Hydroxybenzoyl)-pyrene (**2.2**)

Although **2.1** was successfully synthesised, the very low yield led to initial conclusions that recrystallisation was perhaps a poor method of purification in this system. Therefore, a second end-cap monomer, 1-(4-hydroxybenzoyl)-pyrene (**2.2**) was synthesised. In this case, purification was carried out using column chromatography (60:40 hexane/ethyl acetate as eluent). The following results provide some explanation for the low reaction yield.

In the synthesis of **2.2**, the reaction did not go to completion despite an extended (16 h) reaction time. This was confirmed by the large amounts of pyrene starting material recovered from the reaction by column chromatography (R_f = 0.82). Along with the desired mono-substituted product (R_f = 0.54), a disubstituted by-product, bis(4-hydroxybenzoyl) pyrene (R_f = 0.13) was also recovered. The ^{1}H NMR spectra of the isolated pyrene starting material and the di-substituted by-product are shown in Figure 2.6 and Figure 2.7 respectively.

Figure 2.6. ^{1}H NMR spectrum of pyrene recovered by chromatography from the synthesis of **2.2**.

Figure 2.7. Expanded ^{1}H NMR spectrum of bis(4-hydroxy)pyrene by-products recovered by column chromatography from the synthesis of **2.2**.

Work by Harvey and co-workers[9] on the acetylation of pyrene may explain the complex ^{1}H NMR spectrum of the di-substituted by-product shown in Figure 2.7. These researchers found that the di-substituted pyrene is formed as three different regioisomers namely: 1,3-, 1,8- and 1,10-substituted pyrenes. They also showed that these different diacetyl-pyrenes are formed in an approximate 3:1:1 ratio respectively. Based on their findings, the proposed structures of the by-products isolated from the synthesis of 1-(4-hydroxybenzoyl)-pyrene are shown in Figure 2.8. This shows four possible preferred substitution positions in pyrene: 1-, 3-, 8- and 10. As can be observed in Figure 2.7, the ratio of the different bis(4-hydroxybenzoyl)-pyrene by-products cannot be conclusively derived from the ^{1}H NMR alone. Nonetheless, high resolution mass spectrometry confirms that the isolated compound was indeed a mixture of di-substituted hydroxybenzoyl pyrenes (MW = 442.1205, HRMS (ESI) = 443.1275 [M$^+$]).
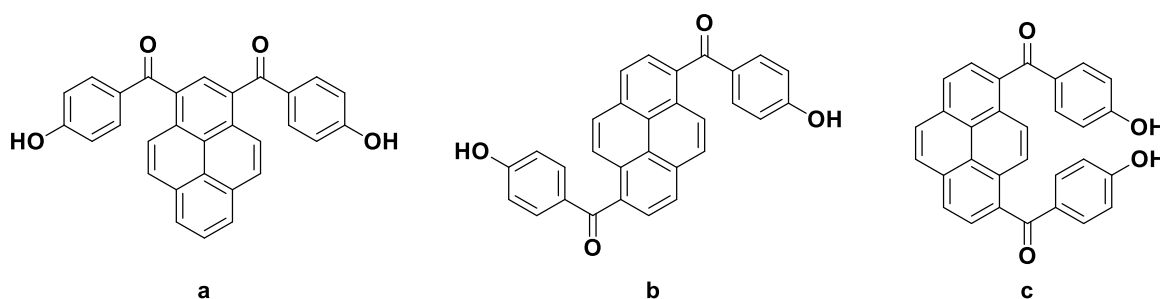
Figure 2.8. Proposed structures of the three regioisomers of the di-substituted pyrene, recovered by column chromatography from the synthesis of **2.2**: **(a)** 1,3-bis(4-hydroxybenzoyl)-pyrene, **(b)** 1,8-bis(4-hydroxybenzoyl)-pyrene and **(c)** 1,10-bis(4-hydroxybenzoyl)-pyrene, on the basis of the work by Harvey et al.[9]

The intended mono-substituted product, 1-(4-hydroxybenzoyl)-pyrene (**2.2**) was, however, successfully isolated in much improved yield (26%) compared to that obtained from the synthesis of its fluoro-counterpart **2.1** (2%). The ^{1}H NMR spectrum (Figure 2.9) confirms the successful synthesis of **2.2** with the corresponding splitting pattern of two doublets each with intensity 2H resulting from the 4-hydroxybenzoyl aromatic protons. As expected, with the formation of the carbonyl bond at the 1-pyrene position, the symmetry of pyrene has been disrupted and no longer shows the simple pattern of pyrene itself (Figure 2.6).

Figure 2.9. ^{1}H NMR spectrum showing the aromatic region of **2.2** synthesised in neat triflic acid and purified by column chromatography.
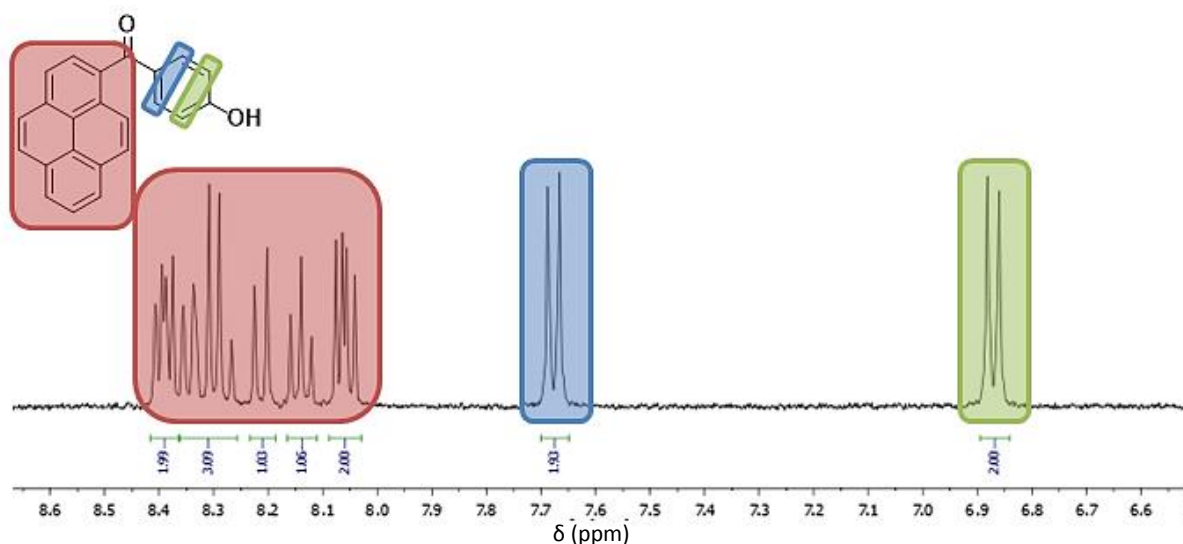
Although the final yield had considerably improved with the use of column chromatography as a purification technique, the above reaction is still an inefficient route to the end-caps. First, a yield of 26% remains poor in the synthesis of large quantities of end-cap for subsequent polymerisation. Second, the results show that the above conditions tend to give di-substituted by-products despite the presence of unreacted pyrene starting material. It thus seemed that increasing the proportion of pyrene would do little to improve the yield. A longer reaction time might well lead to even more di-substituted or even perhaps tri-substituted by products. This led to seeking a different method to synthesise the end-caps.

2.3.2.2 Improved synthetic method using triflic acid as *catalyst*

Flamholc et al.[10] have reported the successful synthesis of 1-pyrenyl ynones via Friedel-Crafts acylation. This approach differed from that described above in that the reaction was carried out with only catalytic amounts of triflic acid and using dichloromethane as solvent. The reaction was said to complete in 2 h instead of 16 h. This procedure was the starting point, in the present work, for a new approach to synthesis of benzoylpyrene end-caps.

The procedure was first adapted (as detailed in Scheme 2.4) in the synthesis of **2.1**, and was immediately successful, with a yield of 88% after purification by column chromatography. Figure 2.10 shows the ^{1}H NMR spectrum of **2.1** synthesised using the adapted method. It

corresponds well with the ^{1}H NMR spectrum of the same compound synthesised in neat triflic acid previously shown in Figure 2.5.
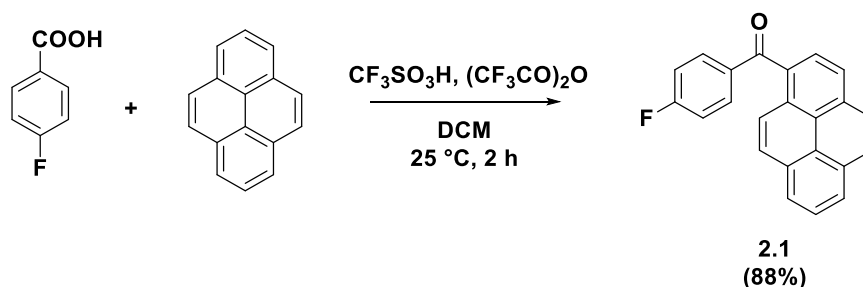
Scheme 2.4. Improved synthesis of **2.1** using catalytic amounts of triflic acid.
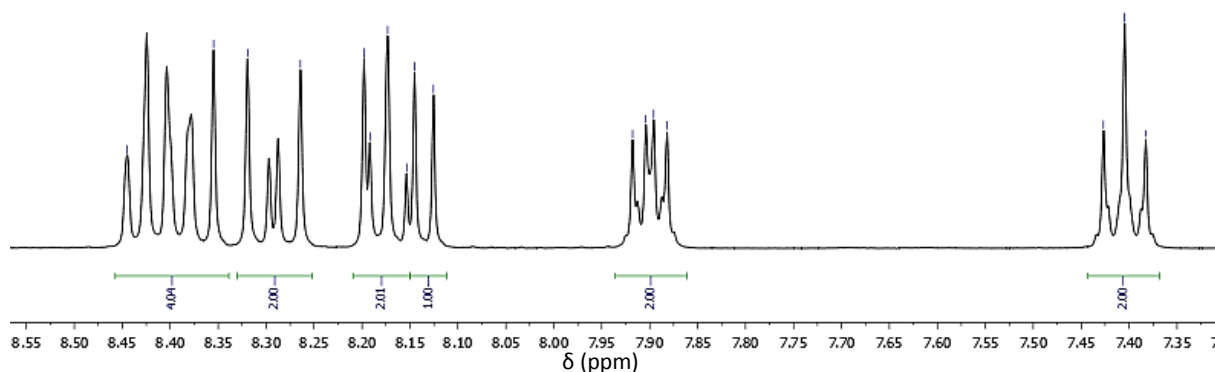
Figure 2.10. ^{1}H NMR spectrum of **2.1** synthesised using catalytic amounts of triflic acid.

This synthetic method was also adapted for 1-(4-hydroxybenzoyl)-pyrene (**2.2**) with similar success. The product formed as a yellow precipitate in the interphase when the reaction was quenched in water, with a yield of 58%. The ^{1}H NMR spectrum (Figure 2.11) suggested a pure product and did not require additional purification. HRMS confirmed that the product was indeed **2.2**, with purity (DSC) estimated at 98%. Attempts to improve the yield involved systematic addition of the catalyst (triflic acid) to up to 4-fold excess, addition of further 4-hydroxybenzoic acid and extending the reaction time, but none of these approaches increased the yield significantly.
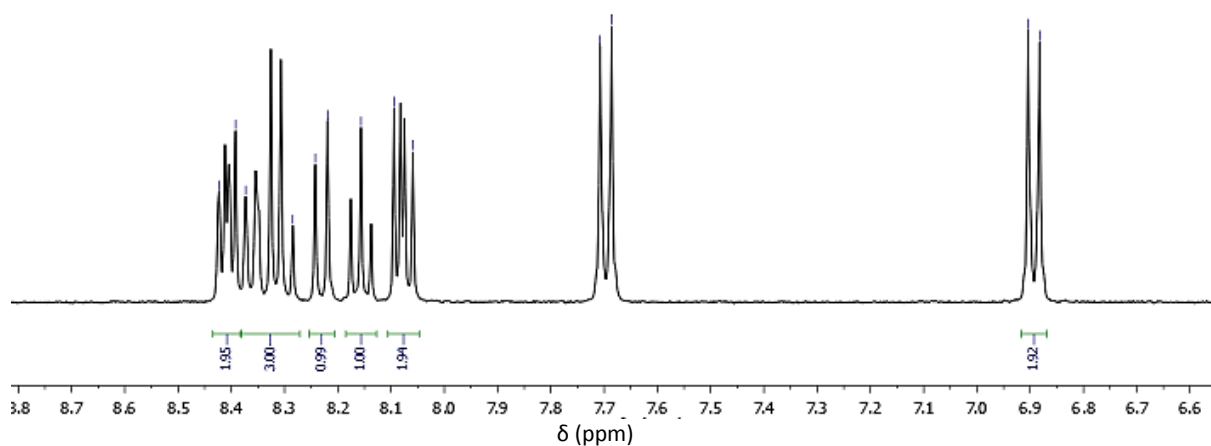
Figure 2.11. ^{1}H NMR spectrum of **2.2**, synthesised using catalytic amountes of triflic acid.

2.3.3 Polymerisation with benzoylpyrene end-caps

Following the synthesis of 4-fluoro- and 4-hydroxybenzoylpyrene as end-capping monomers, the next step was to synthesise end-functionalised PAEKs and poly(ether sulfone)s (PES). The reaction mechanism is similar to the polycondensation shown in Scheme 2.1. However, unlike the previous polymerisation that was carried out in diphenyl sulfone at high temperature (300 °C), the following polymerisations were carried out in refluxing DMAc/toluene, with Dean-Stark azeotropic distillation of water. The end-cap was added with the co-monomers at the start of the reaction in order to again achieve a one-pot polycondensation with *in situ* functionalisation. Initially, the polymerisation was attempted by using end caps at 5% per mole of the limiting co-monomers, but at this ratio it was difficult to obtain conclusive evidence of successful end-capping by ^{1}H NMR spectroscopy. Moreover, fluorescence spectroscopy analysis also proved inconclusive in confirming polymer functionalisation. The end-cap was thus next added at 20 mol% per mole of limiting co-monomer, to afford a X_n of approximately 10.

2.3.3.1 Analysis of benzoyl pyrene end-capped PAEK

The functionalised polymer **2.5** (Figure 2.12) was synthesised by nucleophilic polycondensation of 1,3-bisfluorobenzoylbenzene, 4,4'-hexafluorobisphenol-A and **2.1** in DMAc. 4,4'-Hexafluorobisphenol-A was chosen as the co-monomer to give good solubility for the polymer at modest temperatures, as the polymerisation conditions (200 °C) are mild compared to the polycondensations previously employed (300 °C). Analysis by ^{1}H NMR spectroscopy indicated that the pyrenyl-functionalised polymer had been synthesised.

However, this alone could not conclusively confirm that the polymer was quantitatively terminated by the pyrenyl end cap. Several steps were taken to determine the success of the polymer functionalisation, which will be discussed in the next section.
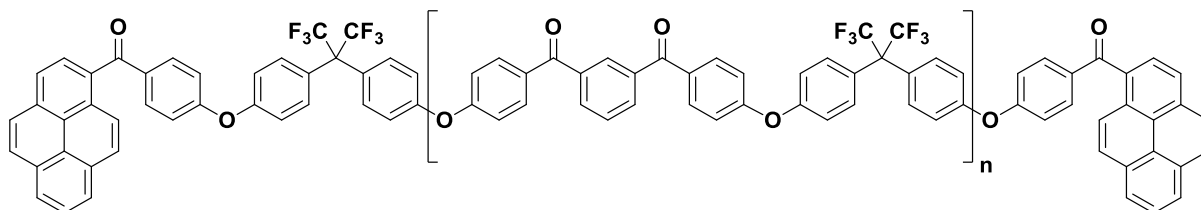
Figure 2.12. Structure of **2.5**.

Considering the ^{1}H NMR spectrum of **2.5** shown in Figure 2.13, the resonances from the protons on the polymer chain repeat unit are easily assigned. The multiplet at 7.11-7.15 ppm and the triplet at 7.21 ppm integrate between them to 88H, which would account for the protons adjacent to the ether linkage, if the degree of polymerisation is taken to be X_n = 10. The doublet at 7.48 ppm correlates well with the proton environments adjacent to the carbonyl groups. The distorted triplet at 7.69 ppm which integrates to 10H suggests that it can be assigned to the proton at the centre of the 3-ring, co-monomer residue (labelled **k**). The proton *para* to this (labelled **i**) which lies between the two carbonyl groups of the difluoro co-monomer may possibly be the apparent singlet at 8.08 ppm, although there is significant overlap with the multiplets on either side of it. This resonance would be close to reported literature values for this type of ^{1}H environment.[5] The multiplets at 8.02-8.06 and 8.10 and 8.34 ppm integrate altogether to approximately 18H, and thus are highly likely to arise from the terminal pyrenyl groups (9H each).
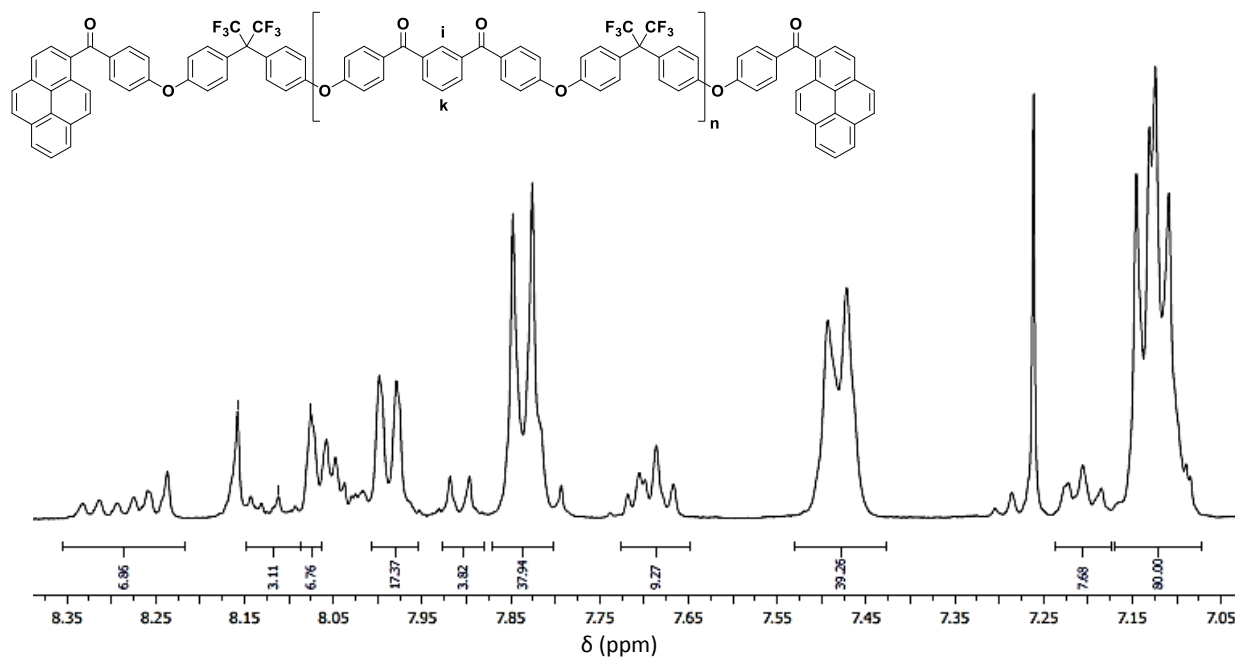
Figure 2.13. Expanded ^{1}H NMR spectrum of **2.5**. The mutiplets at 8.34-8.10 ppm are attributed to the protons of the pyrenyl end-cap.

In order to confirm successful functionalisation of the polymer, an identical but unfunctionalised polymer (**2.6**), capped with the monofunctional 4-hydroxybenzophenone was synthesised (Figure 2.14). Since the only difference between the two polymers is their end-caps, it follows that the NMR spectra of the two polymers should only differ in the regions of the pyrene end-cap. Considering the spectra of the two polymers compared in Figure 2.15, the highlighted area around 8.30 ppm shows that polymer **2.5** has additional resonances that are not observed in the spectrum of the control polymer. This difference between the two spectra indicates that polymer **2.5** has been successfully functionalised, as the two spectra are otherwise almost identical.
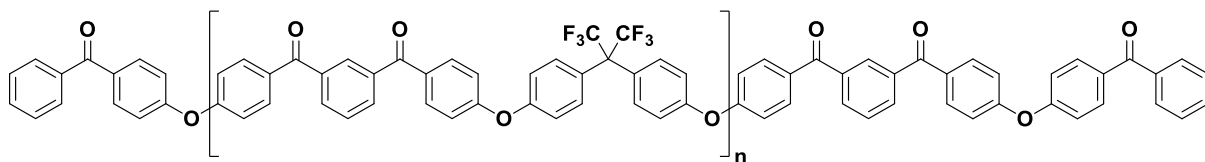
Figure 2.14. Structure of polymer **2.6**, synthesised with 4-hydroxybenzophenone terminal groups.
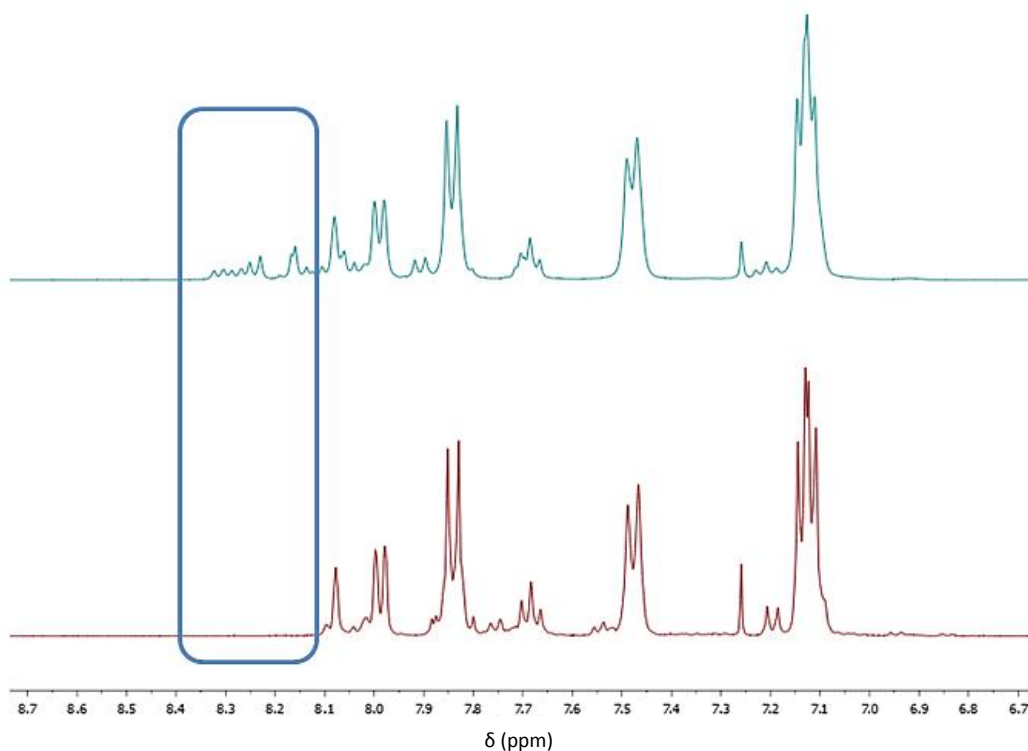
Figure 2.15. ^{1}H NMR spectra of the functionalised polymer **2.5** (blue) and control polymer **2.6** (red). The highlighted area shows the difference in the terminal groups of the two polymers.

Fluorescence spectroscopy was again used to look for further evidence of functionalisation. Figure 2.16 shows the fluorescence spectra of the two polymers. A solution of polymer **2.5** in CHCl$_3$/HFiPA (6:1 v/v) displayed the strong fluorescence emission that is characteristic of pyrenyl residues at around 470 nm when exposed to a UV-light source (λ = 400 nm). It also shows the complete absence of fluorescence in the case of the control polymer **2.6**. Given that the only difference between the two polycondensations was the addition of pyrenyl end-groups, the spectra clearly demonstrate that **2.5** has been successfully functionalised.
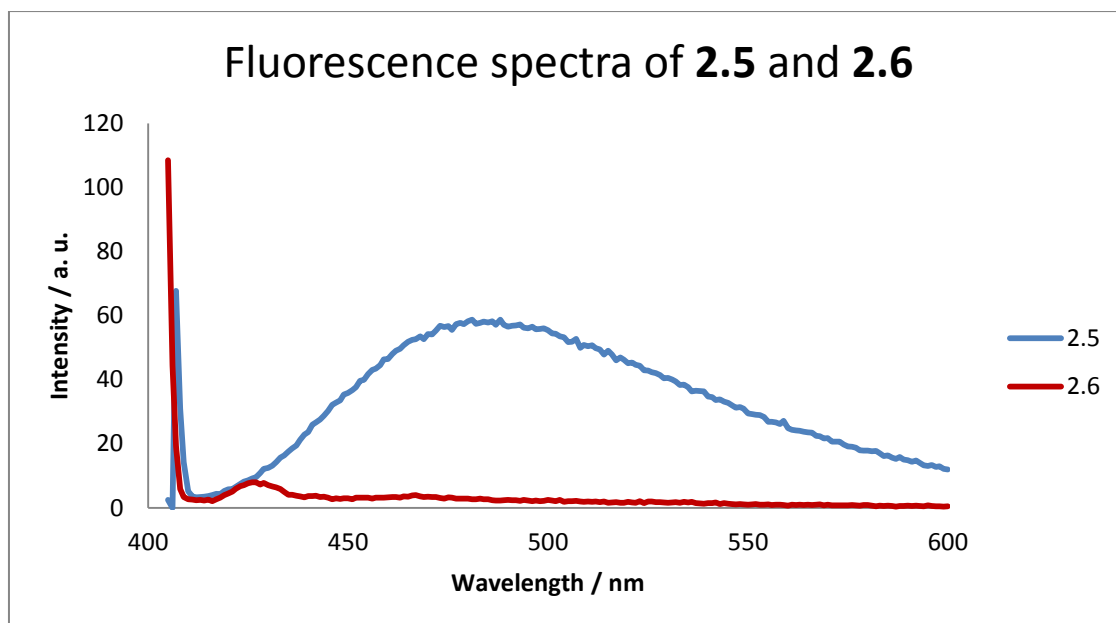
Figure 2.16. Fluoresence spectra (in CHCl$_3$/HFiPA (6:1 v/v), 10^{-7} M solutions) of polymer **2.5** in showing emission at 470 nm compared with the control polymer **2.6**, which did not fluoresce under UV light (λ = 400 nm).

As a model for polymer functionalisation, a small molecule (**2.8**) was synthesised for comparison. As can be seen in Figure 2.17, the small molecule is analogous to a benzoyl pyrene-capped homopolymer of **2.5**, making it a good model for studying the end-capping of the polymer.
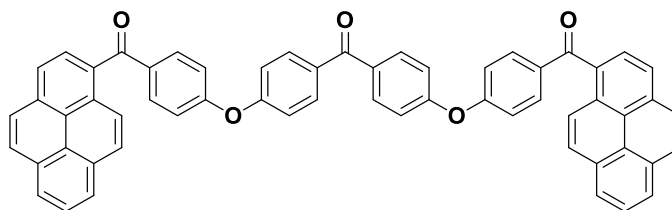
Figure 2.17. Structure of small molecule **2.8**, a model for the functionalised polymer **2.5**.

The ^{1}H NMR spectrum of the model compound **2.8** is shown in Figure 2.18. The two doublets in the highest field are attributed to the protons adjacent to the ether bonds. The two doublets downfield arise from the protons adjacent to the carbonyls. Unlike the spectrum of polymer **2.5** itself (Figure 2.13), the pyrenyl resonances are cleanly separated, with no overlap with the rest of the proton resonances from the small molecule. The pyrenyl proton resonances for the small molecule **2.8** have identical chemical shift and splitting patterns as

the pyrenyl resonances of its end-capped polymer counterpart, providing very good evidence that polymer **2.5** has indeed been successfully functionalised.
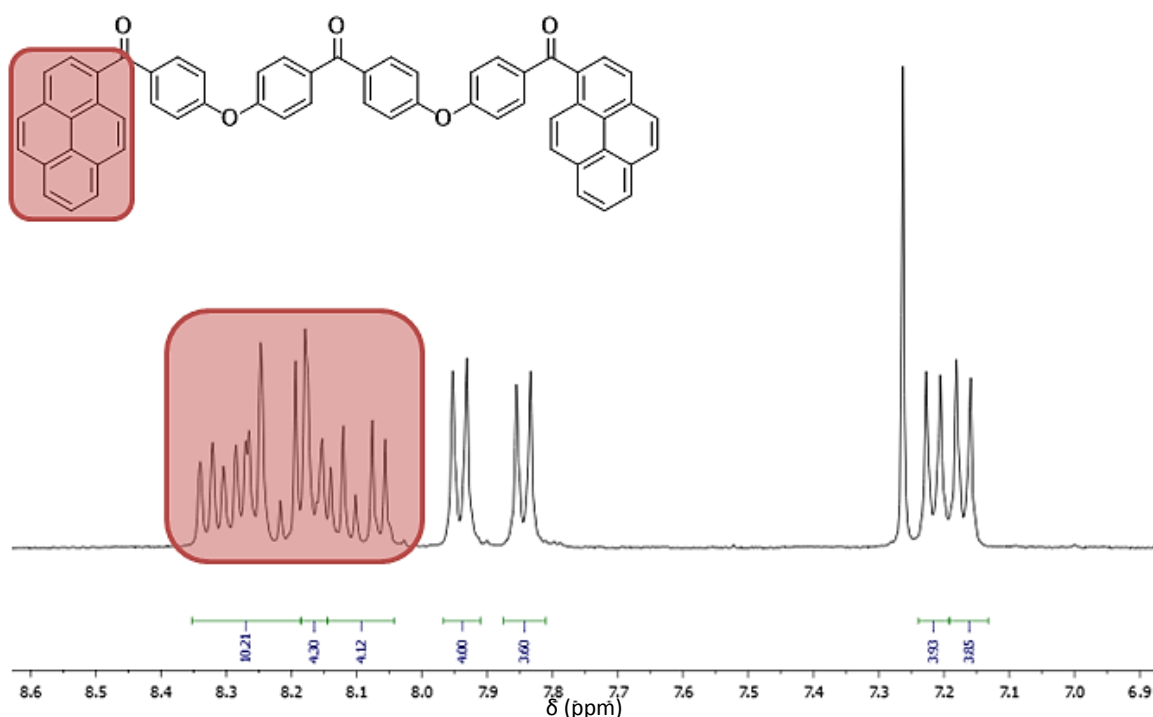
Figure 2.18. ^{1}H NMR spectrum of small molecule model compound **2.8**.

2.3.3.2 Analysis of benzoyl pyrene end-capped PES

Following on from the polycondensation using 1-(4-fluorobenzoyl)-pyrene as the end-capping monomer (giving polymer **2.5**), 1-(4-hydroxybenzoyl)-pyrene (**2.2**) was used to end-functionalise a poly(ether sulfone) (PES) (**2.7**, Figure 2.19) using identical polymerisation conditions. The synthesis of an amorphous soluble PES allows a comparison between η_{inh} values and average molecular weight data obtained from gel permeation chromatography (GPC) analysis. This would better confirm the number of repeat units and the polydispersity (Đ) which is the measure of the distribution of molecular mass in a given polymer.[11] All PAEKs described thus far tend to be insoluble in common GPC solvents. PESs such as **2.7** on the other hand, are readily soluble in GPC solvents.[12] Before any molecular weight analysis was carried out, ^{1}H NMR spectroscopy showed that polymer **2.7** had been end-capped with **2.2** (Figure 2.19).
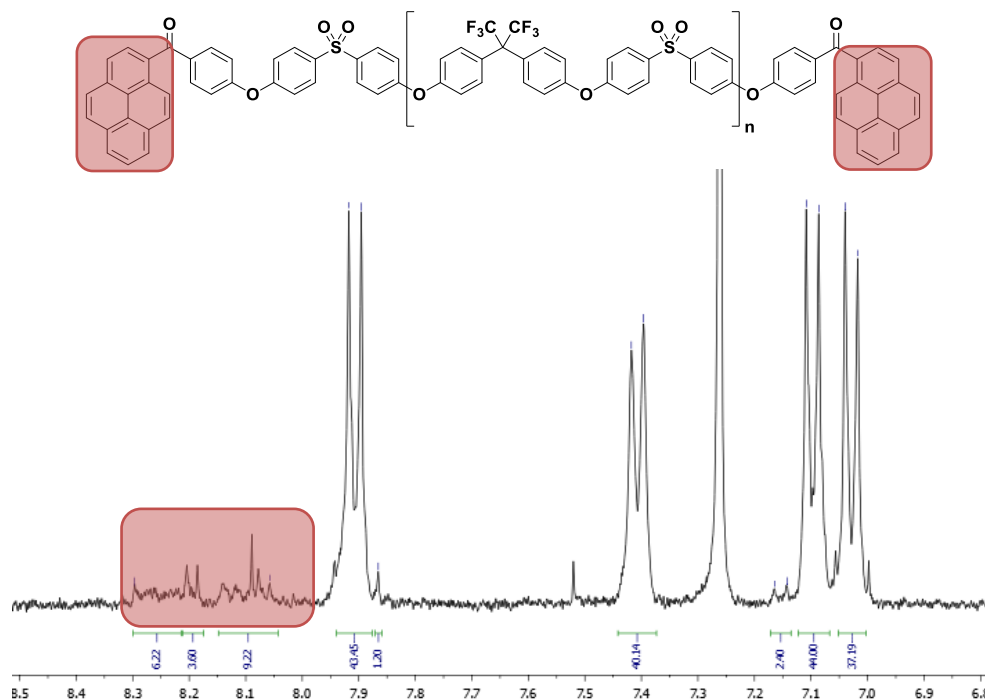
Figure 2.19. ^{1}H NMR spectrum of **2.7**.

Viscosity (η_{inh}) measurements give a qualitative indication of the average molecular weight of a polymer, with values of 0.5-1.0 dL g^{-1} being generally considered to indicate a high molecular weight polymer. Polymer **2.7** gave an η_{inh} measurement in CHCl$_3$/HFiPA (6:1 v/v) of 0.15 dL g^{-1}. The GPC analysis showed it had a weight-average molecular weight (M$_w$) of 24,000 and a number-average molecular weight (M$_n$) of 4,000, hence the *Đ* given by *Đ* = M_w / M_n is 5.59. A *Đ* that tends toward unity indicates that the molecular weight distribution of the polymer is essentially uniform, i.e. the polymer is monodisperse.[13] The high *Đ* value for **2.7** gives an indication that the polymerisation conditions may not be well-controlled. This can be expected in a one-pot polymerisation with a mono-functional end-group. Effectively, 20 mol% of the reactants are terminating monomers and can therefore cap the polymer at any point in the reaction, leading to a polymer with a wide range of chain lengths. The broad molecular weight distribution of **2.7** (Figure 2.20) is thus taken to be an artefact of an effective functionalisation reaction. A significant amount of the GPC analyte as highlighted in Figure 2.20, can be attributed to cyclic oligomers (e.g. trimers and dimers). These cyclic oligomers are by-products of the polymerisation, and are known to form more readily in polycondensations at high dilution conditions.[14]

Figure 2.20. Molecular weight distribution curve (GPC) of **2.7**, *Đ* = 5.59.

2.3.4 Direct end-capping of poly(ether ketone)s

The polymers discussed thus far all involved first the synthesis of an end-capping monomer followed by addition to the monomers in a separate polycondensation reaction, which finally results in a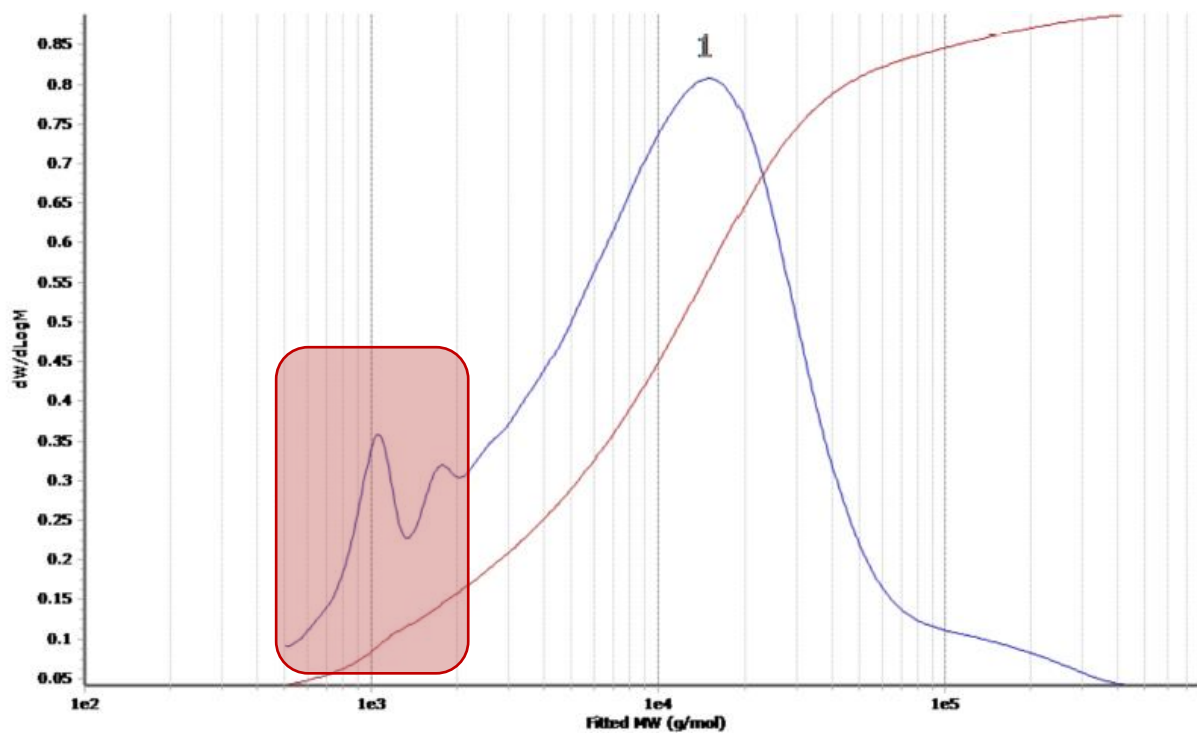 functionalised polymer. The polycondensation and functionalisation itself is a one-step reaction at high temperature. It was postulated in the present work that perhaps, using different chemistry, a functionalised polymer could be synthesised via a one-step reaction. This work focused on an all-aromatic system with the PAEKs synthesised by electrophilic polycondensation at ambient temperature.

2.3.4.1 Synthesis of a model compound for direct end-capping

Initially, a model for the direct functionalisation reaction was planned in order to show a successful synthetic route to a functionalised small molecule (**MC1**). The small molecule is formed from an electrophilic aromatic substitution reaction between oxydibenzoic acid and pyrene in neat triflic acid as shown in Scheme 2.5.
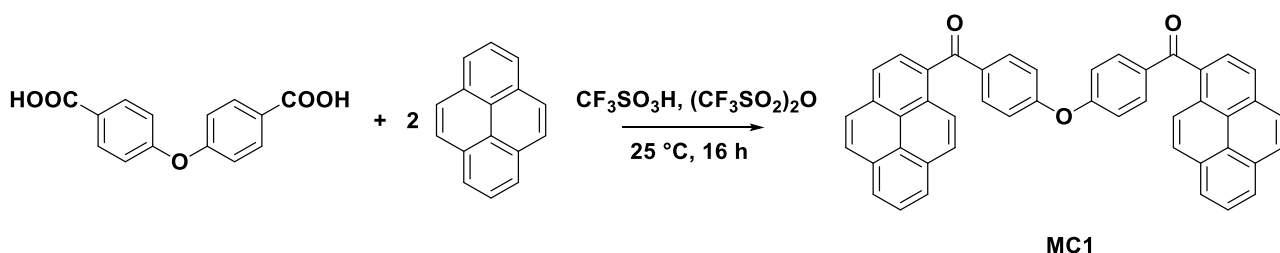
Scheme 2.5. Synthesis of proposed model compound (**MC1**) for direct end-capping.

In order to avoid the multiple substitution of pyrene previously observed in neat triflic acid reactions, a large excess of pyrene was used. As it transpired, despite the large excess of pyrene in the system, the reaction still produced multiply substituted pyrenyl compounds as the ^{1}H NMR spectrum in Figure 2.21 shows. Considering the multiplet at 7.21-7.15, this peak would be expected to be a simple doublet had the synthesis produced the model compound **MC1**. However, the multiplet shows at least three distinct proton resonances, indicating at least the same number of proton environments. Similarly, the pyrenyl resonances show more proton environments than were expected for the desired product. Comparing the spectra of the two model compounds **2.8** and **MC1**, Figure 2.18 shows a definite singly-substituted pyrene (**2.8**) while Figure 2.21 shows multiply substituted pyrenes giving a more

complex spectrum (**MC1**). Proceeding from this evidence of multiple substitution in pyrene, a different approach to the proposed *in situ* end-capping was explored.
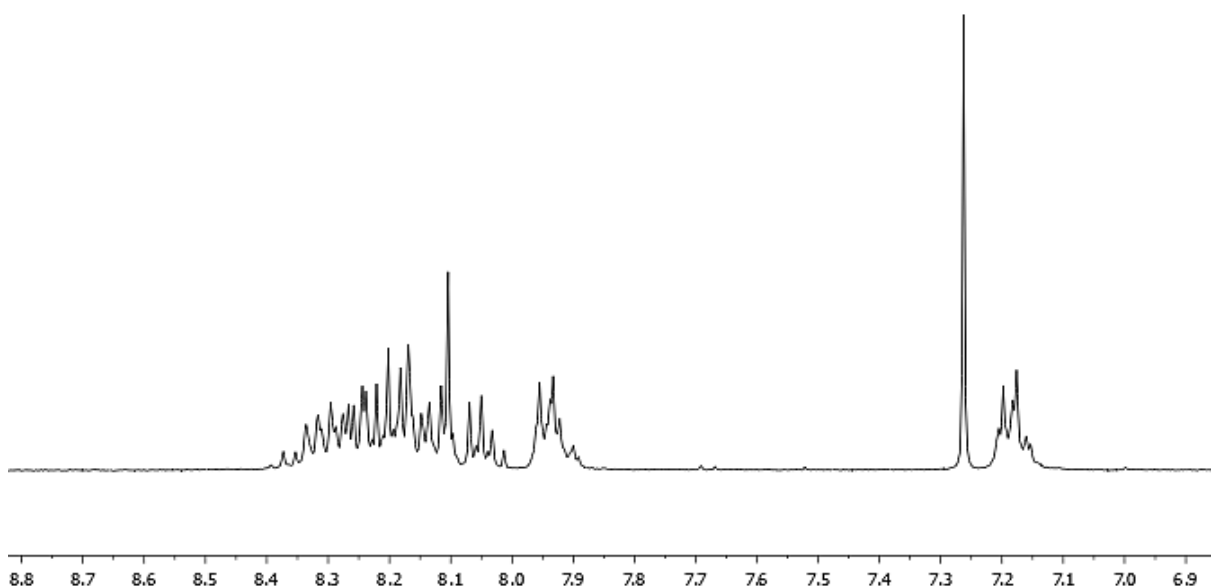
Figure 2.21. ^{1}H NMR spectrum of **MC1**.

2.3.4.2 Electrophilic direct end-capping polycondensation

Until now, all polymerisations described in this work have been one-step polycondensation with end-capping. Next however, a two-step, one-pot polymerisation was used in order to avoid potential multiple substitutions incorporating pyrene groups along the polymer chain. The polycondensation, in neat triflic acid was with co-monomers 1,4-diphenoxybenzene and oxydibenzoic acid. Oxydibenzoic acid was added in 20 mol% excess to ensure that the polymer chain is terminated with carboxylic acid functional groups that can subsequently react with pyrene thus forming a functionalised polymer. The co-monomers were stirred in triflic acid for 16 h which allowed the polymer chain to achieve a higher molecular weight (η_{inh} (H$_2$SO$_4$): 0.22 dL g^{-1}) than the polymers synthesised via a nucleophilic route such as **2.4** and **2.5** (η_{inh} (H$_2$SO$_4$); 0.19 and 0.12 dL g^{-1}, respectively). After this extended chain-growth reaction, an excess of pyrene was added and the reaction was stirred for a further 16 h to afford the functionalised polymer **2.9** (Scheme 2.6).
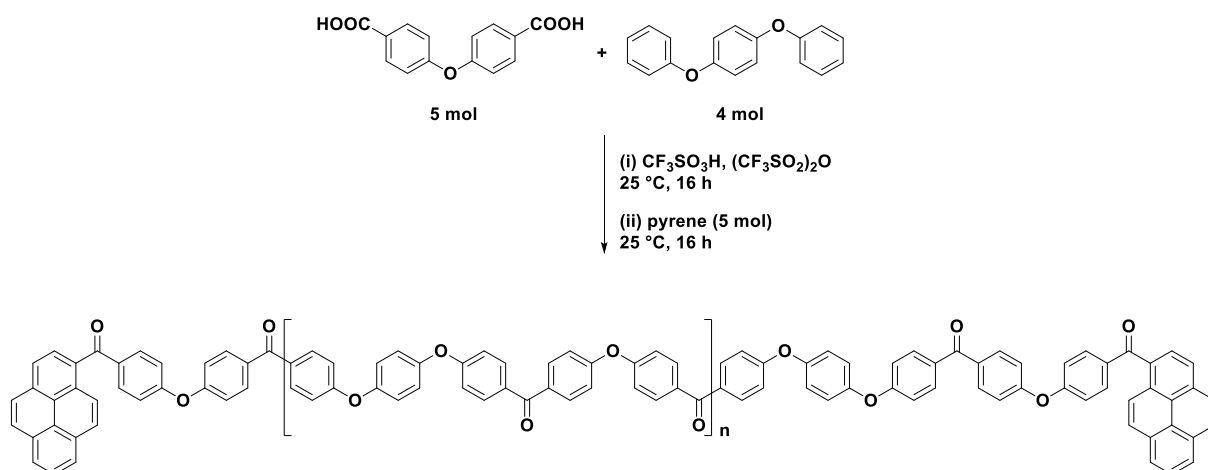
Scheme 2.6. Two-step polymerisation and end-capping via electrophilic aromatic substitution to produce functionalised polymer **2.9**.

Using this approach, polymer **2.9** has been successfully functionalised with pyrene following a two-step polycondensation via an electrophilic route. The ^{1}H NMR spectrum of **2.9** (Figure 2.22) shows the pyrene resonances as singly substituted. The pyrene resonances are similar to those previously observed for 1-(4-hydroxybenzoyl)-pyrene (**2.2**, Figure 2.11). There was no evidence of di-substituted pyrene in the spectrum of polymer **2.9**, unlike that observed for both end-cap **2.1** and model compound **MC1** when synthesised in neat triflic acid. One of the measures taken to ensure that the polymers would be functionalised was to add a large excess of pyrene (greater than 2-fold). In this case, it is very likely that the excess pyrene available in the system contributes to ensuring that pyrene will only be singly substituted. Thus it acts only as an end-capping monomer rather than acting as a linking group along the polymer chain. This polymer displayed a T_g of 155 °C, consistent with formation of a high molecular weight polymer. It also shows a high T_m of 342 °C, which is characteristic of highly crystalline PAEKs.
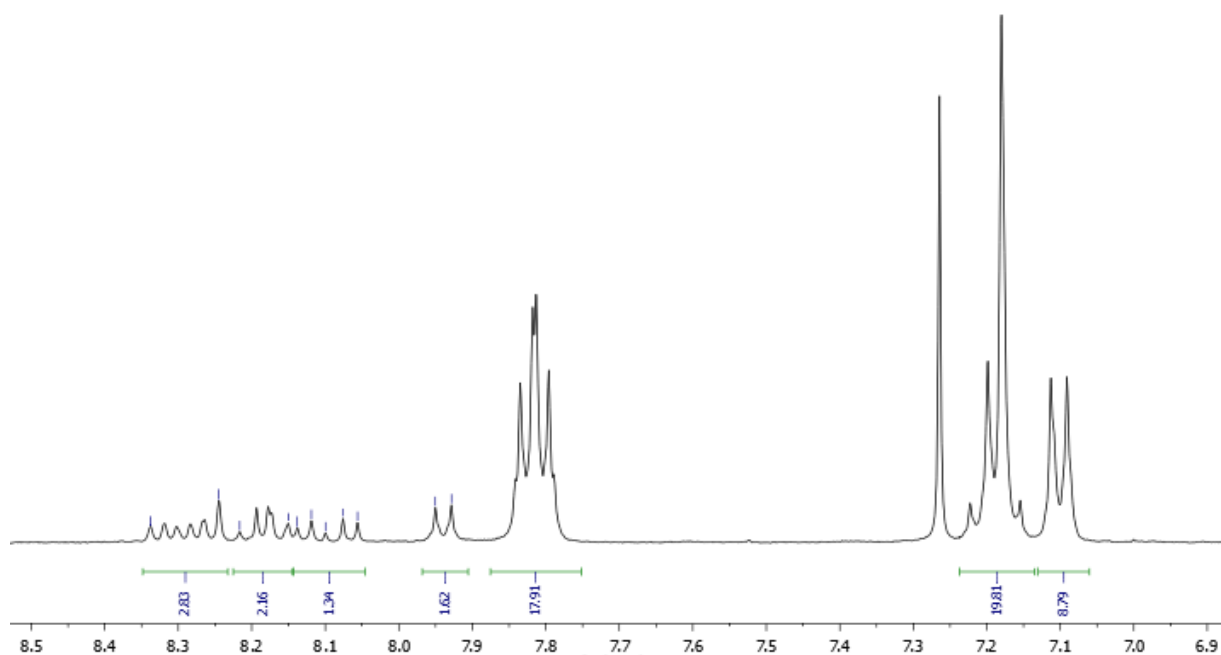
Figure 2.22. ^{1}H NMR spectrum of **2.9** synthesised via electrophilic direct endcapping polycondensation

2.3.5 Models for π-π interactions between polymers

The polymer end-capping discussed above is just the first step in the synthesis of π-electron-rich PAEKs which are to be studied for their potential in supramolecular polymer blends for composite matrices. This present section is concerned with initial studies which explored the binding interaction between complementary units in such polymer blends, with polyimides acting as the electron-poor components.

Computational modelling (molecular mechanics, *Materials Studio*) suggested that polymer chain-folds comprising a pyromellitic diimide unit linked by a biphenyl chain (Figure 2.23) would provide a good geometry for binding the pyrenyl end-group of a second polymeric component. As can be seen in Figure 2.23, the polyimide forms a chain-folded structure with the benzoyl pyrene end-group of polymer **2.5** intercalated between the pyromellitimide and biphenylene-disulfone linker of the polyimide. This can also be said to be π-π stacked as the distance between the aromatic groups is approximately 3.4 Å, which is consistent with previously reported types of attractive but non-bonding intermolecular interactions.[15]
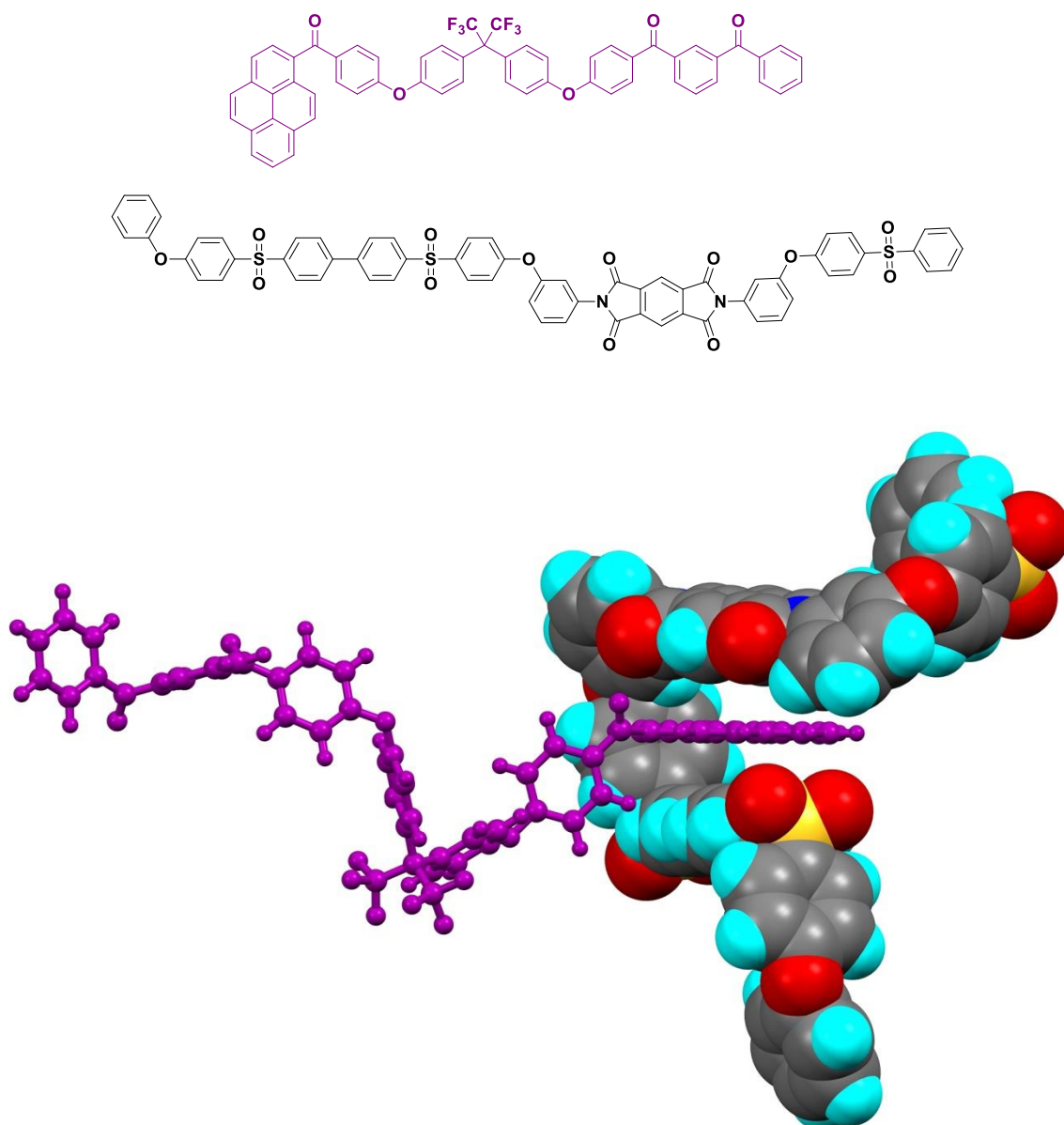
Figure 2.23. Energy-minimised computational model showing π-π stacked polyimide (space-filled) and benzoyl pyrene terminated PAEK **2.5** (purple).

Similarly, computational modelling shows the small molecule **2.8**, (the model compound for the functionalised PAEK) stacked within a macrocyclic ether-imide-sulfone cage **2.11**, which is in turn a model for the polyimide chain fold. The minimised computational model shows a π-π stacked supramolecular interaction (Figure 2.24).

2.8

2.11
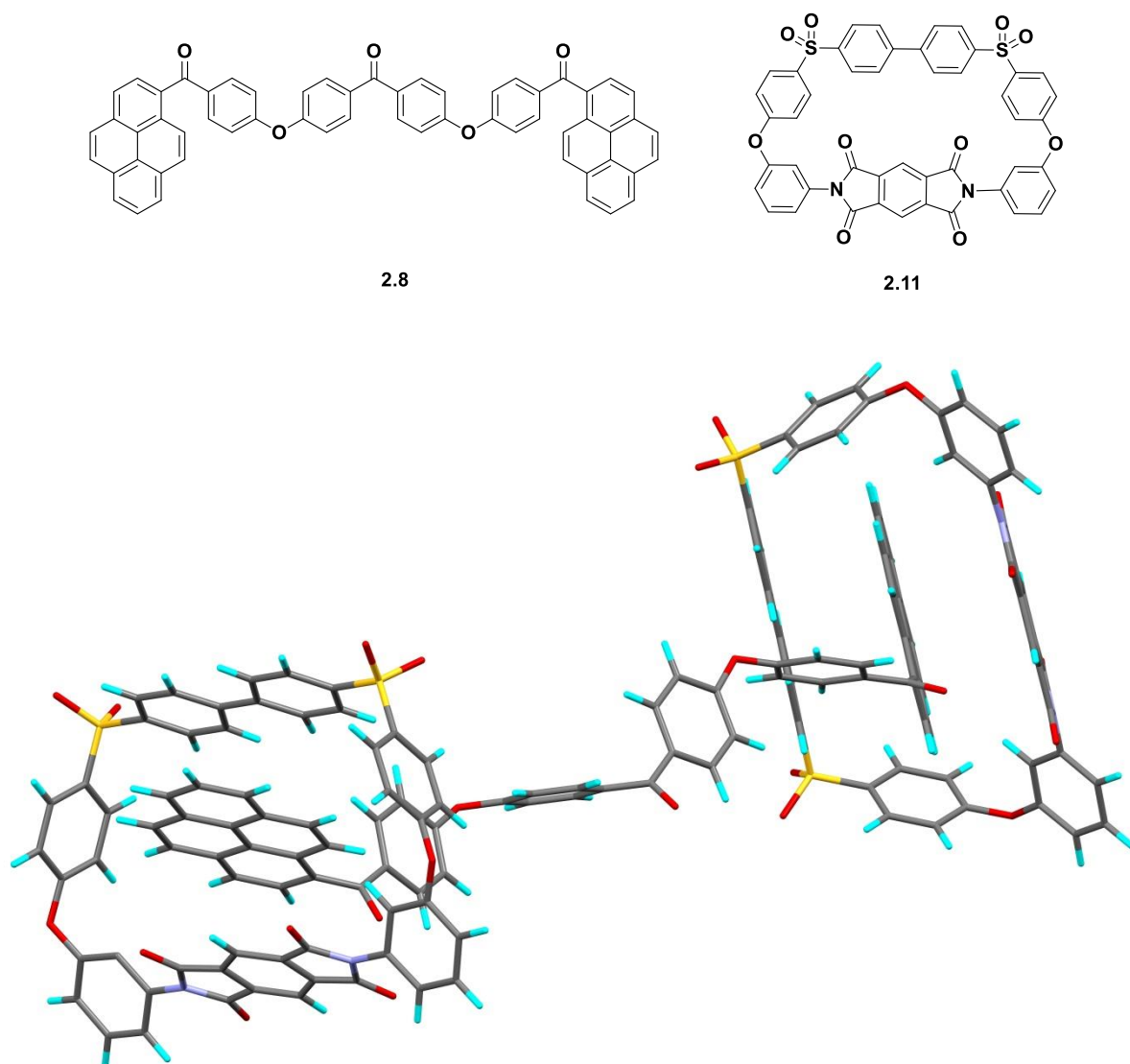
Figure 2.24. Minimised computational model showing π-π stacking between **2.8** and **2.11** which are the small molecule models for an end-functionalised PAEK and polyimides, respectively.

2.3.5.1 Crystal structures

Single crystal X-ray analysis was carried out by Dr A. M. Chippindale on **2.1**, which provided information on the site of benzoylation, the molecular conformation, and crystal packing within the unit cell (Figure 2.25). The single crystals described below were grown via solvent/non-solvent vapour exchange. The compound was dissolved in CDCl$_3$ and diffused against MeOH as the non-solvent over a period of 4 weeks.
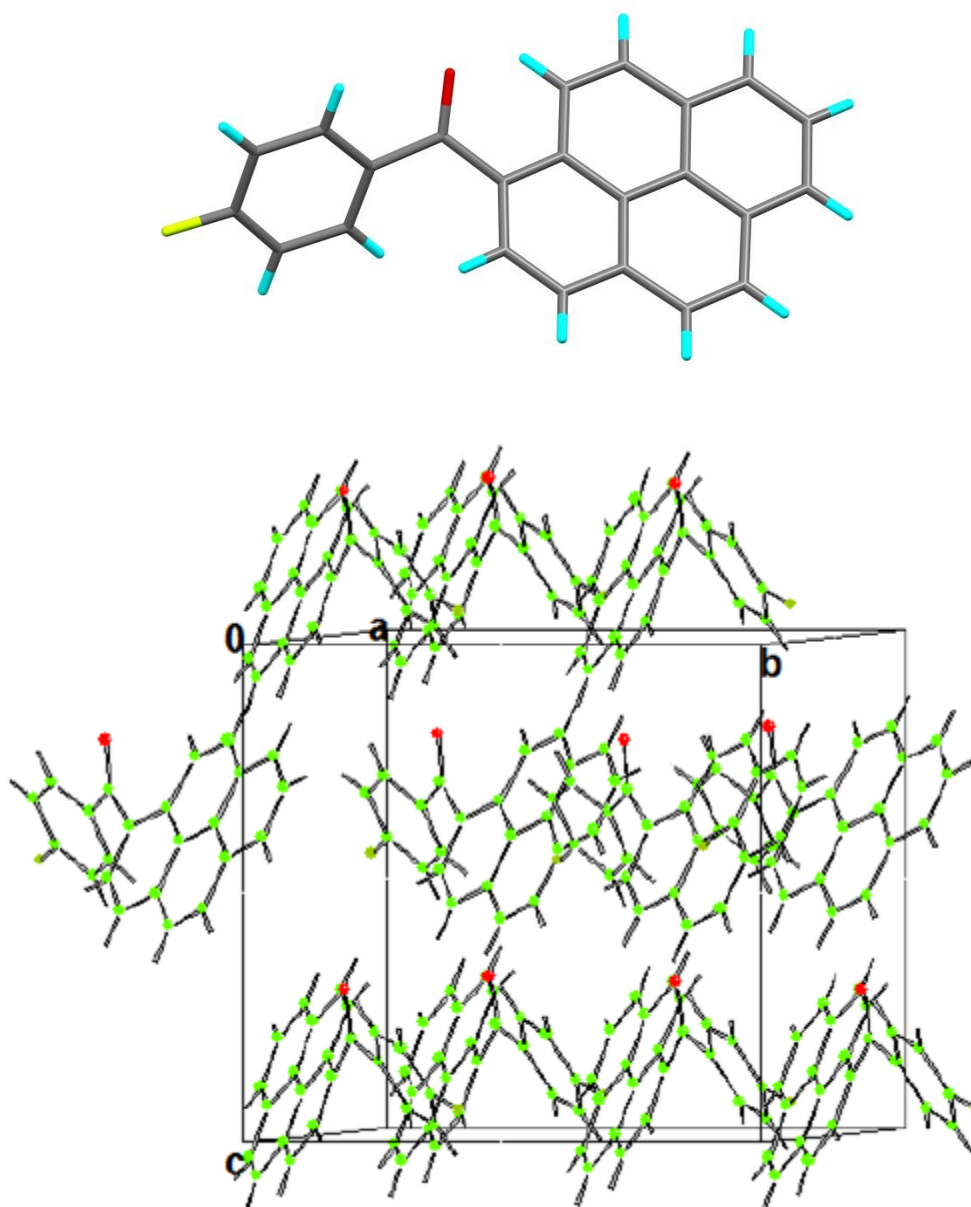
Figure 2.25. Structure of **2.1** obtained from single crystal X-ray analysis (top) and packing and arrangement within a unit cell (bottom).

Additionally, single crystals of **2.2** complexed with macrocycle **2.11** were also obtained (Figure 2.26). The resulting X-ray structure (again by Dr A. M. Chippindale) shows that the pyrenyl substituent of the end-cap forms a π-π stacking interaction with the macrocyclic pyromellitimide unit with a typical interatomic distance of 3.4 Å. Also shown is the packing of the complex within the unit cell, which is of particular interest as it shows hydrogen bonding between the hydrogen of the hydroxybenzoyl group of one end-cap molecule and a carbonyl oxygen atom of an adjacent macrocyclic imide. Hydrogen bonding is known to aid

and direct self-assembly of polymers into supramolecular polymer arrays.[16] The structure also quite clearly shows that the hydroxybenzoyl groups are not π-stacking even though they are parallel to each other. This is evident in their interatomic distance of 4.4 Å.

2.2   **2.11**
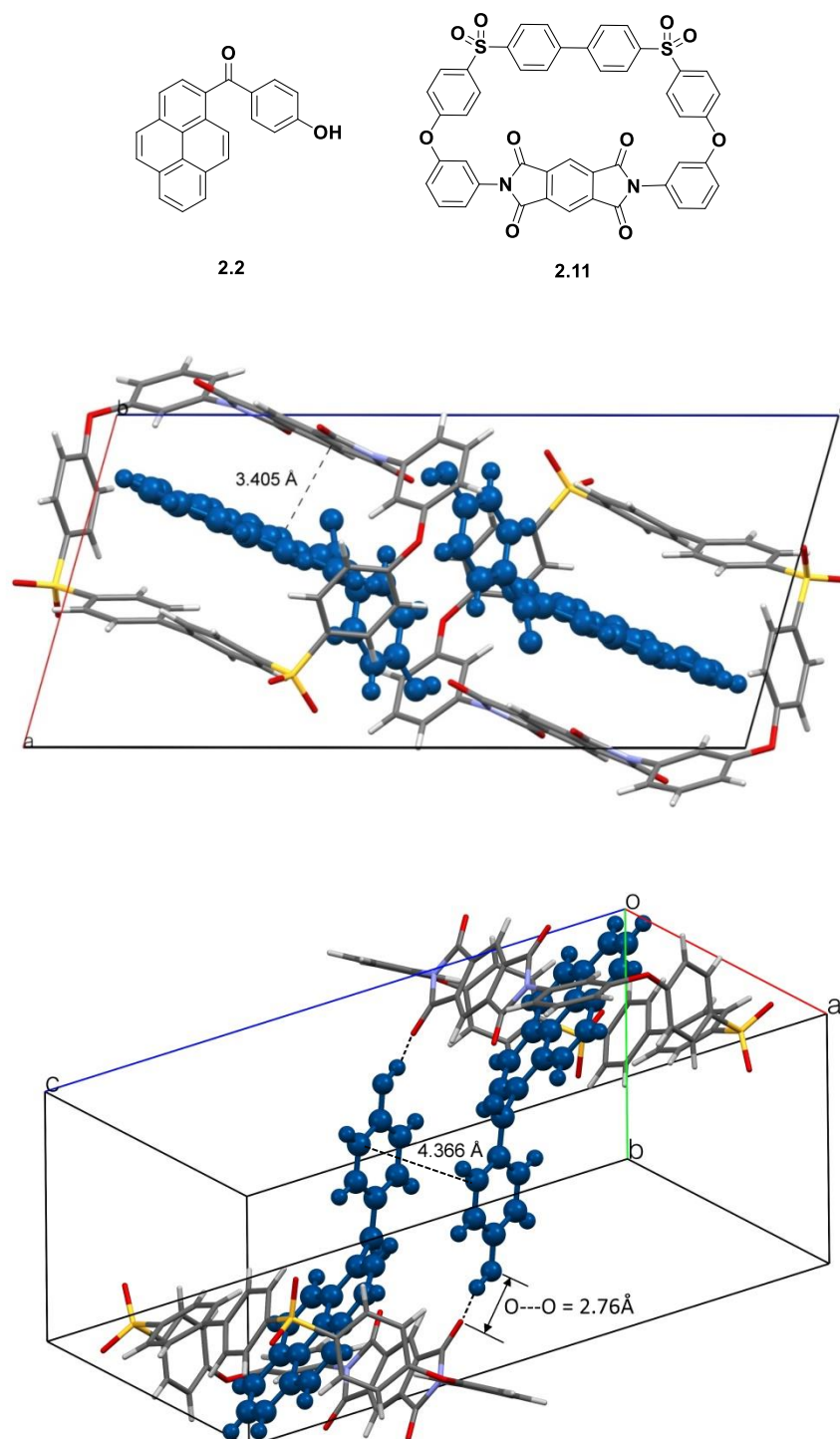
Figure 2.26. Top: X-ray diffraction of the complex between **2.2** and **2.11** showing π-π stacking. Bottom: The same complex showing O---O separation of 2.76 Å, which is indicative of the presence of a hydrogen bond.

2.3.5.2 NMR titration experiments

A series of ^{1}H NMR studies were carried out to confirm complexation of a pyrenyl-functionalised PAEK with a chain-folding polyimide. In a model study, such complexation was explored using the end-cap **2.2** and the macrocyclic chain-fold analogue **2.11** (Figure 2.27).
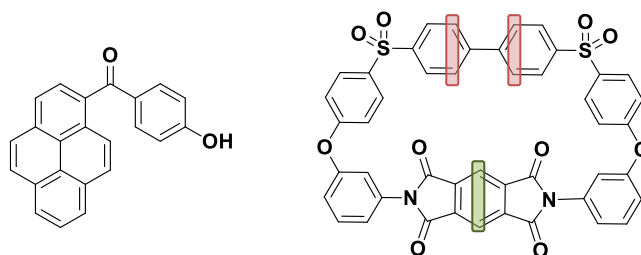
Figure 2.27. Structures of the compounds in the NMR titration experiment, **2.2** and macrocycle **2.11**.

A ^{1}H NMR spectrum of the macrocycle was first run, and progressively increasing amounts of end-cap were then added as shown in Figure 2.28. As 1-(4-hydroxybenzoyl)pyrene is added to the macrocycle in increasing molar ratios from 1:0 through to 1:2 (macrocycle:pyrene), marked upfield shifts in the proton resonances in the pyromellitimide (green) and biphenyl (red) units are observed. It should be noted that, above a 1:1 macrocycle to end-cap molar ratio, the shift of the pyromellitimide proton cannot be absolutely distinguished among the other resonances but its shift is estimated in Figure 2.28 by the green dashed line. The large observed upfield shifts of the macrocyclic resonances confirm strong complexation of the two molecules. An upfield shift indicates that the aromatic ring-current of the pyrenyl end-cap is shielding the macrocyclic protons from the NMR magnetic field.[17]

Macrocycle : end-cap
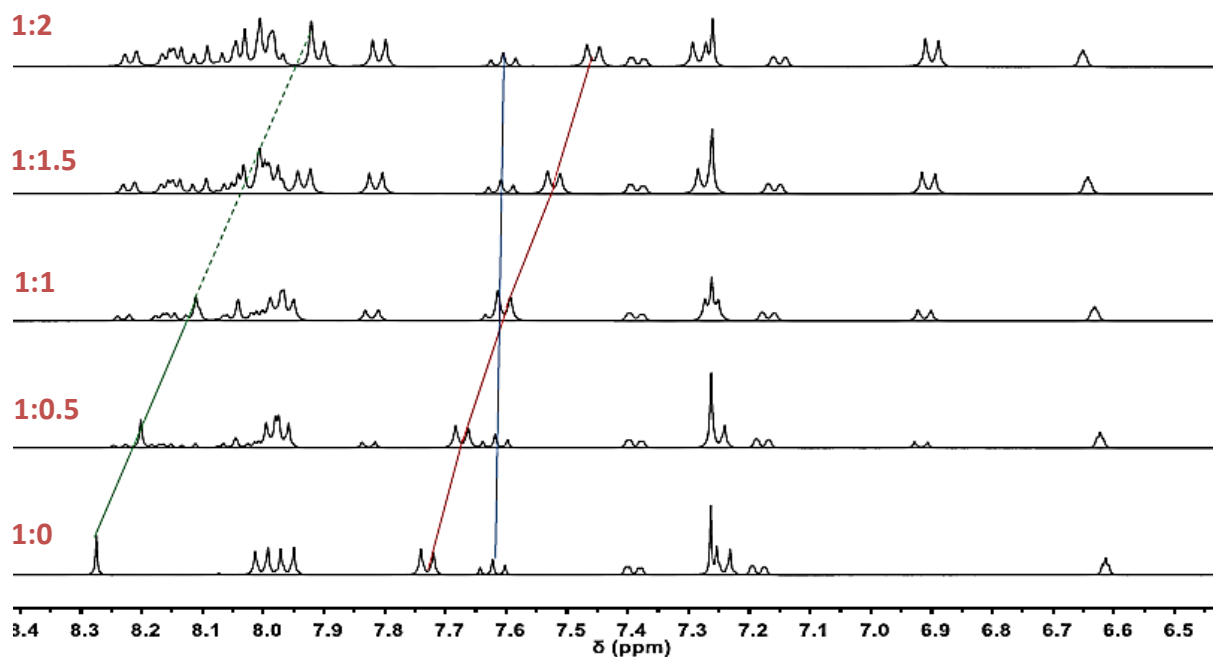
Figure 2.28. ^{1}H NMR spectra showing upfield shifts in the macrocycle **2.11** protons (green and red lines) as more **2.2** is added.

To further explore the potential π-π stacking interactions between the polyimide and the functionalised poly(ether ketone), model compound **2.8** was used in a similar titration study in order to investigate its possible complexation with **2.11** (Figure 2.29).
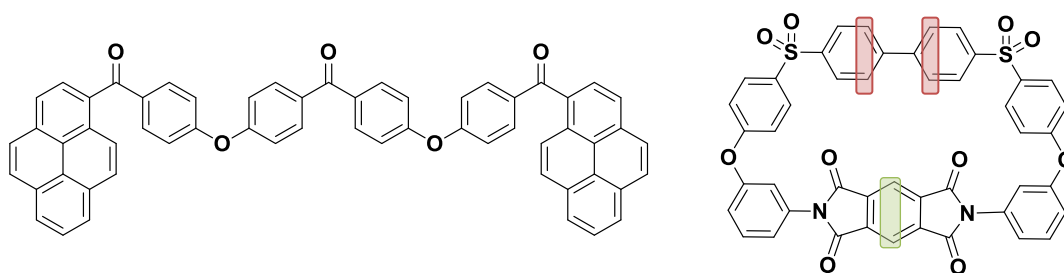
Figure 2.29. Structure of model compound **2.8** and macrocycle **2.11** for the ^{1}H NMR titration experiment.

As with the complexation between the macrocycle and 1-(4-hydroxybenzoyl)pyrene, there was good evidence of complexation between the model compound and the macrocycle. As can be seen in Figure 2.30, there is a clear upfield shift of the biphenylene resonances (red) upon the addition of **2.2**. The resonance from the pyromellitide protons (8.30 ppm) is partly obscured by the proton resonances of the pyrenyl group in **2.2** in high loading, but its projected upfield shift is reliably indicated by the green dashed line.
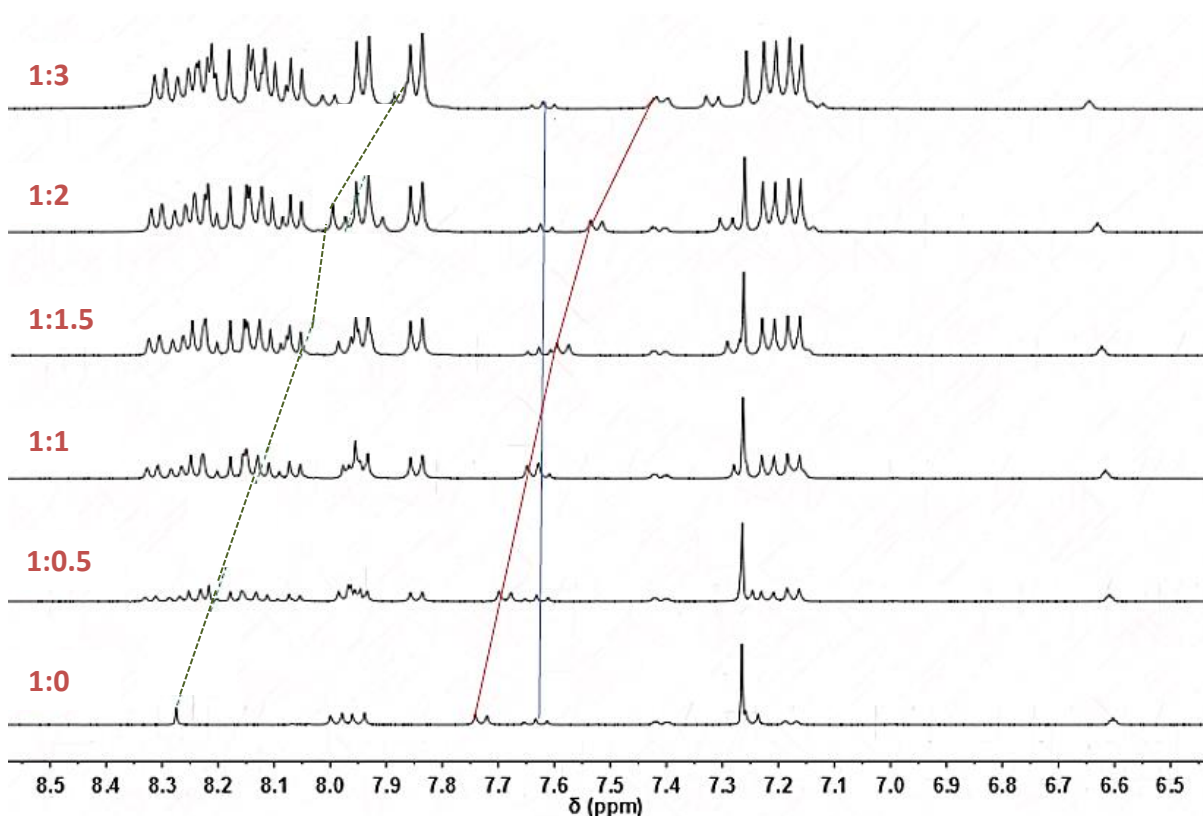
Figure 2.30. Stacked ^{1}H NMR spectra showing upfield shifts in macrocycle proton resonances as oligomeric model compound **2.8** is titrated with macrocycle **2.11**.

2.3.6 Additional end-cap studies

With the successful synthesis of the benzoylpyrene end-capping compounds, several attempts were made to synthesise different end-caps with three to five π-conjugated rings. Adapting the same synthetic procedure as for 1-(4-hydroxybenzoyl)-pyrene (**2.2**), the syntheses of anthracene-, triphenylene- and perylene-based end-caps were explored.

Attempts to synthesise a pure (4-hydroxybenzoyl)-anthracene using the same method as for **2.2** were not successful. It is suspected that the product has been made, but some starting material still remained in the crude product, and several attempts to purify the crude material were unsuccessful. Triphenylene on the other hand, was proved entirely unreactive towards 4-hydroxybenzoic acid. No evidence of substituted triphenylene was found, and virtually all the starting material was recovered.

Adapting the synthetic method to produce benzoyl*perylene* end-groups (Scheme 2.7) was much more successful, enabling isolation of the new compound 1-(4-fluorobenzoyl)-perylene **2.3**. It is envisaged that future work could explore PAEKs terminated with these π-electron rich substituents. Perylene has been recently used in functionalising polymers to form supramolecular healable polymer systems and is definitely worth exploring for use in high-performance polymers.[18] The crude product from this reaction required purification by column chromatography. The pure product was confirmed to be **2.3** by HRMS (m/z: 375.1179 [$C_{27}H_{16}OFNa^+$], calculated: 375.1180 [$M+Na^+$]). Furthermore, single crystal X-ray diffraction confirmed successful synthesis of the target compound, and showed the site of benzoylation at the 1-position (Figure 2.31).
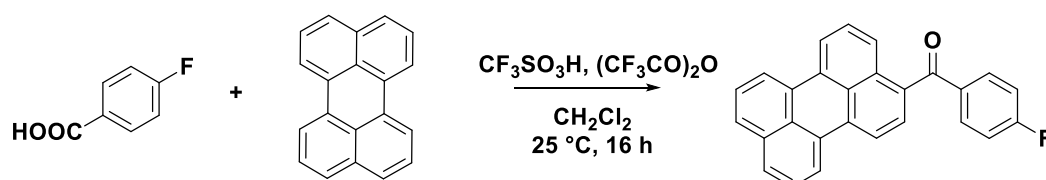
Scheme 2.7. Reaction scheme between 4-fluorobenzoic acid and perylene to produce **2.3**.
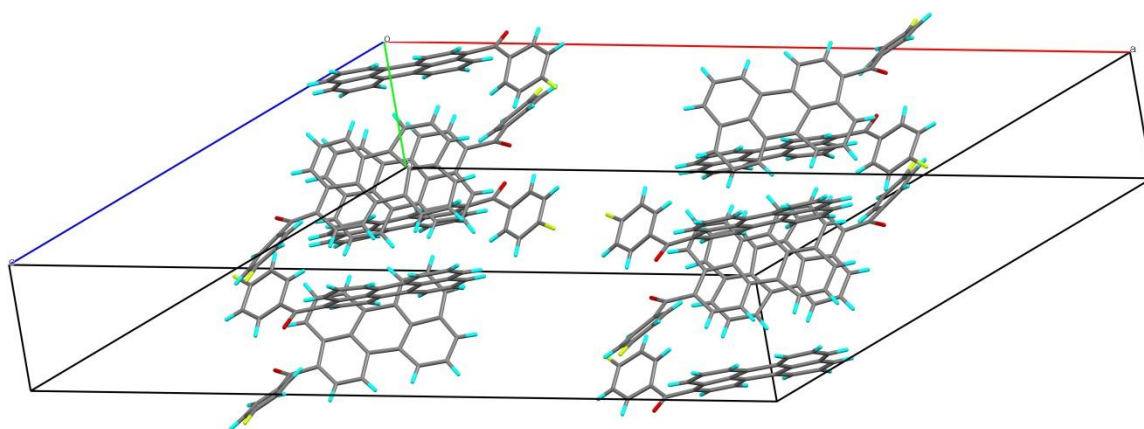
Figure 2.31. X-ray crystal analysis of **2.3**, confirming successful synthesis of 1-(4-fluorobenzoyl)-perylene.

2.4 Conclusions

This chapter details the synthesis of three novel π-electron rich compounds that are suitable for end-capping poly(ether ketone)s and poly(ether sulfone)s. The route to the synthesis of these end-caps involves Friedel-Crafts type acylations of pyrene and perylene with a substituted benzoic acid, using only catalytic amounts of trifluoromethanesulfonic acid. The pyrenyl end-caps were used in the direct functionalisation of poly(ether ketone)s and poly(ether sulfone)s via nucleophilic polycondensation. The end-capping was jointly demonstrated by NMR and fluorescence spectroscopy, and inherent viscosity and GPC measurements supported the findings, showing the polymers are of approximately the expected molecular weights.

It was also demonstrated that a two-step electrophilic polycondensation followed by end-capping is a viable route to producing functionalised polymers. The electrophilic polycondensation was carried out at room temperature over 16 h in neat trifluoromethane sulfonic acid as both the solvent and catalyst. The polymer isolated via this method was found to have a relatively high molecular weight as indicated by its inherent viscosity and supported by the high glass transition temperature measurements.

Initial studies have demonstrated π-π stacking interactions between model compounds for interacting macromolecules. Single crystal X-ray diffraction showed that 1-(4-hydroxybenzoyl)-pyrene binds within a pyromellitimide biphenyl macrocycle, which is a model of a π-electron deficient system. Binding interactions in solution have also been demonstrated by ^{1}H NMR spectroscopy.

2.5 Experimental

2.5.1 Materials

1,3-Bis(4-fluorobenzoyl)benzene, 4,4'-dihydroxybenzophenone, 1-hydroxypyrene, 3-aminophenol, 4,4'-bis[(4-chlorophenyl)sulfonyl]-1,1'-biphenyl, pyromellitic dianhydride, 1,4,5,8-naphthalenetetracarboxylic dianhydride, pyrene, trifluoromethanesulfonic acid, *N,N*-dimethylacetamide, acetone, methanol, ethanol, ethyl acetate, dichloromethane, deuterated chloroform and deuterated dimethylsulfoxide were purchased from Sigma Aldrich, UK. Perylene, diphenyl sulfone, trifluoroacetic anhydride, trifluoromethanesulfonic

anhydride and diphenyl sulfone were purchased from Alfa Aeser, UK. Sodium hydroxide, potassium hydroxide, potassium carbonate and hexane were purchased from Fisher Scientific, UK. 1,1,1,3,3,3-Hexafluoro-2-propanol was purchased from Apollo Scientific, UK. All materials were used as supplied unless stated otherwise.

2.5.2 Endcap synthesis

2.5.2.1 1-(4-fluorobenzoyl)-pyrene (2.1)

A solution of 4-fluorobenzoic acid (760 mg, 5.4 mmol), trifluoroacetic anhydride (750 µL, 5.4 mmol) and DCM (35 mL) was stirred for 5 minutes. Pyrene (1 g, 4.9 mmol) was added followed by triflic acid (480 µL, 5.4 mmol) and the solution was stirred for 3 h. Water (25 mL) was added to the reaction mixture. The aqueous layer was separated and extracted with DCM. The combined organics were dried over Mg_2SO_4, filtered, then the solvent removed *in vacuo*. The product was purified by column chromatography (DCM), yielding the pure product **2.1** as a yellow-green solid (1.41 g, 88%).
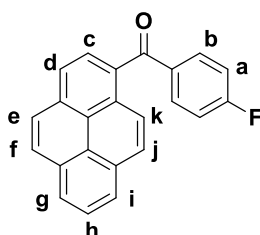
2.1

M.p.: 129 °C; HRMS (ESI) m/z: 325.1022 [$C_{28}H_{14}OFNa^+$], calculated: 325.1023 [M+Na$^+$]; ^{1}H NMR (400 MHz, DMSO-d_6): δ (ppm) 8.44-8.35 (m, 4H **c, d, e, f**), 8.32-8.26 (m, 2H **g, i**), 8.20-8.15 (m, 2H **h, j**), 8.14 (d, *J* = 8.0, 1H **k**), 7.90 (app q, *J* = 8.0, 5.6 2H **b**), 7.40 (t, *J* = 8.8, 2H **a**); ^{13}C NMR (100 MHz, DMSO-d_6): δ (ppm) 196.1, 166.5, 163.9, 134.7, 134.6, 133.1, 132.5, 130.7, 129.9, 129.2, 128.8, 128.7, 127.2, 126.8, 126.6, 126.4, 126.1, 124.2, 124.0, 123.5, 116.0, 115.8; IR: v_{max}/ cm^{-1} 1640 (C=O), 1592 (C=C Ar), 1226 (C-F).

2.5.2.2 1-(4-hydroxybenzoyl)-pyrene (2.2)

This compound was synthesised following the procedure for **2.1**, but replacing 4-fluorobenzoic acid with 4-hydroxybenzoic acid (740 mg, 5.4 mmol). Water (25 mL) was added to the reaction mixture. The yellow precipitate was filtered and washed with water

until a neutral filtrate was obtained. The title compound **2.2** was recovered as a pale yellow solid without further purification (0.92 g, 58%).
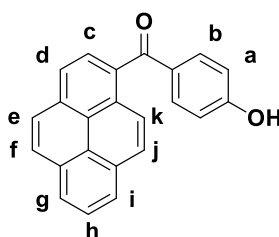
2.2

M.p.: 245 °C; HRMS (ESI) m/z: 323.1066 [$C_{23}H_{15}O_2Na^+$], calculated: 323.1067 [M+Na$^+$]; ^{1}H NMR (400 MHz, DMSO-d_6): δ (ppm) 8.42-8.39 (m, 2H **c, d**), 8.39-8.28 (m, 3H **e, f, g**), 8.23 (d, J = 9.2, 1H **i**), 8.16 (t, J = 7.6, 1H **h**), 8.09-8.06 (app q, J = 4.8, 2H **j, k**), 7.70 (d, J = 8.8, 2H **b**), 6.89 (d, J = 8.8 2H **a**); ^{13}C NMR (100 MHz, DMSO-d_6): δ (ppm) 195.8, 170.3, 162.7, 134.0, 132.8, 131.9, 130.7, 130.1, 129.2, 128.6, 128.5, 128.2, 127.3, 126.7, 126.1, 125.8, 124.3, 124.2, 115.5 59.7; IR: ν$_{max}$/ cm^{-1} 3352 (O-H broad), 1572 (C=C Ar), 1276 (C=O).

2.5.2.3 1-(4-fluorobenzoyl)-perylene (2.3)

This compound was synthesised following the procedure for **2.1**, but with perylene (1.231 g, 4.9 mmol) replacing pyrene. The product was purified by column chromatography (DCM/ hexane 80/20) yielding **2.3** as a bright orange solid (1.08 g, 59%).
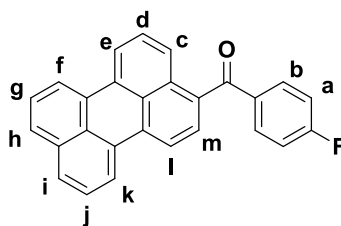
2.3

M.p. (DSC): 204 °C; HRMS (ESI) m/z: 375.1179 [$C_{27}H_{16}OFNa^+$], calculated: 375.1180 [M+Na$^+$]; ^{1}H NMR (400 MHz, DMSO-d_6): δ (ppm) 8.51-8.47 (m, 4H **e, f, k, l**), 7.95-7.83 (m, 5H **b, h, i, m**), 7.65-7.59 (m, 4H **c, d, g, j**), 7.41 (t, J = 8.8, 2H **a**); ^{13}C NMR (100 MHz, DMSO-d_6): δ (ppm) 196.3, 134.7, 134.1, 133.4, 132.9, 132.8, 131.7, 130.9, 130.0, 129.1, 128.6, 12834, 128.0, 127.1, 127.0, 125.1, 122.1, 121.5, 121.3, 119.4, 116.1, 113.8; IR: ν$_{max}$/ cm^{-1} 1646 (C=O), 1596, 1498 (C=C Ar), 1552, 1262, 1226 (C-F).

2.5.3 Synthesis of pyrenyl end-capped polymers

2.5.3.1 Hydroxypyrene terminated poly(ether ketone ether ketone ketone) (2.4)

A mixture of 1,3-bis(4-fluorobenzoyl)benzene (1.23 g, 3.83 mmol), 4,4'-dihydroxybenzophenone (3.477 g, 3.48 mmol), 1-hydroxypyrene (152 mg, 0.70 mmol), Na$_2$CO$_3$ (0.47 g, 4.40 mmol) and diphenyl sulfone (16 g) was heated to 300 °C under argon for 3 h. The polymer solution was poured onto a sheet of aluminium, cooled and ground to a powder before extracting with acetone (200 mL). The powder was filtered then was extracted four times with refluxing acetone, and then in a Soxhlet extractor with refluxing acetone for 16 h. The powder was extracted five times with boiling water, and then a final four times with refluxing acetone. The suspension was then filtered, the precipitate dried at 110 °C under vacuum for 16 h, affording the functionalised poly(ether ketone) **2.4** as a colourless powder (0.83 g, 42%).
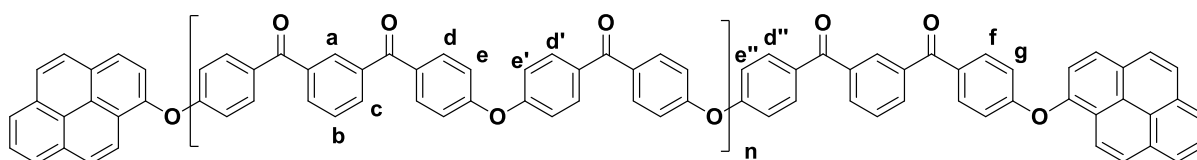
2.4

T_g: 175 °C; T_c: 190 °C; T_m: 289°C; η_{inh} (H$_2$SO$_4$): 0.19 dL g^{-1}; ^{1}H NMR (400 MHz, CDCl$_3$/(CF$_3$)COOH 3:1 v/v): δ (ppm) 8.22-8.18 (m, 10H, py), 8.12-8.08 (m, 19H (expected 27H), **a**, **c**), 7.95 (app t, J = 9.2, 58H (expected 60H), **d**, **d'**, **d''**), 7.90 (d, J = 4.4, 4H, **f**), 7.87-7.83 (m, 6H, py), 7.77 (t, J= 7.6, 9H **b**), 7.25 (app t, J = 4.8, 64H (expected 60H), **e**, **e'**, **e''**), 7.04 (d, J = 8.4, 4H **g**); ^{13}C NMR (175 MHz, CDCl$_3$/(CF$_3$)$_2$CHOH 6:1 v/v): δ (ppm) 199.6, 199.2, 161.6, 160.6, 137.1, 137.0, 134.7, 133.9, 133.7, 133.7, 133.6, 133.4, 133.3, 132.1, 131.5, 131.4, 131.4, 131.2, 129.2, 129.1, 119.2, 119.0, 118.9, 116.3, 116.1; IR: v_{max} / cm^{-1} 1665 (C=O), 1585, 1500 (C=C Ar), 1239 (C-O).

2.5.3.2 Benzoyl pyrene terminated poly(ether hexafluoroisopropylidene ether ketone ketone) (2.5)

A solution of potassium carbonate (508 mg, 0.65 mmol), DMAc (30 mL) and toluene (25 mL) was heated under reflux for 1 h with azeotropic distillation of water. 1,3-bisfluorobenzoylbenzene (1.038 g, 2.95 mmol), 4'4-hexafluorobisphenol (1.095 g, 3.25 mmol) and **2.1** (195 mg, 0.60 mmol) were added and heated over 4 h under reflux and the

toluene-water azeotrope was removed. The reaction mixture was heated at reflux for 16 h before being cooled and the product precipitated in brine and then filtered off. The precipitate was dissolved in CHCl$_3$ and then re-precipitated in MeOH, filtered off, and dried at 120 °C under vacuum for 16 h to afford **2.5** as a colourless solid (1.22 g, 52%).

2.5
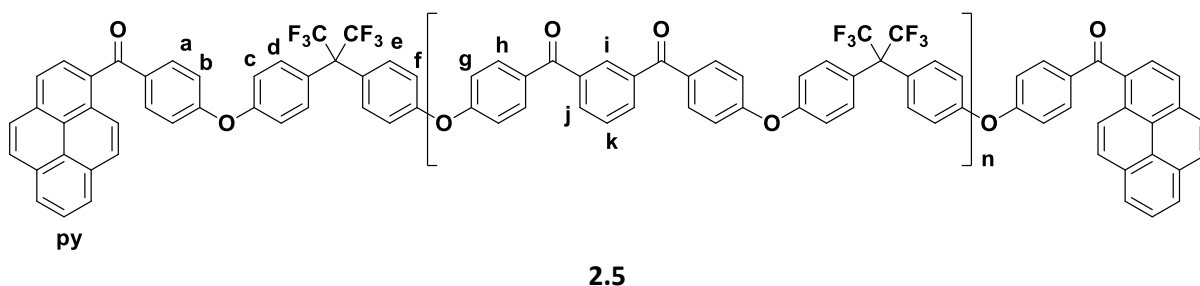
T_g: 143 °C; η_{inh} (H$_2$SO$_4$): 0.12 dL g^{-1}; ^{1}H NMR (700 MHz, CDCl$_3$/(CF$_3$)$_2$CHOH 6:1 v/v): δ (ppm) 8.34-8.10 (m, 10H py), 8.08 (s, *J* = 8.0, 10H **i**), 8.06-8.02 (m, 8H, py), 7.99 (d, *J* = 7.6, 20H **j**), 7.91 (d, *J* = 8.4, 4H **a**), 7.84 (d, *J* = 8.8, 40H **e**), 7.69 (t, *J* = 7.6, 10H **k**), 7.48 (d, *J* = 8.4, 40H **h**), 7.21 (m, 8H **b**), 7.15-7.11 (m, 80H **g, f**) ppm; ^{13}C NMR (175 MHz, CDCl$_3$/(CF$_3$)$_2$CHOH 6:1 v/v): δ (ppm) 198.5, 132.6, 156.2, 138.1, 134.4, 133.6, 132.4, 131.3, 130.1, 129.4, 126.0, 125.9, 123.2, 123.1, 120.3, 120.3, 120.0, 118.5, 117.6, 117.5, 117.5; IR: ν_{max} / cm^{-1} 1660 (C=O), 1594, 1500 (C=C Ar), 1244 (C-O), 1170 (C-F).

2.5.3.3 Poly(ether hexafluoroisopropylidene ether ketone ketone) (2.6)

This polymerisation was carried out using the same conditions as for **2.5**, but using the following monomers 1,3-bisfluorobenzoylbenzene (1.048 g, 3.23 mmol), 4'4-hexafluorobisphenol (1.00 g, 2.93 mmol) and 4-hydroxybenzophenone (115 mg, 0.590 mmol) to afford **2.6** as a colourless powder (1.69 g, 76%).

2.6
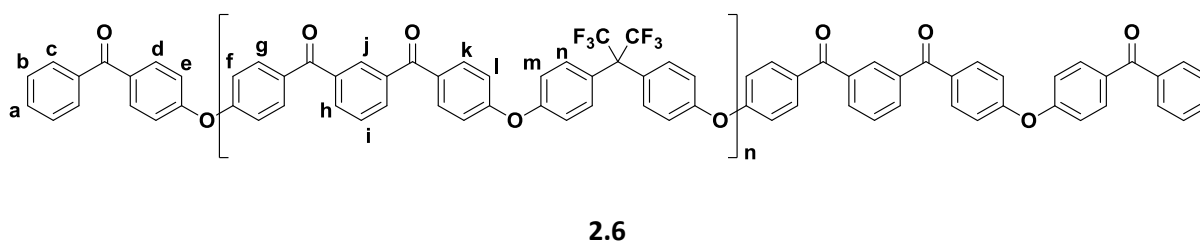
T_g: 143 °C; η_{inh} (H$_2$SO$_4$): 0.14 dL g^{-1}; ^{1}H NMR (700 MHz, CDCl$_3$/(CF$_3$)$_2$CHOH 6:1 v/v): δ (ppm) 8.09 (s, 7H (expected 11H), **j**), 8.01-7.73 (m, 76H (expected 74H), **c, d, g, h, k**), 7.70 (t, *J* = 4.0, 11H **i**), 7.75 (t, *J* = 4.0, 4H (expected 6H) **a, b**), 7.50 (d, *J* = 4.0, 40H **n**), 7.22 (d, *J* = 0.4, 4H, **e**),

7.15-7.10 (m, 84H **f, l, m**); ^{13}C NMR (175 MHz, CDCl$_3$/(CF$_3$)$_2$CHOH 6:1 v/v): δ (ppm) 198.2, 162.2, 155.7, 135.6, 137.5, 134.0, 133.1, 132.1, 130.8, 130.8, 129.7, 129.0, 128.6, 125.4, 125.4, 122.6, 122.6, 119.9, 119.8, 119.8, 119.7, 119.6, 119.5, 117.9, 117.0, 117.0, 117.0, 116.9; IR: v$_{max}$ / cm^{-1} 1660 (C=O), 1594, 1500 (C=C, Ar), 1238 (C-O), 1170 (C-F).

2.5.3.4 Benzoyl pyrene functionalised poly(ether hexafluoroisopropylidene ether sulfone) (2.7)

This polycondensation was carried out under the same conditions as for **2.5**, using the following monomers bis(4-chlorophenyl)sulfone (1.96 g, 6.82 mmol), 4'4-hexafluorobisphenol (2.09 g, 6.21 mmol) and 4-hydroxybenzoylpyrene (0.40 g, 1.24 mmol), to afford **2.7** as a colourless powder (3.38 g, 76%).

2.7
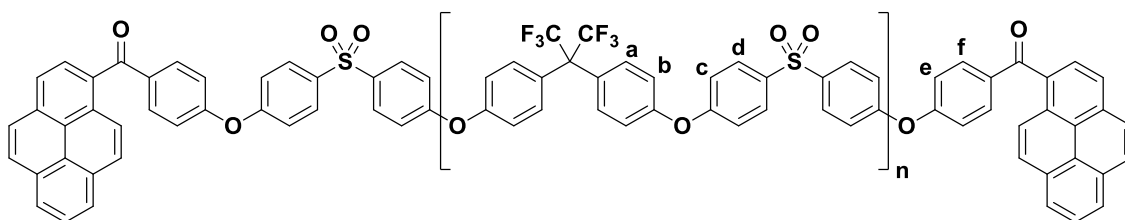
T_g: 157 °C; η$_{inh}$ (CHCl$_3$/(CF$_3$)$_2$CHOH 6:1 v/v): 0.17 dL g^{-1}; ^{1}H NMR (400 MHz, CDCl$_3$/(CF$_3$)$_2$CHOH 6:1 v/v): δ (ppm) 8.30-8.06 (m, 18H py), 7.91 (d, J = 8.8, 44H **d**), 7.87 (obscured d, 2H (expected 4H), **f**), 7.41 (d, J = 8.8, 40H **a**), 7.10 (d, J = 8.8, 44H **c**), 7.15 (d, J = 8, 2H (expected 4H), **e**) 7.03 (d, J= 9.2, 38H (expected 40H), **b**); ^{13}C NMR (100 MHz, CDCl$_3$/(CF$_3$)$_2$CHOH 6:1 v/v): δ (ppm) 174.1, 161.8, 155.9, 134.8, 133.9, 132.5, 130.0, 127.6, 127.3, 125.9, 125.8, 125.3, 119.8, 119.7, 39.0, 35.5, 20.5; IR: v$_{max}$ / cm^{-1} 1720 (C=O), 1580, 1485 (C=C Ar), 1241 (C-O), 1151 (S=O), 1104(C-F); GPC (RI, THF): M$_n$ = 4,000 M$_w$ = 24,000, Đ = 5.59.

2.5.3.5 4,4'-Bis(1,4-oxybenzoylpyrene)benzophenone (2.8)

This compound was prepared following the procedure for **2.5**, but in reduced quantity. Reagents and solvents were as follows: potassium carbonate (97 mg, 0.70 mmol), DMAc (15 mL), toluene (10 mL), 4,4'-dihydroxybenzophenone, (66 mg, 0.31 mmol) and **2.1** (100 mg, 0.62 mmol). The reaction mixture was cooled, precipitated in brine, filtered, washed with methanol then dried for 16 h at 100 °C *in vacuo* to give the title compound **2.8** as a colourless powder (0.137mg, 54%).
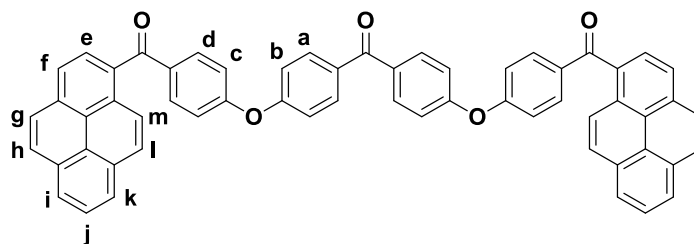
2.8

T_g (onset): 112 °C. T_m: 195-198 °C; HRMS (ESI) m/z: 823.2489 [$C_{59}H_{85}O_5Na^+$], calculated: 823.2479 [M+Na$^+$]; ^{1}H NMR (400 MHz, CDCl$_3$): δ (ppm) 8.34-8.22 (m, 10H **e, f, g, h, i**), 8.20-8.10 (m, 4H, **j, k**), 8.08-8.03 (m, 4H, **l, m**) 7.94 (d, J = 8.8, 4H **a**), 7.85 (d, J = 788, 4H **d**), 7.22 (d, J = 8.8, 4H **b**), 7.17 (d, J = 8.8, 4H **c**); ^{13}C NMR (100 MHz, CDCl$_3$): δ (ppm) 197.0, 160.5, 159.6, 134.4, 133.4, 133.1, 133.0, 132.4, 131.2, 130.7, 129.6, 129.6, 129.2, 128.9, 127.2, 126.6, 126.5, 126.1, 126.0, 124.8, 124.6, 124.4, 123.8, 118.8, 118.6; IR: ν_{max} / cm^{-1} 1758 (C=O), 1584, 1500 (C=C, Ar), 1238, 1152 (C-O).

2.5.4 Pyrene terminated poly(ether ether ketone ether ketone) (2.9)

A solution of oxydibenzoic acid (1.29 g, 5 mmol), 1,4 diphenoxybenzene (1.04 g, 4 mmol), and trifluoroacetic anhydride (1.5 mL) in trifluoromethanesulfonic acid (30 mL) was stirred for 16 h. Pyrene (1.01 g, 5 mmol) was added to the solution, which was then stirred for a further 20 h. The solution was precipitated dropwise into water and the solid was filtered off and washed with water until the washings tested neutral for pH. The precipitated polymer was then extracted in refluxing 20% EtOH solution, followed by refluxing 20% EtOH solution containing 1% NaOH, then washed with water, then finally extracted three times in refluxing acetone. The suspension was then filtered, and the polymer dried at 90 °C for 16 h to yield **2.9** as a yellow solid (2.10 g, 66%).

2.9
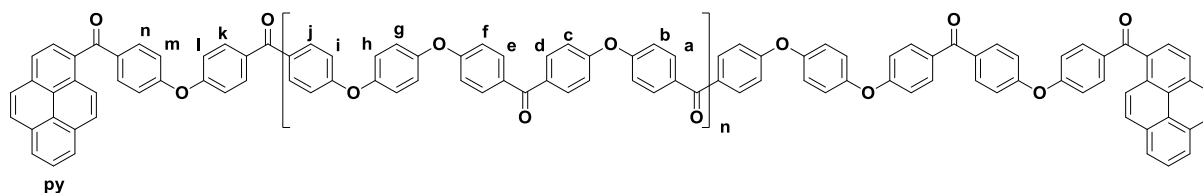
T_g: 155 °C; T_m: 342 °C; η_{inh} (H$_2$SO$_4$): 0.22 dL g^{-1}; ^{1}H NMR (400 MHz, CDCl$_3$/(CF$_3$)$_2$CHOH 6:1 v/v): δ (ppm) 8.34-8.06 (m, 6H, py), 7.94 (d, J = 8.8, 2H, py), 7.82 (app dd, J= 6.8, 2.0, 18H **a, d, e, j, k, n**), 7.21-7.14 (app q, J = 8.8, 6.4, 20H **b, c, f, i, l, m**), 7.09 (d, J = 8.8 8H **g, h**) ppm; ^{13}C NMR (100 MHz, CDCl$_3$/(CF$_3$)$_2$CHOH 6:1 v/v): δ (ppm) 134.2, 134.1, 133.2, 132.3, 131.6, 131.5,

130.9, 130.2, 130.2, 130.1, 129.9, 127.5, 127.1, 127.0, 126.8, 125,9, 124.65, 124.3, 124.2, 123.1, 122.4, 120.3, 119.3, 119.2, 117.5; IR: ν_{max} / cm^{-1} 1662 (C=O), 1587, 1511 (C=C, Ar), 1242, 1151 (C-O).

2.5.5 Macrocycle synthesis

2.5.5.1 4,4'-Bis[4-(3-aminophenoxy)benzenesulfonyl)-1,1'-biphenyl] (diamine,2.10)

3-Aminophenol (6.55 g, 60 mmol) was added to a refluxing suspension of K$_2$CO$_3$ (5.53 g, 40 mmol) in DMAc (250 mL) and toluene (100 mL). The solution was heated at reflux for 1 h, with Dean-Stark removal of water. 4-4' Bis(4-chlorobenzenesulfonyl)biphenyl (10.61 g, 20 mmol) was added to the solution and the remaining toluene was distilled off. The solution was then heated at 190 °C for 48 hours. The reaction mixture was cooled to room temperature, precipitated into distilled water (1 L) and the solid was filtered off and washed with water then MeOH. The precipitate was then dried under vacuum for 2 h at 110 °C. The crude product was recrystallized from 2-methoxyethanol to afford diamine **2.10** as a beige powder (11.0 g, 84.0%). This synthesis was also reproduced multiple times on a 25 g scale.
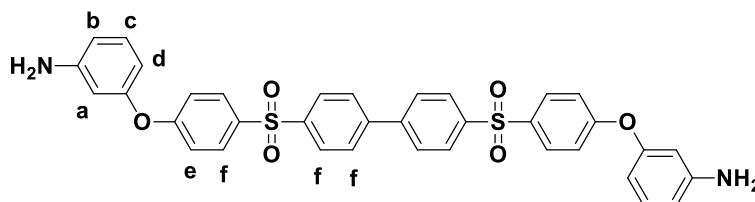
2.10

M.p. (DSC): 240 °C; HRMS (ESI) m/z: 649.1466 [C$_{18}$H$_{15}$O$_8$N$_2$S$_2$Na$^+$], calculated: 649.1462 [M+Na$^+$]; ^{1}H NMR (400 MHz, DMSO-d_6): δ (ppm) 8.05-7.94 (m, 12H **f**), 7.12 (d, J = 7.2, 4H **e**), 7.06 (t, J = 7.1, 2H **c**), 6.44 (d, J = 6.4, 2H **a**), 6.25 (t, J = 6.2, 2H **b**), 6.21 (d, J = 8, 2H **d**), 5.33 (s, 2NH$_2$); ^{13}C NMR (100 MHz, DMSO-d_6): δ (ppm) 161.9, 155.3, 150.8, 143.1, 141.4, 133.9, 130.4, 130.1, 128.6, 127.8, 117.8, 110.7, 106.8, 105.0; IR: ν_{max}/ cm^{-1} 3455 (N-H stretch), 3362 (N-H stretch), 1510 (N-H bend), 1486 (C=C, Ar) 1246 (C-O).

2.5.5.2 Cyclo-{4,4'-bis[4-(3-aminophenoxy)benzenesulfonyl]-1,1'-biphenyl-N,N'-bis(3-phenylene-pyromelliticdiimide}

(Pyromellitimide macrocycle, 2.11)

A solution of pyromellitic dianhydride (0.54 g, 2.5 mmol) and diamine **2.10** (1.62 g, 2.5 mmol) in anhydrous DMAc (50 mL) was added via syringe pump over 26 h into refluxing anhydrous DMAc (100 mL). After a further 24 h under reflux, the reaction mixture was cooled, was concentrated to 50 mL on the rotary evaporator, and precipitated into water (800 mL). The resulting solid was filtered off, washed with methanol, and dried under vacuum for 16 h at 100 °C. The product was purified using by column chromatography (8% ethyl acetate in DCM) to afford **2.11** as a pale yellow powder (0.42 g, 21%).
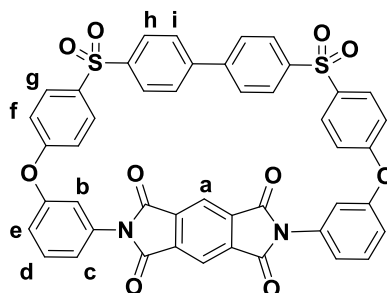
2.11

HRMS (ESI) m/z: 1683.1985 [$C_{92}H_{52}O_{20}N_4S_4Na^+$], calculated: 1683.1950 [$M+Na^+$]; ^1H NMR (400 MHz, $CDCl_3/(CF_3)_2CHOH$ 6:1 v/v): δ (ppm) 8.27 (s, 2H **a**), 8.01 (d, J = 8.0, 4H **h**), 7.97 (d, J = 8.8, 4H **g**), 7.73 (d, J = 8.0, 4H **i**), 7.62 (t, J = 8.4 2H **d**), 7.38 (dd, J = 8.0, 2, 2H), 7.24 (d, J = 9.2, 2H), 7.19 (d, J = 8.8, 2H), 6.62 (t, J = 4, 2H **b**); ^{13}C NMR (100 MHz, $CDCl_3/(CF_3)_2CHOH$ 6:1 v/v): δ (ppm) 165.2, 160.8, 157.4 144.0, 136.9, 135.4, 131.4, 131.1, 130.3, 128.3 125.5, 122.1, 121.0, 120.6, 119.5,117.1, 115.1; IR: v_{max} / cm^{-1} 3061 (C-H, Ar stretch), 1720 (C-O, amide), 1570 (C=C, Ar), 1368 (C-N) 1259 (C-O-C), 1152 (S=O) 1107 (C-N).

2.6 References

[1] G. Crevecoeur and G. Groeninckx, *Macromolecules*, 1991, **24**, 1190-1195.

[2] R. J. Karcha and R. S. Porter, *J. Polym. Sci: Part B: Polym. Phys.*, 1993, **31**, 821-830.

[3] B. W. Greenland, S. Burattini, W. Hayes and H. M. Colquhoun, *Tetrahedron*, 2008, **64**, 8346-8354.

[4] A. J. Zych and B. L. Iverson, *J. Am. Chem. Soc.*, 2000, **122**, 8898-8909.

[5] D. Williams and I. Fleming, *Spectroscopic Methods in Organic Chemistry,* McGraw-Hill, New York, 6th Edition, 2008.

[6] H. Q. Nimal Gunaratne, C. Richard Lagrick, A. V. Puga, K. R. Seddon and K. Whiston, *Green Chem.,* 2013, **15**, 1166.

[7] F. M. Winnik, *Chem. Rev.* 1993, **93**, 587-617.

[8] H. M. Colquhoun and D. F. Lewis, *Polymer*, 1988, **29**, 1902-1908.

[9] R. G. Harvey, J. Pataki and H. Lee, *Org. Prep. Proc. Int.,* 1984, **16**, 144-148.

[10] R. Flamholc, D. Plazuk, J. Zakrzewski, R. Metivier, K. Nakatani, A. Makal and K. Wozniak, *RSC Adv.*, 2014, **4**, 31594-31601.

[11] J. K. Stille, *J. Chem. Ed.,* 1981, **58**, 862-866.

[12] T. Yamashita, H. Tomitaka, T. Kudo, K. Horie and I. Mita, *Polym. Degrad. Stabil.*, 1993, **39**(1), 47-54.

[13] R. G. Gilbert, M. Hess, A. D. Jenkins, R. G. Jones, P. Kratochvíl, and R. F. T. Stepto. *Pure Appl. Chem.*, 2009, **81**, 351-353.

[14] P. Hodge and S. D. Kamau, *Angew. Chem. Int. Ed. Engl.*, 2003, **42**, 2412-2414.

[15] J. Huand and M. Kertesz, *J. Am. Chem. Soc.*, 2007, **129**, 1634-1643.

[16] T. F. A. De Greef, M. M. J. Smulders, M. Wolffs, A. P. H. J. Schenning, R. P. Sijbesma and E. W. Meijer, *Chem. Rev*., 2009, **109**, 5687-5754.

[17] S. Nagaoka, *J. Chem. Educ.*, 2007, **84**, 801.

[18] L.R. Hart, N.A. Nguyen, J.L. Harries, M.E. Mackay, H.M. Colquhoun and W. Hayes, *Polymer*, 2015, **69**, 293-300.

Chapter 3

Blends of end-capped poly(aryl ether ketone)s with chain-folding polyimides as matrices for composites

3.1 Abstract

A supramolecular polymer blend formed via π-π stacking interactions between π-electron rich PAEKs and a π-electron deficient sulfonyl-biphenyl polyimide is described herein. The T_g of the PAEKs increased with the addition of the polyimide in the blend. A blend which exhibited a single, broad T_g has been synthesised, indicating that a substantially compatible blend was produced. Systematic changes in the structure of the polyimide, namely the incorporation of an all-aromatic m-terphenylene co-monomer and pairs of π-electron poor pyromellitic diimide units has further increased the T_g of the PAEK in the blend. A pilot scale supramolecular polymer blend consisting of a pyrene-terminated PEKK and m-terphenylene polyimide was synthesised and used as the binding polymer for samples of carbon fibre composites. Mechanical properties of the supramolecular polymer composites were measured against commercial PEKK composites.

3.2 Introduction

Carbon fibre reinforced polymers are lightweight composite materials that can achieve a very high level of strength and toughness. The binding polymers are often thermoset resins such as epoxies, but thermoplastic polymers such as PAEKs (Figure 3.1) are also used.[1] By using PAEK-based composites, manufacturers could eliminate the additional step of curing epoxies in autoclaves. PAEKs show excellent mechanical properties, high thermal stability and good resistance to chemical degradation.[2] Moreover, thermoplastic composites made from PAEKs can achieve very much higher levels of toughness than cross-linked, thermoset materials, even when the latter are toughened with reactive thermoplastic additives.[3]

Figure 3.1. Some industrially useful PAEKs.

The main reason for the toughness of thermoplastics such as PEEK™ is the linear nature of the polymer structure,[4] and crystallinity in these thermoplastics results in high melting temperatures, strength, stiffness and solvent resistance.[5] However, the insolubility of PEEK™ in organic solvents makes solution-prepregging into carbon fibre very difficult (a prepreg is a fibrous material to which a resin has been applied, prior to fabrication of the final composite structure). The very high melt viscosity of PEEK™ also inhibits good fibre-wetting and coating of carbon fibre by the polymer during composite production.[6]

In order to overcome the difficulties of achieving good surface-wetting of a carbon fibre tow (an untwisted bundle of continuous filaments that is commonly woven into carbon fibre fabrics), one current approach is to reduce the viscosity of PEEK™ by dissolving it in diphenyl sulfone at or near the polymer melting point (340 °C).[7] This solution is then used to suffuse the tow and the solvent is then removed and recycled by sublimation at around 400 °C.[8] A different approach involves the dispersal of micronized PEEK™ in water, and using the resulting low-viscosity suspension for prepregging.[9] These approaches can both achieve a good prepreg, but do not address the difficulty of consolidating a composite with a high melt viscosity matrix. As such, the molecular weight of the matrix polymer must be carefully specified so that it is low enough for composite processing to be possible, while being just high enough to retain a reasonable level of toughness.[10]

The present work was motivated by the potential use of supramolecular self-assembly in a thermoplastic matrix. This novel approach involves the use of a low molecular weight polymeric additive that is designed to act as a plasticiser and flow promoter at high temperatures. The use of such an additive will thus enhance melt processing of the composite. At low temperatures, the additive is designed to behave as a non-covalent cross-linking agent. This would enhance the effective molecular weight of the polymer matrix and the material could thus demonstrate higher modulus and higher levels of toughness.

Recent work[11] has shown that polymer blends in which electron-rich chain termini of one polymer intercalate into the electron-poor chain folds of a second polymer can be both compatible and readily-healable. In the present work, this concept is extended to polymer systems in which high levels of thermal and mechanical performance might be expected, namely blends of a functionalised, semi-crystalline PAEK and a chain-folding polyimide.

3.3 Results and discussion

The novel PAEKs described in this chapter are end-functionalised by pyrenyl substituents and these give the polymer π-electron rich functionality. The pyrenyl functionality has been shown to form a π-π stacked intermolecular "bond" with electron-deficient diimide groups, as discussed in Chapter 2. The present chapter explores the results of extending this concept of self-assembly to blends of aromatic PAEKs and chain-folding polyimide systems.

3.3.1 Polymer synthesis

Two semi-crystalline PAEKs (Figure 3.2) were prepared by high-temperature polycondensation of 4,4'-dihydroxybenzophenone with 1,3-bis(4-fluorobenzoyl)benzene in diphenyl sulfone. The only difference between the two polymers is in their terminal groups. One polymer was synthesised with 1-oxypyrene terminal group (**3.5**), while the other was terminated with 4-oxybenzoyl benzene end-group (**3.6**) which display no π-stacking functionality and thus act as a control for **3.5**. The syntheses of these polymers were discussed in detail in Chapter 2.
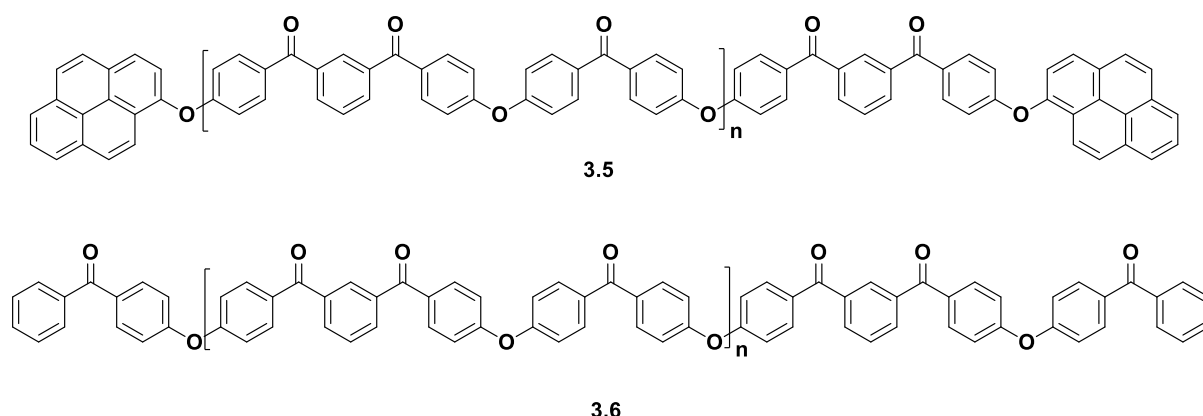

3.5

3.6

Figure 3.2. Structure of pyrenyl-capped PAEK **3.5** and unfunctionalised PAEK **3.6**.

Inherent viscosities (η_{inh}) measured on 0.1% solutions in H_2SO_4 gave an indication of the relative molecular weights of the PAEKs. Polymer **3.5,** with η_{inh} of 0.38 dL g^{-1} was synthesised by including 2 mol% of 1-hydroxypyrene terminal groups in the polycondensation. This was designed to control the molecular weight as well as to functionalise the polymer. The end-groups clearly represent only a very small proportion of the polymer by weight, and so can be relatively costly without greatly affecting the cost of polymer production. Similarly, polymer **3.6** was synthesised with the incorporation of 2 mol% of 4-hydroxybenzophenone in the polycondensation and had η_{inh} of 0.30 dL g^{-1}. The η_{inh} values agree, qualitatively, with those expected for capped polymers of medium to high molecular weight (0.3 - 0.5 dL g^{-1}).

The T_g values of both polymers were identical, at 153 °C. The aim of this study was then to introduce an additive, in this case an amorphous chain-folding polymer containing electron deficient diimide moieties into which the terminal groups of **3.5** can intercalate. Since T_g is a property of the amorphous phase, and the terminal groups are located in the amorphous region of the PAEK, the polyimide would be expected to raise the T_g of the PAEK in the blend. Additionally, the polymer blend would exhibit *pseudo*-high molecular weight in ambient temperatures as the two polymers are physically and reversibly (but not chemically) cross-linked. Figure 3.3 shows a graphical representation of this reversible supramolecular interaction between the two polymers.
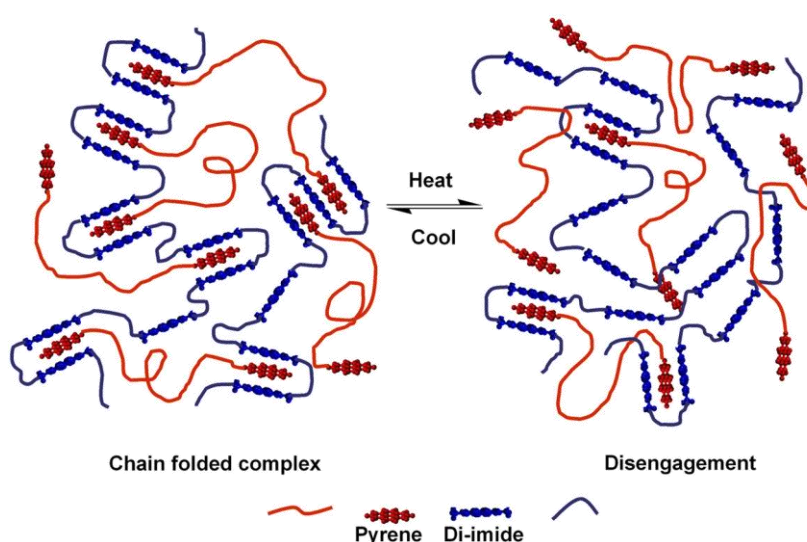

Figure 3.3. Schematic representation of the reversible supramolecular interaction between a pyrene-functionalised PAEK and a polyimide. (Schematic reproduced with permission of H. M. Colquhoun.)

3.3.2 Polymer blends with a polyimide from pyromellitic anhydride

3.3.2.1 Polyimide synthesis

The functionalised PAEK with its electron-rich terminal groups was to be blended with electron deficient polyimides. The polyimides were synthesised by a two-step reaction between a diamine and a dianhydride, as shown in Scheme 3.1. The first step is the formation of poly(amic acid) at ambient temperature in a polar aprotic solvent. The poly(amic acid) is then isolated as a solid film before thermal ring closure and imidisation via dehydration at high temperatures.[12]
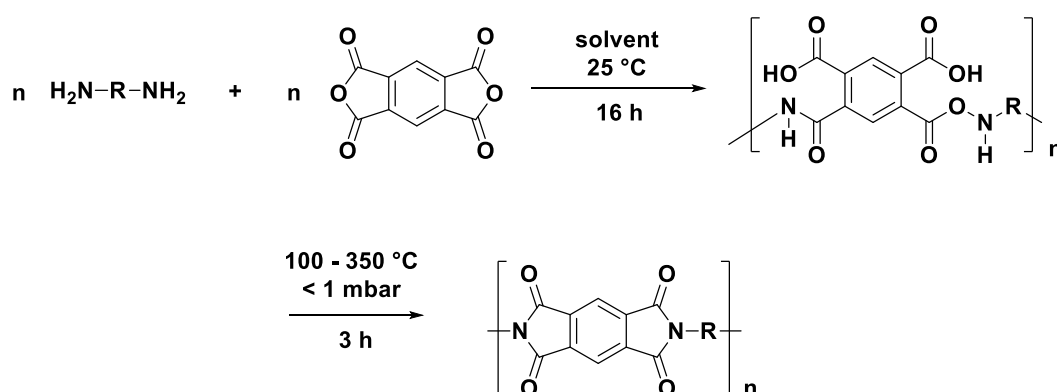
Scheme 3.1. Representative two-stage synthesis of a polyimide by reaction of pyromellitic dianhydride with a diamine via the poly(amic acid). The solvent is generally a dipolar aprotic solvent such as DMF or DMAc.

The first polyimide studied in this series was a poly(imide-sulfone) **3.9** formed from the imidisation of a biphenylene-disulfone diamine (**3.2**) and pyromellitic dianhydride (Figure 3.4). Polyimide **3.9** was found to have a T_g of 283 °C and an η_{inh} of 0.37 dL g^{-1}. This polymer has previously been shown to have electron-deficient chain-folds which provide binding sites for complementary electron-rich pyrenyl tweezer-type molecules.[13]
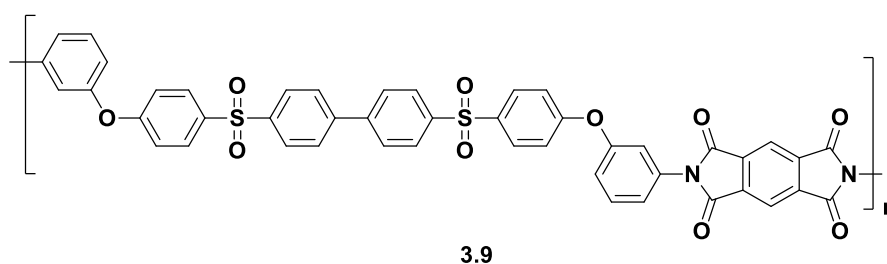
3.9

Figure 3.4. Structure of polyimide **3.9**.

A computational model of the supramolecular interaction, shown in Figure 3.5, suggested that the two polymers **3.5** and **3.9** could potentially form a compatible blend. It is expected that the intercalation of the end-groups of **3.5** into the chain-folds of **3.9** can only occur in the amorphous phase, where the functionalised chain ends are necessarily found. Thus, the likewise amorphous high-T_g polyimide **3.9** will potentially have the effect of increasing the T_g of **3.5**. The resulting T_g of the polymer blend would be a weighted average of the T_g of the individual polymers comprising the blend. For instance, in a 75/25 wt/wt blend of **3.5** and **3.9**, perhaps 50% of the PAEK will exist in the crystalline phase. It follows that the amorphous phase will therefore comprise **[3.5·3.9]** in a 37.5:25 weight ratio, giving an expected weighted average T_g for the blend of *ca.* 220 °C.
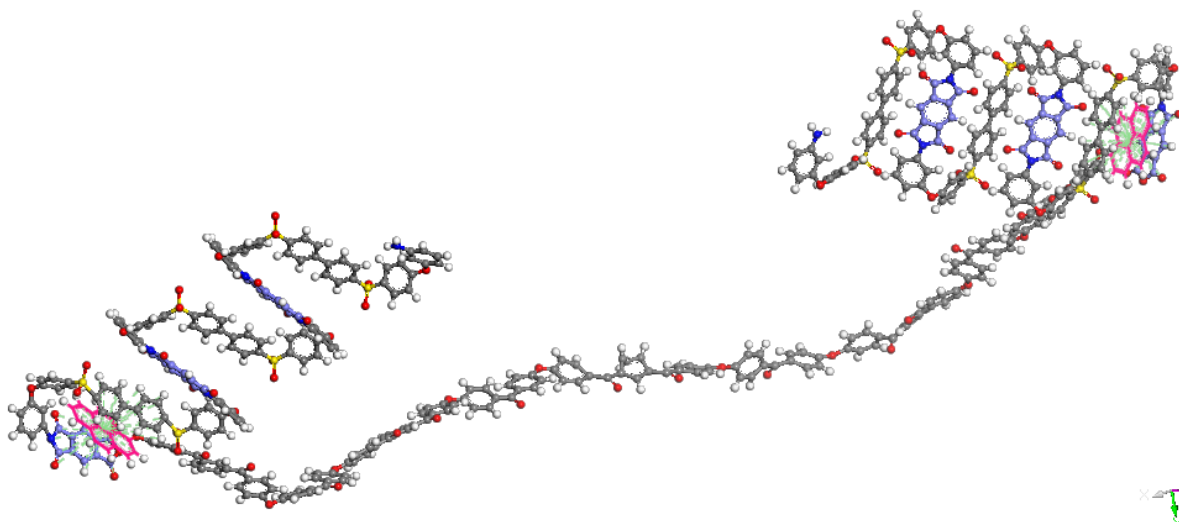

Figure 3.5. Computational model showing geometry optimisation (molecular mechanics) of the interacting polymers in blend **[3.5·3.9].** The pyrenyl terminal groups of **3.5** (magenta) are shown to be intercalated into the complementary chain folds of the polyimide **3.9** (blue).

The η_{inh} measurements suggest that **3.5** has a slightly higher molecular weight than **3.6**. These PAEKs were synthesised with a chain-terminating unit in the polymerisation thus limiting the molecular weight. The two PAEKs have similar melting points (Table 3.1). Conversely, polyimide **3.9** was designed to have a relatively low molecular weight for an uncapped polyimide.[14] In this way, the polyimide may act as a plasticiser for the PAEK in the blend, and later in the fabrication of carbon fibre composites. Polyimide **3.9** did not show a melting point within the temperature range studied (20 °C to 400 °C) and is thus considered

amorphous. A summary of η_{inh} values and phase transition temperatures of the three polymers is given in Table 3.1.

Table 3.1. Inherent viscosity values and phase transition temperatures of PAEKs and polyimide.

Polymer	η_{inh}^{a} / dL g^{-1}	T_g^{b} / °C	T_m / °C
3.5	0.38	153	299
3.6	0.30	151	300
3.9	0.37	283	–

^{a} η_{inh} was measured in a capillary viscometer for 10 g dm^{-3} solutions (**3.5** and **3.6** in 96% H_2SO_4 and **3.9** in NMP).
^{b} T_g and T_m were measured from DSC second heating scans, 10 °C min^{-1}.

3.3.2.2 Polymer blends in 1:1 weight ratio

Polymer blends were prepared by dissolving both components to give a 10% (w/v) solution in CHCl$_3$/HFiPA (6:1 v/v). The blend was then precipitated in methanol, filtered, extracted with methanol, and finally dried. The first two blends were 50/50 w/w ratio for both **[3.5·3.9]** and the control blend **[3.6·3.9]**. The thermal behaviour of the blends was then characterised by DSC in terms of their T_g values. The T_g of a fully compatible blend, is a single weight-average of its individual components, but incompatible or partly-compatible blends would show two T_g values.[15]

Figure 3.6 shows the DSC thermograms of **[3.5·3.9]** and its individual parent polymers. It can be observed that the blend **[3.5·3.9]** exhibits two T_gs, one for each of the corresponding polymers that make up the blend. This clearly indicates that **3.5** and **3.9** do not form a fully compatible blend, but it is noteworthy that the T_g arising from PAEK **3.5** has increased by some 5 °C in the blend. Conversely, the T_g of **3.9** has decreased considerably (by approximately 40 °C) in the blend, implying that the PAEK is more soluble in the polyimide than vice-versa.
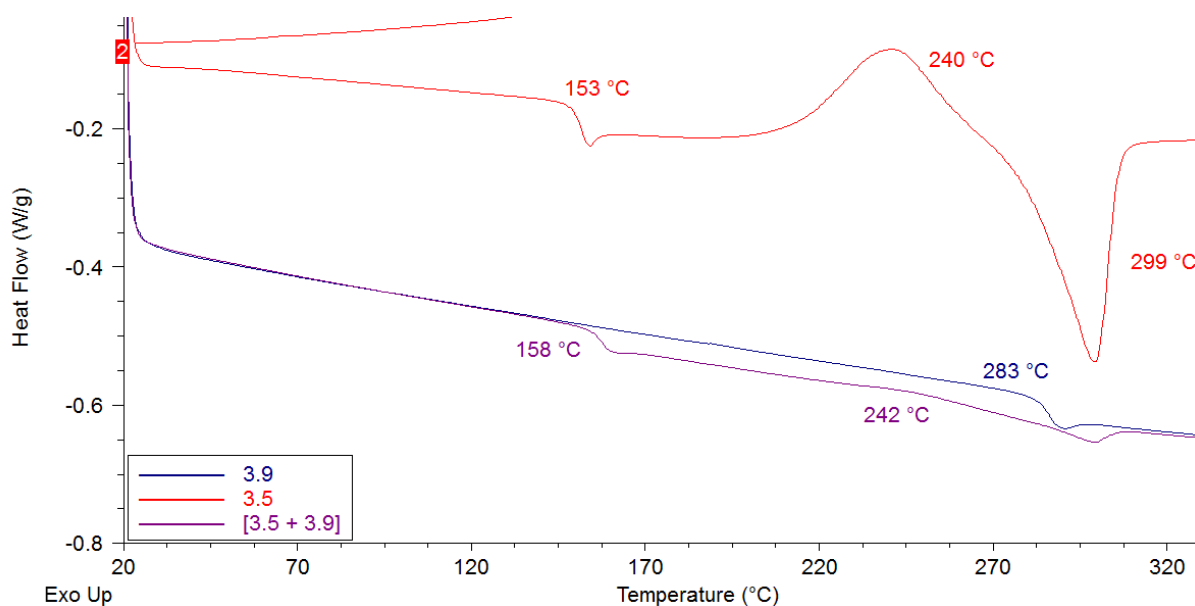
Figure 3.6. Partial DSC thermograms of polymers **3.5** (red), **3.9** (blue) and **[3.5·3.9]** (purple), showing the T_gs of the polymers and blend (second heating scan, 10 °C min^{-1}). Polymer **3.5** shows a T_{cc} at 240 °C and a T_m at 299 °C.

For comparison, the DSC thermogram of the control blend **[3.6·3.9]** is shown in Figure 3.7. This control blend also displayed two T_gs indicating that **3.6** and **3.9** also formed an incompatible blend. For blend **[3.6·3.9]**, the T_g of the PAEK has also increased by some 5 °C, similar to the pyrenyl blend. In contrast, the T_g of the polyimide in the control blend decreased only by some 13 °C. These results indicate that the PAEK terminated with 1-oxypyrene forms a more compatible blend with polyimide **3.9** than does the unfunctionalised PAEK.
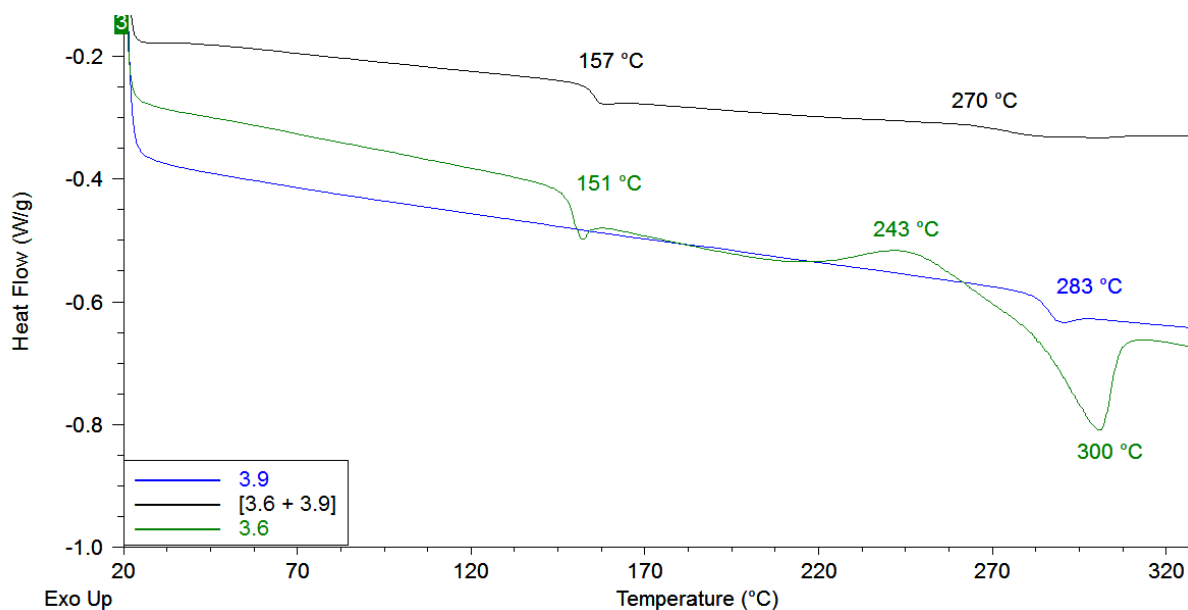
Figure 3.7. Partial DSC thermograms of **3.6** (green), **3.9** (blue) and **[3.6·3.9]** (black), showing the T_g of the polymers and blend (second heating scan, 10 °C min^{-1}). Polymer **3.6** shows a T_{cc} at 243 °C and a T_m at 300 °C.

3.3.2.3 Series of blends with different ratios of polymers

A series of blends which contained varying ratios of PAEK **3.5** to polyimide **3.9** were investigated in order to determine whether a different ratio of the two polymers would produce a more compatible blend. Blends of **[3.5·3.9]** were thus prepared containing 1:10, 1:3, 1:1, 3:1 and 10:1 weight ratios of **3.5** to **3.9**. The thermal behaviour across the series of blends is shown in Figure 3.8. The T_g of **3.5** alone was measured as 153 °C. It can be observed that the T_g of the PAEK in the blends increases with addition of polyimide **3.9**. This can be seen in every one of the blends, even a marginal increase with just addition of 10% **3.9**. However, across the series, over the entire composition range studied, the blends exhibited two glass transition temperatures. This indicates that PAEK **3.5** and polyimide **3.9** do not form a fully compatible blend. It has been reported that the crystallisation of miscible polymer blends can cause a phase segregation leading to the expression of two different T_gs corresponding respectively to the two single phases.[16,17] In this present work, the biggest increase in the PAEK T_g was observed for the blend with 1:3 **[3.5·3.9]** with an increase of 13 °C. It was also observed that the crystallinity of the PAEK **3.5** decreases with addition of more polyimide. In case of blends comprising greater than 50% **3.5** (10:1 and 3:1), the T_{cc} and T_m of **3.5** are clearly observed. The T_m peaks of **3.5** may be obscuring the T_g of polyimide

3.9 in the blend. In the blends with less than 50% **3.5** (1:3 and 1:10), there are no observable peaks assigned to T_{cc} or T_m.
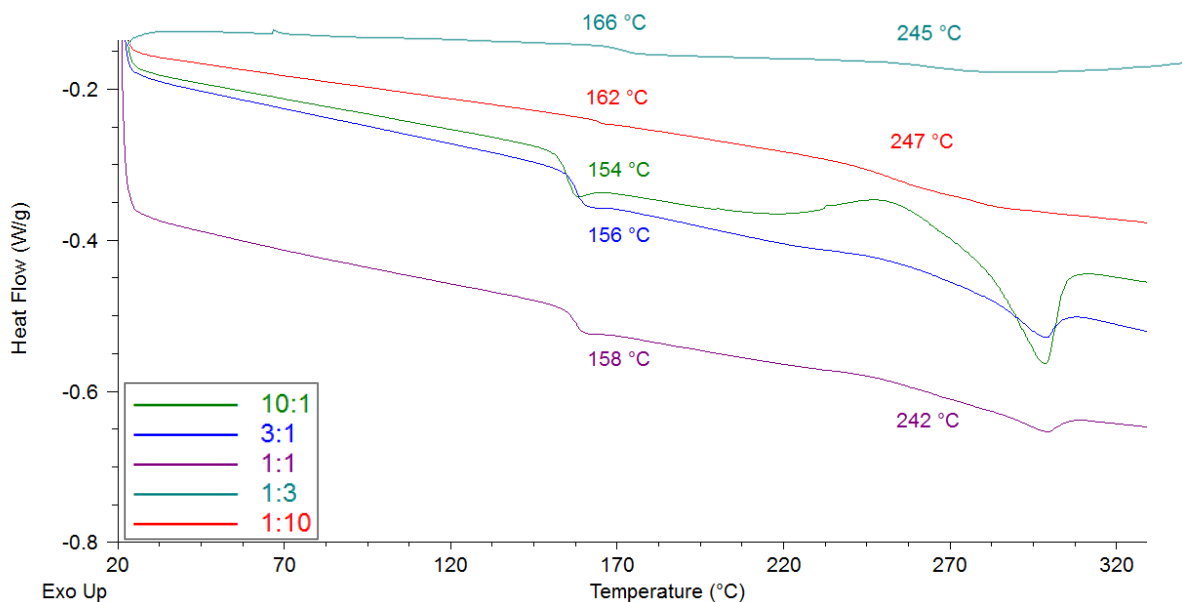

Figure 3.8. Partial DSC thermograms of **[3.5·3.9]** (second heating scan, 10 °C min^{-1}). Legend indicates the w/w ratios of **3.5**:**3.9**.

3.3.3 Blend of a PAEK with a naphthalene-diimide based copolymer

Further to the results of the blending studies with **3.9**, it was postulated that a polyimide containing a more strongly π -stacking co-monomer would bind more effectively to the pyrenyl terminal groups of **3.5**. Thus, co-polyimide **3.10** was synthesised by polycondensation of the chain-folding diamine **3.2** with equimolar quantities of naphthalene and pyromellitic dianhydrides (Figure 3.9).
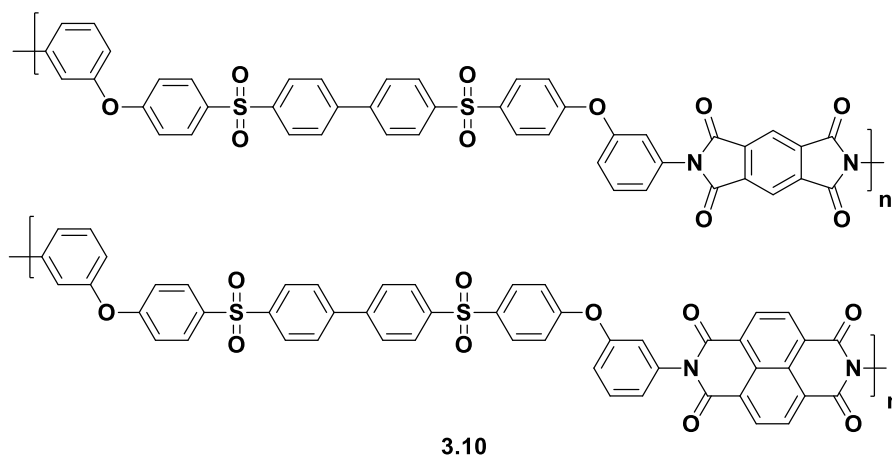
3.10

Figure 3.9. Structure of co-polyimide **3.10**, synthesised from co-monomers pyromellitic dianhydride and 1,4,5,8-naphthalenetetracarboxylic dianhydride in a 1:1 molar ratio.

Co-polyimide **3.10** was synthesised under similar polymerisation conditions as for **3.9**, with a 1:1 molar ratio of pyromellitic dianhydride and 1,4,5,8-naphthalenetetracarboxylic dianhydride. The T_g of **3.10** was measured as 309 °C. The pyrene-terminated PAEK **3.5** was then solution-blended with **3.10** as per the previously described methods to afford blend **[3.5·3.10]**. The phase transitions of this blend were analysed by DSC (Figure 3.10). It was found that in the blend, the T_g of the PAEK has increased by only 2 °C, from 153 °C to 155 °C. It was also observed that the blend has two T_g's with the T_g for **3.10** decreasing by some 22 °C in the blend. It is clear that polymers **3.5** and **3.10** do not form a compatible blend, despite the incorporation of a more electron deficient co-monomer in naphthalene dianhydride.
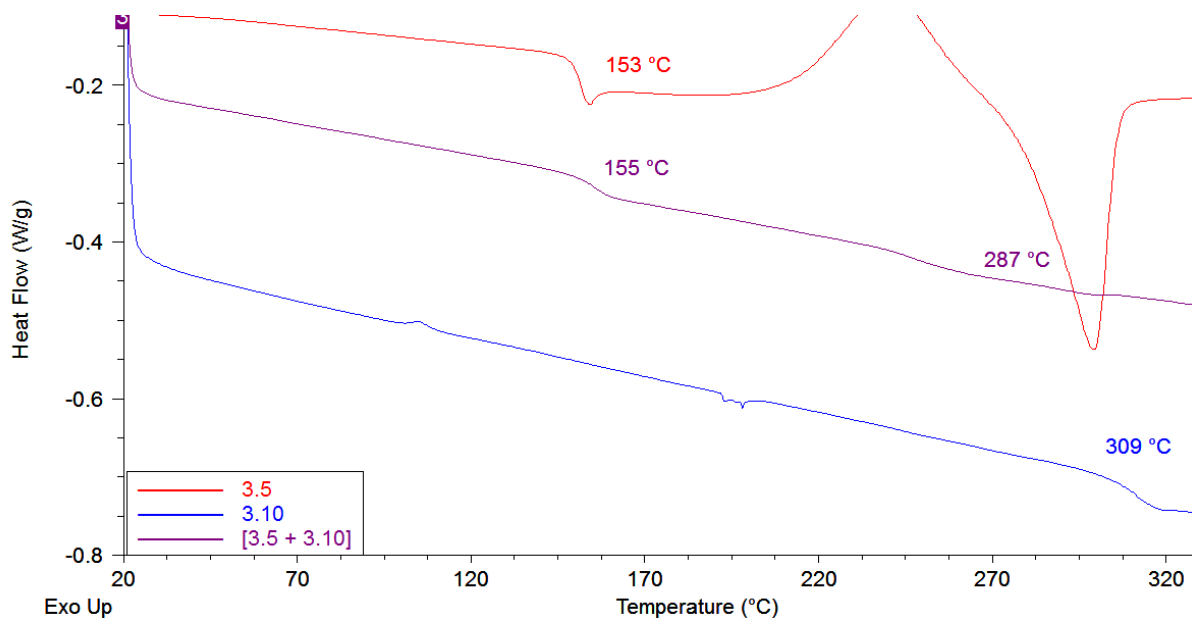
Figure 3.10. DSC thermograms (second heating scan, 10 °C min^{-1}) of PAEK **3.5** (red), polyimide **3.10** (blue) and blend **[3.5·3.10]** (purple).

3.3.4 Blends of PAEKs with a co-polyimide based on *m*-terphenylene diamine

The next polyimide (**3.11**) to be explored contained a new type of chain-fold with potentially stronger binding characteristics. This novel chain-fold is based on *m*-terphenylene diamine and contains two imide units forming a binding site (Figure 3.11). Introducing *m*-terphenylene diamine as a co-monomer also allows a more precise definition of the number and density of chain-folded binding sites. Previous work[18] has shown that two adjacent diimide residues produce much stronger binding of pyrenyl units than the diimide-biphenylenedisulfone chain-fold present in polyimide **3.9**.
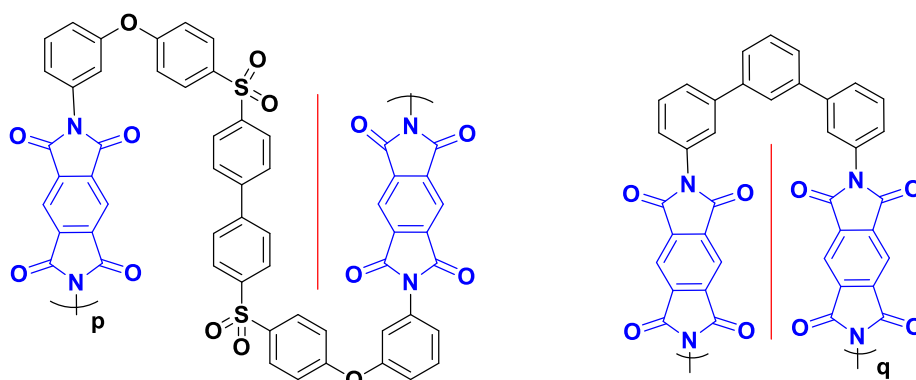

Figure 3.11. A comparison of the two different binding sites in polyimide **3.11**. The incorporation of 20 mol% of the *m*-terphenylene co-monomer results in two diimide units forming a chain-folding binding site (shown at the right). The red line represents a pyrenyl group intercalating into the binding site of the polyimide.

The synthesis of *m*-terphenylene diamine was achieved by Suzuki coupling.[19] First, the dinitro precursor (**3.3**) is obtained from the reaction of 1,3-dibromobenzene with an excess of 3-nitrophenylboronic acid in the presence of palladium acetate as catalyst. The resulting dinitro compound is then reduced with a poly(hydrosiloxane) to yield the *m*-terphenyl diamine (**3.4**). Scheme 3.2 shows the two-step synthesis of **3.4**.
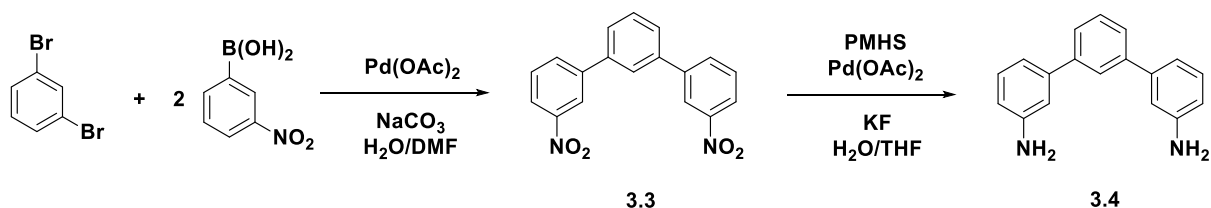
Scheme 3.2. Synthesis of *m*-terphenylene diamine **3.4** from the reduction of **3.3** with palladium (II) acetate as catalyst and polymethylhydrosiloxane (PMHS) as the reducing agent.

The co-polyimide **3.11** (Figure 3.12) was synthesised using similar conditions to **3.9**, but with the incorporation of 20 mol% *m*-terphenylene diamine as co-monomer. The inclusion of this diamine as a co-monomer retains the all-aromatic character of the polyimide and so should maintain the thermo-oxidative stability and high T_g characteristics of polyimides.

3.11
(p = 4, q = 1)
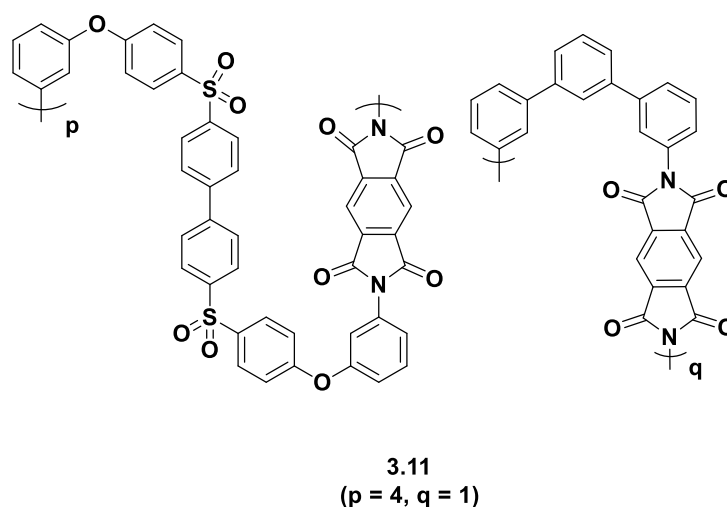
Figure 3.12. Structure of co-polyimide **3.11** (p = 4, q = 1).

Co-polyimide **3.11** was solution-blended with the pyrenyl-PAEK **3.5** (1:1 weight ratio) using the blending procedure previously described, to form blend **[3.5·3.11]**. Figure 3.13 shows the DSC thermogram of blend **[3.5·3.11]**, in which only a single, broad T_g was observed for the blend. The T_g of **3.5** (153 °C) is increased by 20 °C upon incorporation of polyimide **3.11** in the blend. The incorporation of 20% *m*-terphenylene co-monomer with its two diimide

units per binding site has thus produced a significant improvement in the T_g of the PAEK in blend **[3.5·3.11]** compared with the situation in which there is only one diimide per binding site, in blend **[3.5·3.9]**. The additional diimide unit clearly produces a stronger π-π stacking interaction between the 1-oxypyrene end groups of PAEK **3.5** and the diimide units in the polyimide **3.11**. However, it must be emphasised that the new T_g of 173 °C is not a weight average of the two copolymers in the blend. Indeed it is well below the expected T_g of a 1:1 weight ratio blend, and further work is required to investigate the reasons for this. Nevertheless, blend **[3.5·3.11]** gave the most significant results, in terms of enhancing the lower of the two original T_gs, of the three polyimides studied in blends with the pyrene-ended PAEK **3.5**.
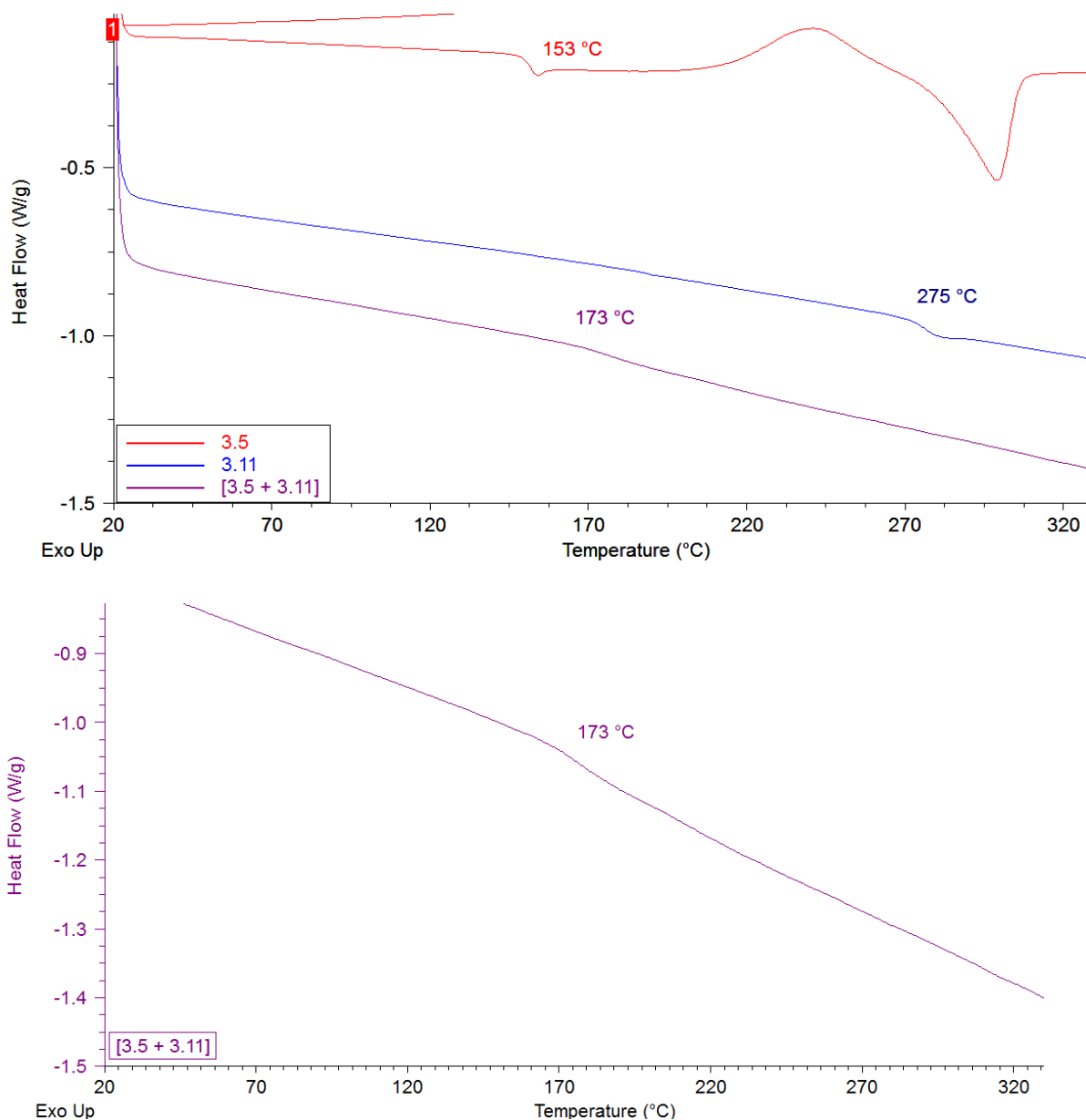
Figure 3.13. Top: DSC thermograms (second heating scan, 10 °C min^{-1}) showing PAEK **3.5** (red), polyimide **3.11** (blue) and blend **[3.5·3.11]** (purple). Bottom: Vertical expansion of DSC thermogram of blend **[3.5·3.11]**.

As a comparison, polyimide **3.11** was solution blended with the control PAEK **3.6** to form blend **[3.6·3.11]**. The DSC thermogram of blend **[3.6·3.11]** (Figure 3.14) shows the T_g of the PAEK **3.6** has increased some 12 °C in the blend compared with the non-blended sample. However, the blend displayed two T_gs, corresponding to both of its polymeric components. This indicates that blend **[3.6·3.11]** has not formed a fully compatible blend.
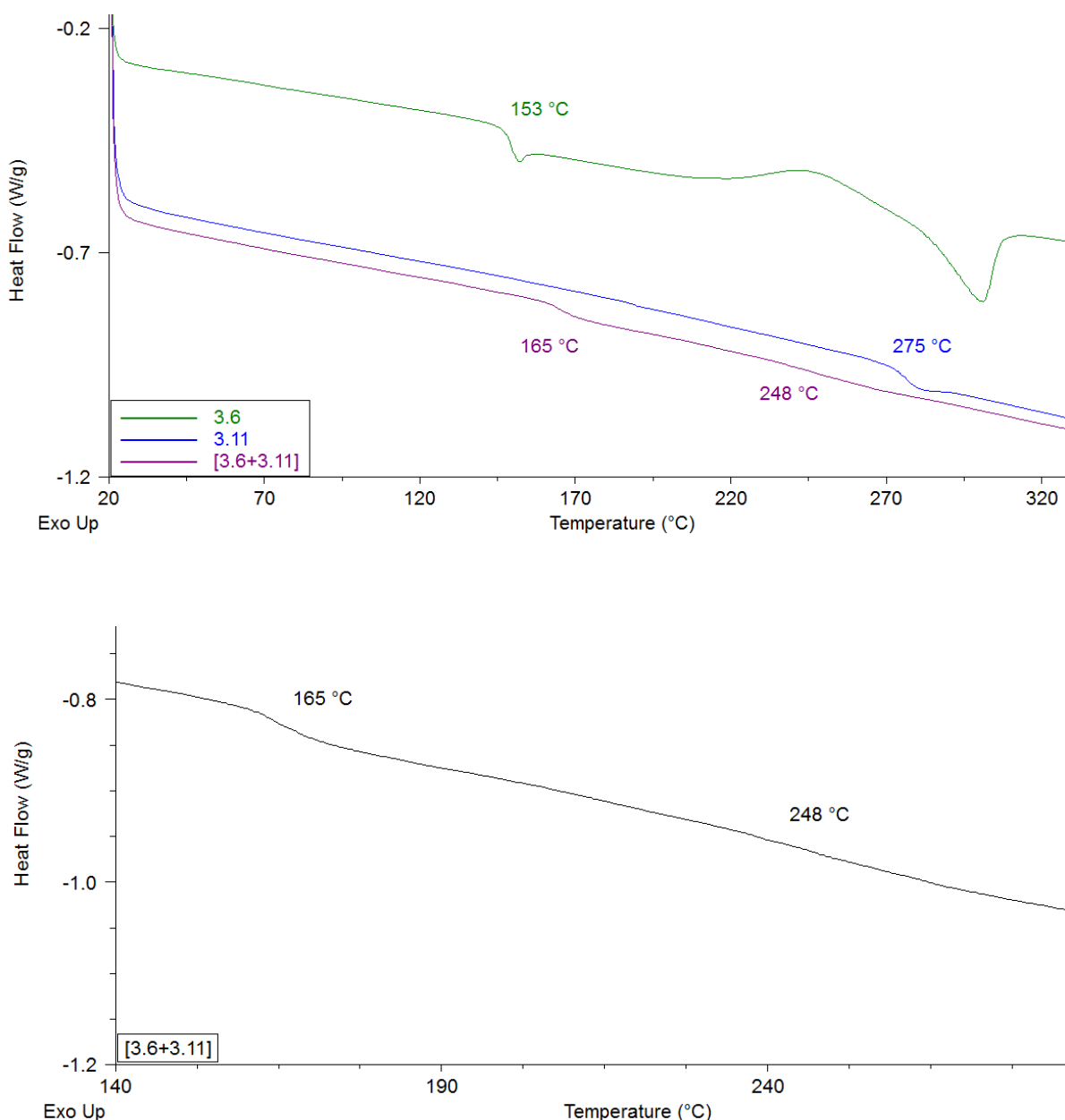

Figure 3.14. Top: DSC thermograms (second heating scan, 10 °C min^{-1}) showing PAEK **3.6** (green), polyimide **3.11** (blue) and blend **[3.6·3.11]** (purple). Bottom: Vertical expansion of DSC thermogram of blend **[3.6·3.11]**.

3.3.5 Steps toward composite production

Among the polyimides tested, co-polyimide **3.11** was able to modestly increase the T_g of the PAEK in the blend. Not only this, the copolymer blend **[3.5·3.11]** displayed a single T_g which is indicative of a compatible blend. Therefore, when it came to producing polymer blends for carbon fibre composite production and testing, polyimide **3.11** was the chosen copolymer. For composite production, each composite plaque requires 40 g of polymer matrix for the mould. Taking into consideration cost, timescale, and availability of equipment, a 5:3 weight ratio of PAEK to polyimide was chosen for composite production. The model copolymer blend used for scale-up was **[3.5·3.11]**. However, the quantities required for the composite mould are near to industrial pilot-scale and several modifications to both to the PAEK and the polyimide were required.

3.3.5.1 Chemical imidisation

Polyimide **3.11** was originally synthesised on a research scale of up to 3 g per batch. The high temperatures (>220 °C) and vacuum treatment required for thermal imidisation of the poly(amic acid) meant that the dehydration step was carried out in a small drying tube. As such, this technique was unfeasible for synthesising polyimide on the large scale (>100 g) required for composite production. Chemical imidisation is, however, a potentially better synthetic method for producing large quantities of polyimide. It does not require a combination of high temperature and high vacuum, so larger quantities can be made per polymerisation. The structure of polyimide **3.12** synthesised via chemical imidisation is shown in Figure 3.15. Phthalic anhydride was added to control the molecular weight of the polyimide. The dehydration step proceeds by reaction of the poly(amic acid) with acetic anhydride and a basic catalyst,[20] in this case pyridine. This approach yielded the required 100 g of polyimide **3.12** for the copolymer blend. This dehydration method is less commonly used in the preparation of polyimide films. Indeed, **3.12** was isolated as a brown powder.
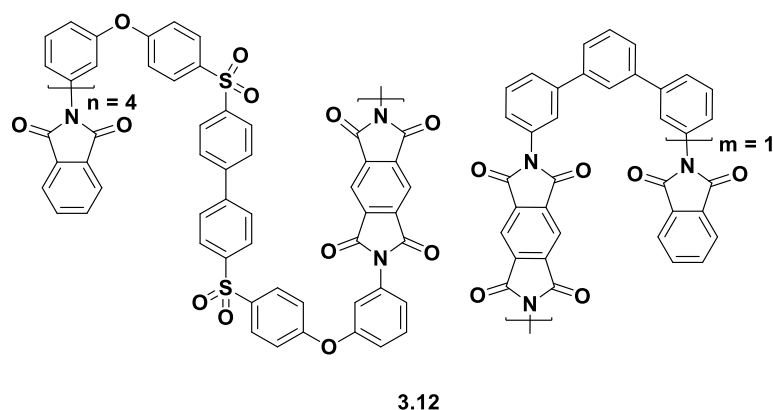
3.12

Figure 3.15. Polyimide **3.12** synthesised via chemical imidisation.

3.3.5.2 Functional PAEK synthesis

The PAEK that was used in the copolymer blend for the composite matrix was one of the industry standard materials, known as poly(ether ketone ketone) (PEKK). As shown in Figure 3.17, this copolymer is different from **3.5** and **3.6** that were used in the initial blends study. It was synthesised at Cytec Aerospace Materials Ltd (Wilton) via electrophilic co-polycondensation of terephthaloyl chloride, isophthaloyl chloride with 1,4-bis(4-phenoxybenzoyl)benzene in the presence of aluminium chloride. The ratio of terephthaloyl chloride to isophthaloyl chloride was not disclosed to the present author. However, as with the previous polymer blends studied in this work, two different PAEKs were produced (Figure 3.16), one a pyrenyl end-capped PEKK (**3.7**) and the other (as a control polymer) PEKK with benzoyl terminal groups (**3.8**).
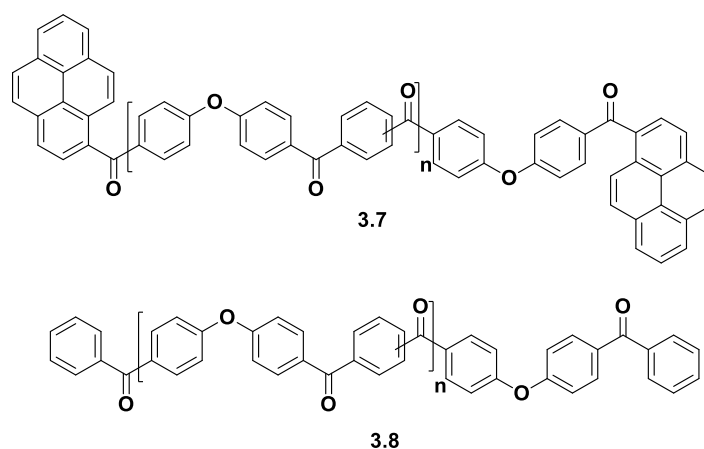

3.7

3.8

Figure 3.16. Structures of pyrenyl-terminated PEKK (**3.7**) and control PEKK (**3.8**).

The end-capping monomer for **3.7** was pyrene-1-carbonyl chloride (**3.1**), which was synthesised by reaction of pyrene-1-carboxylic acid with oxalyl chloride in toluene, after drying the solvent by azeotropic distillation of water (Figure 3.17).
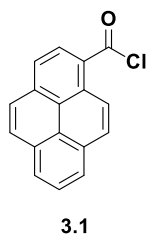

3.1

Figure 3.17. Structure of acyl chloride **3.1**, the terminating reagent for copolymer **3.7**.

The synthesis of this acyl chloride[21] did not require an amide catalyst (typically DMF in the literature) to produce an iminium intermediate. It instead proceeded by nucleophilic substitution by the chloride ion from oxalyl chloride, a proposed mechanism for which is shown in Scheme 3.3.
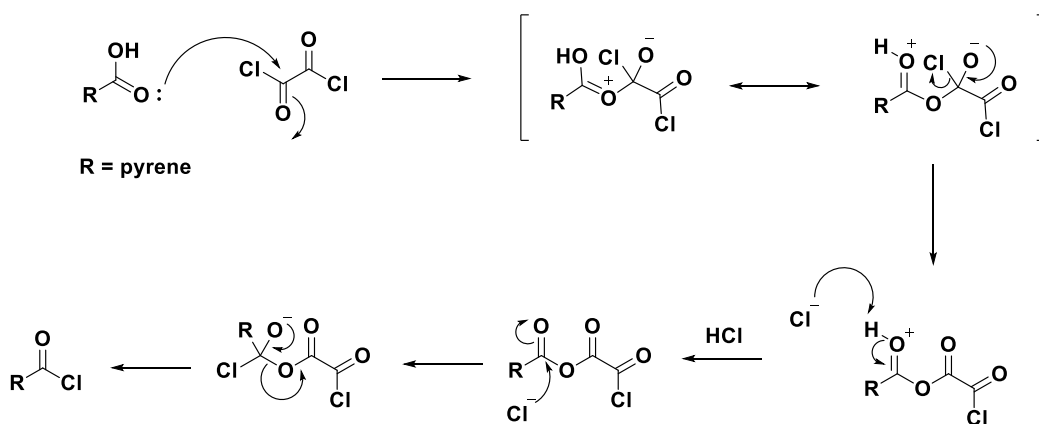
Scheme 3.3. Proposed mechanism for the synthesis of **3.1** from the nucleophilic substitution reaction between pyrene carboxylic acid and oxalyl chloride.

The pyrenyl-terminated PEKK was synthesised by including acyl chloride **3.1** with the co-monomers at the beginning of the polymerisation, to produce **3.7** (Figure 3.17). The average inherent viscosity of **3.7** in 96% sulfuric acid was 0.66 dL g^{-1}, with η_{inh} for different batches ranging from 0.53 − 0.75 dL g^{-1}. Similarly, the control PEKK **3.8** was synthesised by inclusion of benzoyl chloride to control the molecular weight of the polymer. The average η_{inh} of **3.8** in

sulfuric acid was 0.56 dL g^{-1}. There were initial concerns with respect to the differences in the η_{inh} of the two polymers. It is possible that some of the pyrene acyl chloride **3.1** used to cap **3.7** has hydrolysed to reform the carboxylic acid.[22] An end-cap that has hydrolysed will be less reactive than **3.1**. If this were the case, the polymer chain has the potential to grow longer with a decreased amount of end-caps available as the polymerisation progresses. It was the later batches of **3.7** that gave the highest η_{inh} measurements. However, fluorescence spectroscopy analyses of all samples of **3.7** (in CHCl$_3$/HFiPA 6:1 v/v) showed strong fluorescence under UV light, indicating at least partly successful end-capping.

3.3.5.3 Spin blending

The small-scale polymer blends heretofore discussed all involved solution blending. That is, taking each polymeric component, making up a concentrated solution and then re-precipitating to form a blend. This approach is fundamentally unfeasible on the larger scale as it is highly wasteful of resources. It was therefore replaced by the more straightforward spin blending method. In spin blending, the two polymers in the solid, finely-powdered form are physically spun in a tilted, rotating flask until a homogenous mixture is achieved. In the case of the PEKK-polyimide blends, a 5:3 weight ratio was used. Fortuitously, the control benzoyl-PEKK **3.8** and pyrenyl-PEKK **3.7** have a profoundly different appearances compared to polyimide **3.12** (colourless, bright yellow and brown, respectively). Thus a visibly homogenous mixture from spin blending of the two polymers was easily identifiable.

3.3.6 Composite production

There were two main stages involved in taking the polymer blend to carbon fibre composite production. The first was preform production and drying which were carried out at the Cytec Aerospace Materials production site in Wrexham. The preform was then stored until it is heat-pressed into plaques, which was carried out at Cytec's Wilton research laboratories.

3.3.6.1 Preform preparation

The first step in composite production was to prepare a preform mould which is composed of the polymer matrix and the carbon fabric. Preforms are dry, fibrous material prefabricated into a desired shape. The resulting material is a flexible plaque wrapped in a film. For each of the systems studied, a polymer slurry (40 g in 120 g water) was prepared. The slurry also contained *ca.* 0.5% non-ionic surfactant and ca. 0.5% defoamer. The slurries

of both PEKK-polyimide blends were found to be more viscous than the commercial PEKK standard.

Nine panels were prepared in total, six with 0° layup of fabric and three with alternating +45° and -45° layup of fabric. This arrangement of fibre orientation ensures that there are no weak planes in any fibre direction. A release film was place on the mould. The first carbon fabric (0° layup) was placed in the mould. A seventh of the slurry solution was placed on top and distributed evenly. This step raised an issue with the viscous slurry of both **[3.7·3.12]** and **[3.8·3.12]** blends, which had to be applied with a brush into the fabric. The process was repeated with each ply, alternating the 0° and 45° fabric. A final layer of polymer slurry was placed on the top ply of fabric. The release film was then loosely folded over and then the mould and preform placed in a vacuum autoclave oven at 90 °C until dry. The matrices of the composite preforms are thermoplastic polymers and thus can be stored at ambient temperature for an indefinite period of time.

3.3.6.2 Platen pressing

The next stage of composite production was hot pressing. This involved the use of high temperatures and pressures to fuse together all the layers of the composite panel. To prepare the composite, a release-polymer was placed on top of the preform and covered with a layer of release film and a metal frame was placed on top (Figure 3.18). All the layers were then placed between two metal plates.

Figure 3.18. The composite preform is placed on a metal plate with a release film then a release polymer and a metal frame is placed on top of it (left). A second release film and metal plate is placed on top (right).

The plates were then placed in the centre of a Platen press preheated to 375 °C. Over 20 minutes, the press plates were brought together slowly, with the plates fully closed for the final 5 minutes. A pressure of 50 bar was then applied and held for 20 minutes. This pressure was held whilst the press was cooled. The Platen press was cooled below the polymer T_g before the plates were removed. When the plates were ready, the composite was removed from the steel plate using a hammer and chisel (Figure 3.19). All three polymer matrix systems produced composite plaques of 2.0 - 2.1 mm thickness.
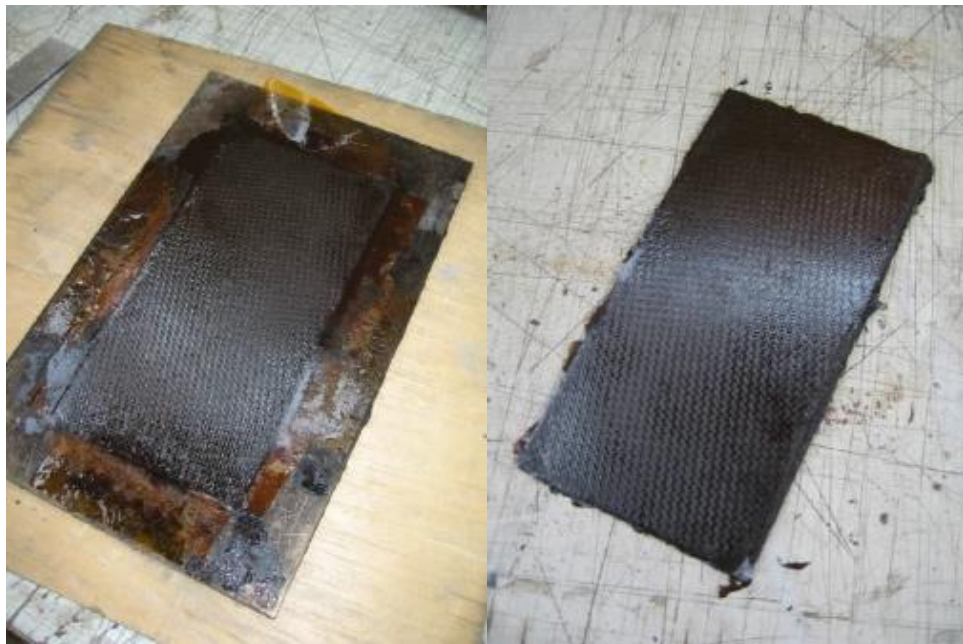

Figure 3.19. After the press has cooled, the metal plates are removed. The carbon fibre composite is then released from the metal frame.

3.3.7 Composite testing

Three different kinds of carbon fibre composite materials were produced in this study: composites of the commercial PEKK, blend **[3.7·3.12]** and blend **[3.8·3.12]**. All three were produced using the methods described above. The thermal characteristics of the materials were evaluated by DMA, and the morphologies of the materials were investigated by ESEM.

3.3.7.1 Environmental Scanning Electron Microscopy (ESEM)

Taking commercial PEKK as the standard morphology for carbon fibre composites allows a direct comparison for the PAEK-polyimide blends. Figure 3.20 shows an electron micrograph of the commercial PEKK composite. The commercial PEKK composite displayed good wetting

of the fibres. There are no observable holes between the layers of fabric. The method of producing the preform has been optimised at Cytec for this particular polymer matrix, and is an actual commercial product.
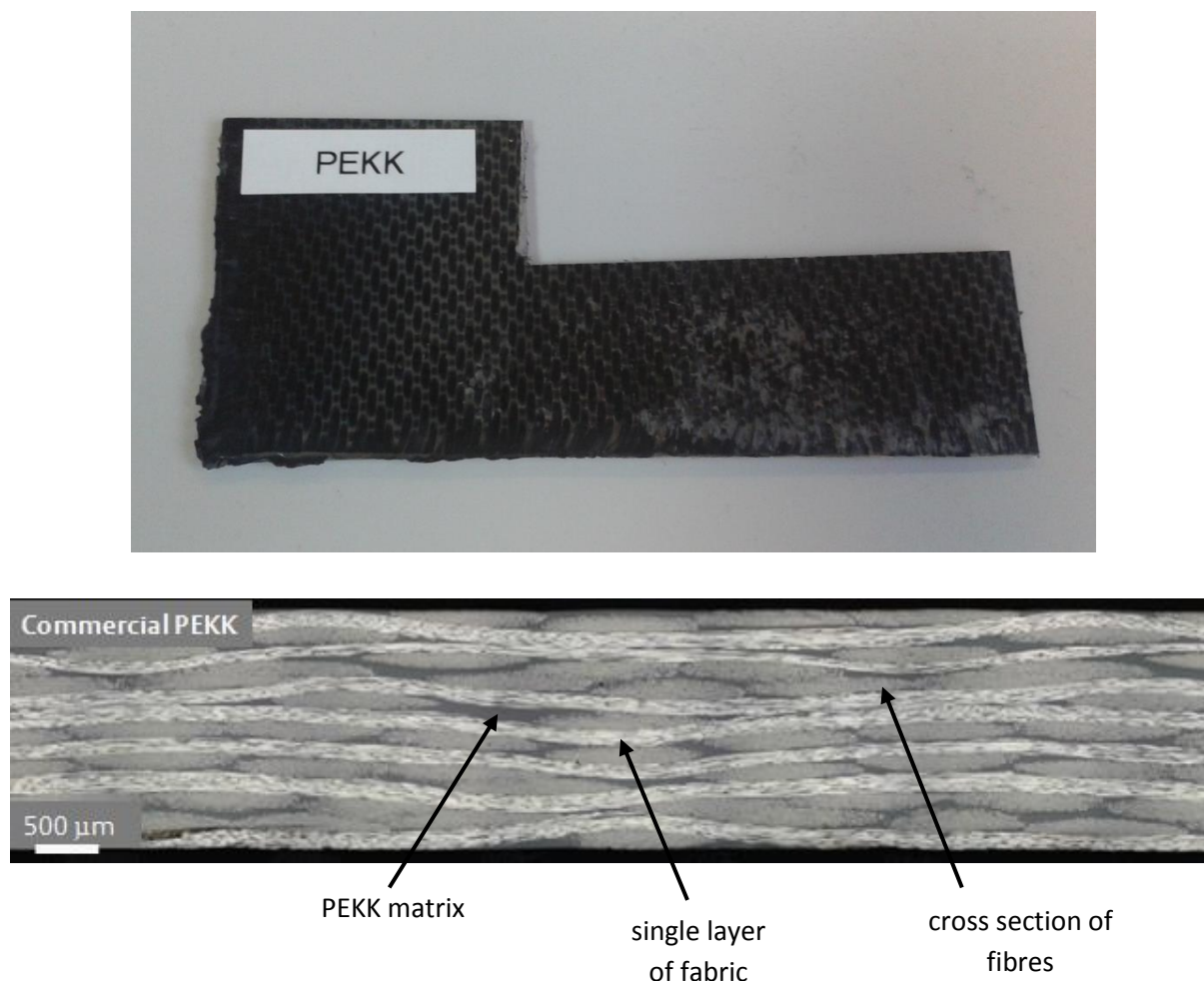

Figure 3.20. A photo of the commercial PEKK composite (top) and an electron micrograph of the same carbon fibre composite (bottom).

In comparison, an electron micrograph of the **[3.7·3.12]** composite, which has a pyrenyl-PAEK and polyimide blend matrix is shown in Figure 3.21. This composite has also achieved excellent fibre wetting as can be seen by the flecks of grey in the white of the fabric layers. However, there are gaps between the layers of fabric layup as can be observed by the black holes between the central layers. The larger gaps are concentrated in the inner layers of the composite and only very small gaps can be observed in the outer layers of the composite. There were several differences between PEKK and **[3.7·3.12]** that may account for the gaps. The observed difference in the viscosity between the slurries of the two polymers may have

caused poor binding between the fabrics. The preform slurry of blend **[3.8·3.12]** also displayed a more viscous suspension than that of PEKK, and a comparison between the electron micrographs of **[3.7·3.12]** and **[3.8·3.12]** may help resolve the origin of the gaps. The addition of the anionic surfactant and de-foaming agent, although in small quantities, may have also affected the adhesion of blend **[3.7·3.12]** between the layers.
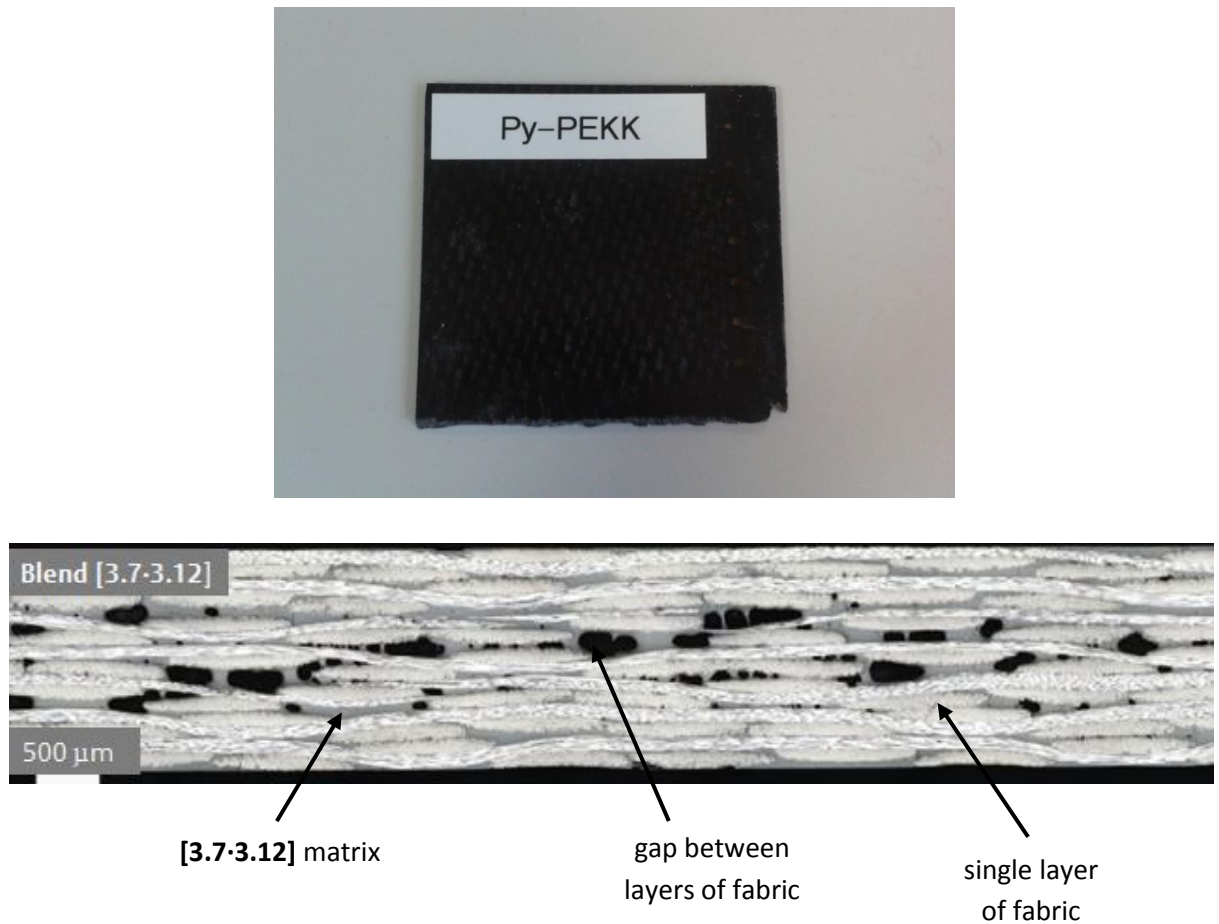

Figure 3.21. A photo of the **[3.7·3.12]** composite (top) and electron micrograph of the same composite, made with pyrenyl-PEKK/polyimide blend (bottom). The black sections are gaps between the layers.

An electron micrograph of the **[3.8·3.12]** composite, which has the control benzoyl-PAEK and polyimide blend matrix is shown in Figure 3.22. This composite has again achieved overall good fibre wetting. However, in contrast to the **[3.7·3.12]** composite, there are holes in between the carbon filaments within the layers of the fabric as indicated by the black regions. As it was with blend **[3.7·3.12]** (Figure 3.21), there are gaps between the layers of fabric layup given by the black areas between the layers. Comparing the three electron

micrographs, the viscosity of the preform slurries may have played a part in adhesion of the matrix to the carbon fabric. The less viscous PEKK had no observable holes between the fabric layers while the two blend matrices had holes between fabric layers.

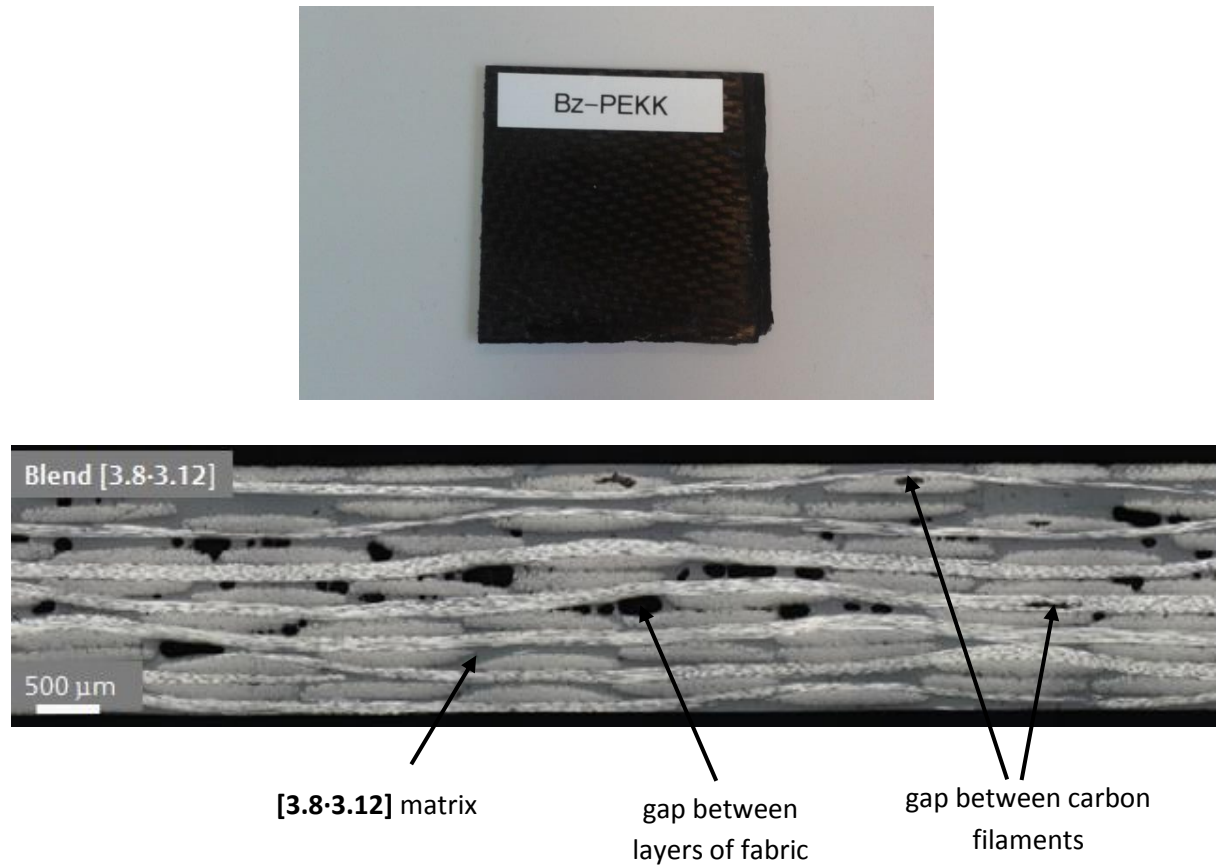[3.8·3.12] matrix gap between layers of fabric gap between carbon filaments

Figure 3.22. A photo of the **[3.7·3.12]** composite (top) and an electron micrograph of **[3.8·3.12]** composite, made with unfunctionalised PAEK/polyimide blend (bottom). The black areas represent gaps (voids) between the layers and gaps between carbon filaments within the fabric layers.

3.3.7.2 Dynamic Mechanical Analysis

DMA measures the storage modulus, loss modulus and tan delta of a material as it is deformed when a sinusoidal stress is applied.[23] After scanning a sample, any of the above parameters can be used to define the T_g of a material. The T_g of the composites in this present work were determined by measuring the storage modulus (E' onset) and tan delta. The E' onset occurs at the lowest temperature and relates to the mechanical failure of the material. The tan delta peak occurs at the highest temperature and is a measure of the midpoint between the glassy and rubbery states of a polymer.[24] The T_g values of the composites are summarised in Table 3.2.

Table 3.2. A summary of T_g values for the composite samples determined by DMA

T_g	Commercial PEKK	Blend [3.7·3.12]	Blend [3.8·3.12]
E' onset / °C	123	162	163
tan delta / °C	152	176	184

The composite made with commercial PEKK polymer matrix was found to have an E' onset of 123 °C. The E' onset of the blend **[3.7·3.12]** composite was 162 °C and for **[3.8·3.12]** it was found to be 163 °C. It would appear that the T_g of the material (as defined by E' onset) has increased by 40 °C in the blend with polyimide in both the pyrenyl- and unfunctionalised PAEK. However, considering the tan delta parameter for measuring T_g, there was a more modest increase in the T_g of PEKK from 152 °C to 176 °C in blend **[3.7·3.12]** and to 184 °C in blend **[3.8·3.12]**.

The latter tan delta result is the opposite of what was expected as blend **[3.7·3.12]** with its pyrenyl-terminated PAEK was expected to form a more compatible blend with the polyimide than the unfunctionalised PAEK contained in blend **[3.8·3.12]**. Indeed, the model polymeric blends **[3.5·3.9]** and **[3.5·3.11]** previously discussed in Section 3.2.4 showed that the blend with the pyrenyl terminal groups displayed a higher T_g than its benzoyl terminated counterpart. The discrepancies in the *composite* T_g values could, however, have been affected by the different levels of defects (interlayer gaps) in the composite materials. More extensive investigations of composite thermo-mechanical properties are clearly needed to resolve this issue.

The discrepancy in the values of T_g measured by DMA also calls to attention the difference between the mean η_{inh} of polymers **3.7** and **3.8**, with the former giving a value some 0.10 dL g^{-1} higher than the latter. Since the η_{inh} of a polymer is in general, proportional to its molecular weight, it can be inferred that **3.7** has a higher molecular weight than **3.8**. A rudimentary consideration of the Flory-Fox equation (Chapter 1) relates the number-average molecular weight of a polymer to its T_g. The equation indicates that T_g is dependent on free volume, which is in turn dependent on the average molecular weight of the polymer. A lower molecular weight results in lower T_g whereas increasing molecular weights result in an asymptotic approach to the maximum T_g.[25] It thus follows that copolymer **3.7**, with its higher mean η_{inh}, should have displayed a higher T_g.

3.3.7.3 Instron mechanical testing

A further key mechanical measurement is the interlamellar shear strength (ILSS) of a composite sample. The ILSS is the resistance of a layered composite to internal forces that tend to produce a sliding motion between the layers of the material.[26] Layers slide pass one another along the plane that is parallel to the direction of the force, and when the material splits, it is a failure in shear.[27]

In a carbon fibre composite, the polymer matrix displays about a tenth of the strength of the carbon fibre reinforcement.[28] When a material fails in this case, it is the strength of the polymer matrix that is being measured, as this is the component that fails first. The measurements indeed reflect what was observed in the ESEM. The commercial PEKK sample recorded the highest shear strength (Figure 3.23). This is as expected as there was excellent adhesion of the polymer matrix between the layers of carbon fabric. In the case of the two polymer blend samples, **[3.7·3.12]** and **[3.8·3.12]** gave a lower ILSS. This is not, however, a true reflection of the strength of the matrix material as the samples are inherently weakened by the holes in the matrix between the carbon fibre layers.

It was found that that the shear strength of the interface of matrix and carbon fibre reinforcement is strongly correlated to the fibre-matrix adhesion.[29] Therefore, when a material breaks, it will fail first where holes are present as this is the weakest point.[30] Perhaps what can be surmised from the data is that there may be more defects (holes) in the matrix of **[3.7·3.12]** than **[3.8·3.12]**. This then provides a more quantitative

measurement of the gaps in the matrix as the **[3.7·3.12]** composite sample has a mean ILSS approximately 20 MPa lower than **[3.8·3.12]** (Figure 3.24).
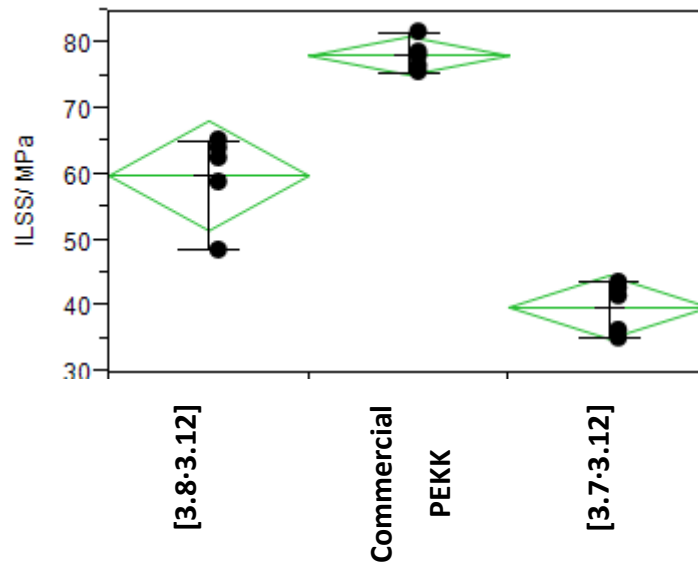

Figure 3.23. ILSS measurements of the three composite samples.

The flexural strength of the samples was also measured. The flexural strength of a material may be described as the stress in a material just before it yields in a "bending" fracture test. In a composite, it is the measure of the maximum fibre stress at failure on the side where tension is applied on a sample. A material reaches the limit of its flexural strength when it fractures under an applied stress. As can be seen in Figure 3.24, the **[3.7·3.12]** composite sample fails at a lower flexural stress than the other two samples. Flexural failure occurs when a crack propagates in the material. In a three-point flexural test, failure occurs due to bending failure, shear failure and sometimes due only to matrix cracking.[31]

A baseline carbon fibre used in the aerospace industry has a tensile strength of over 3500 MPa, and a generic commercial epoxy resin composite has a flexural strength of over 1800 MPa.[32] Taking these values as guidelines, it may appear that the samples of **[3.7·3.12]** composite failed because of a weakness in the polymer matrix. However, it must be reiterated that the gaps in the matrix generated during preform production are undoubtedly a factor in weakening the sample regardless of the inherent properties of the polymer matrix. Indeed, the performance of a composite material depends strongly on the quality of adhesion at the fibre-matrix interface.[33] In the case of **[3.7·3.12]** composite, there is clearly

poor adhesion between the matrix and carbon fabric interface, although this alone cannot explain the large difference in the measure flexural strength of **[3.7·3.12]** and **[3.8·3.12]**.
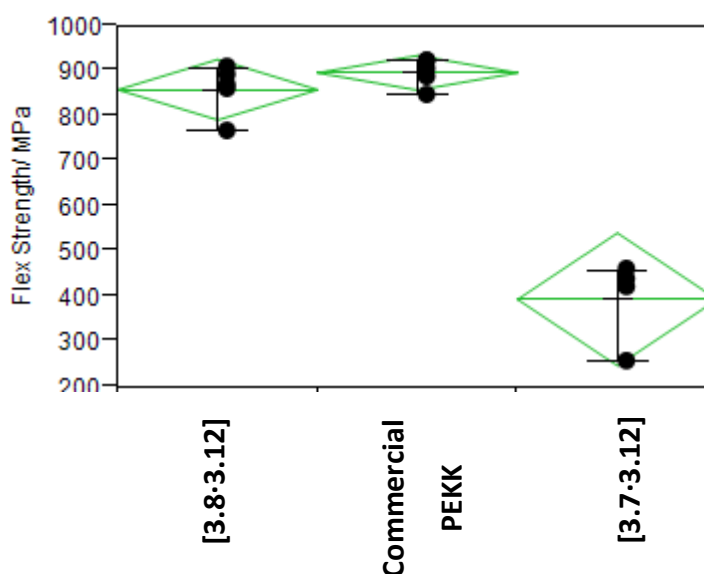

Figure 3.24. Flexural strength measurements of the three composite samples.

3.4 Conclusions

The polycondensation of 4,4'-dihydroxybenzophenone with 1,3-bis(4-fluorobenzoyl)benzene and a monofunctional 1-hydroxypyrene has produced a π-electron rich pyrenyl end-capped PAEK. Blends of this polymer with polyimides containing electron deficient residues successfully led to the formation of complementary π-π stacked complexes. Systematic changes in the glass transition temperature showed that blend formation involved some degree of positive interaction between the two components.

An apparently compatible, homogenous blend has been produced with a polyimide containing *m*-terphenylene diimide units. This blend exhibited a single broad glass transition temperature, albeit lower than the expected value for a polymeric blend of this type. The high glass transition temperature of polyimides had a positive effect of increasing the glass transition temperature of the overall blends with PAEKs.

Carbon fibre composites were produced with a blend of pyrene functionalised PEKK and *m*-terphenylene polyimide as the matrix material. Under ESEM examination, the composite

was found to have gaps between the matrix and the carbon fibre layers. This suggests that the polymer blend has poor adhesion to the carbon fabric. As a result, the poor adhesion at the interface of the composite may have cause the early failure of the material in the mechanical testing. The experimental composite showed a much lower interlamellar shear strength and flexural strength than commercial composites.

3.5 Experimental

3.5.1 Materials

1,3-bis(4-fluorobenzoyl)benzene, dihydroxybenzophenone, 1-hydroxypyrene, 4-hydroxybenzophenone, 3-aminophenol, 4,4'-bis[(4-chlorophenyl)sulfonyl]-1,1'-biphenyl, poly(methylhydrosiloxane), pyromellitic dianhydride, 1,3-dibromobenzene, 1,4,5,8-naphthalenetetracarboxylic dianhydride, oxalyl chloride, *N,N*-dimethylacetamide, acetone, methanol, deuterated chloroform and deuterated dimethylsulfoxide were purchased from Sigma Aldrich, UK. Potassium fluoride, diphenyl sulfone and acetic anhydride were purchased from Alfa Aeser, U.K. Sodium carbonate, potassium carbonate, *N,N*-dimethylformamide and toluene were purchased from Fisher Scientific, U.K. 3-Nitrophenylboronic and 1-pyrenecarboxylic acid were purchased from Tokyo Chemical Industry, U.K. Palladium (II) acetate was purchased from Lancaster Synthesis Ltd. 1,1,1,3,3,3-hexafluoro-2-propanol was purchased from Apollo Scientific, U.K. Samples of PEKK were provided by Cytec Aerospace Materials, UK. All materials were used as purchased unless stated otherwise.

3.5.2 Monomers and end-capping reagents: synthetic procedures

3.5.2.1 1-Pyrene acyl chloride (3.1)[34]

A suspension of 1-pyrene carboxylic acid (5 g, 19.7 mmol) in toluene (150 mL) was heated at reflux for 2 h with azeotropic distillation of water. The suspension was cooled to 60 °C. Oxalyl chloride (5 g, 40.7) was then added to the suspension, and heated to reflux over 3 h. The resulting yellow solution was cooled to room temperature and concentrated under vacuum. The yellow precipitate that formed was filtered, washed with methanol (50 mL) and dried under vacuum at 90 °C for 24 h to yield the title compound **3.1** as yellow crystals (4.80 g, 92%). This synthesis was reproduced multiple times on the same scale.
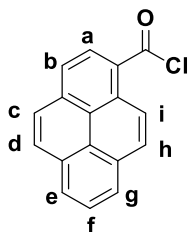
3.1

M.p. (DSC) 210 °C; ^{1}H NMR (400 MHz, CDCl$_3$): δ (ppm) 9.08 (d, *J* = 9.6, 1H **a**), 8.95 (d, *J* = 8.4, 1H **b**), 8.37-8.34 (m, 3H **c, d, f**), 8.28 (d, *J* = 8.8, 1H **e**), 8.23 (d, *J* = 8.4 Hz, 1H **g**), 8.15-8.12 (m, 2H **h, i**); ^{13}C NMR (100 MHz, DMSO-*d$_6$*): δ (ppm) 169.0, 133.6, 130.6, 130.1, 130.0, 129.6, 129.4, 129.1, 128.4, 127.2, 126.2, 1246, 124.4, 124.3, 123.9, 123.3 ; IR: ν$_{max}$ / cm^{-1} 1755 (C=O), 1503 (C=C), 1187 (C-H), 904 (C-H), 842 (C-Cl).

### 3.5.2.2 4,4'-Bis[4-(3-aminophenoxy)benzenesulfonyl)-1,1'-biphenyl] (3.2)

The synthesis and characterisation of this monomer has been previously described (as **2.10**) in Chapter 2 .
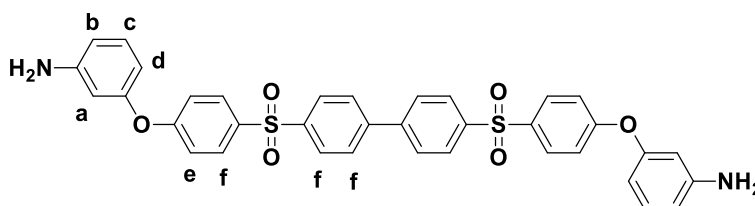

3.2

3.5.2.3 3,3"-Dinitro-*m*-terphenyl (3.3)[35]

1,3-dibromobenzene (0.47 g, 2 mmol), 3-nitrophenyl boronic acid (1.33 g, 8 mmol), Na$_2$CO$_3$ (0.85 g, 8 mmol), Pd(OAc)$_2$ (435 mg, 0.02 mmol), was stirred in a mixture of water (7 mL) and DMF (6 mL) at 60 °C for 16 h. The product was precipitated in water, filtered off and washed with methanol, then water, then methanol once again before drying under vacuum for 16 h to give the product **3.3** as a grey powder (0.55 g, 85%). This synthesis was reproduced several times on a 5 g scale.
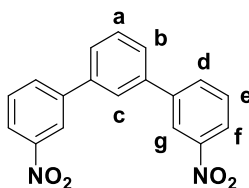
3.3

M.p. (DSC) 210 °C; HRMS (ESI) m/z: 320.0799 [$C_{18}H_{12}N_2O_4$], calculated: 320.0797; ^{1}H NMR (400 MHz, DMSO-d_6): δ (ppm) 8.59 (s, 2H **g**), 8.30 (d, J = 7.6, 2H **f**), 8.28 (d, J = 8.0, 2H **d**), 8.16 (s, 1H **c**), 7.86 (d, J = 8.0, 2H **b**) 7.79 (t, J = 8.4, 2H **e**) 7.67 (t, J = 7.6, 1H **a**); ^{13}C NMR (100 MHz, DMSO-d_6): δ (ppm) 148.5, 141.4, 138.8, 133.7, 130.4, 130.1, 127.3, 125.9, 122.36, 121.8; IR: ν$_{max}$ / cm^{-1} 1528 (N-O), 1344 (C-N), 888 (C-H Ar).

3.5.2.4 *m*-Terphenylene diamine (3.4)[36]

A solution of palladium(II) acetate (0.012 g, 0.05 mmol) and **3.3** (0.32 g, 1 mmol) in tetrahydrofuran (5 mL) was stirred until homogenous. A solution of potassium fluoride (0.23 g, 4 mmol) in water (2 mL) was added dropwise. Liquid polymethylhydrosiloxane (0.48 mL, 8 mmol) was then added dropwise. The solution was stirred for 3 hours. Diethyl ether (25 mL) was added to the reaction mixture and the organic phase was separated and concentrated under vacuum. The resulting oil was extracted with chloroform to yield the desired diamine as a brown oil **3.4** (0.21 g, 77%). This synthesis was reproduced several times on a 5 g scale.
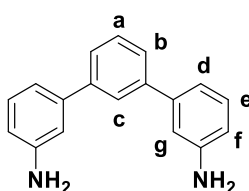

3.4

HRMS (ESI) m/z: 261.1384 [$C_{18}H_{17}N_2$], calculated: 261.1392; ^{1}H NMR (400 MHz, DMSO-d_6): δ (ppm) 7.58 (s, 1H **c**), 7.39 (m, 3H **a**, **b**), 7.01 (t, J = 7.02, 2H **e**), 6.79 (s, 2H **g**), 6.72 (d, J = 6.7, 2H **d**), 6.47 (d, J = 6.5, 2H **f**) 5.06 (s, 2NH$_2$); ^{13}C NMR (100 MHz, DMSO-d_6): δ (ppm) 149.1, 141.5, 140.9, 129.4, 129.1, 125.2, 124.6, 114.4, 113.2, 112.2; IR: ν$_{max}$ / cm^{-1} 3367 (N-H) 1598 (N-H bend), 1478 (C-N), 907 (N-H wag).

3.5.3 Poly(aryl ether ketone)s: synthetic procedures

3.5.3.1 Pyrene-end-capped poly(ether ketone) (3.5)

A mixture of 1,3-bis(4-fluorobenzoyl)benzene (2.75 g, 8.52 mmol), 4,4'-dihydroxy-benzophenone (1.79 g, 8.36 mmol), 1-hydroxypyrene (100 mg, 0.46 mmol), Na_2CO_3 (0.98 g, 9.20 mmol) and diphenyl sulfone (35 g) was heated to 300 °C under argon, with mechanical stirring, for 3 h. The polymer solution was poured onto a sheet of aluminium and ground to a powder in an ultracentrifuge mill before extracting in acetone (200 mL). The powder was filtered off and extracted four times with refluxing acetone, and then in a Soxhlet extractor with refluxing acetone for 16 h. The powder was extracted five times with boiling water, and then a final four times with refluxing acetone. The suspension was then filtered, the precipitate dried at 110 °C under vacuum for 16 h, affording the functionalised poly(ether ketone) **3.5** as a pale brown powder (2.62 g, 61%).


3.5
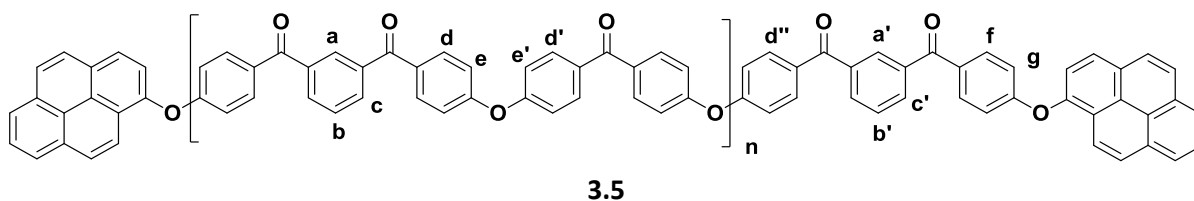
T_g = 153 °C; T_m = 299 °C; η_{inh} (H_2SO_4) = 0.38 dL g^{-1}; ^{1}H NMR (700 MHz, CDCl$_3$/(CF$_3$)$_2$CHOH 6:1 v/v): δ (ppm) 8.30-8.21 (m, 6H (expected 10H), py), 8.17 (s, 25H **a**), 8.13 (s, 2H, **a'**) 8.06 (d, *J* = 4.4, 52H **c**, **c'**), 7.93-7.89 (app dd, *J* = 8.4, 4.8, 208H **d**, **d'**, **d''**, **f**), 7.86-7.78 (m, 8H, py) 7.75 (t, *J*= 4.4, 1H **b**, **b'**), 7.25 (app t, *J* = 4.4 260H (expected 204), **e**, **e'**, solvent), 7.14 (d, *J* = 4.8, 4H **g**) ppm; ^{13}C NMR (100 MHz, CDCl$_3$/(CF$_3$)$_2$CHOH 6:1 v/v): δ (ppm) 198.9, 198.6, 161.3, 160.4, 137.5, 134.2, 133.1, 132.89, 132.7, 131.6, 130.7, 129.8, 129.0, 119.2, 118.9; IR: ν$_{max}$ / cm^{-1} 1660 (C=O), 1587, 1508 (C=C Ar), 1242 (C-O-C).

3.5.3.2 Control poly(ether ketone) (3.6)

A mixture of 1,3-bis(4-fluorobenzoyl)benzene (5.49 g, 17.04 mmol), 4,4'-dihydroxybenzophenone (3.58 g, 16.72 mmol), 4-hydroxybenzophenone (0.18 g 0.92 mmol), Na_2CO_3 (1.95 g, 18.4 mmol) and diphenyl sulfone (35 g) was heated with mechanical stirring to 300 °C under argon for 3 h. The solution was then poured onto a sheet of aluminium, ground to a powder before extracting in acetone (200 mL). The powder was filtered then

was extracted four times with refluxing acetone, and then in a Soxhlet extractor with refluxing acetone for 16 h. The powder was extracted five times with boiling water, and then a final four times with refluxing acetone. The suspension was then filtered, the precipitate was dried at 110 °C under vacuum for 16 h, affording the poly(ether ketone) **3.6** as a white powder (7.37 g, 86%).


3.6
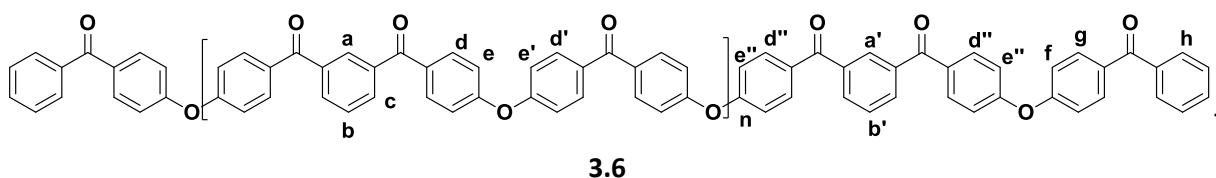
T_g = 151 °C T_m = 300 °C; η_{inh}: 0.30 dL g^{-1}; ^{1}H NMR (400 MHz, CDCl$_3$/(CF$_3$)$_2$CHOH 6:1 v/v): δ (ppm) 8.14 (s, 14H **a**), 8.08 (s, 2H, **a'**) 8.03 (d, J= 8.0, 31H (expected 30H), **c**), 7.88 (app t, J = 8.8, 129H (expected 120H), **d, d'**), 7.80-7.76 (m, 12H, **d''**, **g**), 7.73 (t, J= 7.6, 16H, **b, b'**), 7.55 (app t, J = 8, 4H, **h**), 7.24-7.21 (m, 130H (expected 120H), **e, e', e''**), 7.14-7.11 (m, 7H (expected 6H), **i, j**), 6.96 (d, J= 8.4, 4H, **f**); ^{13}C NMR (100 MHz, CDCl$_3$/(CF$_3$)$_2$CHOH 6:1 v/v): δ (ppm) 198.4, 198.2, 161.2, 160.3, 137.5, 134.2, 133.1, 132.8, 132.6, 131.6, 130.8, 130.0, 129.0,128.6, 119.1, 118.9, 115.4; IR: v_{max}/cm^{-1} 1651 (C=O), 1589, 1497 (C=C Ar), 1240 (C-O).

3.5.3.3 Commercial PEKK

The following polymers were synthesised at the Cytec Aerospace Materials research laboratories, Wilton, UK. The exact quantities of the monomers, reagents and MW-controlling agents were classed as proprietary information and were not disclosed to the present author.

### 3.5.3.3.1 Pyrenyl-end-capped PEKK (**3.7**)

Terephthaloyl chloride, isophthaloyl chloride, 1,4-bis(4-phenoxybenzoyl)benzene, **3.1** and AlCl$_3$ were added to DCM (250 mL) at -20 °C. The solution was heated at 20 °C for 4 h. The resulting slurry was filtered, extracted three times with an acidic methanol solution, followed by water, until a neutral pH was obtained, to yield polymer **3.7** as a yellow powder (40 g).
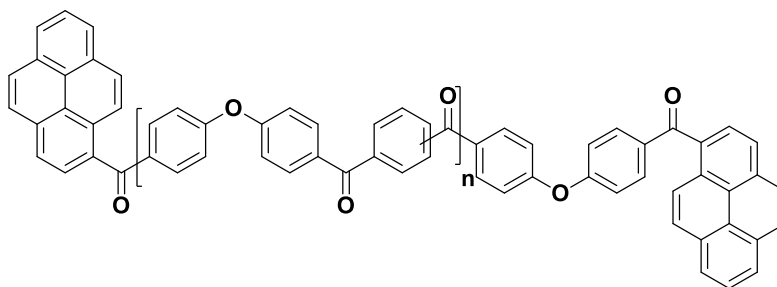
3.7

T_g = 140 °C T_c = 318 °C T_m = 335 °C; η_{inh} = 0.66 dL g^{-1}; ^{1}H NMR (400 MHz, CDCl$_3$/(CF$_3$)$_2$CHOH 6:1 v/v): δ (ppm) 8.15 (s, 1H), 8.03 (d, J= 8, 2H), 7.93-7.90 (m, 30H), 7.73 (t, J= 7.6, 1H), 7.24-7.21 (m, 18H); ^{13}C NMR (100 MHz, CDCl$_3$/(CF$_3$)$_2$CHOH 6:1 v/v): δ (ppm) 197.6, 197.4, 161.1, 161.0, 141.0, 137.8, 134.2, 133.4, 133.2, 131.2, 130.4, 130.1, 130.0, 129.3, 120.8, 119.3; IR (ν$_{max}$ cm^{-1}) 1643 (C=O), 1583, 1494 (C=C Ar), 1236 (C-O-C).

3.5.3.3.2 Control PEKK (**3.8**)

Terephthaloyl chloride, isophthaloyl chloride, 1,4-bis(4-phenoxybenzoyl)benzene, benzoyl chloride and AlCl$_3$ were added to DCM (250 mL) at -20 °C. The solution was heated at 20 °C for 4 h. The resulting slurry was filtered, extracted three times with an acidic methanol solution, followed by water until the filtrand was lithmus neutral, to yield the polymer **3.7** as a colourless powder (36 g). This polymer was reproduced several times on the same scale.
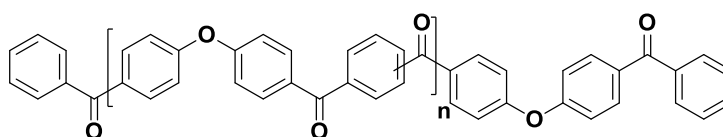

3.8

T_g = 143 °C T_c = 323 °C T_m = 332 °C; η_{inh} = 0.56 dL g^{-1}; ^{1}H NMR (400 MHz, CDCl$_3$/(CF$_3$)$_2$CHOH 6:1 v/v): δ (ppm) 8.15 (s, 1H), 8.04 (d, J = 8, 2H), 7.93-7.90 (m, 22H), 7.72 (t, J = 8, 1H), 7.24-7.21 (m, 14H); ^{13}C NMR (100 MHz, CDCl$_3$/(CF$_3$)$_2$CHOH 6:1 v/v): δ (ppm) 197.3, 197.1, 160.8, 160.7, 140.7, 137.6, 134.0, 133.1, 133.0, 132.0, 131.0, 130.2, 130.0, 129.8, 129.7, 1129.7, 129.0, 128.6, 120.5, 119.1; IR (ν$_{max}$ cm^{-1}) 1652 (C=O), 1586, 1491 (C=C Ar), 1241 (C-O-C).

3.5.4 Polyimides and co-polyimides: synthetic procedures

### 3.5.4.1 Chain-folding polyimide from pyromellitic anhydride (3.9)

Pyromellitic dianhydride (0.273 g, 1.25 mmol) was added to a solution of diamine **3.2** (0.811 g, 1.25 mmol) in DMAc (5 mL). The solution was stirred for 20 h then transferred to a Petri dish and heated at 80 °C under vacuum for 2 h. The remaining film was heated sequentially to 120 °C for 10 minutes, 150 °C for 10 minutes, 180 °C for 10 minutes, 210 °C for 10 minutes and finally at 250 °C for 2 h. The resulting polyimide film was dissolved in DMF and reprecipitated in methanol to give colourless beads. The polyimide was dried at 80 °C under vacuum for 2 hours, then extracted with refluxing chloroform for 3 hr, and finally dried under vacuum at 100 °C for 2 hours to afford polyimide **3.9** as colourless beads (0.89 g, 86%).

3.9
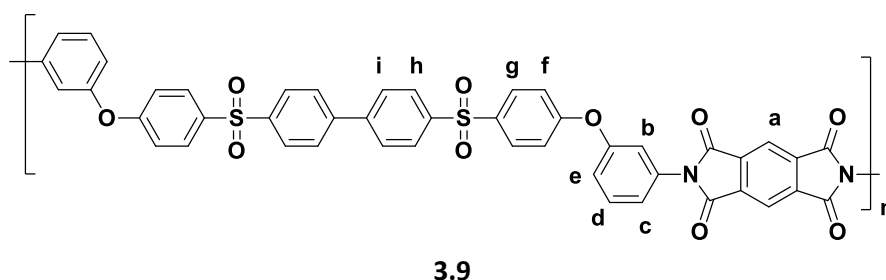
T_g = 283 °C; η_{inh} (NMP) = 0.37 dL g^{-1}; ^{1}H NMR (400 MHz, CDCl$_3$/(CF$_3$)$_2$CHOH 6:1 v/v): δ (ppm) 8.46 (s, 2H **a**), 7.96 (d, J = 8.0, 4H **g**,), 7.89 (d, J = 8.8, 4H **h**), 7.82 (s, 2H **b**) 7.73 (d, J = 8, 4H **i**), 7.60 (t, J = 8.8, 2H **d**), 7.32 (d, J = 8, 2H **c**), 7.30-7.16 (m, 6H **e**, **f**); ^{13}C NMR (100 MHz, CDCl$_3$/(CF$_3$)$_2$CHOH 6:1 v/v): δ (ppm) 165.2, 137.0, 130.0 128.5, 128.0, 125.6, 125.5, 122.8, 122.7, 120.0, 119.9, 118.4, 117.1; IR: v_{max} / cm^{-1} 1722 (C=O), 1580 (C=C Ar), 1486 (C=C, Ar),1368 (C-N), 1236 (C-N), 1150 (S=O), 1104 (C-O).

3.5.4.2 Chain-folding co-polyimide from pyromellitic dianhydride and 1,4,5,8-naphthalenetetracarboxylic dianhydride (3.10)

This co-polyimide was synthesised following the procedure for **3.9**, but using the following monomers: pyromellitic dianhydride (0.13 g, 0.62 mmol), 1,4,5,8-naphthalenetetracarboxylic dianhydride (0.16 g, 0.62 mmol) and diamine **3.2** (0.80 g, 1.23 mmol) to afford co-polyimide **3.10** as colourless beads (0.51 g, 49%).

3.10
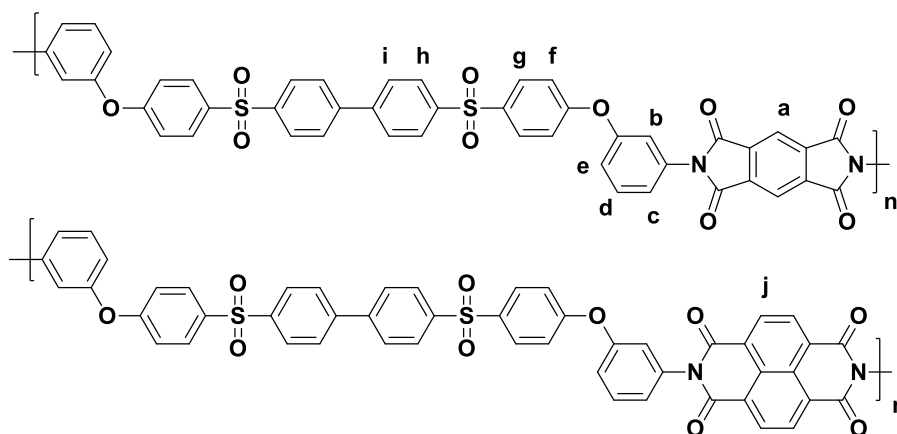
T_g = 309 °C; η_{inh} (NMP) = 0.27 dL g^{-1}; ^{1}H NMR (400 MHz, CDCl$_3$/(CF$_3$)$_2$CHOH 6:1 v/v): δ (ppm) 8.82 (s, 4H **j**), 8.44 (s, 2H **a**), 7.96 (d, J = 8.0, 9H **g**,), 7.88 (d, J = 7.9, 9H **h**), 7.79 (d, J = 7.7, 9H **b**) 7.65-7.56 (m, J = 8, 5H **i**), 7.32 (d, J = 7.3, 2H **c**), 7.21-7.14 (m, 2H$_e$, 16H **f**); ^{13}C NMR (100 MHz, CDCl$_3$/(CF$_3$)$_2$CHOH 6:1 v/v): δ (ppm) 165.8, 163.9, 162.2, 162.1, 156.3, 155.6, 144.7, 140.0, 136.9, 133.5, 133.4, 132.2, 131.6, 131.48, 131.2, 129.8, 129.7, 128.6, 127.8, 127.1, 126.6, 124.6, 123.0, 121.6, 120.7, 120.0, 118.8, 118.5; IR: v_{max} / cm^{-1} 1676 (C=O), 1583 (C=C Ar), 1481 (C=C, Ar),1366 (C-N), 1231 (C-N), 1150 (S=O), 1100 (C-O).

3.5.4.3 Chain-folding co-polyimide from *m*-terphenylene diamine (20 mol%) and pyromellitic dianhydride (3.11)

This co-polyimide was synthesised following the procedure for **3.9**, but with the following monomers and solvent: pyromellitic dianhydride (0.68 g, 3.13 mmol), diamine **3.2** (1.62 g, 2.5 mmol) and diamine **3.4** (0.16 g, 0.63 mmol) in DMAc (10 mL). The resulting film was dissolved in DMF and reprecipitated in methanol to give colourless beads. The co-polyimide was dried at 80 °C under vacuum for 2 hours to afford **3.11** as colourless beads (2.13 g, 90%).

3.11
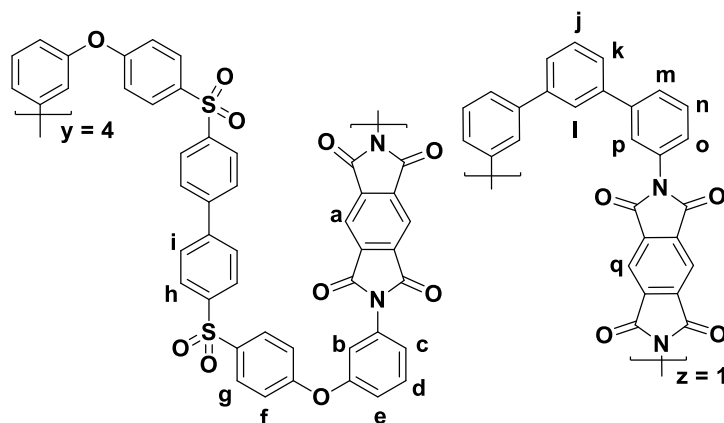
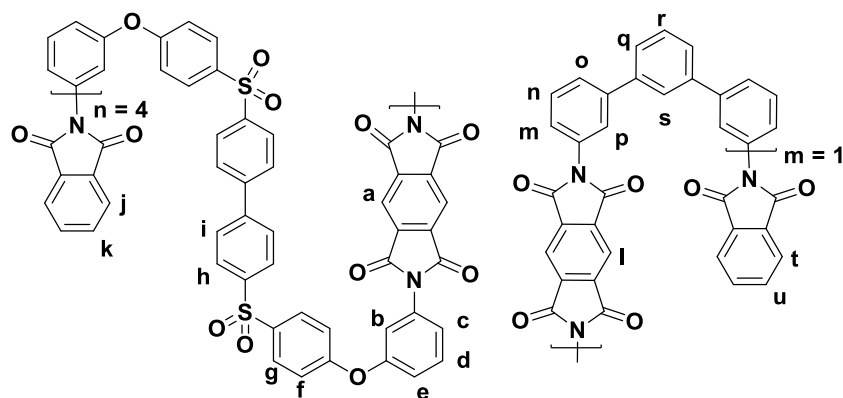T_g = 277 °C; η_{inh} (NMP) = 0.57 dL g^{-1}; ^{1}H NMR (400 MHz, CDCl$_3$/(CF$_3$)$_2$CHOH 6:1 v/v): δ (ppm) 8.47 (s, 3H (expected 2H), **q**), 8.45 (s, 5H, **a**), 8.05 (app d, *J* = 7.6, 12H, **i, k, l**), 7.96 (d, *J* = 7.6, 16H, **g**), 7.88 (d, *J* = 8.4, 16H, **h**), 7.84 (s, 4H, **b**), 7.72 (d, *J* = 8.0, 16H, **i**), 7.67-7.63 (m, 5H, **j, m, p**), 7.60 (t, *J* = 7.6, 8H, **d**), 7.42-7.37 (m, 2H, **o**), 7.30 (app d, 8H, **c**), 7.21-7.15 (m, 26H **e, f, n**) ^{13}C NMR (100 MHz, CDCl$_3$/(CF$_3$)$_2$CHOH 6:1 v/v): δ (ppm) 165.7, 162.1, 155.7, 144.7, 140.0, 137.0, 133.3, 131.5, 131.1, 129.8, 128.5, 127.6, 123.1, 121.6, 121.1, 118.5; IR: ν_{max} / cm^{-1} 1720 (C=O), 1582 (C=C Ar), 1483 (C=C, Ar), 1233 (C-N), 1151 (S=O), 1103 (C-O).

3.5.4.4 Chain-folding co-polyimide from *m*-terphenylene diamine (20 mol%) and pyromellitic dianhydride by the chemical imidisation route (3.12)

A solution of **3.2** (18.13 g, 28 mmol) and **3.4** (1.82 g, 7 mmol) in DMAc was stirred for 1 hr before the addition of pyromellitic dianhydride (7.62 g, 35 mmol) and phthalic anhydride (0.258 g, 1.74 mmol). The solution was stirred for 16 h and then acetic anhydride and pyridine were added and stirred for 1.5 h before heating the reaction mixture to 85 °C for 4 h. The solution was precipitated in methanol, filtered and dried under vacuum at 80 °C for 12 h, and then heated under vacuum at 200 °C for 5 h. The resulting solid was ground in an ultracentrifugal mill to yield polyimide **3.12** as a brown powder (22.64 g, 85%). This synthesis was repeated several times at the same scale.

3.12

T_g = 258 °C; η_{inh} (NMP) = 0.34 dL g^{-1}; ^{1}H NMR (400 MHz, CDCl$_3$/CF$_3$COOH 3:1 v/v): δ (ppm) 8.52 (s, 8H, **a**), 8.34 (s, 1H, **l**), 8.04 (d, J = 8, 30H (expected 21H), **i, o, q, s**) 7.96 (d, J = 8.8, 25H, **e**), 7.74 (d, J = 8, 27H, **f, m, n, p, r**), 7.62-7.58 (m, 15H, **b, c**), 7.40 (d, J = 6.4, 2H, **j**), 7.34 (d, J = 8, 30H, **h, g**), 7.30 (app d, 2H, **t**), 7.27 (t, J = 4, 9H, **d, k**), 7.12 (app d, J = 7.6, 2H, **u**); ^{13}C NMR (100 MHz, CDCl$_3$/CF$_3$COOH 3:1 v/v): δ (ppm) 165.7, 162.2, 155.3, 144.5, 140.1, 13.0, 133.2, 131.6, 130.9, 130.5, 130.0, 128.8, 128.4, 127.9, 123.1, 121.0, 120., IR: ν_{max} / cm^{-1} 1720 (C=O), 1580 (C=C Ar), 1485 (C=C, Ar), 1366 (C-N), 1241 (C-N), 1151 (S=O), 1104 (C-O-C).

3.5.5 Blending procedures

3.5.5.1 Solution blending

The method of solution blending of **3.5** and **3.9** is given here as a generic procedure for the preparation of polymeric blends.

Polymer **3.9** (0.25 g, 0.29 mmol) was added to a solution of **3.5** (0.25 g, 0.50 mmol) in DMAc and stirred for 5 minutes. The resulting blend was precipitated in methanol, filtered off and extracted in boiling methanol. The solid was finally washed with ether before drying under vacuum for 3 h to give pale cream polymer flakes (0.38 g, 76%).

3.5.5.2 Spin blending

The spin blending of **3.7** and **3.12** is given here as a generic procedure for the preparation of polymeric blend **[3.7·3.12]**.

A 250 mL round bottomed flask was charged with **3.7** (25 g) and **3.12** (15 g) and spun using a rotary evaporator until the powders were thoroughly mixed and a homogenous dispersion was achieved.

3.6 References

[1] H. M. EL-Dessouky and C. A. Lawrence, *Composites: Part B*, 2013, **50**, 429.

[2] C. Gao, S. Zhang, X. Li, S. Zhu and Z. Jiang, *Polymer*, 2014, **55**, 119-125.

[3] T. E. Attwood, P. C. Dawson, J. L. Freeman, L. R. J. Hoy, J. B. Rose and P. A. Staniland, *Polymer*, 1981, **22**, 1096–1103.

[4] M. T. Bishop, F. E. Karasz, P. S. Russo and K. H. Langley, *Macromolecules*, 1985, **18**, 86–93.

[5] Y. Lee and R. S. Porter, *Polym. Eng. Sci.*, 1986, **26**, 633-639.

[6] I. Fukawa and T. Tanabe, *J. Polym. Sci. Part A: Polym. Chem.,* 1993, **31**, 535-546.

[7] H. M. Colquhoun and D. F. Lewis, *Polymer,* 1988, **29,** 1902-1908.

[8] I. Manolakis, P. Cross, S. Ward and H. M. Colquhoun, *J. Mater. Chem.,* 2012, **22**, 20458-20464.

[9] A. Texier, R.M. Davis, K.R. Lyon, A. Gungor, J. E. McGrath, H. Marand and J.S. Riffle, *Polymer,* 1993, **34**, 896.

[10] H. Q. N. Gunaratne, C. R. Langerick, A. V. Puga, K. R. Seddon and K. Whiston, *Green Chem.,* 2013, **15**, 1166-1172.

[11] S. Burattini, H. M. Colquhoun, J. D. Fox, D. Friedmann, B. W. Greenland, P. J. F. Harris, W. Hayes, M. E. Mackay and S. J. Rowan, *Chem Commun.,* 2009, **28**, 6717–6719.

[12] D. K. Brandom and G. L. Wilkes, *Polymer*, 1994, **35**, 5672–5677.

[13] Z. Zhu, C. J. Cardin, Y. Gan, and H. M. Colquhoun, *Nature Chem.*, 2010, **2**, 653–660.

[14] T. Altares Jr., D. P. Wyman and V. R. Allen, *J. Polym. Sci. A Polym. Chem.*, 1964, **2**, 4533–4544.

[15] G. Crevecoeur and G. Groeninckx *Macromolecules,* 1991, **24**, 1190–1195.

[16] A. A. Goodwin and G. P. Sinmon, *Polymer*, 1996, **37**, 991-995.

[17] L. H. Sang and K. W. Nyon, *Polymer*, 1997, **38**, 2657-2663.

[18] S. Burattini, B. W. Greenland, W. Hayes, M. E. Mackay, S. J. Rowan and H. M. Colquhoun, *Chem. Mater.*, 2011, **23**, 6–8.

[19] R. J. Rahaim, Jr. and R. E. Maleczka, Jr., *Org. Lett.*, 2005, **7**, 5087–5090.

[20] M. H. Brink, D. K. Brandom, G. L. Wilkes and J. E. McGrath, *Polymer*, 1994, **35**, 5018–5023.

[21] Y. Nagata, T. Nishikawa and M. Suginome, *Chem. Commun.*, 2012, **48**, 11193–11195.

[22] R. K. Dieter, *Tetrahedron*, 1999, **55**, 4177–4236.

[23] K. P. Menard, *Dynamic Mechanical Analysis: a Practical Guide*, CRC Press, London, 2008.

[24] W.K. Goertzen and M.R. Kessler, *Composites: Part B*, 2007, **38**, 1–9.

[25] L. H. Cragg, T. E. Dumitru and J .E. Simkins, *J. Am. Chem. Soc.*, 1952, **74**, 1977–1979.

[26] G. V. Reddy, T. S. Rani, K. C. Rao and S. V. Naidu, *J. Reinf. Plast. Compos.,* 2009, **28**, 1665–1677.

[27] F. Abali, A. Pora and K. Shivakumar, *J. Compos. Mater.,* 2003, **37**, 453-464.

[28] L. Di Landro and M. Pegoraro, *J. Mater. Sci.*, 1987, **22**, 1980–1986.

[29] S. Deng, L. Ye and Y.-W. Mai, *Adv. Compos. Mater.*, 1998, **7**, 169-182.

[30] J. W. Mar and K. Y. Lin, *J. Aircraft*, 1997, **14,** 703–704.

[31] S. Priya and S. K. Rai, *J. Ind. Tex.*, 2006, **35**, 217–226.

[32] Toray Carbon Fibres America, Inc. T300 Technical Data Sheet No. CFA-001.

[33] J. Schultz, L. Lavielle and C. Martin, *J. Adhesion*, 1987, **23**, 45-60.

[34] Y. Nagata, T. Nishikawa and M. Suginome, *Chem. Commun.*, 2012, **48**, 11193–11195.

[35] L. Liu, Y. Zhang and B. Xin, *J. Org. Chem.*, 2006, **71**, 3994–3997.

[36] R. J. Rahaim, Jr. and R. E. Maleczka, Jr., *Org. Lett.*, 2005, **7**, 5087–5090.

Chapter 4

Controlled monomer-sequence randomisation in the synthesis of poly(aryl ether ketone)s

4.1 Abstract

The effects of varying the alkali metal cation in the high temperature nucleophilic synthesis of a semi-crystalline PAEK have been systematically investigated, and striking variations in the sequence distributions and thermal characteristics of the resulting polymers were found Polycondensation of 4,4'-dihydroxybenzophenone with 1,3-bis(4-fluorobenzoyl)benzene in the presence of an alkali metal carbonate M_2CO_3 (M = Li, Na, K or Rb) as base, affords a range of different polymers that vary in the distribution pattern of two-ring and three-ring monomer units along the chain. Li_2CO_3 gives an alternating and highly crystalline polymer, but the degree of sequence-randomisation increases progressively as the alkali metal series is descended, with Rb_2CO_3 giving a fully random and non-thermally-crystallisable polymer. Randomisation during polycondensation is shown to result from transetherification of the polymer by fluoride ions. An isolated sample of alternating-sequence polymer is thus converted to a fully randomised material on heating with RbF.

4.2 Introduction

Long-fibre composites based on semi-crystalline engineering polymers such as PEEK[1] and PEKK[2] as matrices (Figure 4.1) have gained significant attention in recent years.[3] The high crystalline melting points (T_m) of poly(aryl ether ketone)s (PAEKs), which are typically 340 – 380 °C, result in retention of significant mechanical strength and stiffness even at

temperatures well above their T_gs.[4] However, such melting points also require correspondingly high composite fabrication temperatures of up to 420 °C.[5]
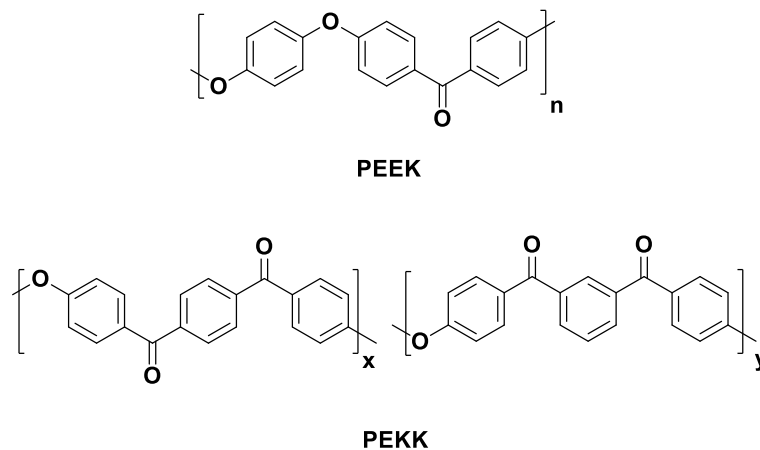

Figure 4.1. Some thermoplastic aromatic matrix polymers used in carbon fibre composites

Herein is described the study of a lower-melting but still crystallisable PAEK matrix polymer (**N4**; Figure 4.2) derived from the nucleophilic polycondensation of 4,4'-dihydroxybenzophenone with 1,3-bis(4-fluorobenzoyl)benzene. The synthesis of this polymer (T_g = 152 °C; T_m = 285 °C) has been briefly noted in a conference paper.[6] The combination of a T_g somewhat higher than that of PEEK (T_g = 143 °C; T_m = 343 °C) and a significantly lower melting point would enable more facile processing; thus making it a potentially very viable polymer matrix for composites.

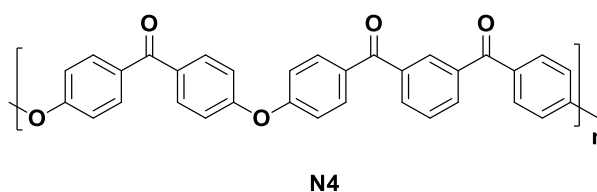**Figure 4.2.** Structure of polymer **N4** (N = "nucleophilic").

The polymer from the nucleophilic polycondensation mentioned above might initially be expected to comprise an alternating sequence of 2-ring and 3-ring monomer residues. A rigorously alternating structure of this type has in fact been obtained from the *electrophilic* polycondensation of 4,4'-diphenoxybenzophenone with isophthaloyl chloride (Scheme

4.1).[7,8] The resulting semi-crystalline polymer (**E4**) shows thermal characteristics (T_g = 147 °C; T_m = 310 °C) similar to that of the "nucleophilic" polymer **N4** (T_g = 152 °C; T_m = 285 °C), though the melting point of **E4** is noticeably higher.


E4
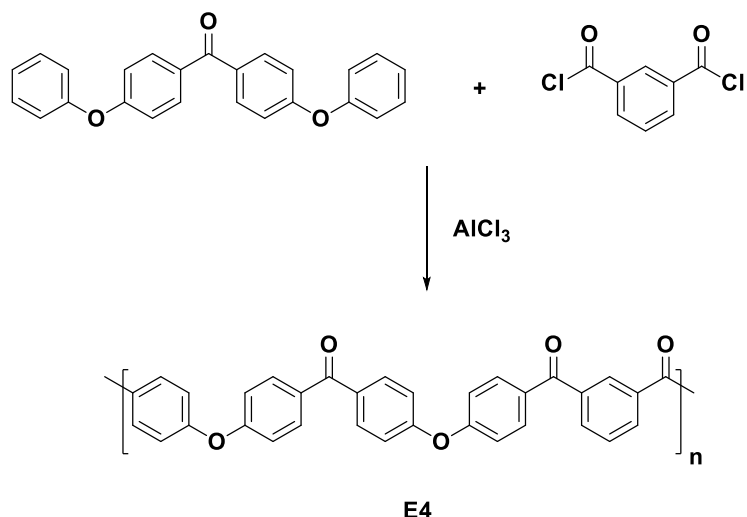
Scheme 4.1. Synthesis of polymer **E4** (E = "electrophilic").[7] The structures shown for **N4** (Figure 4.2) and **E4** are merely different representations of the same polymer chain sequence.

The work described in the chapter demonstrates that the difference in melting point is highly significant, as the different melting points and degrees of crystallinity (χ_c) of the "nucleophilic" polymers were found to be influenced by the nature of the alkali metal carbonate used in the synthesis. This variability is shown to relate to the degree of sequence-randomisation occurring in polycondensation, an effect resulting from reversible cleavage of the ether linkages during growth of the polymer chain growth.[9,10] This randomisation would of course not be expected in the electrophilic synthesis (Scheme 4.1).

4.3 Results and discussion

Polycondensation of a bis(4-fluoroaryl)ketone with 4,4'-dihydroxybenzophenenone in diphenyl sulfone as solvent at 300 °C in the presence of an alkali metal carbonate M_2CO_3 as base (Scheme 4.2; M = Na, K or Rb), afforded high molecular weight PAEKs **4.1**, **4.2** and **4.3** respectively, with inherent viscosities in the range 0.60 − 0.80 dL g^{-1}. A slight molar excess of the difluoroketone was used to control the final molecular weight. These polymers may also

be symbolised as PEKEK*m*K, poly(ether ketone ether ketone ketone) containing *meta*-phenylene linkages.
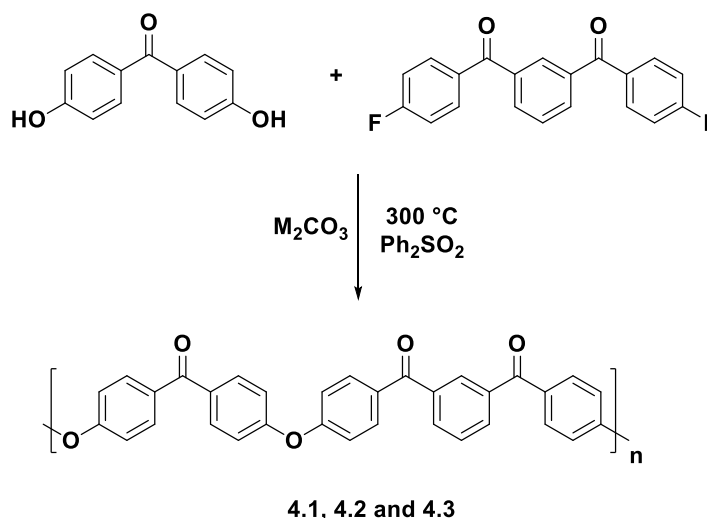
4.1, 4.2 and 4.3

Scheme 4.2. Synthesis of polymers **4.1**, **4.2** and **4.3** (M in M_2CO_3 = alkali metal).

4.3.1 Variation in crystallisability between the three "nucleophilic" polymers (4.1, 4.2, 4.3)

4.3.1.1 DSC analysis

Following exhaustive extraction of the DPS solvent and inorganic salts, the three polymers were dried and analysed by DSC. After the first heating scan to 350 °C, the samples were cooled at 10 °C min^{-1}. None of the polymers showed evidence of crystallisation on cooling from the melt, and the polymers were then reheated at the same rate (Figure 4.3). Polymer **4.1** (Na_2CO_3) showed a T_g of 149 °C, followed by a cold crystallisation exotherm peaking at 245 °C, and finally a crystal melting endotherm at 300 °C. The other two polymers, **4.2** (K_2CO_3) and **4.3** (Rb_2CO_3), showed only T_gs at 151 and 153 °C, respectively, on the second heating scan. It seemed possible that the observed variation in crystallisability between the three polymers could result from differences in the sequence distributions of the monomer residues along the polymer chain. Transetherification with sequence randomisation has previously been shown to occur during the nucleophilic synthesis of PAEKs in which both the monomer residues in the chain are activated towards nucleophilic attack adjacent to the ether linkage.[9,10]
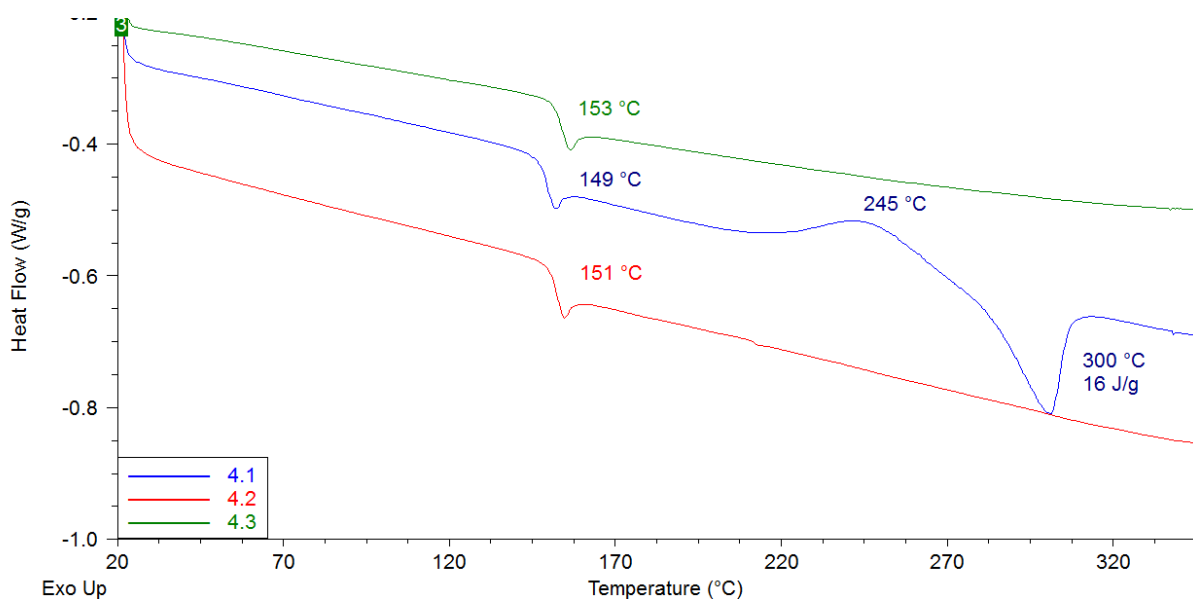
Figure 4.3. DSC thermograms of second heating scans for **4.1** (blue), **4.2** (red) and **4.3** (green).

4.3.1.2   Powder X-ray diffraction

Powder X-ray diffraction data supported the hypothesis that **4.1** is more highly crystalline than **4.2** and **4.3**, as is evident in Figure 4.4. Crystalline regions in the polymer produce sharp peaks in the diffraction pattern. The three polymers give fairly similar powder X-ray diffraction peaks, but the difference is that polymer **4.1** produced much stronger crystalline reflections than the other two polymers. As shown in Figure 4.4, the d-spacing at approximately 4.3 Å which becomes more crystalline. This may be attributed to a more efficient crystalline phase packing of polymer **4.1**, with its alternating monomer residues. Furthermore, 4.3 Å is the separation found between parallel aromatic rings of two hydroxybenzoyl residues previously discussed in this thesis (*cf.* Figure 2.26). The monomer residues presented in this present chapter is very similar to a hydroxybenzoyl residue. The increase in crystallinity is comparable with the DSC analysis (Figure 4.3), wherein **4.1** showed thermal crystallisability and the other two polymers did not.
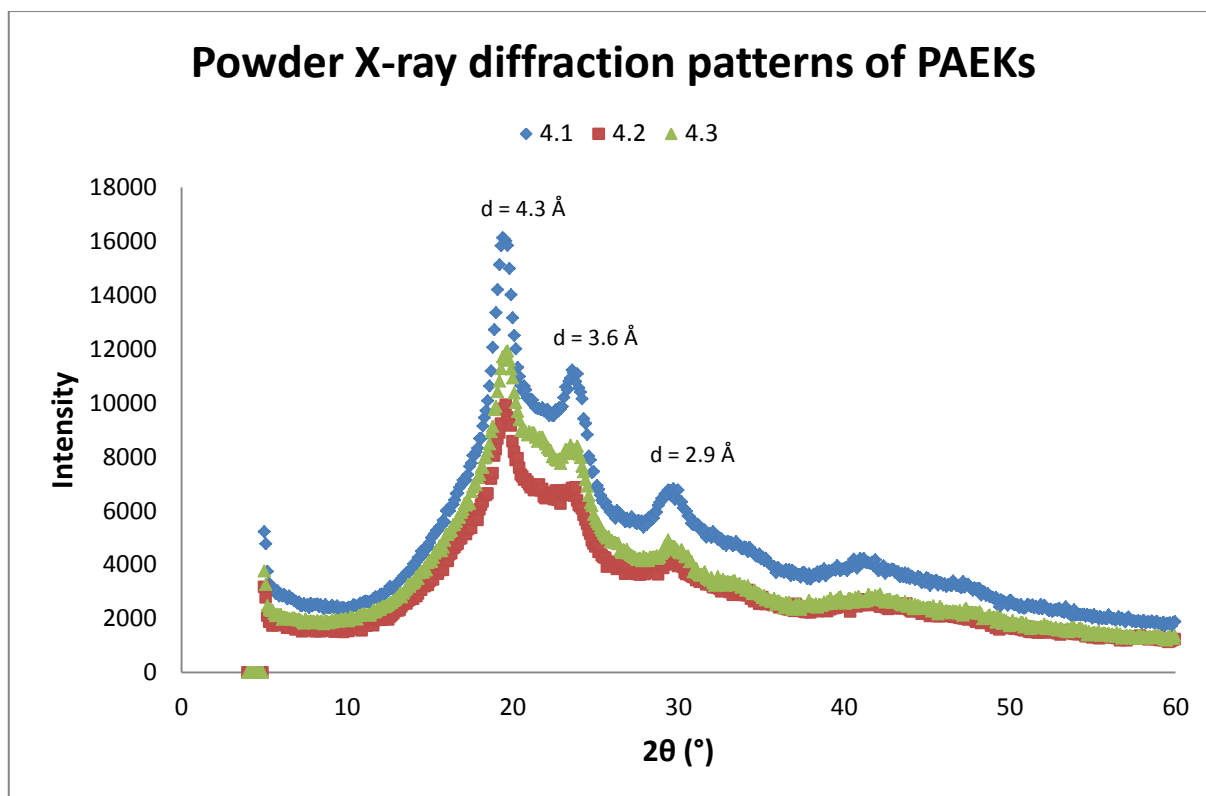
Figure 4.4. Powder X-ray diffraction pattern of polymers **4.1**, **4.2** and **4.3** with assigned values for the most intense interplanar spacings.

4.3.2 ^{13}C NMR analysis of resonances in the C-O-C region

The possibility that monomer sequence randomisation influenced the crystallisability of polymers was confirmed by ^{13}C NMR analysis. Figure 4.5 shows useful diagnostic resonances in the range δ = 160-162 ppm which corresponds to the aromatic carbons attached directly to ether oxygens. Polymer **4.1** shows only two peaks in this region, corresponding to the two different carbons of this type (one for each type of co-monomer residue; two-ring or three-ring) that would be expected from in the simple alternating structure (EKEK*m*K)$_n$. The other two polymers however, show two additional 'inner' peaks in the ^{13}C-O-C region, with the relative intensity of these peaks increasing substantially from **4.2** to **4.3**. This demonstrates that there are more distinct ^{13}C-O-C environments in **4.2** and **4.3** than in **4.1**, and the next sections will identify the different ^{13}C-O-C environments.
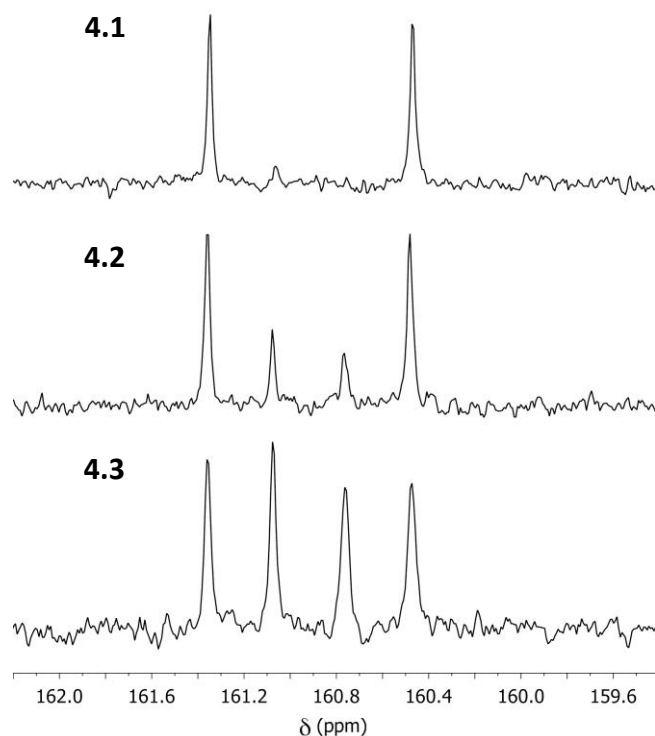
Figure 4.5. ^{13}C NMR resonances in the C-O-C region for polymers **4.1**, **4.2** and **4.3**.

4.3.3 Assignment of co-monomer resonances

In order to aid the assignment of ^{13}C-O-C peaks to the specific two-ring and three-ring co-monomer residues, a dimethyl substituted polymer (**4.7**), analogous to **4.1** was synthesised. This involved first the synthesis of the dimethyl bisphenol co-monomer (**4.6**, Scheme 4.3) followed by polycondensation with 1,3-bis(4-fluorobenzoyl)benzene.

The dimethyl bisphenol co-monomer was synthesised by the direct condensation of *o*-cresol with 4-hydroxy-3-methylbenzoic acid in triflic acid, which gave very pure 3,3'-dimethyl-4,4'-dihydroxybenzophenone (**4.6**). Bisphenol **4.6** was then polymerised with 1,3-bis(4-fluorobenzoyl)-benzene in the presence of Na_2CO_3 (Scheme 4.3) to give polymer **4.7**. These conditions are identical to the polymerisation conditions that produced polymer **4.1**. It is expected that the ^{13}C NMR spectrum of **4.7** will be similar to **4.1**, as the only difference between the two polymers are the bisphenol co-monomers.
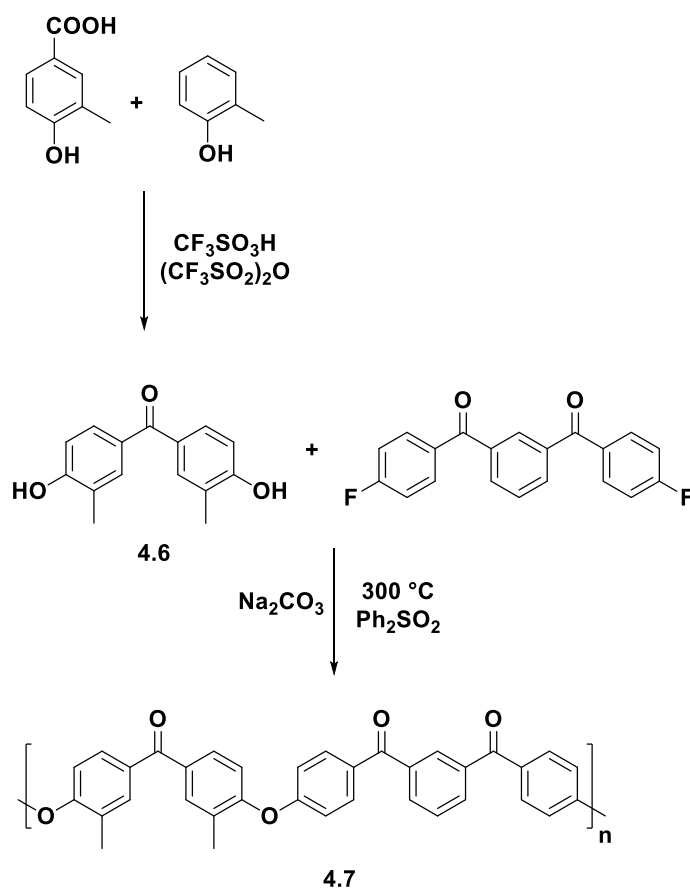
Scheme 4.3. Synthesis of bisphenol **4.6** and its polycondensation with 1,3-bis(4-fluorobenzoyl)-benzene to give poly(ether ketone) **4.7**.

The ^{13}C NMR spectrum of polymer **4.7** (Figure 4.6) shows two resonances assigned to the two carbons directly attached to ether oxygen. The difference between this spectrum and the spectrum for **4.1** is that the lower field ^{13}C-O-C peak (labelled **b**) is shifted only very slightly (around 0.25 ppm) relative to its position in the spectrum of **4.1**, whereas the peak labelled **a**, has shifted substantially upfield by some 2.9 ppm. This result strongly suggests that the lower field resonance stems from the ^{13}C-O-C carbon associated with the three-ring residue, which is chemically unchanged in the "dimethyl" polymer **4.7**. It then follows that the strongly shifted, higher field resonance can be assigned to the two-ring residue, in which the methyl substituents are *ortho* to its ^{13}C-O-C carbons.
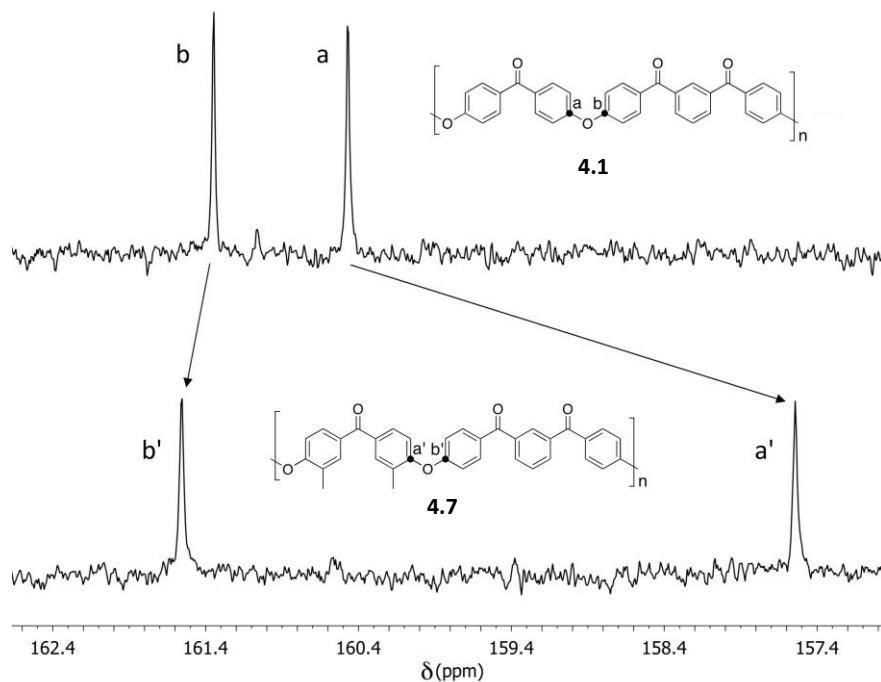
Figure 4.6. ^{13}C NMR spectra in the C-O-C region for polymers **4.1** and **4.7**.

4.3.4 Assignment of randomised sequence resonances

The ^{13}C NMR spectra of polymers **4.2** and **4.3** showed two additional "inner" peaks in the ^{13}C-O-C region (Figure 4.5). The increased multiplicity of the peaks suggests sequence-randomisation could be occurring, and indeed the new peaks proved assignable to sequences comprising two adjacent two-ring residues and two adjacent three-ring residues. These assignments were achieved by first doping a sample of polymer **4.2** with the homopolymer PEK*m*K[6] which resulted in the enhancement of the intensity of the peak at 161.1. This indicates that the lower field "inner" peak results from ^{13}C-O-C of two adjacent three-ring residues. Next, a sample of PEK[4] was added to **4.2**, which resulted in the increase of the intensity of the peak at 160.8. This shows conclusively that the higher field "inner" peak corresponds to two adjacent two-ring residues (Figure 4.7).
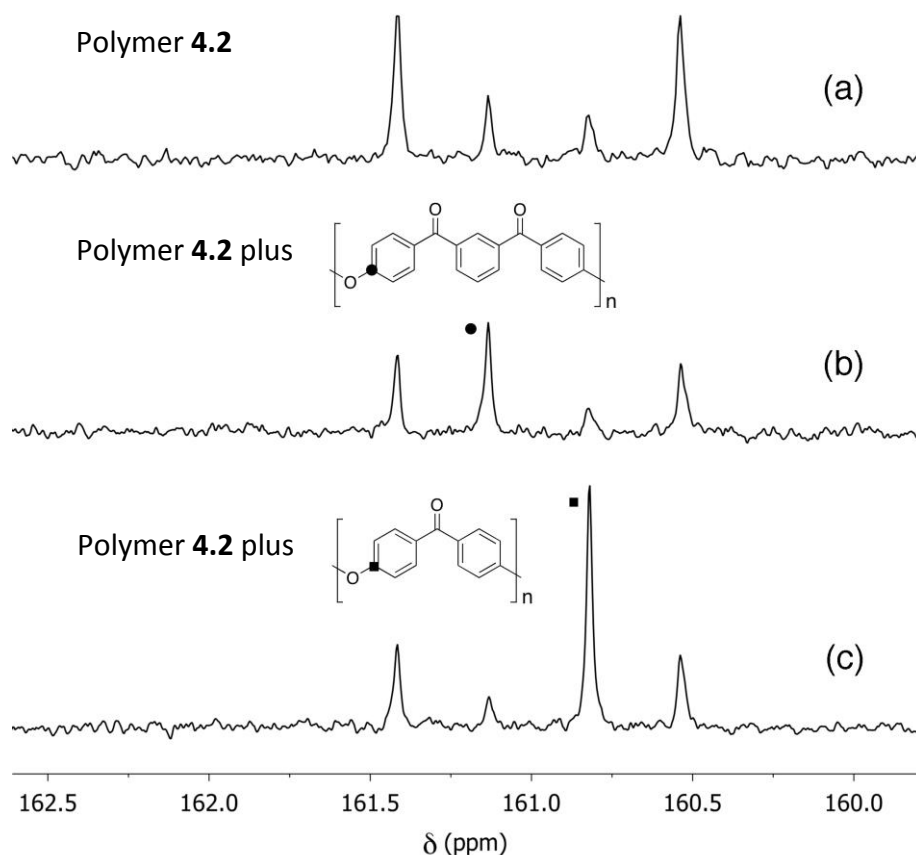
Figure 4.7. ^{13}C NMR resonances in the C-O-C region for (a) polymer **4.2**; and the same polymer doped with (b) PEK*m*K or (c) PEK.

4.3.5 Sequence probabilities and ^{13}C NMR intensities

The ^{13}C NMR spectrum of polymer **4.3**, produced using Rb$_2$CO$_3$ as base, showed even more extensive sequence randomisation than **4.2**, now with four peaks of *equal* intensity in the ^{13}C-O-C region (Figure 4.5). Analysis of the probability distribution for the three possible dimer sequences around the ether linkages in this copolymer shows that a completely random polymer would contain KEK, KEK*m*K and K*m*KEK*m*K sequences in the relative proportions 1:2:1. Calculating the sequence probability for **4.3** (Table 4.1), the probability of a three-ring being followed by a two-ring monomer residue is 0.25, and the same for the probability of a two-ring being followed by a three-ring residue. The probability of two two-ring residues being adjacent to each other is also 0.25 and the same is true for a three-ring followed by another three-ring residue. Thus all the possible sequences are accounted for, as the sum of all the probabilities is 1. This distribution would consequently give rise to four

^{13}C NMR resonances of equal intensity (1:1:1:1), as the unsymmetrical KEK*m*K sequence contains two distinct C-O-C carbons.

Table 4.1. Calculation of the sequence probabilities for polymer **4.3**, produced with Rb$_2$CO$_3$ as base.

Possible doublet sequences	^{13}**C NMR pattern**
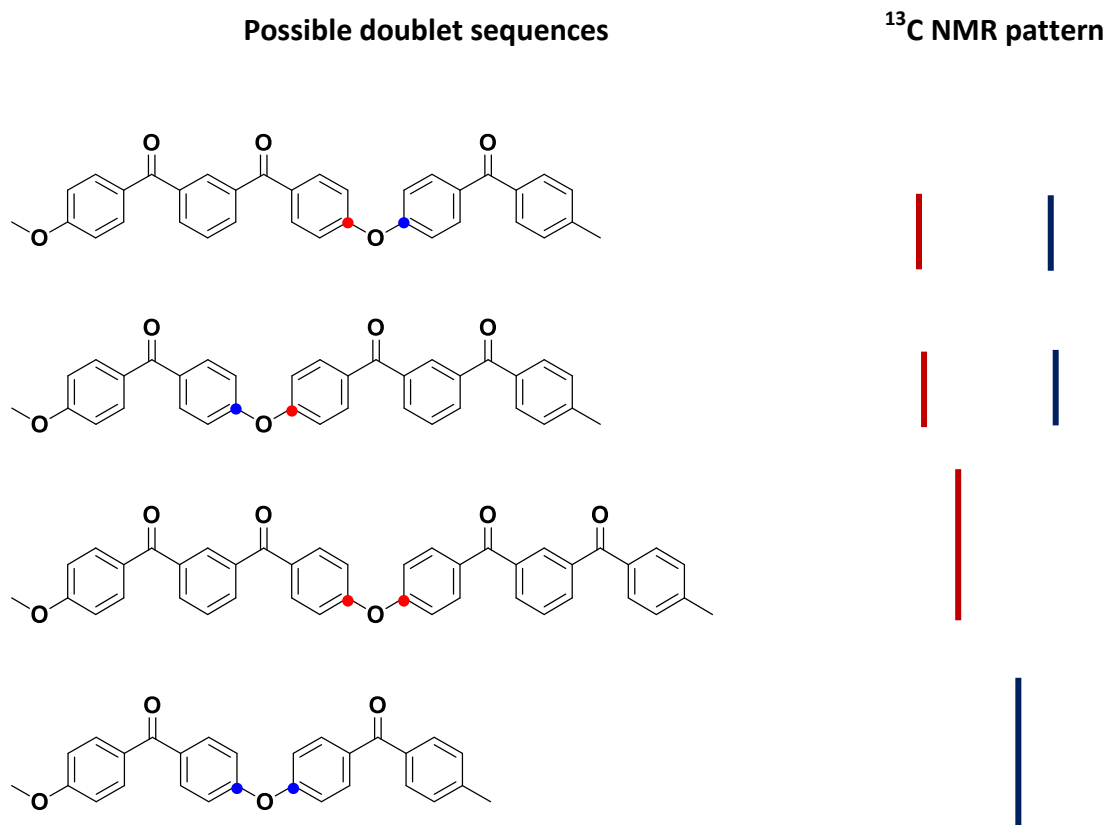
If the degree of randomness is 100%, then the probability of a three-ring being followed by a two-ring is 0.5 x 0.5 = 0.25 and the same for a two-ring being followed by a three-ring.

The probability of a three-ring being followed by a three-ring is then also 0.5 x 0.5 = 0.25, and the same is true for a two-ring being followed by a two-ring.

Summing the resonances for each sequence now gives four lines in the ratio 1:1:1:1. The sum of probabilities is 1, so these comprise all possibilities.
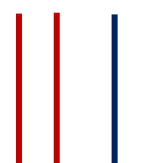
A similar calculation indicates that the intensity ratios observed (ca. 3:1:1:3) in the spectrum of polymer **4.2** which was synthesised with K_2CO_3 as base correspond to approximately 50% randomisation, relative to a fully alternating sequence. Thus, the probability of a three-ring being followed by a two-ring residue is now 0.375, and the same for a two-ring being followed by a three-ring residue. The probability of two adjacent two-rings is then 0.125, and again the same for a two three-ring sequence. The sum of probabilities for the above four sequences is 1, therefore all possible sequences are accounted for. The resonances for each sequence would now give four peaks in the ratio 3:1:1:3 (Table 4.2).

Table 4.2. Calculation of the sequence probabilities for polymer **4.2**, produced with K_2CO_3 as base.

Possible doublet sequences	**^{13}C NMR pattern**

If the degree of randomness is 50%, then the probability of a three-ring being followed by a two-ring is 0.5 x 0.75 = 0.375 and the same for a two-ring being followed by a three-ring.
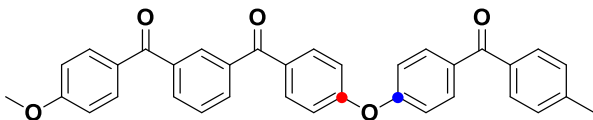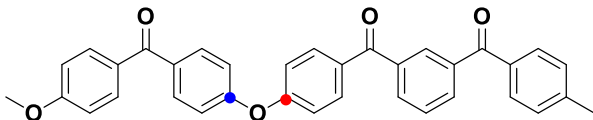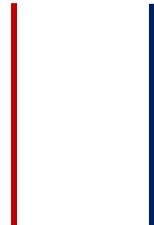
The probability of a three-ring being followed by a three-ring is then also 0.5 x 0.25 = 0.125, and the same is true for a two-ring being followed by a two-ring.

Summing the resonances for each sequence now gives four lines in the ratio 3:1:1:3. The sum of probabilities is 1, so these comprise all possibilities.

Now considering the fully alternating polymer **4.1** produced with Na_2CO_3 as base, just two ^{13}C NMR resonances of equal intensity in the C-O-C region is observed since the only possible co-monomer sequences are a two-ring followed by a three-ring residue and a two-ring followed by a three-ring residue, both with probability 0.5. Therefore it is expected to produce two peaks of equal intensity (Table 4.3).
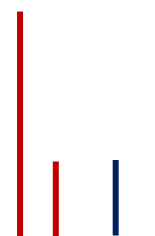
Table 4.3. Calculation of the sequence probability for polymer **4.1**, produced with Na_2CO_3.

Possible doublet sequences	^{13}C NMR pattern

Choosing monomers at random from two possible alternatives means that the probability of the first is 0.5, but the probability of the second is fully defined, i.e. 1.

In a fully alternating polymer, the only possible doublet sequences are three-ring followed by two-ring and two-ring followed by three-ring, both with probability 0.5 x 1 = 0.5.

Total probability is then 1 so all possible sequences are accounted for. The sum of all the resonances for each sequence would give two lines in the ratio 1:1.

It is worth noting that the original report of polymer **N4** indicated that it was synthesised using a mixture of Na_2CO_3 and K_2CO_3 and that its melting point was 285 °C,[11] which is significantly lower than for polymer **4.1** (300 °C). It thus seems very probable that a significant degree of sequence-randomisation in **N4** had also occurred in that work. In fact, even **4.1** is unlikely to be 100% alternating as its melting point is still slightly lower than that of the "electrophilic" polymer **E4** (310 °C). Moreover, the ^{13}C NMR spectrum of **4.1**, shown in Figure 4.5 reveals a very weak but still just detectable "inner" resonance corresponding to the symmetric, non-alternating sequence K*m*KEK*m*K. The relationships between polymers **4.1 – 4.3**, identified in the present work, are summarised in Figure 4.8.
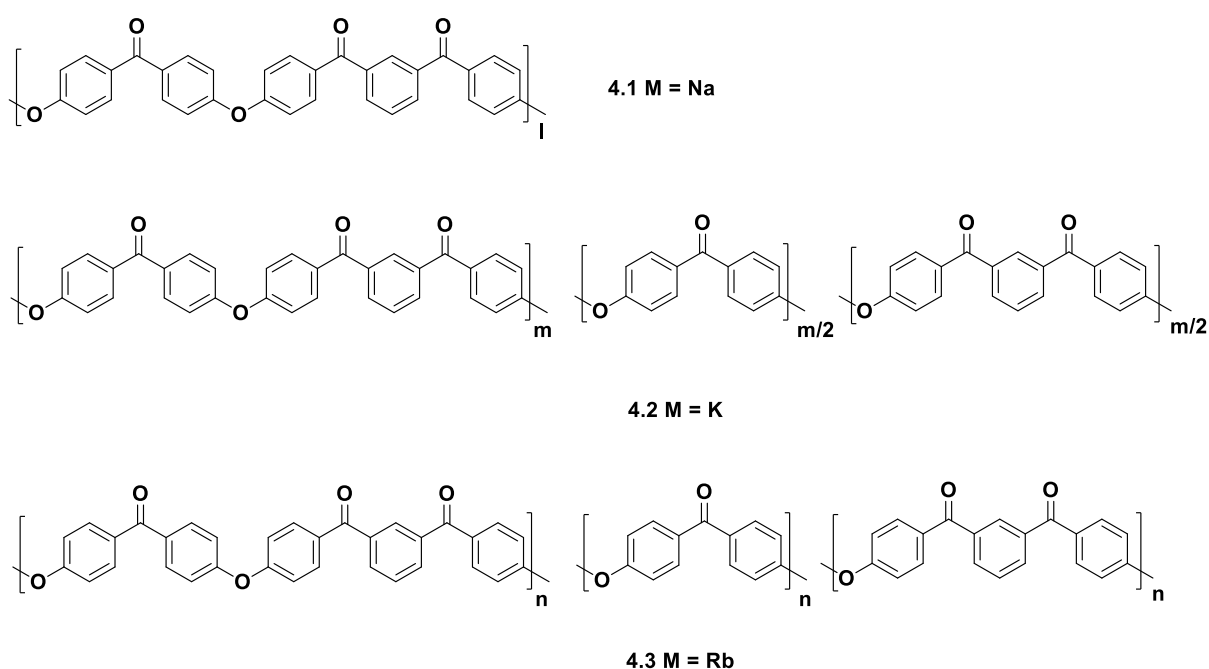
Figure 4.8. Representations of the chain sequences in polymers **4.1** (almost entirely alternating), **4.2** (semi-random) and **4.3** (fully randomised), arising from the use of different alkali metal carbonates M_2CO_3 in the nucleophilic polycondensation shown in Scheme 4.2.

4.3.6 Mechanism of sequence-randomisation of monomer residues

A number of possible mechanisms have been proposed for transetherification that occurs during the synthesis of PAEKs, but all depend on reversible, nucleophilic cleavage of the ether linkages (Scheme 4.4). Candidate nucleophiles in the system include the carbonate

and fluoride anions. Indeed K_2CO_3 has previously been shown to induce a small degree of sequence randomisation in a PAEK, albeit requiring very high reaction temperatures (340 °C) and prolonged reaction times (6 h).[11]
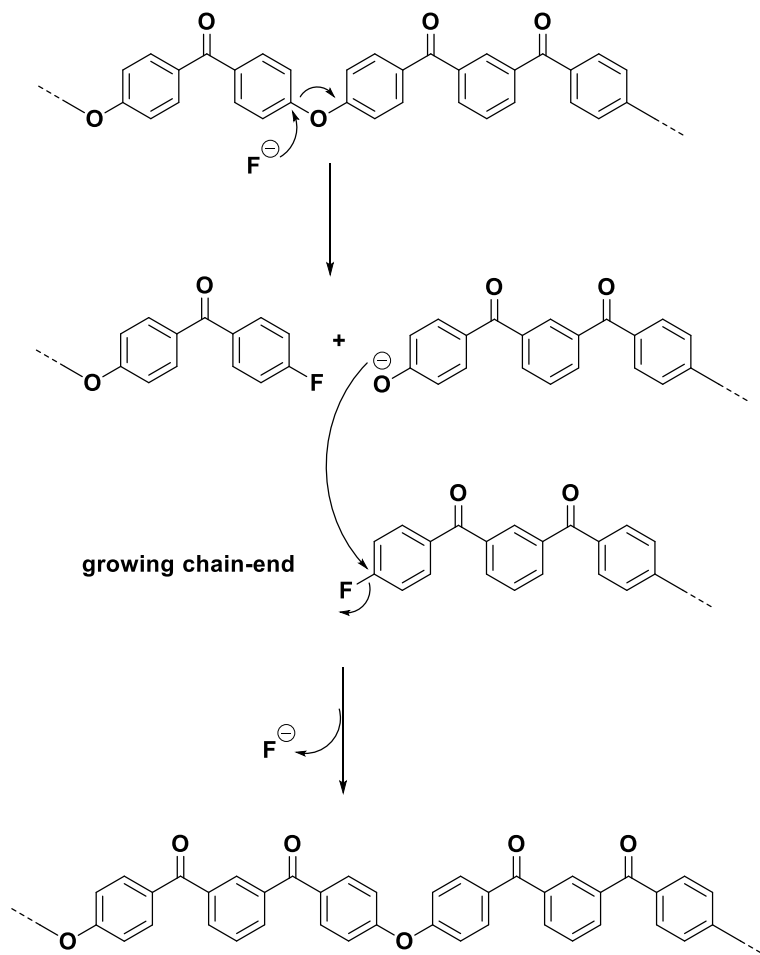
Scheme 4.2. Partial mechanism for fluoride-catalysed sequence randomisation in the synthesis of polymers **4.1 – 4.3**. The initial chain cleavage by fluoride can occur at either the two-ring or three-ring monomer residue. The fluoro- end-group resulting from this reaction can subsequently regenerate a fluoride anion by reaction with a phenoxide monomer or end-group.

The fluoride ion can be a very strong nucleophile in dipolar aprotic solvents,[12,13] but its effectiveness in this system would depend both on the solubility of the fluoride salt involved and on the extent of pairing with its counter-ion in solution. The larger the counter-ion, the weaker the ion-pairing and the more soluble the salt, so RbF should be much more effective than NaF, with KF somewhere in between (r_{ionic} = 1.16, 1.52, 1.66 Å for 6-coordinate Na$^+$, K$^+$, and Rb$^+$ respectively).[14] It has been suggested here that the relatively low solubility of NaF in

polar aprotic solvents such as diphenyl sulfone inhibits fluoride-catalysed transetherification in a poly(ether sulfone ether ketone) system, leading to a predominantly alternating structure.[15] In contrast, both the increased solubility and reduced ion-pairing in KF will promote fluoride-catalysed transetherification, so that a more random structure was produced. This report is fully consistent with the experimental results discussed above for sequence-randomisation in the synthesis of polymer **4.1 – 4.3**.

In the present work, sequence-randomisation catalysed by fluoride ion was demonstrated conclusively by treatment of the alternating polymer **4.1** with RbF in diphenyl sulfone, at the same concentrations, temperature and time as in polymer synthesis. The result was completely clear-cut, with the diagnostic ^{13}C-O-C resonances (Figure 4.9) for the product, **4.4**, changing from two equal intensity resonances in **4.1** (alternating structure) to four equal intensity resonances (random-sequence structure), exactly as in polymer **4.3**.

(a) Polymer **4.1**
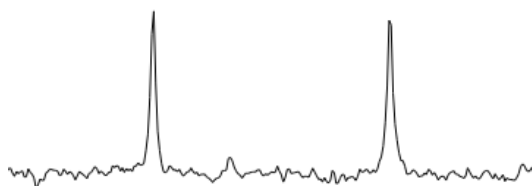
(b) Polymer **4.1** treated with RbF

producing **4.4**
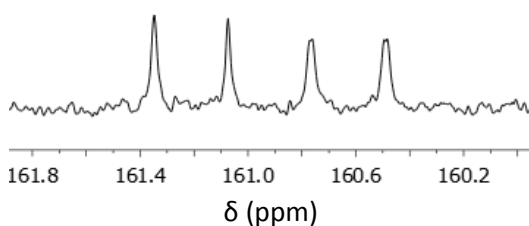
Figure 4.9. ^{13}C NMR spectra showing ^{13}C-O-C resonances of (a) Polymer **4.1** produced with Na_2CO_3 (almost entirely alternating structure) and (b) polymer **4.4** (fully randomised) produced by treating the as-made polymer **4.1** with RbF.

4.3.7 Polymer made with Li_2CO_3 as base

As a final test of the proposed mechanism for sequence-randomisation, the polycondensation shown in Scheme 4.2 was carried out using *lithium* carbonate as base. The extremely low solubility of LiF in organic solvents[16] should strongly inhibit fluoride-catalysed transetherification and indeed, as shown in Figure 4.10, resonances arising from sequence randomisation were scarcely discernable in the ^{13}C NMR spectrum of the resulting polymer (**4.5**).

(a) Polymer **4.5**

M = Li

(b) Polymer **4.3**

M = Rb
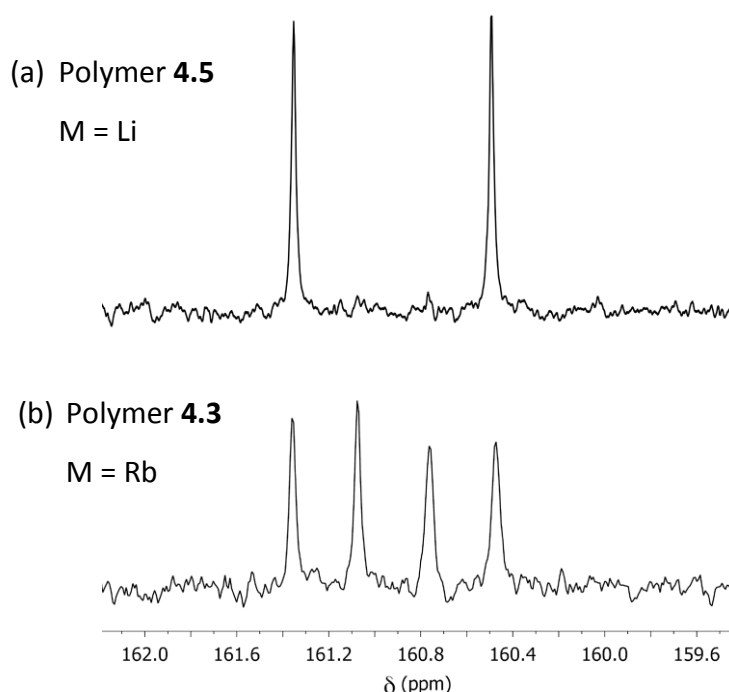
Figure 4.10. ^{13}C NMR resonances in the C-O-C region for polymers (a) **4.5** (alternating) compared with (b) **4.3** (fully randomised), made with different alkali metal carbonates M_2CO_3, illustrating the virtual absence of sequence-randomisation in the former polymer.

As shown in the DSC thermogram (Figure 4.11), polymer **4.5** crystallised from the melt (T_c = 215 °C), unlike the other polymers described in this chapter. Polymer **4.5** also showed a slightly higher T_m value than **4.1** (304 °C vs. 300 °C) and a much higher χ_c (ΔH_m = 49 vs. 16 J/g), presumably the consequences of a more perfectly alternating sequence of monomers along the polymer chain.
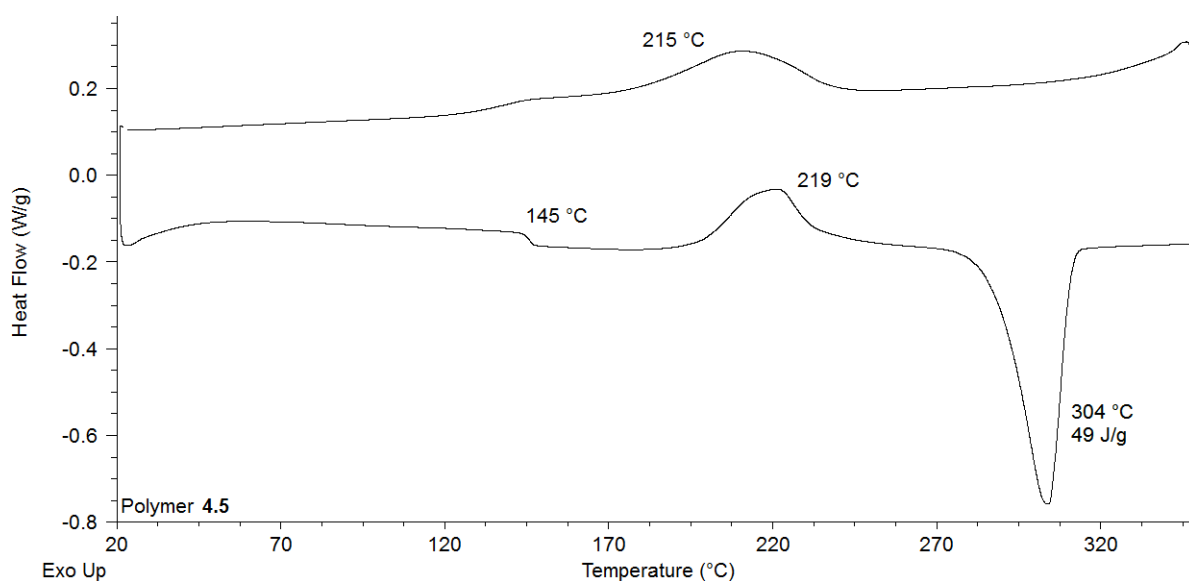
Figure 4.11. DSC thermogram of second heating and subsequent cooling scans for polymer **4.5**.

4.4 Crystal and molecular structure of PEKEK*m*K

The structure was solved, in collaboration with Professor H. M. Colquhoun, by diffraction-modelling using computational simulation software (*Cerius2*, v. 3.5) from Accelrys, San Diego, and was refined manually against experimental X-ray fibre data from a sample of PEKEK*m*K that had been synthesised using Na_2CO_3 as base (**4.1**). Fibres were drawn over a hotplate set at 400 °C, to five times their original length, and were then annealed at constant length for 16 h at 220 °C. X-ray fibre diffraction patterns were obtained from a vertically-oriented fibre using an Oxford Diffraction *Gemini* single crystal diffractometer, with Cu-Kα radiation (λ = 1.5418 Å). Patterns were obtained by averaging four images with the fibre at 0°, 90°, 180°, and 270° rotations about the vertical axis. The most highly-resolved fibre pattern thus obtained is given in Figure 4.12, below, with *d*-spacings shown on the pattern-calibration rings:

128
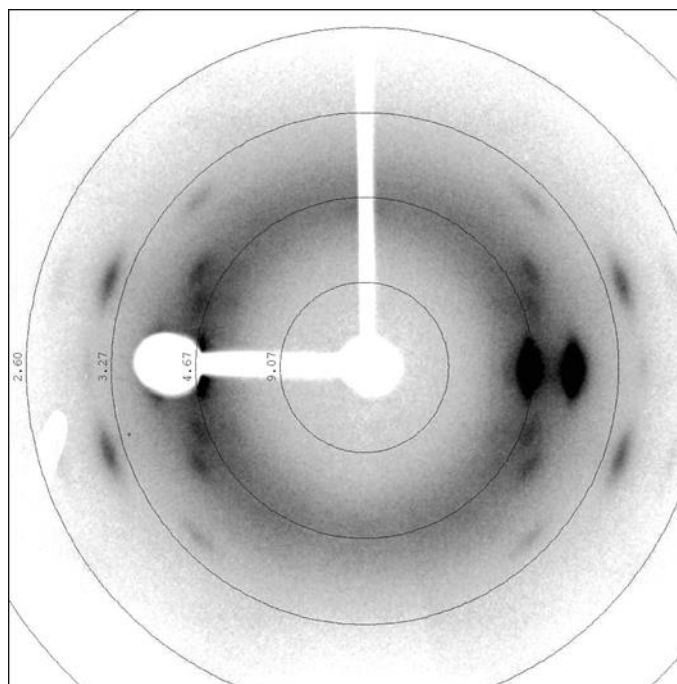
Figure 4.12. X-ray fibre diffraction pattern of PEKEK*m*K.

An initial model for the polymer repeat unit (5 rings) was built using conformational data from the previously-determined structure[17] of a closely-related polymer known as "PK99"[18,19], in which 4,4'-biphenol replaced the 4,4'-dihydroxybenzophenone used in the synthesis of PEKEK*m*K, in polycondensation with 1,3-bis(4-fluorobenzoyl)benzene (Figure 4.13).
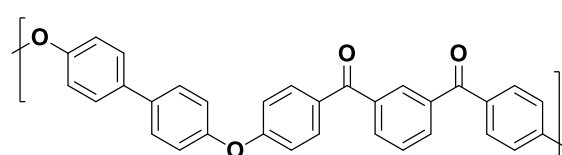
"PK99" (5-ring repeat)
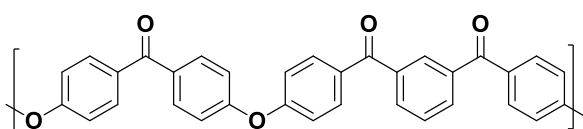
PEKEKmK (5-ring repeat)

Figure 4.13. Model repeat units of PK99 and PEKEK*m*K.

In the present work, a single, 5-ring repeat unit of PEKEK*m*K (Figure 4.13) was constructed using the same molecular parameters as were found for the chain in PK99. The latter structure had shown that the two 1,3-carbonyl groups are not coplanar with their associated aromatic ring (as had been assumed in earlier studies)[18-20] but are twisted by some 20° in the same direction, out of the plane of the ring. This conformation had originally been identified in the single-crystal X-ray structure of a model oligomer (Figure 4.14) based on a central 1,3-dicarbonyl-phenylene unit,[17] and the same "twisted" conformation was thus also adopted in the present study.
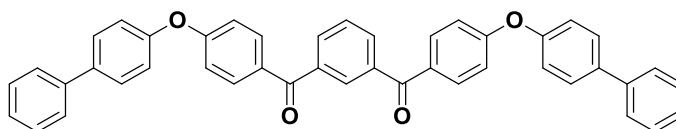
Figure 4.14. Structure of the model oligomer of PK99 from which a conformation for PEKEK*m*K was adopted.

A single, 5-ring chemical repeat unit, with the chain conformation as described above, was constructed in in *Cerius2*, but the overall conformation of this unit suggested that linking such units together would give a curved rather than linear chain conformation. A second 5-ring chemical repeat unit was therefore built, with a conformation that was a mirror-image of the first repeat, and linking the two units gave a linear 10-ring unit in which the two isophthaloyl rings are tilted to opposite sides of the chain (Figure 4.15).
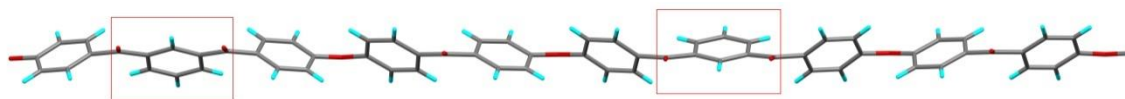
Figure 4.15. A linear 10-ring unit of PEKEK*m*K, with the two isophthaloyl rings tilted to opposite sides of the chain.

Using this 10-ring repeat as the "monomer", a single chain of PEKEK*m*K was constructed in an orthorhombic 10 Å x 10 Å unit cell using the "Crystal Builder" tool in *Cerius2*, which automatically aligns the polymer chain with the *c*-axis, as is conventional in polymer crystallography. This chain was placed at the origin and, on the basis of numerous known poly(ether ketone) structures,[17,21] a second chain was generated at the centre of the cell by

applying the *b*-glide operation [-x+1/2, y+1/2, z]. The *a* and *b* dimensions were then re-set to 7.80 and 6.07 Å respectively (the values found for PK99), and the *c*-dimension was set by the modelling program to 51.51 Å.

The structure was then energy-minimised with fixed (orthorhombic) unit cell dimensions, using a version of the Dreiding-2 force field that had previously been optimised for aromatic polymer structures.[22,23] Next, the unit cell lengths were allowed relax during a second cycle of energy minimisation, affording values of *a* = 7.62, *b* = 6.01 and *c* = 49.97 Å. A fibre pattern simulated from this structure gave an extremely encouraging (though not quite exact) match to the experimental pattern shown above. Repeated manual adjustment of the cell lengths, followed by re-minimisation and comparison between simulated and experimental fibre patterns led to optimised unit cell dimensions of *a* = 7.68, *b* = 6.04 and *c* = 49.50 Å.

At this point, the structure was searched for space-group symmetry using the "Find Symmetry" tool in *Cerius2*, resulting in assignment of the body-centred orthorhombic space group *Ima2*. However, applying this space group to the structure resulted in the chain-axis being realigned by the program parallel to *a* rather than to *c*. The lattice was therefore re-set to correct this, resulting in the final space group being defined as *Ic2m*. The structure was finally re-minimised in this space group, with fixed cell dimensions, and the resulting structure is shown in Figure 4.16, projected (top to bottom) along the *a*, *b* and *c* axes of the unit cell. The asymmetric unit (Figure 4.17) comprises 2.5 aromatic rings, one ether linkage and 1.5 carbonyl groups. Representative bond lengths and angles from the final structure are shown.
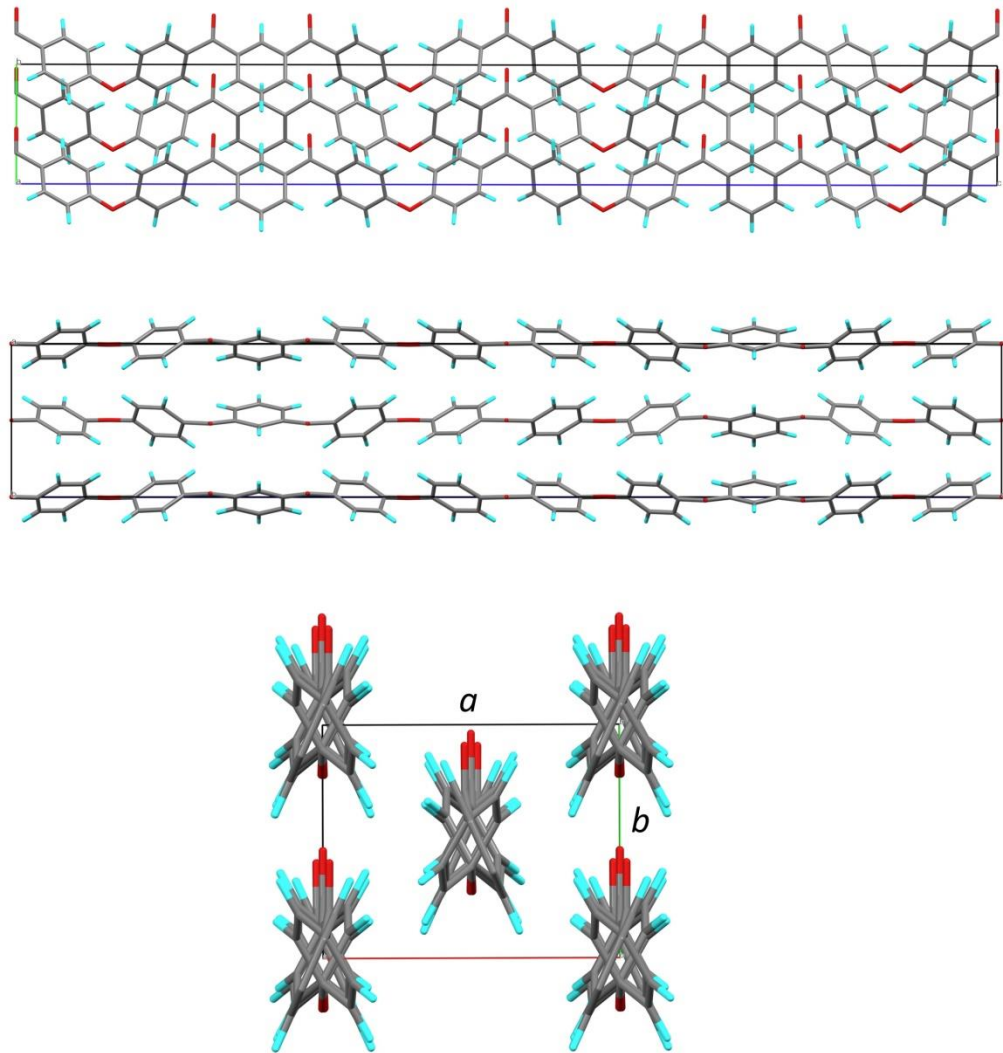
Figure 4.16. PEKEK*m*K in the space group *Ic2m*, with the final structure projected along the *a*, *b* and *c* axes of the unit cell (top to bottom).
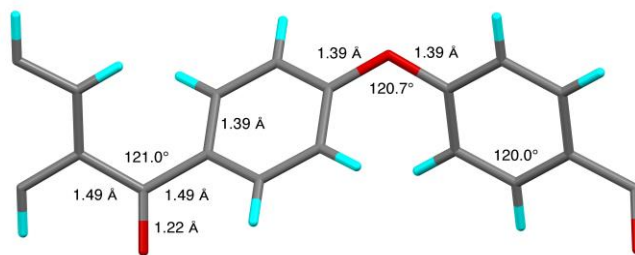
Figure 4.17. The asymmetric unit of PEKEK*m*K, with representative bond lengths and angles.

Fully quantitative comparison between experimental and simulated fibre patterns is not possible in *Cerius2*, but direct overlay of the fibre pattern simulated from the above

structure on the experimental pattern (Figure 4.18) shows qualitatively excellent agreement in the positions and intensities of the predicted and observed reflections. Further refinement of the structure could undoubtedly be achieved, but it seems clear that the present model is, at worst, a very good approximation to the structure of polymer PEKEK*m*K.
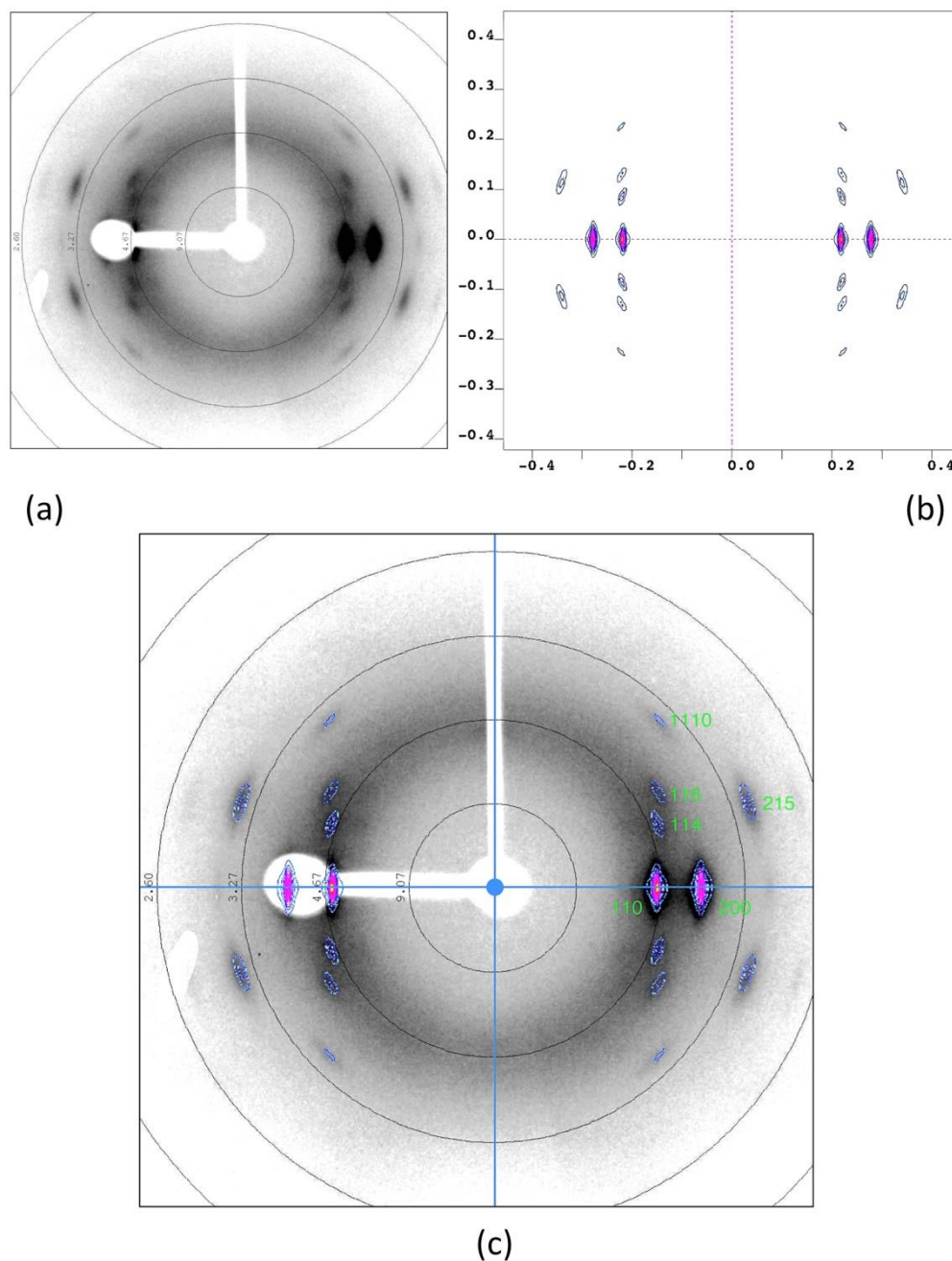
Figure 4.18. (a) Experimental, (b) simulated fibre patterns and (c) direct overlay of the two patterns.

4.5 Conclusions

Sequence-randomisation, via transetherification, during the nucleophilic synthesis of a PAEK involving fluoride displacement from a bis(4-fluoroaryl)ketone can be controlled by varying the alkali metal cation (Li^+, Na^+, K^+, or Rb^+) present during polycondensation. Substitution of Na_2CO_3 by K_2CO_3 as base produces a PAEK with a more random distribution of subunits. When Rb_2CO_3 is used as base, the arrangement of monomer subunits within the chain is almost entirely random. Polycondensation in the presence of Li_2CO_3 produced an essentially alternating arrangement of monomer residues.

This sequence-randomisation is a result of reversible nucleophilic cleavage by fluoride ions of ether linkages activated by electron-withdrawing carbonyl groups. The very low solubility of LiF in dipolar aprotic solvents such as diphenyl sulfone prevents transetherification, thus leading to an essentially entirely alternating structure. The degree of transetherification increases with the ionic radius of the alkali metal involved, and a proposed mechanism in which fluoride ions reversibly cleave the growing polymer chain is substantiated by a direct demonstration of sequence-randomisation in the presence of RbF. The crystallisability of the polymer from the melt declines markedly as the degree of sequence-randomisation increases as demonstrated by differential scanning calorimetry and powder X-ray diffraction. A crystal structure for the alternating polymer has been simulated by computational modelling and shown to be in good agreement with experimental X-ray diffraction data from a highly oriented fibre.

4.6 Experimental

4.6.1 Materials

1,3-Bis(4-fluorobenzoyl)benzene, 4,4'-dihydroxybenzophenone, trifluoroacetic acid, rubidium carbonate, 12-crown-4, acetone, diethyl ether, methanol, deuterated chloroform and deuterated dimethylsulfoxide were purchased from Sigma Aldrich, UK. Lithium carbonate, trifluoromethanesulfonic anhydride and diphenyl sulfone were purchased from Alfa Aeser, UK. Samples of polymers PEK and PEK*m*K were provided by Cytec Industries, UK. Sodium carbonate, potassium carbonate and tetrahydrofuran were purchased from Fisher Scientific, U.K, ground into a fine powder, sealed under argon and stored in a vacuum

desiccator until use. 1,1,1,3,3,3-Hexafluoro-2-propanol was purchased from Apollo Scientific, U.K. All materials were used without further purification unless stated otherwise.

4.6.2 Polymer 4.1

A mixture of 1,3-bis(4-fluorobenzoyl)benzene (4.60 g, 14.3 mmol), 4,4'-dihydroxybenzophenone (3.00 g, 14.0 mmol), Na_2CO_3 (1.63 g, 15.4 mmol) and diphenyl sulfone (35 g) was heated with stirring to 300 °C under argon. After 3 h, the polymer solution was poured onto a sheet of aluminium and allowed to cool. The resulting solid was milled to a fine powder, and then stirred in acetone (200 mL) at room temperature for 30 min. The powder was filtered off then was next extracted with 4 x 200 mL of refluxing acetone, and then overnight in a Soxhlet extractor with refluxing acetone. The powder was extracted with 5 x 200 mL of boiling water and then finally with 4 x 200 mL of refluxing acetone. The resulting purified material was dried at 110 °C under vacuum for 16 h, affording polymer **4.1** as a beige powder (5.65 g, 81%).
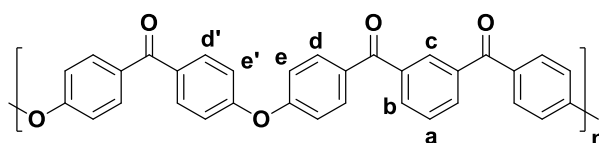
4.1

T_g = 149 °C; T_c = 245 °C; T_m = 300 °C; η_{inh} (H_2SO_4): 0.62 dL g^{-1}; ^{1}H NMR (400 MHz, CDCl$_3$/(CF$_3$)$_2$CHOH 6:1 v/v): δ (ppm) 8.18 (s, 1H **c**), 8.07 (d, J = 7.6, 2H **b**), 7.91 (m, 8H **d, d'**), 7.75 (t, J = 7.6, 1H **a**), 7.26 (d, J = 8.0, 8H **e, e'**) ppm; ^{13}C NMR (100 MHz, CDCl$_3$/(CF$_3$)$_2$CHOH 6:1 v/v): δ (ppm) 199.1, 198.8, 161.4, 160.5, 137.5, 134.2, 133.1, 132.8, 132.6, 131.6, 130.8, 129.0, 119.1, 118.8; IR: v_{max}/ cm^{-1} 2997 (C-H), 1655 (C=O), 1588 (C-C), 1238 (C-O-C), 1161 (C-O-C).

4.6.3 Polymer 4.2

This polymer was obtained using the procedure described for polymer **4.1**, but with potassium carbonate (2.13 g, 15.4 mmol) replacing sodium carbonate to give polymer **4.2** as a beige powder (6.00 g, 86%).

T_g = 151 °C; η_{inh} (H_2SO_4): 0.78 dL g^{-1}; ^{1}H NMR (400 MHz, CDCl$_3$/(CF$_3$)$_2$CHOH 6:1 v/v): δ (ppm) 8.19 (s, 1H), 8.08 (d, J = 7.6, 2H), 7.92 (m, 8H), 7.76 (t, J = 7.6, 1H), 7.26 (d, J = 8.0, 8H) ppm; ^{13}C NMR (100 MHz, CDCl$_3$/(CF$_3$)$_2$CHOH 6:1 v/v): δ (ppm) 199.4, 199.0, 161.4, 161.1, 160.8, 160.5, 134.3, 133.1, 132.8, 132.8, 132.6, 131.8, 131.6, 130.8, 129.0, 119.8, 118.8; IR: ν$_{max}$ / cm^{-1} 2985 (C-H), 1656 (C=O), 1591 (C-C), 1240 (C-O-C), 1163 (C-O-C).

4.6.4 Polymer 4.3

The same procedure as described for polymer **4.1** was used, but replacing sodium carbonate with rubidium carbonate (3.56 g, 15.4 mmol) and using a 5 mol% excess of 1,3-bis(4-fluorobenzoyl)benzene (4.74 g, 14.70 mmol) to control the molecular weight, afforded polymer **4.3** as a beige powder (5.35 g, 77%).

T_g = 153 °C; η_{inh} (H_2SO_4): 0.73 dL g^{-1}; ^{1}H NMR (400 MHz, CDCl$_3$/(CF$_3$)$_2$CHOH 6:1 v/v): δ (ppm) 8.12 (s, 1H), 8.01 (d, J = 7.6, 2H), 7.86 (m, 8H), 7.70 (t, J = 7.6, 1H), 7.21 (d, J = 8 Hz, 8H); ^{13}C NMR (100 MHz, CDCl$_3$/(CF$_3$)$_2$CHOH 6:1 v/v): δ (ppm) 199.0, 198.7, 161.3, 161.1, 160.8, 160.4, 137.4, 134.2, 133.1, 132.8, 132.6, 132.5, 131.8, 131.6, 130.8, 129.0, 119.1, 118.9; IR: ν$_{max}$ / cm^{-1} 3000 (C-H), 1654 (C=O), 1588 (C-C), 1497 (C-C), 1236 (C-O-C), 1160 (C-O-C).

4.6.5 Polymer 4.4

Polymer **4.1** (2.20 g), RbF (1.49 g, 14.3 mmol) and diphenyl sulfone (35 g) were heated with stirring at 300 °C under argon for 2 hours. Using the same work-up procedure as described for polymer **4.1** gave polymer **4.4** as a tan powder (1.05 g, 47%).

T_g = 153 °C; η_{inh} (H_2SO_4) = 0.44 dL g^{-1}; ^{1}H NMR (100 MHz, CDCl$_3$/(CF$_3$)$_2$CHOH 6:1 v/v): δ (ppm) 8.13 (s, 1H), 8.01 (d, J = 7.6 Hz, 2H), 7.87 (m, 8H), 7.70 (t, J = 7.6 Hz, 1H), 7.20 (d, J = 8.0 Hz, 8H); ^{13}C NMR (100 MHz, CDCl$_3$/(CF$_3$)$_2$CHOH 6:1 v/v): δ (ppm) 197.6, 197.4, 161.0, 160.7, 160.4, 160.1, 137.5, 134.0, 133.1, 132.8, 131.9, 131.7, 130.9, 129.8, 128.9, 119.1, 118.9; IR: ν$_{max}$ / cm^{-1} 2982 (C-H), 1655 (C=O), 1589 (C-C), 1497 (C-C), 1238 (C-O-C).

4.6.6 Polymer 4.5

The same procedure as described for polymer **4.1** was used, but replacing sodium carbonate with lithium carbonate (1.13 g, 15.4 mmol) and using an additional 2 x 200 mL of boiling water at the extraction stage. The polymer was then extracted with 12-crown-4 ether in

tetrahydrofuran for 48 h to ensure removal of lithium fluoride. The polymer as then filtered off, washed with acetone, diethyether, boiling water, followed by more acetone. This gave polymer **4.5** as a colourless powder (5.53 g, 78%).

T_g = 143 °C; T_c = 219 °C; T_m = 304 °C; η_{inh} (H_2SO_4): 0.40 dL g^{-1}; ^{1}H NMR (400 MHz, $CDCl_3$/$(CF_3)_2$CHOH 6:1 v/v): δ (ppm) 8.13 (s, 1H), 8.01 (d, J = 7.6 Hz, 2H), 7.87 (t, 8H), 7.70 (t, J = 7.6 Hz, 1H), 7.20 (dd, J = 8, 4 Hz, 8H); ^{13}C NMR (100 MHz, $CDCl_3$/$(CF_3)_2$CHOH 6:1 v/v): δ (ppm) 196.8, 196.6, 160.5, 159.6, 137.1, 133.5, 132.6, 132.3, 131.3, 130.4, 129.3, 128.5, 118.6, 118.4; IR: v_{max}/ cm^{-1} 1653 (C=O), 1588 (C-C), 1496 (C-C), 1235 (C-O-C), 1161 (C-O-C).

4.6.7 3,3'-Dimethyl-4,4'-dihydroxybenzophenone (4.6)

A solution of 4-hydroxy-3-methylbenzoic acid (3.00 g, 19.7 mmol) and *o*-cresol (2.27 g, 21 .0 mmol) in a mixture of trifluoromethanesulfonic anhydride (3.40 mL, 21.0 mmol) and trifluoromethanesulfonic acid (30 mL) was stirred under nitrogen for 18 h. The solution was then added dropwise into stirring water (800 mL). The precipitate was filtered off, washed repeatedly with boiling water, then with a 0.01M NaOH solution, and finally with cold water until a neutral filtrate was obtained. The solid was dried in a vacuum oven at 90 °C for 5 h to afford bisphenol **4.6** as a colourless powder (3.20 g, 67%).
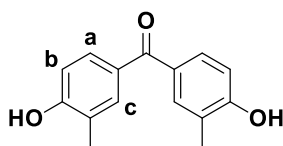
4.6

M.p. (DSC): 248 °C (lit. 247-248 °C)[24]; HRMS (ESI) m/z: 243.1016 [$C_{15}H_{15}O_3$], calculated: 243.1021; ^{1}H NMR (400 MHz, $CDCl_3$/CF_3COOH 6:1 v/v): δ (ppm) 7.65 (d, J = 2.0, 2H, **a**), 7.58 (dd, J = 2.0, 8.4, 2H, **c**), 6.91 (d, J = 8.4, 2H, **b**), 2.31 (s, 6H, CH_3); ^{13}C NMR (100 MHz, $CDCl_3$/CF_3COOH): δ (ppm) 200.36, 158.81, 134.68, 131.75, 129.26, 124.74, 115.06, 15.51. IR: v_{max}/ cm^{-1} 3424 (O-H), 3229 (O-H), 1639 (C=O), 1579 (C-C), 1373 (C-O).

4.6.8 Polymer 4.7

A mixture of bisphenol **4.6** (2.42 g, 10.0 mmol), 1,3-bis(4-fluorobenzoyl)benzene (3.28 g, 10.2 mmol), Na_2CO_3 (1.16 g, 11.0 mmol) and diphenyl sulfone (35 g) was heated with stirring

to 300 °C under argon. The workup procedure for polymer **4.1** was followed to afford polymer **4.7** as a colourless powder (3.40 g, 64%).

4.7
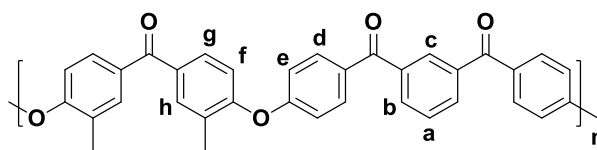
T_g = 168 °C; η_{inh} (H$_2$SO$_4$): 0.44 dL g^{-1}; ^{1}H NMR (400 MHz, CDCl$_3$/CF$_3$COOH 6:1 v/v): δ (ppm) 8.18 (s, 1H, **c**), 8.06 (d, J = 7.6, 2H, **b**), 7.91 (d, J = 7.2 Hz, 4H, **d**), 7.82 (s, 2H, **h**), 7.70-7.65 (m, 3H **a**, **g**), 7.13-7.10 (m, 4H, **e**, **f**) 2.34 (s, 6H, CH$_3$); ^{13}C NMR (100 MHz, CDCl$_3$/(CF$_3$)$_2$CHOH 6:1 v/v): δ (ppm) 215.2, 198.9, 197.9, 161.6, 157.5, 137.3 133.7, 133.0, 132.9, 130.7, 130.5, 129.9, 128.6, 119.2, 115.8, 117.2, 29.8; IR: v_{max} / cm^{-1} 1736 (C-H), 1657 (C=O), 1584 (C-C), 1496 (C-C), 1233 (C-O-C).

4.7 References

[1] A. Wood, D. Pandey, J. Walling, R. Lenferink, S. Wijskamp, R. Day, J. Bennett, A. Nesbitt and J. Methven, Manufacture of high performance thermoplastic composite structures. In: *SAMPE Conf. Proceedings*, Long Beach, USA, 200, **53**, 325/1-325/11.

[2] R. L. Mazur, P. C. Oliveira, M. C. Rezende and E. C. Botelho, *J. Reinf. Plast. Compos.*, 2014, **33**, 749-757.

[3] F. N. Cogswell, *Thermoplastic Aromatic Polymer Composites*, Oxford: Butterworth-Heinemann, 1992.

[4] P. A. Staniland, Poly(ether ketones). In: G. Allen and J. C. Bevington (eds), *Comprehensive Polymer Science*. Oxford: Pergamon, 1989, Vol. 5. pp. 483-497.

[5] K. G. Schmitt-Thomas, Z-G Yang and R. Malke, *Compos. Sci. Technol.*, 1998, **58**, 1509-1518.

[6] P. A. Staniland, *Bull. Soc. Chim. Belges,* 1989, **98**, 667-676.

[7] Z. Qiu, Z. Mo, S. Sheng and C. Song, *Macromol. Chem. Phys.*, 2000, **201**, 2756-2759.

[8] Z. Qiu and W. Yang, *J. Appl. Polym. Sci.*, 2006, **102**, 4775-4779.

[9] H. M. Colquhoun, C. C. Dudman, D. J. Blundell, A. Bunn, P. D. Mackezie, P. T. McGrail, E. Nield, J. B. Rose and D. J. Williams, *Macromolecules*, 1993, **26**, 107-111.

[10] V. L. Rao, P. U. Sabeena and M. R. Rao, *J. Appl. Polym. Sci*, 1999, **73**, 2113-2121.

[11] I. Fukawa, T. Tanabe and H. Hachiya, *Polym. J.*, 1992, **24**, 173-186.

[12] G. C. Finger and C. W. Kruse, *J. Am. Chem. Soc.*, 1956, **78**, 6034-6037.

[13] R. L. Markezich, O. S. Zamek, P. E. Donahue and F. J. Williams, *J. Org. Chem*. 1977, **42**, 3435-3436.

[14] F. A. Cotton and G. Wilkinson, *Advanced Inorganic Chemistry*. 5th ed. Chichester: John Wiley, 1988. pp.1385-1388.

[15] V. Carlier, B. Jambe, J. Devaux, R. Legras and P. T. McGrail, *Polymer*, 1993, **34**, 167-172.

[16] D. A. Wynn, M. M. Roth and B. D. Pollard, *Talanta*, 1984, **31**, 1036-1040.

[17] I. Baxter, H. M. Colquhoun, F. H. Kohnke, D. F. Lewis and D. J. Williams, *Polymer*, 1999, **40**, 607-612.

[18] D. J. Blundell, *Polymer*, 1992, **33**, 3773-3776.

[19] D. J. Blundell, J. J. Liggat and A. Flory, *Polymer*, 1992, **33**, 2475-2482.

[20] L. Bellomo, L. Franco and M. Hill, *Polymer*, 1997, **38**, 5643-5651.

[21] P. C. Dawson and D. J. Blundell, *Polymer*, 1980, **21**, 577-578.

[22] S. L. Mayo, B. D. Olafson and W. A. Goddard II, *J. Phys. Chem.*, 1990, **94**, 8897-8909.

[23] H. M. Colquhoun, D. F. Lewis and D. J. Williams, *Polymer*, 1999, **40**, 5415-5420.

[24] M. H. Hubacher, *J. Am. Chem. Soc.*, 1939, **61**, 2664-2665.

Chapter 5

Fractal-like self-similarity in the ^{1}H NMR spectra of random sequence copolymers

5.1 Abstract

The interaction of polycyclic aromatic molecules pyrene and perylene with binary co-polyimides containing both strongly-binding and weakly binding diimide sequences was found to result in the emergence of fractal-like patterns in the ^{1}H NMR spectra of the polyimide. The polyimide spectrum at high intercalator loadings shows a degree of self-similarity over a range of different length scales. A comparison of relative peak positions and intensities in the ^{1}H NMR spectrum of a ransom copolymer with high intercalator loadings with those predicted on the basis of an underlying mathematical fractal known as the "last-quarter Cantor set" is discussed.

5.2 Introduction

A fractal was described by the mathematician Benoit Mandelbrot as an object that has the property of "being exactly the same at every scale or nearly the same at different scales".[1,2] Fractals are mathematical sets that display a self-similar pattern. These intricate, complex patterns have great importance in the field of mathematics and engineering. One of the best-known examples of fractal patterns is the Mandelbrot set (Figure 5.1), which has become famous not only for its value in mathematics but also for its striking aesthetics. The Mandelbrot set displays an elaborate boundary that reveals repeating detail at increasing magnifications. This boundary also incorporates smaller versions of the main pattern, so that the fractal property of self-similarity applies to the entire set, and not just to its parts.[3]

Many *approximate* (as opposed to mathematically rigorous) fractals occur in nature and they characteristically display a self-similar property over an extended but finite scale. Examples of fractal structures in nature include snowflakes, pineapples, sunflowers and Romanesco broccoli. Figure 5.2 shows the self-similar character of a Romanesco broccoli. The head of the broccoli is made up of a spiral composed of a series of smaller florets. This

self-similar pattern continues at several smaller scales. The pattern is only an approximate fractal since the pattern eventually terminates when the size becomes sufficiently small. Interestingly, the number of spirals on the head of Romanesco broccoli is a Fibonacci number.[4]
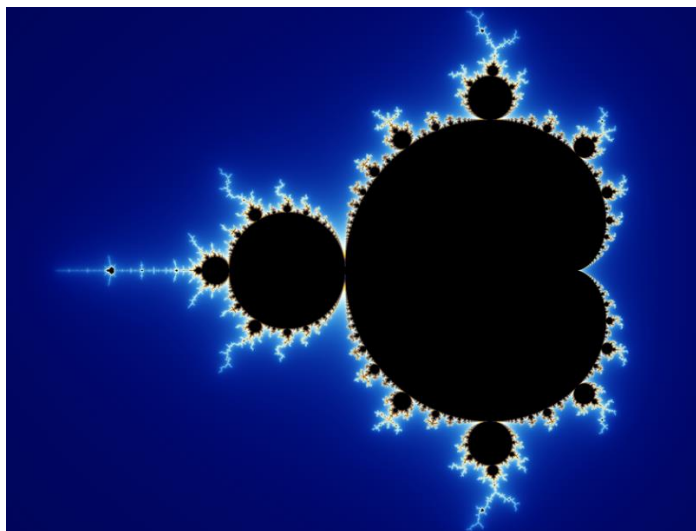
Figure 5.1. Self-similarity in a Mandelbrot set.[5]

Figure 5.2. Romanesco broccoli (an approximate fractal). Note the self-similarity of its structure over several different length scales.[6]

There are many examples of fractal sets in mathematics and nature, as noted above. Extended *molecular* fractals formed by self-assembly of small-molecule components have long been pursued but not achieved until very recently. Generally only scattered or fragmented interactions could be obtained via covalent or coordination bonds in synthetic chemistry.[7,8,9] However, in 2015, the groups of Gottfried and Wu reported the successful assembly and imaging of a defect-free Sierpiński triangle (a well-known mathematical fractal)[10] synthesised on a gold surface by the assembly (through non-covalent halogen-halogen bonding) of dibromo-terphenyl and -quaterphenyl building blocks.[11] Figure 5.3 shows the molecules involved and STM images of the resulting supramolecular Sierpiński triangle.
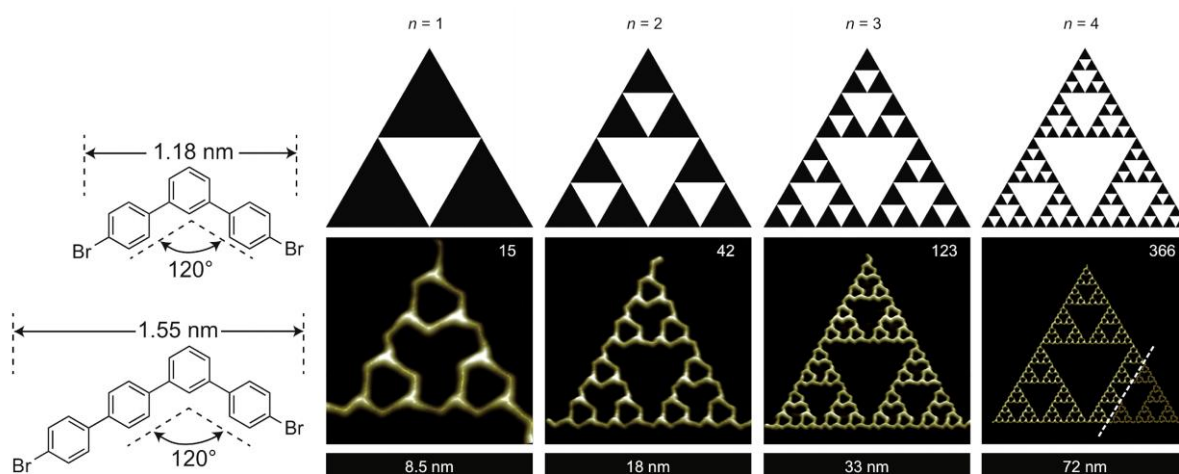
Figure 5.3. Assembly of a molecular Sierpiński Triangle (ST). Mathematical models of the STs (top) and STM images of the growing molecular ST (bottom). The two molecules assemble through noncovalent, multi-centre, Br.....Br halogen bonds. The numbers at upper right in each image indicate the number of molecules that participate in the corresponding molecular ST.[11]

The present chapter discusses the emergence of fractal-type patterns in ^{1}H NMR spectra resulting from the interaction of perdeuterated, polycyclic aromatic intercalator molecules (pyrene-d_{10} and perylene-d_{12}) with a random-sequence co-polyimide. The polymer contains both strongly-binding and weakly binding diimide sequences and at high intercalator loadings its ^{1}H NMR spectrum shows self-similarity over a range of different length scales. The observed fractal pattern is found to arise from a summation, for each possible co-monomer sequence, of ring-current shielding by guest molecules intercalating into polymer chain folds at progressively greater distances from the observed diimide residue.

5.3 Results and discussion

5.3.1 Random copolymer with pyrene-d_{10}

The binary copolymer **5.2** (Figure 5.4) which is the main focus of this chapter was obtained by the thermal polymerisation of naphthalene dianhydride with equimolar quantities of triethylenediamine and sulfonyl biphenyl diamine (**5.1**). The dehydration and subsequent imidisation was carried out at a relatively low maximum temperature of 210 °C to avoid the oxidation of the aliphatic units. This copolymer and its interactions with pyrene were originally studied by Colquhoun and Shaw,[12] and in the present project their results were confirmed and investigations extended to some related copolymers and intercalating agents.
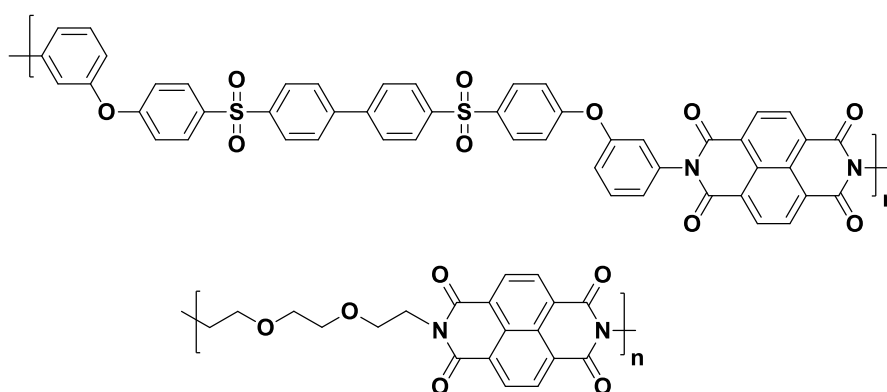
Figure 5.4. Structure of binary copolymer **5.2**.

Figure 5.5 shows the aromatic region of the ^{1}H NMR spectrum of **5.2**, dissolved in a mixture of CDCl$_3$/HFiPA (6:1, v/v). At lowest field, the spectrum shows a well-resolved three-line pattern with integrals 1:2:1. These resonances arise from naphthalene diimide (NDI) residues located between either two aromatic amine residues (Ar-NDI-Ar), two aliphatic residues (Al-NDI-Al), or one of each (Ar-NDI-Al and Al-NDI-Ar). The latter sequence is directionally degenerate and so in a fully random copolymer would be twice as probable to as the other two sequences. This pattern of intensities (1:2:1) thus confirms that the monomer sequence of copolymer **5.2** is genuinely random.
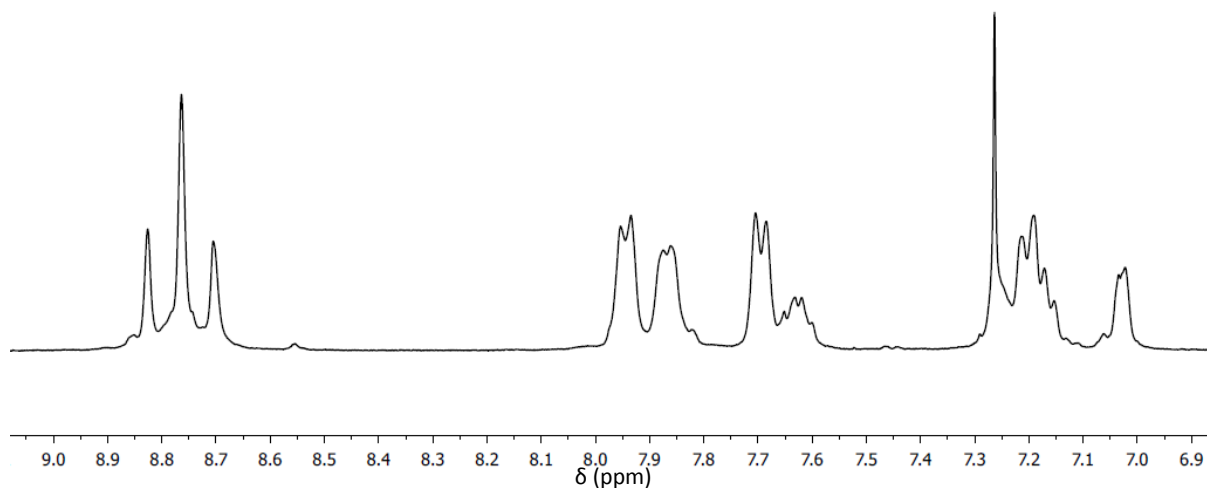
Figure 5.5. Partial ^{1}H NMR spectrum of copolymer **5.2**.

The addition of progressively increasing amounts of pyrene-d_{10} to a solution of **5.2** in CDCl$_3$/HFiPA produced upfield shifts ($\Delta\delta$ up to 0.45 ppm) and splitting of the diimide resonances (Figure 5.6). These effects clearly result from the binding of the pyrene-d_{10} to the polymer chain. The complexation shifts and splittings of the diimide ^{1}H NMR resonances seen in Figure 5.6 evidently result from the ability of pyrene to intercalate into some, but not all, adjacent copolymer chain-folds. The absence of resonances corresponding to bound and unbound diimide residues in **5.2** with pyrene-d_{10} indicates that association and dissociation of the intercalator occur under fast exchange conditions on the NMR timescale,[13] so that only time-averaged spectra are observed.
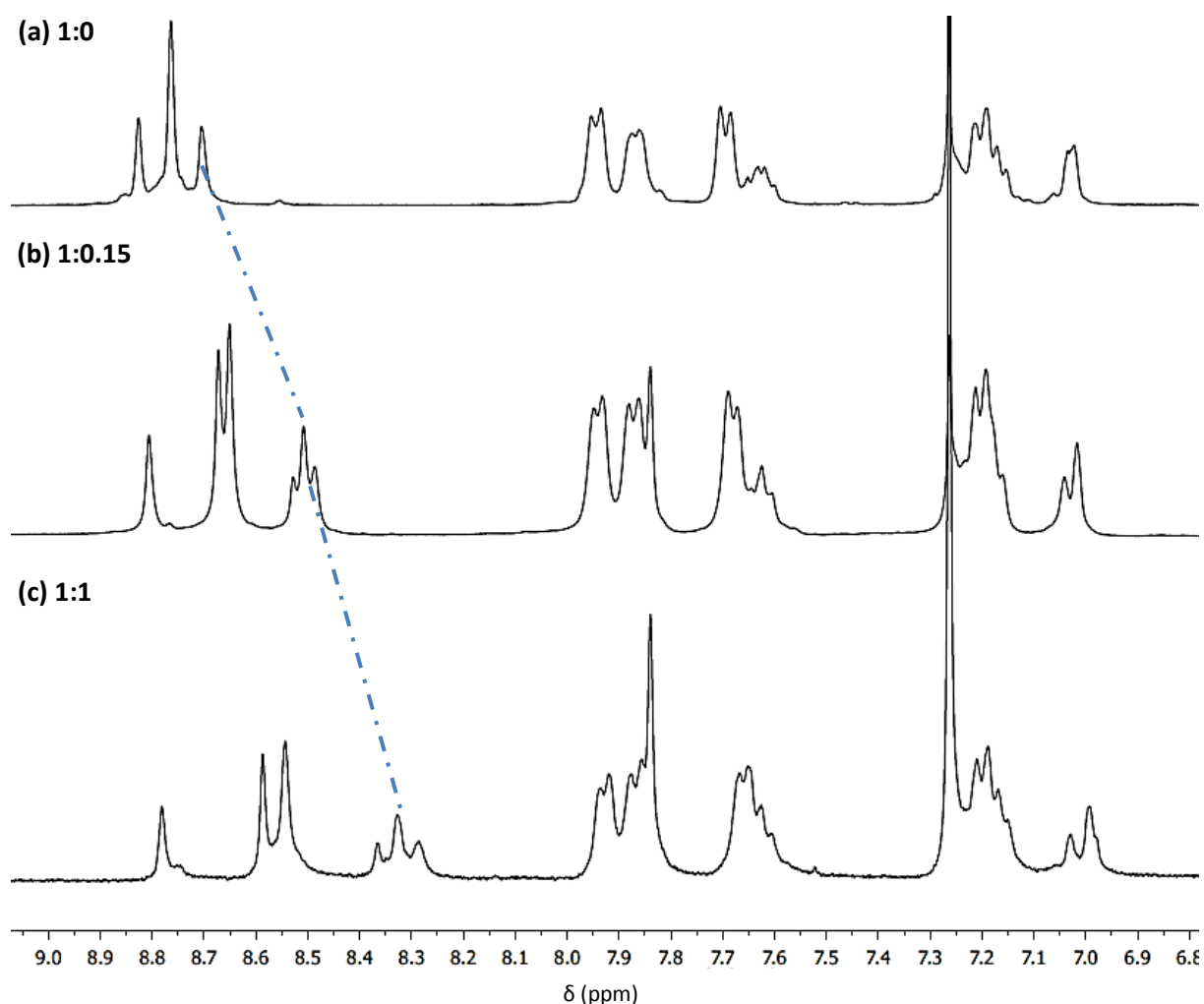
Figure 5.6. ^{1}H NMR spectra of copolymer **5.2** with increasing amounts of pyrene-d$_{10}$.

Specifically, the data can best be interpreted on the (quite reasonable) basis that pyrene intercalates strongly into a sequence of *two* adjacent diimide units connected by the aliphatic linker ("II"), but (to a first approximation) not at all into the sequence comprising *one* diimide plus the essentially non-binding 4,4'-biphenylenedisulfone unit ("IS"), as shown schematically in Figure 5.7. This results in different total degrees of aromatic ring-current shielding of the diimide protons for different sequences.
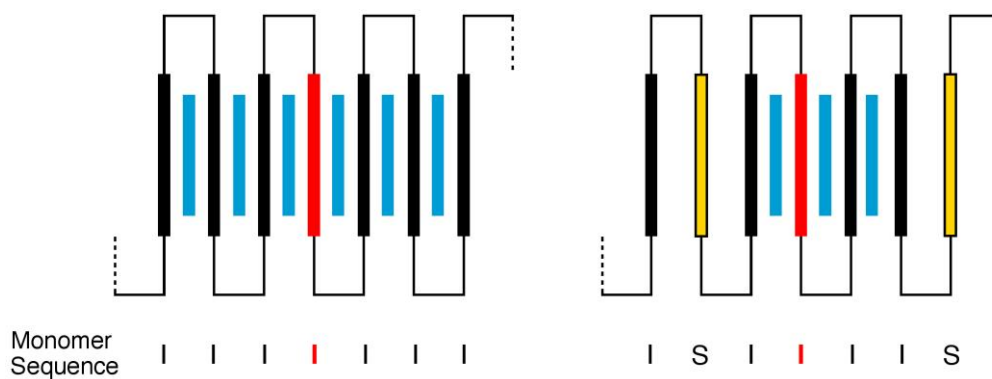
Figure 5.7. Examples of diimide-centred septet sequences (IIIIIII and ISIIIIS) showing how intercalation of pyrene gives rise to a total magnetic shielding that is specific for each sequence. This total shielding, giving rise to the observed complexation shift, is the sum of the shielding contributions from intercalating pyrene molecules at progressively greater distances from the central, observed, diimide unit (shown here in red).

In the spectrum at high pyrene loading (1:1 molar ratio of pyrene to diimide units; Figure 5.6c), the pattern in the diimide region (8.2 to 8.9 ppm) shows evidence of contracting symmetry and self-similarity. Thus, deconvolution of the resonances in Figure 5.6c indicates that the highest field diimide "triplet" (centered at 8.32 ppm) can be interpreted as a copy (scaled down by a factor of about 4), of the entire diimide resonance pattern (lying between 8.20 and 8.80 ppm), of the which the smaller copy is itself a part. This type of self-similarity under a contracting transformation is highly characteristic of fractal geometry. Further splitting of the high field triplet itself emerges at higher pyrene concentrations (Figure 5.10), and although the latter spectrum is complicated to some extent by impurity peaks, the emerging pattern again provides good evidence for self-similarity.

On the basis of this and earlier work, a very recent analysis of the cumulative ring-current shielding model by Colquhoun, Grau-Crespo and co-workers[14] has shown that the self-similar pattern of chemical shifts at high pyrene loadings can be accounted for in terms of an underlying mathematical fractal known as the "last-quarter Cantor set". This set can be generated by a geometric construction that involves dividing a line of unit length into four equal segments and then deleting the last quarter. The procedure is then repeated on each of the remaining three segments. The complete set is obtained by iterating this construction an infinite number of times, but the pattern does not visibly change until after some four or five iterations because the increasing level of detail cannot be resolved by the eye. In Figure

5.8, which shows the first four iterations of the construction, alternate quarters are coloured light and dark blue so that three adjoining quarters do not appear as a single segment.
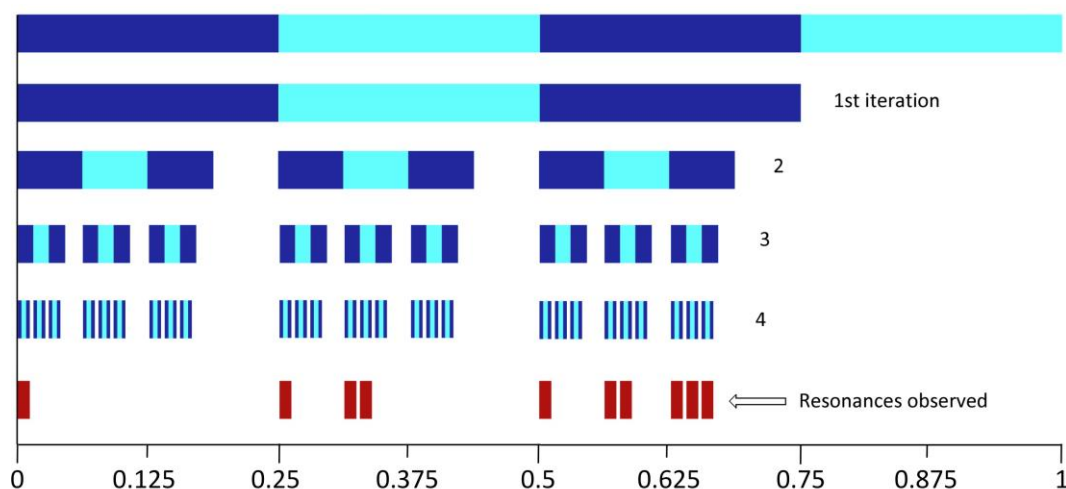
Figure 5.8. Construction of the last-quarter Cantor set (first four iterations) from a line of unit length. The positions shown in red correspond approximately to the chemical shift pattern seen in the diimide region of the ^{1}H NMR spectrum of copolymer **5.2** at high pyrene loadings (Figure 5.6). These clearly represent a selection from the fourth iteration, and it can be shown that the "absent" positions correspond to copolymer sequences that either cannot physically exist within the copolymer chain or cannot be resolved by the intercalation mechanism shown in Figure 5.7.

The approximate self-similarity of the ^{1}H NMR spectrum shown in Figure 5.6c thus emerges as a consequence of the fact that the observed peak positions form part of a Cantor set. This can be seen graphically by contracting both the full set (fourth iteration) and the observed pattern repeatedly by a factor of four (Figure 5.9); the full set shows nearly exact self-similarity, and the observed pattern shows a good approximation to this. Comparison of these patterns with a ^{1}H NMR spectrum simulated from the predicted peak positions for each co-monomer sequence, and with the experimental spectrum of copolymer **5.2** at high loadings of pyrene-d12, are shown in Figure 5.10. Intensities in the simulated spectrum were obtained by calculating the probability of any specific copolymer septet sequence and multiplying the probability by two when the sequence is directionally degenerate.
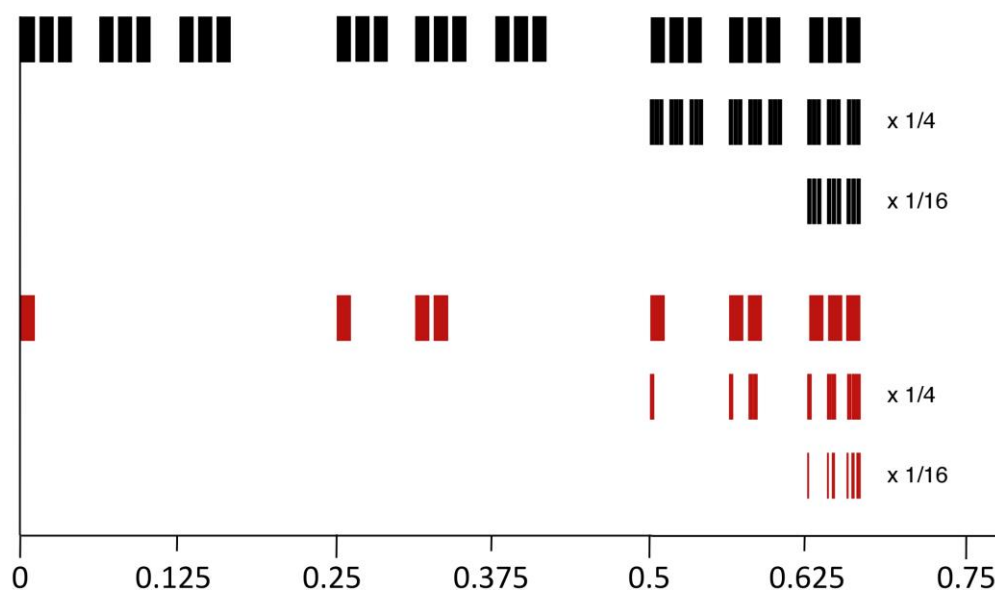
Figure 5.8. Contracting symmetry of the last quarter Cantor set (fourth iteration, top, in black) and of the observed resonance pattern (shown in red). In each case the whole pattern is contracted twice by a factor of four in the horizontal direction.
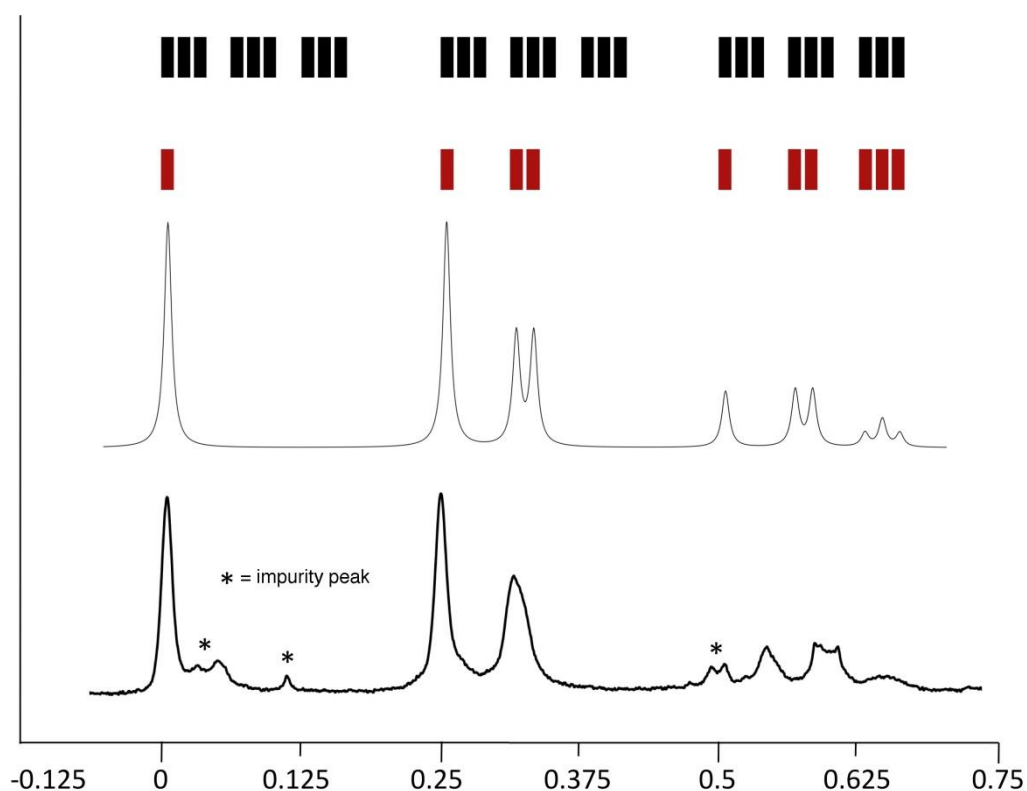
Figure 5.10. Correlation of relative peak positions and intensities in the observed ^{1}H NMR spectrum of copolymer **5.2** at high pyrene loadings (lower spectrum) with those predicted (upper spectrum) on the basis of the last-quarter Cantor set.

5.3.2 Interaction of copolymer 5.2 with perylene-d_{12}

In a further investigation of the structural origins of the fractal-like pattern seen in Figure 5.6c, pyrene was replaced by perylene as the probe molecule in the ^{1}H NMR titration. Progressively increasing amounts of perylene-d_{12} were added to a solution of **5.2** in CDCl$_3$/HFiPA (Figure 5.10). As with pyrene, perylene-d_{12} binds to the copolymer and produces upfield shifts and splittings of the diimide resonances. Perylene produced upfield shifts of up to 0.70 ppm (*cf.* 0.45 for pyrene). This would indicate that perylene has a stronger binding interaction than pyrene with the copolymer, but the pattern at high loadings of perylene is much less well-resolved than with pyrene. Further work is evidently needed to define the spectroscopic consequences of the binding of perylene to this copolymer.
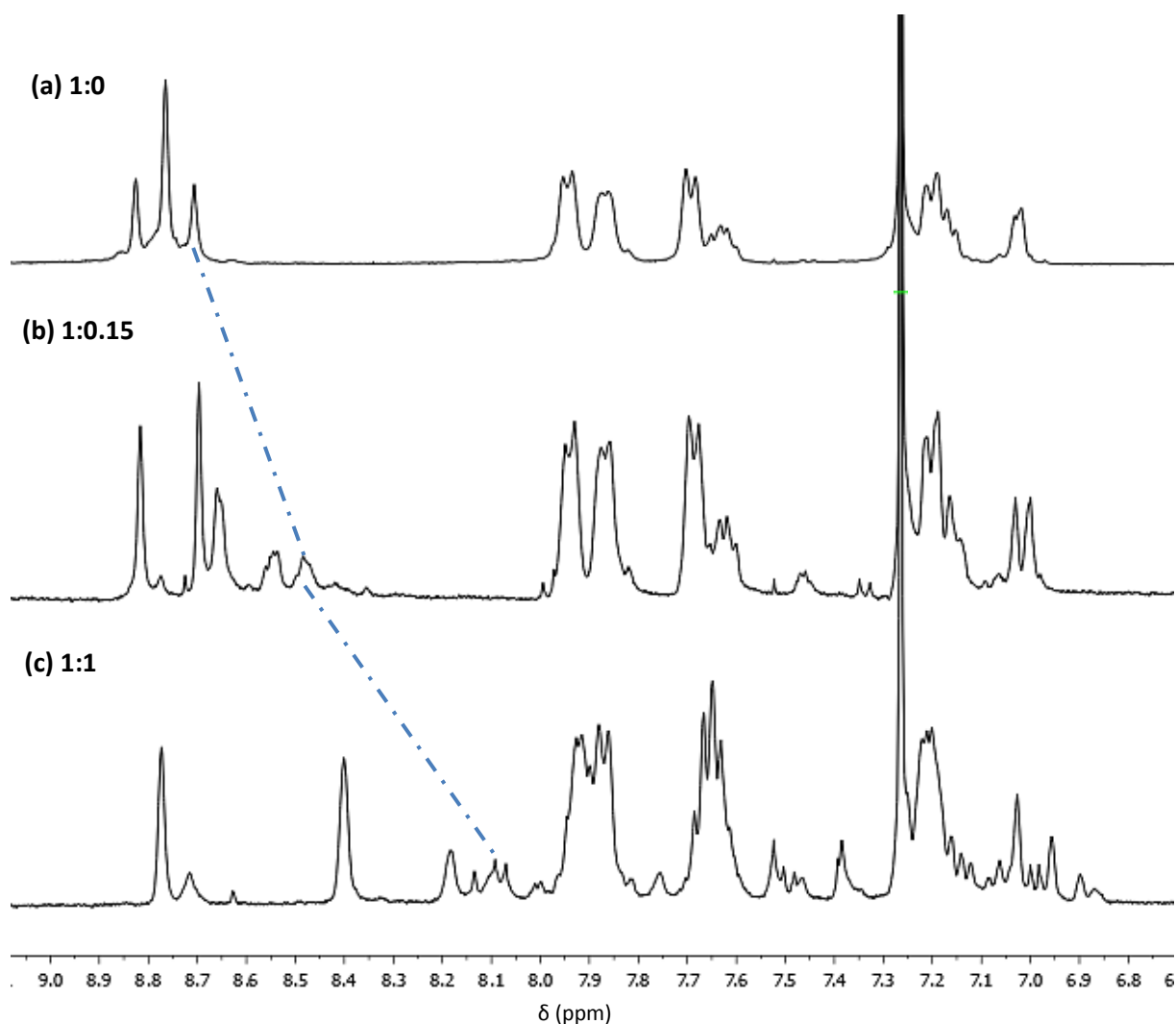
Figure 5.10. ^{1}H NMR spectra of copolymer **5.2** in the presence of increasing levels of perylene-d_{12}.

5.3.3 Interaction of a pyromellitic copolymer with pyrene-d_{10}

An unusual feature of the ^{1}H NMR spectrum of **5.2** (and its complexes with pyrene) is the absence of spin-spin splitting between the two chemically inequivalent diimide protons in unsymmetrically-substituted naphthalene diimide sequences. In order to explore the origins of this effect, a second binary co-polyimide **5.3** (Figure 5.11) was synthesised, now using pyromellitic dianhydride instead of naphthalenetetracarboxylic dianhydride, as the former having only a single type of diimide proton environment.
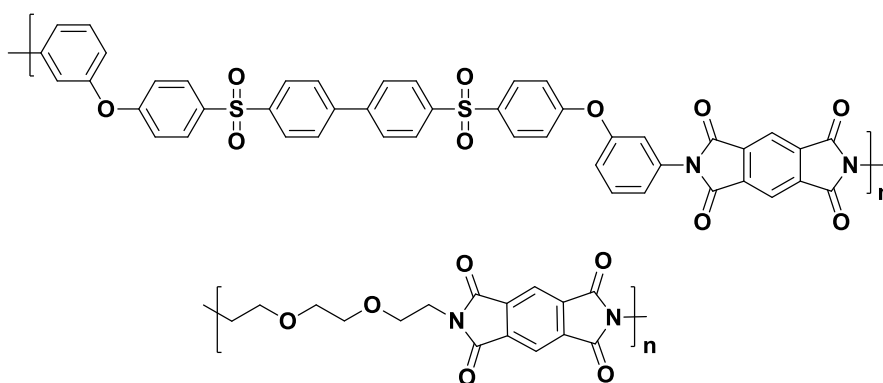
Figure 5.11. Structure of copolymer **5.3**.

The spectroscopic consequences of probe molecules (pyrene and perylene) binding to copolymer **5.3** should theoretically be very similar to those with copolymer **5.2** but with no possible ambiguity arising from inequivalent diimide protons. The ^{1}H NMR spectrum of **5.3** shows a well-resolved three-line pattern in the lowest field region (Figure 5.9). As with copolymer **5.2**, these resonances arise from diimide (now PDI) residues flanked by either two aromatic amine residues (Ar-PDI-Ar), two aliphatic amine residues (Al-PDI-Al) or one of each (Ar-PDI-Al and Al-PDI-Ar). Again, in a fully random 1:1 copolymer the latter would be twice as probable, as it is directionally degenerate. The pattern of integrated intensities (1:2:1) in the diimide region thus confirms that the monomer sequence of this copolymer is genuinely random. There is however a slight broadening (and even a hint of splitting) of the central resonance relative to the outer resonances of the three-line pattern, for which no satisfactory explanation has yet emerged.
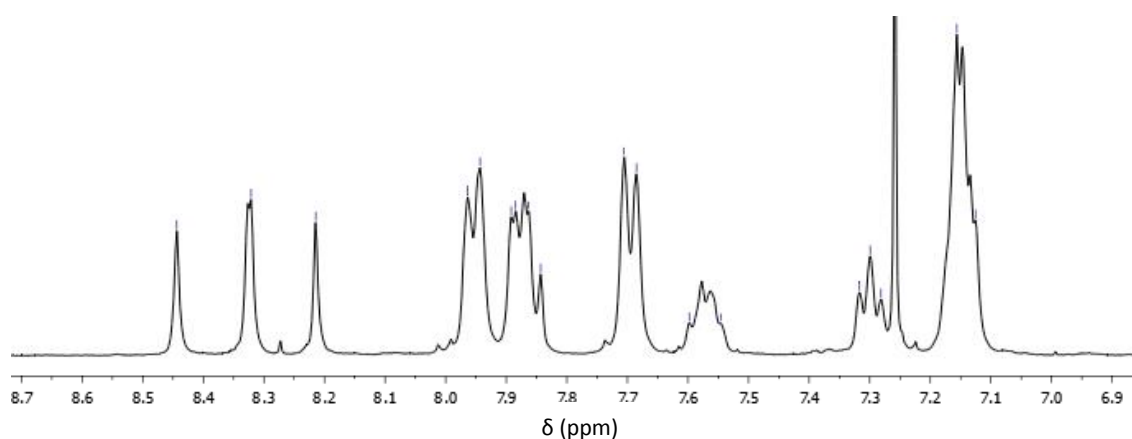
Figure 5.9. Partial ^{1}H NMR of copolymer **5.3**.

Addition of progressively increasing amounts of pyrene-d_{10} to a solution of **5.3** in CDCl$_3$/HFiPA produced once again marked upfield shifts of the copolymer diimide resonances (Figure 5.10). However, disappointingly, there was no indication of the resonance-splitting that gives rise to the fractal-type patterns seen with the corresponding naphthalene-diimide copolymer, so work on this copolymer was not pursued further.
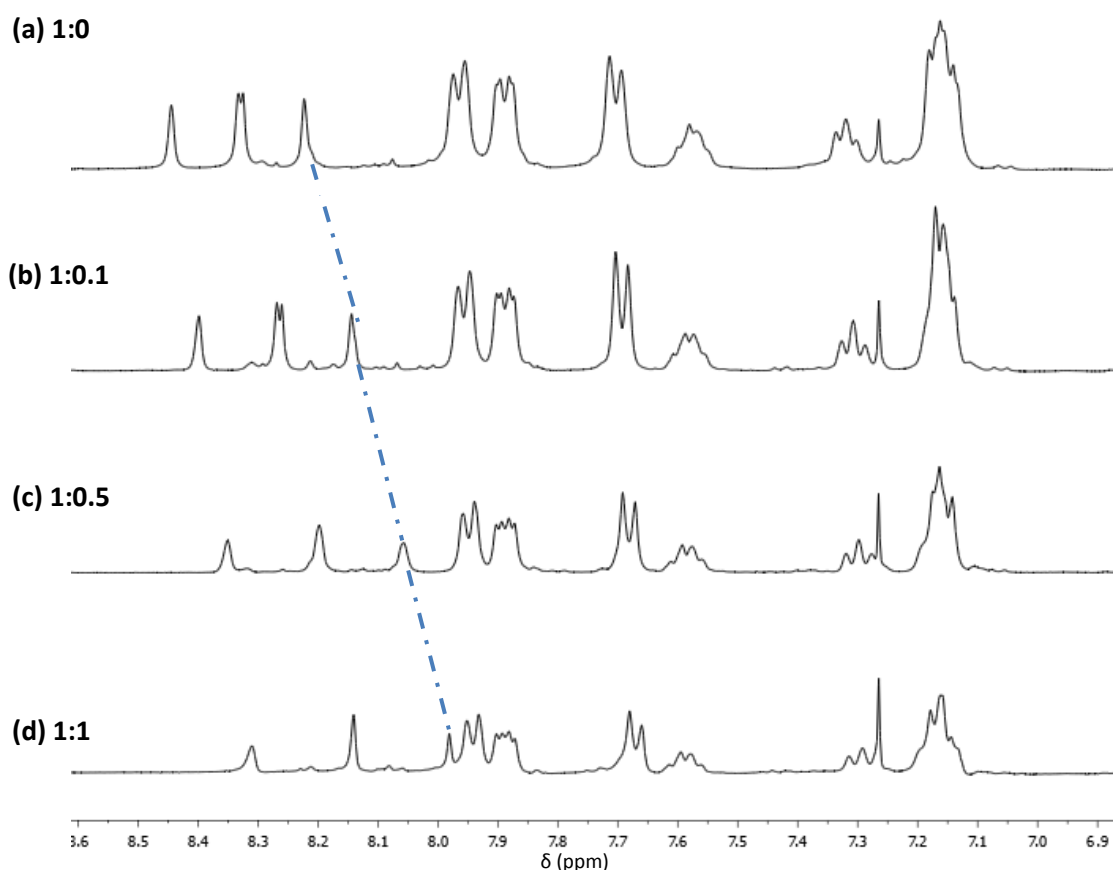
Figure 5.10. ^{1}H NMR spectra of copolymer **5.3** in the presence of increasing amounts of pyrene-d_{10}.

5.3.4 Further observations

In all the spectra of co-polyimides with high loadings of intercalating guest molecules, the upfield shift of the diimide protons in the polymers results in overlap with the resonances of the aromatic diamine residues. It was thus hypothesised that a *fully aliphatic* co-polyimide would be a useful diagnostic polymer for such polymer-guest interactions. In a co-polyimide where both diamine residues are aliphatic, the sole resonances in the low field region would come from the NDI or PDI residue. There would then be no overlap with any resonances shifting upfield on binding pyrene or perylene guest molecules. Several attempts were therefore made to synthesise co-polyimide **5.4** (Figure 5.12). This polyimide is the aliphatic analogue of **5.3** with the sulfonyl diamine (**5.1**) replaced by *trans*-1,4-diaminocyclohexane. However, co-polyimide **5.4** was found to be insoluble in all available deuterated NMR solvents and its interactions with pyrene and perylene could not therefore be investigated.
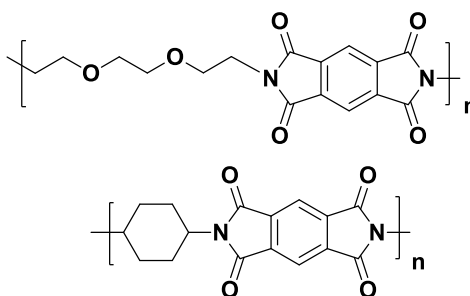
Figure 5.11. Structure of co-polyimide **5.4**.

5.4 Conclusions

This chapter showed the successful synthesis of two different binary copolymers, one of which contained naphthalene diimide residues while the other contained pyromellitic diimide residues. The ^{1}H NMR spectra resulting from the binding of an intercalator molecule (pyrene and perylene) to the diimide residues of the naphthalene diimide co-polymer show a degree of self-similarity over several length scales and demonstrate fractal-like properties. It was observed that perylene binding to the naphthalene diimide co-polymer produced stronger chemical shifts and more complex patterns compared with the binding of pyrene to the same co-polymer.

The co-polyimide containing pyromellitic diimide residues did produce chemical shifts in the ^{1}H NMR spectrum at high pyrene intercalator loadings. However, in this system, a fractal-like pattern was not observed.

At higher intercalator molecule loadings, the naphthalenediimide proton resonances move upfield and eventually overlap with the biphenylenedisulfone unit of the co-polymer. It is desirable to follow the development of the diimide resonance at even higher intercalator loadings. Several attempts were made to synthesise a fully aliphatic binary co-polymer wherein the aromatic region of the ^{1}H NMR would solely exhibit the diimide resonances. However, these attempts were unsuccessful and the polyimide product recovered from the synthesis was highly insoluble.

5.5 Experimental

5.5.1 Materials

4,4'-Bis[(4-chlorophenyl)sulfonyl]-1,1'-biphenyl, poly(methylhydroxysiloxane), 1,4,5,8-naph-thalenetetracarboxylic dianhydride, 1,2-bis(2-aminoethoxy)ethane, 3-trifluoromethyl aniline, *N,N*-dimethylacetamide, acetone, methanol, deuterated chloroform and deuterated dimethylsulfoxide were purchased from Sigma Aldrich UK. Pyrene-d_{10} and perylene-d_{12} were purchased from Alfa Aeser U.K. Pyromellitic dianhydride and trans-1,4-diaminocyclohexane were purchased from Tokyo Chemical Industry U.K. *N,N*-dimethylformamide was purchased from Fisher Scientific U.K. 1,1,1,3,3,3-Hexafluoro-2-propanol was purchased from Apollo Scientific U.K.

5.5.2 4,4'-Bis[4-(3-aminophenoxy)benzenesulfonyl)-1,1'-biphenyl] (5.1)

The synthesis and characterisation of this diamine monomer has been previously described in Chapter 2 as compound **2.10**.
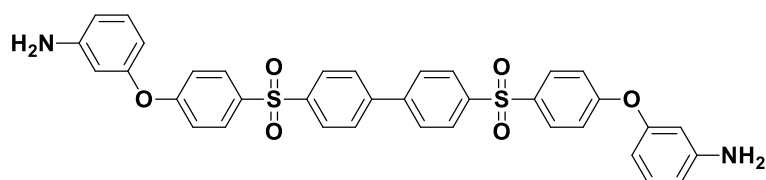
5.1

5.5.3 Naphthalene co-polyimide (5.2)

1,2-Bis(2-aminoethoxy)ethane (0.40 g, 0.62 mmol) was stirred in DMAc (5 mL) for 10 minutes. 4,4'-Bis[(4-chlorophenyl)sulfonyl]-1,1'-biphenyl was then added to the solution and stirred until dissolved. 1,4,5,8-naphthalenetetracarboxylic dianhydride (0.33, 1.2 mmol) was added and the suspension was sonicated for 1.5 h until homogenous. The dark brown solution was then stirred overnight before being transferred to a Petri dish and heated under vacuum to 90 °C for 2hrs to remove the solvent. The resulting film was heated to 150 °C for 30 min, 180 °C for 30 min and finally 220 °C for 2 h to give polyimide 5.1 as a brown film (0.51 g, 70%).
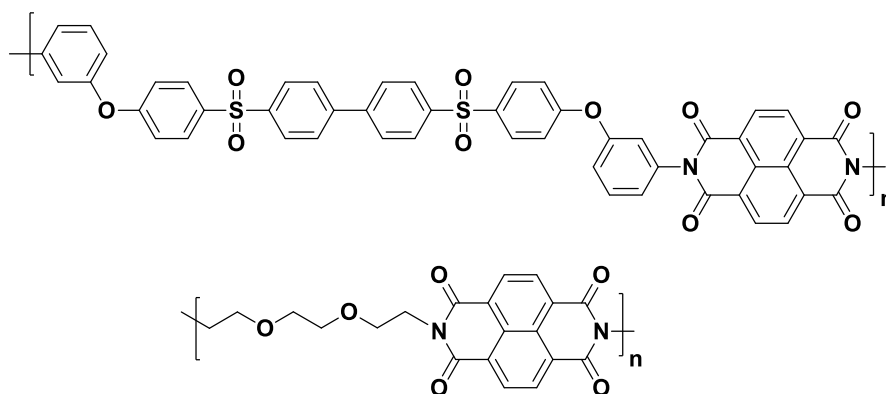
5.2

T_g = 240 °C, T_m (decomp.) 380 °C; η_{inh} (NMP) = 0.28 dL g^{-1}; ^{1}H NMR (400 MHz, CDCl$_3$/(CF$_3$)$_2$CHOH 6:1 v/v): δ (ppm) 8.76 (*app* t, 4H), 7.94 (d, *J* = 7.6, 2H), 7.87 (d, *J* = 5.6, 2H), 7.70-7.60 (m, 3H), 7.21-7.15 (m, 2H) 7.03 (*dist* d, 1H), 3.81 (s, 2H), 3.68 (s, 2H), 3.07 (s, 2H); ^{13}C NMR (100 MHz, CDCl$_3$/(CF$_3$)$_2$CHOH 6:1 v/v): δ (ppm) 163.7, 163.5, 156.0, 144.3, 140.6, 135.3, 134.1, 132.2, 131.7, 131.4, 130.1, 128.5, 128.1, 127.0, 126.8, 126.3, 126.2, 125.0, 121.5, 120.4, 69.7, 68.0, 39.6; IR: ν_{max} / cm^{-1} 1709, 1668 (C=O), 1581 (C=C Ar), 1485 (C=C, Ar), 1341 (C-N), 1247 (C-N), 1153 (S=O), 1107 (C-O), 767 (C-H).

5.5.4 Pyromellitic co-polyimide (5.3)

The same synthetic procedure as **5.1** was followed with the substitution of 1,4,5,8-naphthalenetetracarboxylic dianhydride for pyromellitic dianhydride (0.26 g, 1.2 mmol). This produced the title co-polyimide as a golden film (0.50 g, 83%).

5.3
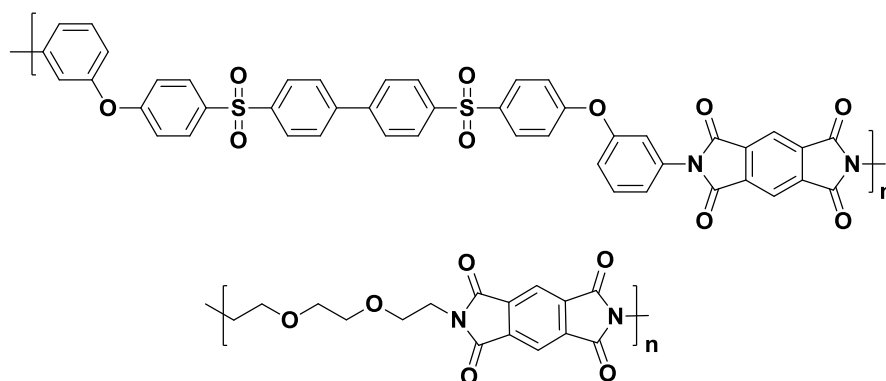
T_g = 217 °C, η_{inh} (NMP) = 0.63 dL g^{-1}; ^{1}H NMR (400 MHz, CDCl$_3$/(CF$_3$)$_2$CHOH 6:1 v/v): δ (ppm) 8.34 (*app* t, 4H), 7.96 (d, *J* = 8.0, 4H), 7.89-7.85 (m, 4H), 7.70 (d, *J* = 8.0, 4H), 7.60-7.55 (m, 2H) 7.30 (*dist* t, 2H), 7.16-7.13 (m, 8H), 3.89 (s, 6H), 3.70 (s, expected 2H), 3.03 (s, 2H), 2.90 (s, 2H); ^{13}C NMR (100 MHz, CDCl$_3$/(CF$_3$)$_2$CHOH 6:1 v/v): δ (ppm) 164.2, 163.7, 163.4, 162.0, 156.1, 144.4, 140.5, 135.4, 133.9, 132.1, 131.8, 131.3, 129.9, 128.4, 127.9, 127.1, 127.0, 126.8, 126.7, 126.2, 126.0, 121.2, 120.1, 118.7, 39.6, 36.8, 32.1; IR: ν$_{max}$ / cm^{-1} 1708, 1662 (C=O), 1581 (C=C Ar), 1486 (C=C, Ar),1342 (C-N), 1244 (C-N), 1152 (S=O), 1100 (C-O).

5.6 References

[1] B. B. Mandelbrot, *The fractal geometry of nature*, New York: W. H. Freeman, 1982.

[2] B. B. Mandelbrot, *Proc. R. Soc. Lond. A*, 1989, **423**, 3-16.

[3] M. Shishikura, *Ann. Math.*, 1988, **147**, 225-267.

[4] M. Kieffer, M. P. Fuller and A. J. Jennings, *Planta*, 1998, **206**, 34-43.

[5] Photograph from B. B. Mandelbrot's lecture: *Fractals and the art of roughness*, 2010. URL: http://www.ted.com/talks/benoit_mandelbrot_fractals_the_art_of_roughness.

[6] Photographed by Miss Corinne E. A. McEwan, University of Reading.

[7] K. Fujibayashi, R. Hariadi, S. H. Park, E. Winfree and S. Murata, *Nano Lett.*, 2007 **8**, 1791-1797.

[8] M. Wang, C. Wang, X.-Q. Hao, J. Liu, X. Li, C. Xu, A. Lopez, L. Sun, M.-P. Song, H.-B. Yang and X. Li, *J. Am. Chem. Soc.*, 2014, **136**, 6664-6671.

[9] R. Sarkar, K. Guo, C. N. Moorefield, M. J. Saunders, C. Wesdemiotis and G. R. Newkome, *Angew. Chem. Int. Ed.*, 2014, **53**, 12182-12185.

[10] W. Sierpinski, *C. R. Acad. Sci. Paris*, 1916, **162**, 629-632.

[11] J. Shang, Y. Wang, M. Chen, J. Dai, X. Zhou, J. Kuttner, G. Hilt, X. Shao, J. M. Gottfried and K. Wu, *Nat. Chem.*, 2015 **7**, 389-393.

[12] J. S. Shaw. PhD Thesis, University of Reading, 2010.

[13] Z. Zhu, C. J. Cardin, Y. Gan and H. M. *Colquhoun*, *Nat. Chem.*, 2010, 2, *653*-660.

[14] J. S. Shaw, R. Vaiyapuri, M. P. Parker, B. W. Greenland, C. A. Murray, K. J. C. Lim, C. Pan, R. Grau-Crespo, C. J. Cardin and H. M. Colquhoun, *manuscript in preparation*.

Chapter 6

Conclusions and future work

6.1 Conclusions

One of the aims of this research project was to increase the thermomechanical performance, primarily defined by the T_g, of semi-crystalline PAEKs for use as composite matrix material. This was achieved by using supramolecular polymer blends of end-functionalised PAEKs and polyimides. Intercalation of the electron-rich termini of the PAEKs into the electron-poor chain-folds of polyimides had the effect of increasing the T_g of the PAEK significantly. Systematic changes to the structure of polyimide led to a polyimide containing *m*-terphenylene diimide units. A blend of the *m*-terphenylene polyimide with 1-oxypyrene terminated PAEK exhibited a single T_g and increased the T_g of the PAEK by some 20 °C in the blend. It was envisioned that the supramolecular "cross-links" represented by the intercalated chain-folds could enhance the effective molecular weight of the PAEK, thus potentially increasing its toughness and modulus. However, as a result of poor adhesion between the layers of carbon fabric, the composite produced with the supramolecular polymer blend as the binding material showed a lower interlamellar shear strength and flexural strength than commercial composites.

A secondary aim of this project was to reduce the melt viscosity of PAEKs to aid pre-pregging and composite fabrication. The polyimide component was kept at a relatively low molecular weight as it was designed to act as a plasticiser the PAEK in the melt. By reducing the overall viscosity in the blend, it would enable more facile pre-pregging and eventual composite production. Carbon fibre composites were produced with a polymer blend of pyrene functionalised PEKK and *m*-terphenylene polyimide as the matrix material. The polymer blend gave a more viscous pre-preg dispersion in water than the commercial standard PEKK. Although the matrix polymer blend achieved good fibre wetting, it had poor adhesion at the interface of the carbon fabric. Further suggestions for improving carbon fibre composite fabrication is discussed below in reference to future work arising from this research project.

The project also investigated the synthesis of several novel end-capping compounds for functionalising PAEKs. A high-yield synthetic route to 4-fluoro- and 4-hydroxybenzoylpyrene was reported. Crystal structures of these compounds were obtained, which provided definitive molecular and crystal packing structure information. Confirmation of the ability of a benzoylpyrene unit to intercalate into a diimide chain-fold was obtained from the X-ray structure of a complex between 4-hydroxybenzoylpyrene and a macrocyclic model imide. The pyrenyl end-caps were used in the direct functionalisation of not only PAEKs but also poly(ether sulfone)s via nucleophilic polycondensation. It was also demonstrated that a two-step electrophilic polycondensation followed by end-capping is a viable route to producing functionalised polymers. The electrophilic polycondensation was carried out at room temperature, and afforded a relatively high molecular weight polymer as indicated by its inherent viscosity and supported by the high T_g measurements.

The mechanism of monomer sequence-randomisation via transetherification during the nucleophilic synthesis of PAEKs was investigated. It was found that the sequence-randomisation is a result of reversible nucleophilic cleavage by fluoride ions of ether linkages activated by electron-withdrawing carbonyl groups. The degree of transetherification increases with the ionic radius of the alkali metal (from carbonates used in the polycondensation) involved.

This thesis also described a short investigation of fractal-like self-similarity observed in the ^{1}H NMR spectra of binary copolymers when complexed with polycyclic aromatic molecules. The intercalation of perdeuterated pyrene and perylene into the chain-folds of a naphthalene diimide binary copolymer produced a degree of self-similarity in the NMR spectrum over several length scales and demonstrated fractal-like properties. It was observed that the binding of perylene produced stronger complexation shifts compared with the binding of pyrene to the same copolymer.

6.2 Future work

6.2.1 End-cap synthesis

The successful synthesis of 1-(4-fluorobenzoyl)perylene end-capping monomer was confirmed by ^{1}H NMR spectroscopy and high resolution ESI-MS. However, attempts to

synthesise the 1-(4-hydroxybenzoyl)perylene analogue have thus far proved unsuccessful. There is evidence of the compound in the ^{1}H NMR spectrum of the reaction product, but purification of the target compound from the perylene starting material remains an obstacle.

It would be useful to obtain quantitative values for the binding constants between the end-caps and the diimide macrocycle. Binding between the two molecules could be quantified using UV-vis spectroscopy using reported dilution methods[1] or by quantitative ^{1}H NMR titration studies[2]. This would allow a quantitative comparison between the different end-capping compounds synthesised during the course of this research project.

It would be worth pursuing a perylenyl-capped PAEK and blending this with polyimide as it is envisioned that perylene would bind more strongly to electron deficient compounds. With the successful acylation of perylene, it would be interesting to see if an electrophilic route would be as viable a way to produce perylene-capped PAEK as it was for pyrene.

6.2.2 Supramolecular polymer blends

The supramolecular polymer blend of a 1-oxypyrene terminated PAEK and the *m*-terphenylene polyimide increased the T_g of the PAEK by some 20 °C in the blend. Although the blend exhibited a single T_g, the value was not a weight-average of the T_g of the two components. Further work is required to resolve the origins of the only modest T_g observed for this type of blend. A phase diagram of T_g versus polyimide content of different blend compositions would be a starting point for this study. Investigations into the morphology of the polymer blends presented in this work were not pursued. It would be of interest and industrial benefit to study any amorphous segregation behaviour in the blend.

Tensile (Instron) testing of the carbon fibre composite showed that the material with the pyrenyl-PEKK and polyimide blend performed less well than other materials tested. As was established in Chapter 3, the failing is due in part to the poor matrix inter-layer adhesion in the carbon fabric. As a short-term solution, investigations on how to adapt the layering process of the composite fabrication for the more viscous polymer blend dispersion could be a way to avoid the formation of defects (holes) in the matrix layers of the composite.

The ratio of the pyrenyl-PEKK and *m*-terphenyl polyimide was designed with the feasibility of a large-scale synthesis in academic laboratory in mind. Without the restrictions of small lab equipment, it would be helpful to produce a type of phase diagram wherein the ideal ratio of polymers with respect to the supramolecular interactions is taken into account. This could produce a more compatible polymer blend, and should therefore improve composite production.

6.3 References

[1] M. B. Nielsen, J. O. Jeppesen, J. Lau, C. Lomholt, D. Damgaard, J. P. Jacobsen, J. Becher and J. F. Stoddart, *J. Org. Chem.,* 2001, **66**, 260-273.

[2] F. La Terra, *PhD Thesis*, University of Reading, 2014.

Chapter 7

Experimental methods

7.1 Polymer blending

7.1.1 Solution blending

Polymer samples were prepared at a concentration of 1 mg mL^{-1}. The polymers were co-dissolved in the named solvent for 30 mins and re-precipitated in MeOH. The resulting precipitate was filtered then extracted in boiling MeOH. The filter was then washed with Et$_2$O before drying in a vacuum oven for 3 h.

7.1.2 Spin blending

Polymer samples were placed in a round bottomed flask and spun in a rotary evaporator until a homogenous powder blend is achieved.

7.2 Carbon fibre composite preform preparation

Preform preparation and drying was carried out in Cytec Industries, Wrexham. For each of the system studied, a polymer slurry (40 g in 120 g water) containing < 0.5% non-ionic surfactant and < 0.5% defoamer was prepared. Nine panels were prepared in total, six of 0° layup of fabric and three of (+45, -45, +45, -45, +45, -45, +45)° layup of fabric. A release film cut larger than the mould was pressed into a 6" x 4" mould. The first carbon fabric (0° layup) was placed in the mould. A seventh of the slurry solution was placed on top and distributed evenly. The process was repeated with each ply, alternating the 0° and 45° fabric. A final layer of polymer slurry was placed on the top ply of fabric. The release film was then loosely folded over and then the mould and preform placed in a vacuum autoclave oven at 90 °C until dry. The preforms were stored at ambient temperature until use.

7.3 Composite pressing

To prepare the composite, a release polymer was placed on top of the preform and covered with a layer of release film and a metal frame is placed on top (Figure 7.1). All the layers are then placed between two metal plates.
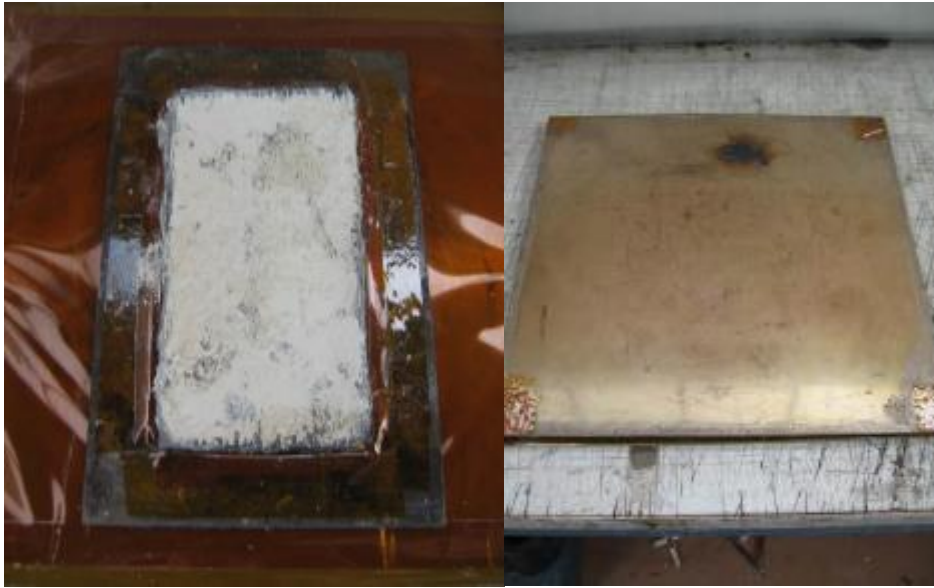
Figure 7.1. The composite preform is placed on a metal plate with a release film then a release polymer and a metal frame is placed on top of it (left). A second release film and metal plate is placed on top (right).

The plates were then placed in the centre of a Platen press preheated to 375 °C (Figure 7.2). The press plates were slowly brought together over 20 mins with the plates fully closed for the final 5 minutes. 50 bar of pressure was then applied and held for 20 mins. This pressure was held whilst the press was cooled (around 45 minutes by air). The Platen press was cooled below the polymer T_g before the plates were removed. Once the plates were cooled, the composite is removed from the steel plate using a hammer and chisel Composite panels of 2.0 - 2.1 mm thickness were produced using the above method.
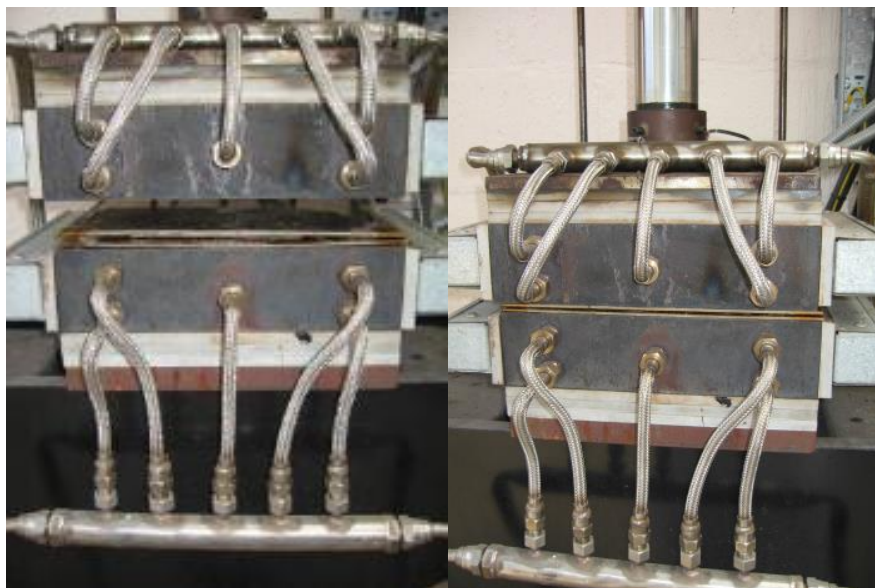
Figure 7.2. The metal plates are placed between a preheated Platen press. The platens are brought together and a pressure of 50 bar is held for 20 mins before cooling.

7.4 Instrumental techniques

7.4.1 Nuclear magnetic resonance spectroscopy

^{1}H and ^{13}C NMR spectra were obtained on a Bruker Nanobay 400 MHz or 700 MHz spectrometer and were referenced to residual solvent resonances or tetramethylsilane. Samples were dissolved in various solvents at room temperature. All values representing chemical shifts, δ, quoted in the assignment of ^{1}H and ^{13}C NMR spectra are in units of ppm.

7.4.2 Infrared spectroscopy

IR spectra were recorded on a Perkin Elmer Spectrum 100 FT-IR spectrometer with a Universal Attenuated Total Reflectance accessory. Monomer samples were analysed as powders whereas polymeric materials were analysed in powder or film form.

7.4.3 Fluorescence spectroscopy

Fluorescence measurements were carried out at 20 °C using a Varian Cary Eclipse fluorescence spectrophotometer. Polymer samples were prepared in 10^{-7} M solutions in $CHCl_3$/TFA (3:1 v/v) or $CHCl_3$/HFiPA (6:1 v/v). Excitation wavelengths were determined from absorbance wavelengths measured from a Varian Cary 300 Bio UV-Visible spectrophotometer.

7.4.4 Mass spectrometry

Mass spectra (electrospray ionisation) were obtained on a LTQ Orbitrap XL with an Accela LC autosampler. Monomer samples were analysed at a concentration of 0.1% (w/v) in acetonitrile or DMSO.

7.4.5 Solution inherent viscosity

Inherent viscosities were measured at 25 °C for 0.1% (w/v) polymer solutions in 96% sulfuric acid (H_2SO_4), in NMP or in a $CHCl_3$ and HFiPA (6:1 v/v) with a Schott-Geräte CT-52 auto-viscometer, using glass capillary No. 53102 (H_2SO_4), No. 53101 (NMP) or No. 53103 ($CHCl_3$/HFiPA) and calculated from Equation 6.1:

Equation 7.1.

$$\eta_{inh} = \left(\frac{\left\{ \ln \frac{t_2}{t_1} \right\}}{c} \right)$$

Where η_{inh} is inherent viscosity (dL g^{-1}), t_1 and t_2 are the flow times of the solvent and polymer solution (s) respectively and c is the concentration of the polymer solution (g dL^{-1}). Final recorded values are expressed as an average of 5 measurements per polymer solution.

7.4.6 Differential scanning calorimetry

Phase transitions of polymers (4-12 mg samples) were identified using a TA Instruments DSC Q2000 under a nitrogen atmosphere. A flow rate of 50 mL min^{-1}, a heating rate of 10 °C min^{-1} and aluminium pans were used. Unless otherwise stated, values of T_g, T_{cc} and T_m were obtained from 2nd heating scans whereas T_c was collected from the 1st cooling scan. T_{cc}, T_m and T_c values were measured as the peak exotherm or endotherm of their respective processes and T_gs were determined from the initial change in the slope of the baseline (onset temperature).

The purities of monomers and small molecules (3-6 mg samples) were identified from the second heating cycles of DSC traces using a Mettler Toledo DSC20 under a nitrogen atmosphere. A flow rate of 50 mL min^{-1} and aluminium pans were used. Data capture and subsequent data analysis were carried out using Mettler STARe software.

7.4.7 Dynamic mechanical analysis

DMA was performed on a TA Q800 DMA using a frequency of 1Hz and a strain of 0.05%. The composite samples were held in place using tensile clamps before heating from 50 to 250 °C at 5 °C min $^{-1}$. The mechanical test methods used were ASTM D2344 (SBS) and ASTM D790B (3 point flex) and both were measured on an Instron 5982 test frame.

7.4.8 Gel permeation chromatography

GPC measurements were performed on an Agilent Technologies 1260 Infinity instrument using a PL gel 5 μm column fitted with a PL gel 5μm guard. THF was used as eluent, with a flow rate of 1 mL min^{-1}. All experimental runs were conducted at 40 °C, employing an UV detector with sampling via automatic sample injection. Molecular weights are referenced to polystyrene standards. Data capture and subsequent data analysis were carried out using Agilent GPC/SEC software. Samples were prepared at a concentration of 2 mg mL^{-1}, with 10 mg of samples dissolved in 5 mL eluent. These solutions were stirred for 16 h at room temperature to fully dissolve the polymer. Each sample was filtered through a 0.2 μm polytetrafluoroethylene membrane prior to injection.

7.4.9 X-ray diffraction

7.4.9.1 Powder diffraction

X-ray powder diffraction data were obtained using a Bruker D8 Advance powder diffractometer. The samples were ground to a fine powder and applied onto a silicon flat plate with a small amount of petroleum jelly. The sample was subjected to Cu-Kα radiation (where λ = 1.5418 Å) with 360° rotations, over the 2θ range 5° to 70°. Intensity data were merged and corrected (subtraction of amorphous regions) for absorption using Bruker Diffrac Plus EVA software, before the powder diffraction data were integrated to give one-dimensional powder data.

7.4.9.2 Fibre diffraction

X-ray fibre patterns of uniaxially oriented fibres were obtained using an Oxford Gemini S Ultra diffractometer (Cu-Kα radiation, λ = 1.5418 Å). Data were collected with sample-to-plate distance of 45 mm and the X-ray beam normal to the plane of the fibre at 90°φ rotations over the 2θ range -90° to +90°.

Uniaxially oriented fibres were obtained by heating polymer samples (approximately 50 mg) at 30 °C above the T_m of the sample upon a sheet of thick aluminium foil on a ceramic hotplate. The polymer melt was formed into a rectangular sheet ~ 0.5 mm in thickness and then quenched rapidly in water. The aluminium foil was dissolved away from the polymer by stirring in a 40% HCl solution for 20 mins, and the polymer sheet was cut into ca. 2mm wide strips which were then manually drawn over a ceramic hotplate (draw ratio > 4) set at 400 °C, and were then annealed at constant length for 16 h at 220 °C.

7.4.9.3 Single crystal diffraction

Single crystal samples were grown via solvent/non-solvent vapour exchange. Samples of benzoylpyrene were dissolved in $CDCl_3$ and diffused against MeOH as the non-solvent over a period of 4 weeks. The single crystals were grown in $CHCl_3$/HFiPA (6:1 v/v) and diffused against hexane as the non-solvent over a period of 6 weeks.

Single crystal X-ray data were obtained using an Oxford Gemini S Ultra diffractometer (Cu-Kα radiation, λ = 1.5418 Å). Data were collected with sample-to-plate distance of 50 mm.

7.4.10   Computational modelling

Model building was performed using Materials Studio software (v.7.0, Accelrys, San Diego, USA). Geometric and energy minimisation of chemical structures was carried out using molecular mechanics with the Accelrys Universal force field.

Computational modelling in Chapters 2 and 4 was carried out using *Cerius2* (version 3.5, Accelrys, San Diego, USA). Energy minimisation of structures was carried out using a modified Dreiding-2 force field (W. A. Goddard III, Caltech).

Appendix: Crystal data

1.   Single Crystal X-ray Data

A.   1-(4-Fluorobenzoyl)pyrene (2.1)

Bond precision: C-C=0.0031 Å   Wavelength=0.71073 Å

Cell: a=3.9729(3)   b=31.006(3)   c=12.3032(6) Å
                                   alpha=90   beta=94.427(5)   gamma=90°
Temperature: 150 K

	Calculated	Reported
Volume Å^3	1511.0(2)	1511.05(19)
Space group	C c	C c
Sum formula	C23 H13 F O	C23 H13 F O
M_r	324.33	324.33
D_x, g cm-3	1.426	1.426
Z	4	4
Mu (mm^{-1})	0.094	0.094
F000	672.0	672.0
F000'	672.33	
h,k,l max	5,44,17	5,41,17
Nref	4700[2361]	2046
Tmin,Tmax	0.992,0.993	0.992,0.993
Tmin'	0.979	

Data completeness = 0.87/0.44   Theta(max) = 30.681
R(reflections) = 0.0425(1875) wR_2(reflections) = wR = 0.0419(1756)
S = 1.140   Npar = 226

B.   1-(4-Fluorobenzoyl)perylene (2.1)

Bond precision: C-C=0.0448 Å   Wavelength=0.71073 Å

Cell: a=37.707(12)   b=13.8814(9)   c=22.338(7) Å
                             alpha=90   beta=144.69(7)   gamma=90°

Temperature: 150 K

	Calculated	**Reported**
Volume Å^3	6758(12)	6758(12)
Space group	P 21/a	P 21/a
Sum formula	C27 H15 F O	C24.92 H13.85 F0.92 O0.92
M_r	374.39	345.61
D_x, g cm^{-3}	1.104	1.104
Z	12	13
Mu (mm-1)	0.072	0.072
F000	2328.0	2328.0
F000'	2329.12	
h,k,l max	56,20,33	55,20,31
Nref	23329	20422
Tmin,Tmax	0.992,0.996	0.990,1.000
Tmin'	0.992	

Data completeness = 0.875   Theta(max) = 31.920
R(reflections) = 0.1768(4701)   wR$_2$(reflections) = wR = 0.1561(2867)
S = 1.139   Npar = 349

C.   Complex of 1-(4-hydroxybenzoyl)pyrene (2.2) with macrocycle 2.11

Bond precision: C-C=0.0082 Å   Wavelength=0.71073 Å

Cell: a=11.6525(5)   b=14.1485(6)   c=22.8678(7) Å
                                    alpha=95.321(3)   beta=102.558(3)
          gamma=111.316(4)°

Temperature: 100 K

	Calculated	Reported
Volume $Å^3$	3366.5(3)	3366.4(3)
Space group	P -1	P -1
Sum formula	$C_{69}H_{40}N_2O_{12}S_2$	$C_{69}H_{40}N_2O_{12}S_2$
M_r	1153.15	1153.21
D_x, g cm^{-3}	1.138	1.138
Z	2	2
Mu (mm^{-1})	0.137	0.137
F000	1192.0	1192.0
F000'	1193.08	
h,k,l max	15,18,29	15,18,29
Nref	15569	15547
Tmin,Tmax	0.989,0.999	0.840,1.000
Tmin'	0.980	

Data completeness = 0.999   Theta(max)= 27.559
R(reflections) = 0.0898(10135)   wR$_2$(reflections) = wR = 0.0882(8649)
S = 1.115   Npar = 766

2. Model for the Crystal Structure of Polymer 4.1 from X-ray Fibre Data

```
_cell_length_a                   7.6800(0)
_cell_length_b                   6.0400(0)
_cell_length_c                  49.5000(0)
_cell_angle_alpha               90.0000(0)
_cell_angle_beta                90.0000(0)
_cell_angle_gamma               90.0000(0)

_symmetry_space_group_name_H-M     'I c 2 m'
_symmetry_Int_Tables_number        46
_symmetry_cell_setting             orthorhombic

_symmetry_equiv_pos_as_xyz
'+x,+y,+z'
'1/2+x,1/2+y,1/2+z'
'-x,+y,-z'
'1/2-x,1/2+y,1/2-z'
'-x,+y,1/2+z'
'1/2-x,1/2+y,+z'
'+x,+y,1/2-z'
'1/2+x,1/2+y,-z'

_atom_site_label
_atom_site_type_symbol
_atom_site_occupancy
_atom_site_fract_x
_atom_site_fract_y
_atom_site_fract_z
    C2    C  1.0000    0.4270    0.3707    0.7741
    C3    C  1.0000    0.5000    0.7588    0.0000
    C5    C  1.0000    0.3919    0.2651    0.7499
    C7    C  1.0000    0.5383    0.6843    0.7499
    C9    C  1.0000    0.4995    0.4081    0.9253
   C10    C  1.0000    0.4134    0.3212    0.9475
   C12    C  1.0000    0.4120    0.4361    0.9717
   C14    C  1.0000    0.4969    0.6377    0.9737
   C15    C  1.0000    0.5831    0.7245    0.9516
   C17    C  1.0000    0.5848    0.6096    0.9274
   C20    C  1.0000    0.4995    0.3924    0.8766
   C21    C  1.0000    0.4112    0.5892    0.8722
   C23    C  1.0000    0.4185    0.6902    0.8471
   C25    C  1.0000    0.5128    0.5939    0.8264
   C26    C  1.0000    0.6007    0.3967    0.8308
   C28    C  1.0000    0.5935    0.2957    0.8559
   C30    C  1.0000    0.5208    0.7069    0.7997
   C32    C  1.0000    0.5016    0.5796    0.7741
    H1    H  1.0000    0.4010    0.2968    0.7912
    H6    H  1.0000    0.3397    0.1179    0.7499
    H8    H  1.0000    0.5909    0.8313    0.7499
   H11    H  1.0000    0.3535    0.1791    0.9460
   H13    H  1.0000    0.3510    0.3750    0.9873
   H16    H  1.0000    0.6430    0.8665    0.9530
   H18    H  1.0000    0.6457    0.6708    0.9118
   H22    H  1.0000    0.3447    0.6573    0.8868
   H24    H  1.0000    0.3565    0.8291    0.8440
   H27    H  1.0000    0.6672    0.3288    0.8162
   H29    H  1.0000    0.6555    0.1570    0.8590
    O4    O  1.0000    0.5000    0.9612    0.0000
   O19    O  1.0000    0.4964    0.2867    0.9015
   O31    O  1.0000    0.5218    0.9094    0.7989
```